EFFECT OF DIVERSE SEISMIC HAZARD ESTIMATES ON PERFORMANCE AND OVERALL COST OF RC SHEAR WALL BUILDINGS IN DUBAI, UAE

by

Nader Essam Aly

A Thesis Presented to the Faculty of the
American University of Sharjah
College of Engineering
in Partial Fulfillment
of the Requirements
for the Degree of

Master of Science in
Civil Engineering

Sharjah, United Arab Emirates

November 2015

Approval Signatures

We, the undersigned, approve the Master's Thesis of Nader Essam Aly

Thesis Title: Effect of Diverse Seismic Hazard Estimates on Performance and Overall Cost of RC Shear Wall Buildings in Dubai, UAE

Signature	**Date of Signature** (dd/mm/yyyy)
Dr. Mohammad AlHamaydeh Associate Professor, Department of Civil Engineering Thesis Advisor	
Dr. Jamal Abdalla Professor, Department of Civil Engineering Thesis Committee Member	
Dr. Mohamed Maalej Professor, Department of Civil and Environmental Engineering University of Sharjah Thesis Committee Member	
Dr. Aliosman Akan Department Head, Department of Civil Engineering	
Dr. Mohamed El-Tarhuni Associate Dean, College of Engineering	
Dr. Leland Blank Dean, College of Engineering	
Dr. Khaled Assaleh Interim Vice Provost for Research and Graduate Studies	

Acknowledgements

I first have to thank Allah Almighty, for blessing me with strength, patience and ability to complete this thesis.

I would like to express my deepest appreciation to my advisor, Dr. Mohammad AlHamaydeh, for his outstanding guidance, motivation and for putting me in the right direction. Without his continuous support, encouragement and valuable contribution, this research would have not been possible. I consider Dr. AlHamaydeh as a mentor who significantly shaped my professional career.

Dedication

This thesis is dedicated to my father, who has always supported me, and to my mother who always dreamt of seeing me in highest positions. It is only with their love, support and prayers that I was able to finish this work successfully.

Abstract

During the last two decades or so, many iconic buildings have been built in Dubai as a result of the rapid economic growth. Unfortunately, several probabilistic seismic hazard studies are reporting substantially diverse estimates for Dubai seismicity. Additionally, the current minimum requirements of Dubai municipality are based on the 1997 Uniform Building Code (UBC'97) with a seismic zone that was recently upgraded following an earthquake in 2013. The aim of this research is to investigate and quantify the impact of the seismic design level on the structural performance and overall cost of contemporary RC Shear wall buildings in Dubai. Twelve reference buildings with heights varying from 6 to 12 stories are designed and detailed following 2012 International Building Code (IBC'12) standards. The buildings are designed with special/ordinary Reinforced Concrete (RC) shear walls for three seismicity levels representing the range of possible estimates in Dubai, namely the high, moderate and low estimates. The seismic performance of the reference buildings is evaluated using pseudo-static nonlinear (push-over) analysis as well as Incremental Dynamic Analysis (IDA). The nonlinear simulation is performed using fully detailed finite element models for the reference buildings. Construction cost and earthquake losses are evaluated and compared for the reference buildings in order to arrive at solid conclusions and sound recommendations. It is found that medium-rise and high-rise RC shear wall buildings are susceptible to significant higher-mode effects. Hence, the current design practice is recommended to account for and consider higher-mode effects and ultimately, trade-off between performance and cost. Furthermore, it is demonstrated that designing for a more conservative (high) seismic hazard level yields substantial enhancements in the overall structural performance. The resulting enhancements in seismic performance are found to outweigh the apparent increase in initial investment by significantly reducing repair and downtime costs. Finally, even when the use of ordinary RC shear walls is permitted by design code (at low seismicity levels), the utilization of special RC shear walls substantially improves the structural response. This structural response improvement is associated with marginal impact on initial investment and a noticeable reduction in repair and down time costs.

Search Terms: Dubai seismic hazard, RC shear walls, fragility analysis, seismic performance, seismic vulnerability, FEMA P695.

Table of Contents

List of Tables

List of Figures

List of Abbreviations

ACI - American Concrete Institute

ACMR - Adjusted Collapse Margin Ratio

AIBC - Abu Dhabi International Building Code

ASCE - American Society of Civil Engineers

CMR - Collapse Margin Ratio

CP - Collapse Prevention

DM - Damage Measure

DSN - Dubai Seismic Network

FEMA - Federal Emergency and Management Agency

GSHAP - Global Seismic Hazard Map Project

IBC - International Building Code

IDA - Incremental Dynamic Analysis

IM - Intensity Measure

IO - Immediate Occupancy

IRIS - Incorporated Research Institutions for Seismology

LFRS - Lateral Force Resisting System

LS - Life Safety

MCE - Maximum Considered Earthquake

MDFS – Multi-Degree of Freedom System

PBEE - Performance Based Earthquake Engineering

PBSD - Performance Based Seismic Design

PEER - Pacific Earthquake Engineering Research Centre

PGA - Peak Ground Acceleration

PGV - Peak Ground Velocity

PHM - Polygonal Hysteretic Model

RC - Reinforced Concrete

SEAOC - Structural Engineers Association of California

SELF - Static Equivalent Lateral Force

SF - Scaling Factor

SHM - Smooth Hysteretic Model

SMRF - Special Moment Resisting Frame

SPSW - Steel Plate Shear Walls

SSF - Spectral Shape Factor

THA - Time History Analysis

UBC - Uniform Building Code

USGS - United States Geological Survey

Chapter 1: Introduction

1.1 Introduction

The United Arab Emirates (UAE) in general, and specifically Dubai, has been undergoing vast economic development in the past two decades. The real estate sector in Dubai has experienced significant investments. As a result, many high rise and iconic buildings have been built to serve as touristic attractions and to accommodate the growing population. Furthermore, in November 2014, Dubai was chosen by the Bureau of International Expositions to host Expo 2020. This announcement significantly affected the real estate sector and the population growth in Dubai. As a result, substantial investments will be taking place to build new residential, commercial and hotel buildings to satisfy the increasing demand. Many of the challenges in the structures design phase come from the level of uncertainty in the assumed loadings, especially dynamic loadings, which have to be resisted by the structure during its service life. Lateral loads such as seismic forces generally exhibit highest degree of uncertainty among other loads. This region suffers from considerable uncertainty in its seismicity level and the design guidelines that should be followed. The seismic hazard of UAE in general and Dubai in specific has been the subject of many researches, such as [12] – [20]. However, unfortunately there is not much consensus in these researches about the seismicity levels that should be designed for in UAE. This could be attributed to the lack of in-depth seismological data and historical recordings of ground motions in this region that should be used in providing comprehensive seismic design guidelines [1]. Although the local authorities of Dubai have set minimum seismic design requirements, the set criteria are actually based on the 1997 Uniform Building Code (UBC'97) [2]. Therefore, the unprecedented growth in the number of buildings in Dubai combined with the lack of consensus on seismic design criteria complicate the vulnerability to earthquakes. It is generally believed that the UAE has low seismicity. Nevertheless, over the past few years, a significant number of regional seismic activities, originating from faults surrounding the UAE, has been recorded by Dubai Seismic Network (DSN) as presented in Figure 1. Additionally, Figure 2 shows some local seismic activities that were also recorded over the period from 2006 to 2014 by DSN. It is unquestionable that earthquakes, if not accounted for in design, could be devastating, and would definitely hinder the economic development of any country. For

instance, on 25 April, 2015 an earthquake with moment magnitude of 7.8 has struck Nepal causing significant damages, killing and injuring many people. The damages were not only restricted to Nepal where the earthquake originated from, but also many neighboring countries were affected, such as India, China and Bangladesh. Another recent earthquake with magnitude of 7.5 has struck north-east Afghanistan on 27th of October, 2015. It initiated landslides, collapsed many buildings and caused significant causalities in parts of both Afghanistan and Pakistan. The main point is that designing structures for seismic forces may or may not increase the initial construction cost, but it will definitely have a significant impact on the life cycle cost and downtime of the structure.

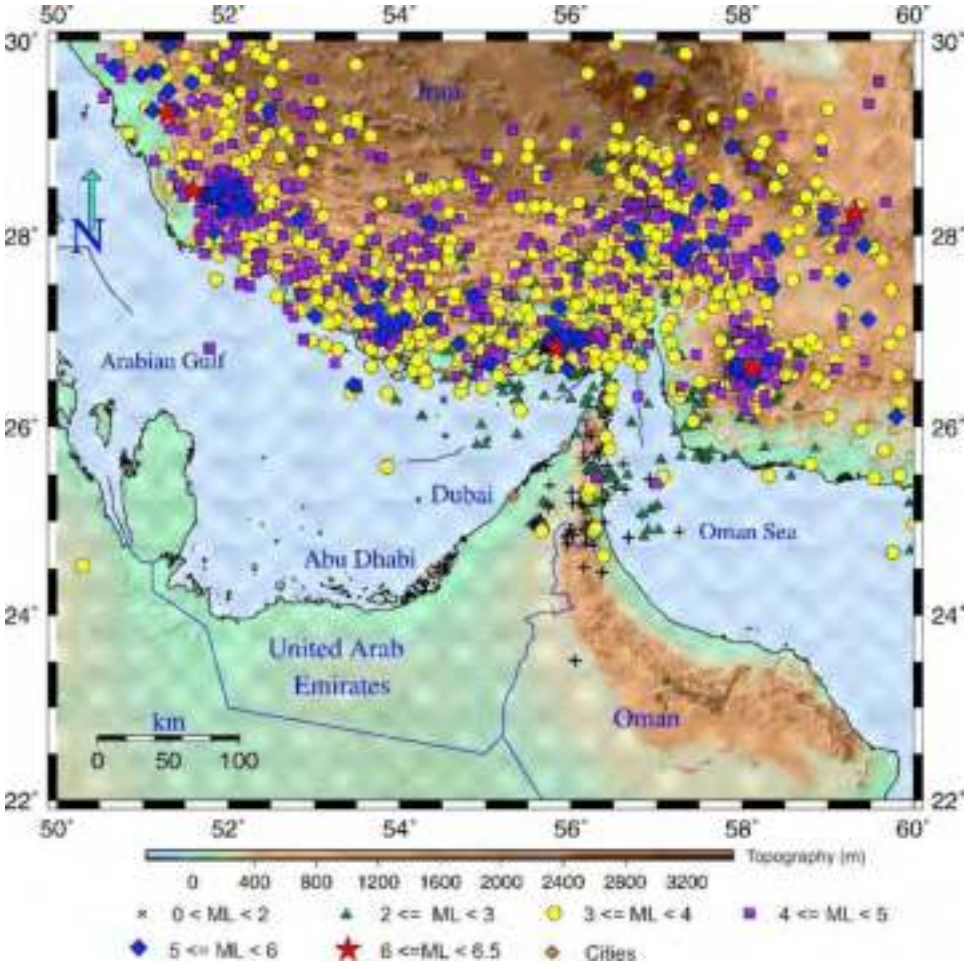

Figure 1: Regional Earthquakes Recorded by DSN [3]

Over the historical prism of the past 100 years, seismic structural analysis and design can be seen to be in constant evolution. It is important to shed light on the

evolving importance of Performance Based Seismic Designs (PBSD) which is the future of earthquake engineering. Following PBSD, the expected behavior of structures under seismic actions can be better understood. Furthermore, PBSD follows techniques that incorporate both geometric and materials nonlinearities such as pseudo static push over analysis, response spectrum analysis and Incremental Dynamic Analyses (IDA) [4]. Evaluating the seismic performance of structures provides engineers with a better understanding of the expected behavior under earthquake excitations. Moreover, it proactively highlights possible design deficiencies and can expect failure mechanisms due to seismic loads. This allows structures to be designed to satisfy pre-set seismic performance objectives rather than being designed following code requirements.

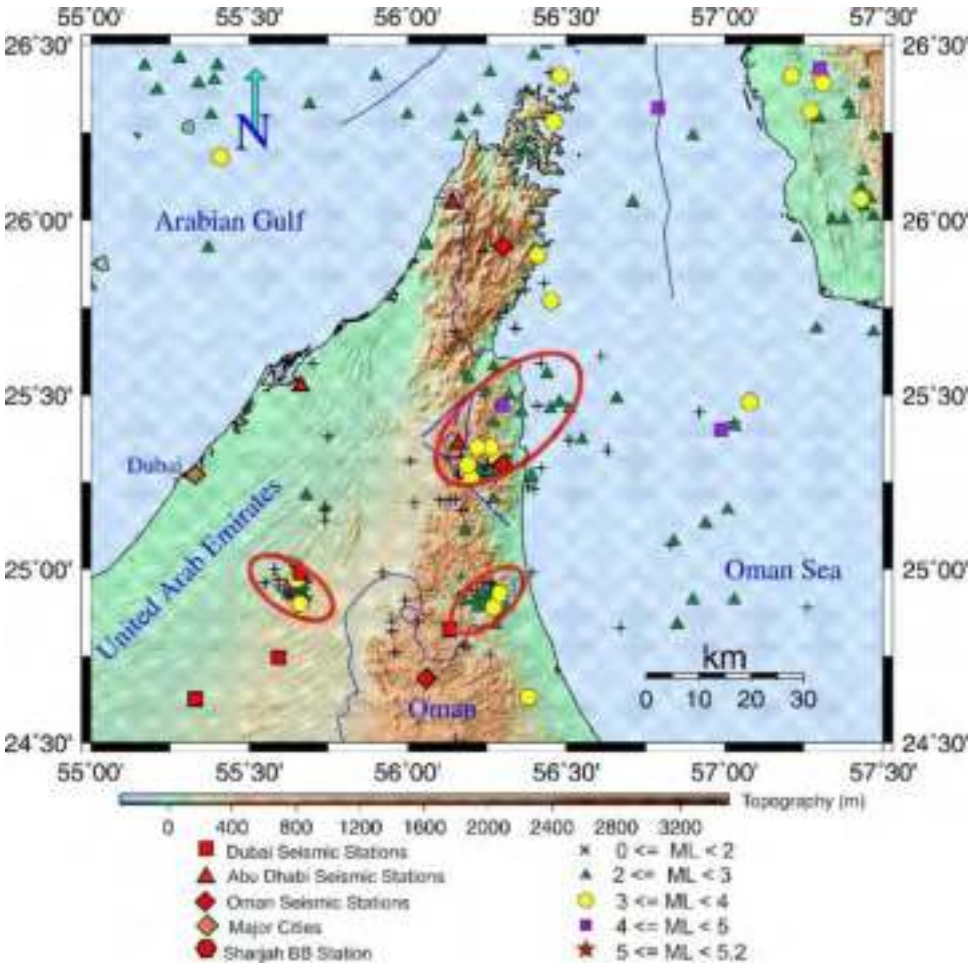

Figure 2: Local Seismicity Recorded by DSN [3]

This research investigates the impact of the seismicity hazard level on the performance, construction, repair and downtime costs of RC shear wall buildings in Dubai. Twelve RC shear wall buildings are designed and detailed following IBC'12 [5] standards. The buildings are 12-story, 9-story and 6-story. These buildings are designed for three different seismic levels representing the current estimated seismicity levels in Dubai, which are high, moderate and low. The different designs are compared based on their design detailing, seismic performance construction and repair costs in order to investigate and quantify the impact of the diverse seismic hazard levels in Dubai.

1.2 Problem Statement

Due to the lack of consensus among the seismic hazard studies for Dubai, it is a quite challenging task for the design firms to pick the design level had they been given the choice. Additionally, the local authorities provide minimum requirements that should be followed based on the UBC'97 code. Furthermore, the municipality has been proactive in adapting to tremors that were felt and measured in UAE in 2013 by raising their minimum requirement to zone 2B for buildings higher than nine stories and 2A for buildings between four to nine stories. Some of the main consequences of the seismic hazard level on the design is the choice of the lateral force resisting system, its detailing requirements, and the implications on construction and repair costs. It is always very crucial to propose designs for structures that are not only economical, but also safe in the short and long runs. The objective of this research is to quantify the impact of the diverse estimated seismicity levels in Dubai on the seismic performance, construction and repair costs of RC shear wall buildings. It was decided to investigate this problem specifically in Dubai due to its rapid economic development and being the business capital of UAE. Additionally, 12-story, 9-story and 6-story RC buildings with shear walls were chosen to target the main sectors of buildings inventory representing the common practice in Dubai.

1.3 Research Significance

This research gains its importance from the fact that there is no clear agreement among all the seismic hazard studies conducted to examine the seismicity hazard level

in Dubai. The diversity in the seismic hazard estimates for Dubai combined with the surrounding seismic activities mandates paying attention to the followed seismic design criteria for buildings. In addition to that, it is usually believed that designing for higher seismic levels will probably yield structures that are considered uneconomical. The proposed research will investigate the consequences of designing RC shear wall buildings for different seismic levels in Dubai. Furthermore, it will provide an insight into the actual impacts of the seismic design level on the design details, seismic performance, construction, repairs and downtime costs. Moreover, it will quantify the effects of using special RC shear walls versus using ordinary RC shear walls for the different estimated seismic levels. Finally, this research once completed is expected to provide a rational guidance for designers and decision makers in choosing the level of detailing in lateral force resisting systems, the design guidelines and criteria for buildings in Dubai.

1.4 Objectives and Scope

The main objectives of this thesis are:

- To investigate the effect of the diverse seismic hazard levels on the design of RC shear wall buildings in Dubai.
- To quantify the impact of the seismic hazard level and buildings' height on the design detailing, construction cost and seismic performance.
- Develop possible recommendations for seismic design criteria in Dubai.

This research is targeting the main inventory of buildings in Dubai having 6 to 12 stories. It is limited to buildings having RC shear walls as their lateral force resisting systems. The reference buildings used in this research have a typical floor and do not have any structural irregularities as defined in IBC'12 [5]. They are designed and detailed for three different seismic levels (high, moderate and low). Furthermore, the seismic performance of the designs is investigated using two types of nonlinear analyses; static and dynamic. The nonlinear analyses are done using a fully detailed fiber model with concentrated plasticity incorporating geometric and material nonlinearities. Furthermore, the Pseudo static push over analysis is displacement controlled and done using linear displacement profile. The IDA is done using a suite of

22 far-field earthquake records specified in FEMA P-695 [6] and obtained from Pacific Earthquake Engineering Research Centre (PEER) NGA database [7]. These records are scaled following FEMA P-695 [6] procedure to match the response spectrum of the highest seismicity estimates in Dubai.

1.5 Methodology

In this research, an extensive review of the literature available about Dubai seismicity, effects of seismicity and performance based earthquake engineering is done. The aim is to quantify the impact of the diverse seismic hazard estimates in Dubai. To achieve that, a total of twelve reference buildings with 12-story, 9-story and 6-story are designed. Each type of building is designed and detailed for the three seismic levels (high, Moderate and Low) with special RC shear walls. However, for the lowest seismic level, the buildings are designed using ordinary RC shear walls and special RC shear walls. The design is done in accordance with the IBC'12 standards [5]. Moreover, the buildings are analyzed and designed to limit their inter-story drift within specified code limits using ETABS commercial package [8]. The design of gravity system is done using spreadsheets and the strength design of the shear walls is done using Quick Concrete Wall program [9]. It should be noted that the gravity system is only designed to resist vertical loads in addition to the deformations compatibility requirements. The quantities of materials are calculated to approximate the construction and repair costs of each building. Furthermore, the buildings' performance is investigated with nonlinear analyses using IDARC-2D [10], which is a software developed at the state University of New York - Buffalo, to perform seismic inelastic analysis of structures [10]. The nonlinear analysis model will be verified by comparing its elastic dynamic characteristics to those obtained from ETABS. Further verifications are done by comparing the nonlinear behavior against available experimental data in the literature. Although the tallest building is only 12-storey, P-Delta effects are included in all buildings since the lateral system is on the perimeter and the highest vertical loads are on the gravity system. The P-Delta effects are included by explicitly modeling the gravity system and pinning the base of columns to represent the assumption that these columns are designed to mainly resist vertical loads. The seismic performance of the buildings is investigated using nonlinear analyses, such as nonlinear pseudo-static

(push over) analysis and nonlinear IDA. Using the Push over analysis and IDA results, capacity curves, IDA curves and fragility curves are produced for the buildings to draw conclusions about the impact of the seismic design level on the seismic performance. Finally, the mean damage state of the buildings at each performance level is used to quantify the amount of losses and to approximate the maintenance and downtime cost.

1.6 Thesis Organization

This thesis is divided into six chapters.

- **Chapter 1: Introduction.** Presents a general introduction of the research background, importance, and its main objectives.
- **Chapter 2: Literature Review.** Provides an extensive overview of the significant seismic hazard studies produced for Dubai. Furthermore, it summarizes some of the previous research findings about the impact of seismicity on design of buildings in Dubai. It presents a brief description of performance based earthquake engineering and its applications.
- **Chapter 3: Buildings Description and Design.** Gives detailed description of the reference buildings used in this research. It summarizes the structural design and details of the different elements in the buildings.
- **Chapter 4: Buildings Seismic Performance Investigation.** Covers the implemented nonlinear analyses assumptions and the results of the performance investigations for the different seismic design levels. It also provides a comparison between the resulting seismic performance for seismicity level-to-level and building-to-building.
- **Chapter 5: Buildings Construction and Maintenance Cost Comparison.** Quantifies the impact of the design seismicity level and performance objectives on construction and repair costs.
- **Chapter 6. Conclusions and Recommendations.** Summarizes the main outcomes, provides recommendations based on the findings and suggests promising extensions.

Chapter 2: Literature Review

2.1 Dubai Seismicity

The level of seismicity in Dubai is not clearly set since there is no strong consensus among researchers about the exact seismic level of UAE or Dubai. However, the number of earthquakes occurring in or close to the UAE has been increasing since 1924 – 2006. Seismicity of the UAE is generally attributed to earthquakes originating from seismic sources that are nearby and remote [11]. Furthermore, the level of seismic activities in the UAE, specifically in Dubai, has been the driving factor for many researches since 1990. Although major seismic activities are rare in the UAE, numerous studies have been conducted in an attempt to provide a clear picture regarding the seismic hazards in Dubai [1]. In general, the available seismic hazard studies show significant diversity in estimating the seismicity hazard of Dubai.

In December 1999, the seismic hazard of Dubai and Abu Dhabi was assessed as a part of the Global Seismic Hazard Map Project (GSHAP). The GSHAP provided Peak Ground Acceleration (PGA) values that correspond to 475 years return period for Europe, Africa and the Middle East. The PGA values that GSHAP provided for Dubai and Abu Dhabi were 0.32g and 0.24g respectively [12]. These values were considered very high and were not based on a specific study of the seismic hazard in UAE that takes in consideration the effects of UAE local seismicity [13].

A specific seismic hazard study was conducted for UAE and nearby countries in 2004 by Abdalla and Al Homoud [14]. Their study incorporated a probabilistic methodology in studying the seismic hazards in UAE. The authors also stated that PGA produced by GSHAP [12] for UAE is highly conservative and was not supported by strong scientific study. The seismicity of UAE is mainly affected by earthquakes originating from both the Zagros fold and thrust belt and the western part of the Makran subduction zone. In fact, the Zagros fold is the second highest seismic active source in Iran while there is no major earthquake activities originating from the western Makran subduction zone [14]. The study used Zagros thrust attenuation equations and was based on assuming bed rock conditions for the sites covered in the study. It produced PGA maps for UAE and nearby countries with 10% probability of being exceeded in 50 and 100 years. Furthermore, it generated a seismic zoning map that is applicable for several

building codes, such as the 1997 Uniform Building Code (UBC97') for the same area. It estimated a PGA, based on 475 years return period, of 0.15g for Dubai [14].

In 2006, Sigbjornsson and Elnashai [15] provided a seismic hazard study specifically for Dubai, UAE. In their investigation they focused on providing a comprehensive seismic study for Dubai compatible with latest requirements for seismic design. Additionally, they shed the light on the significant impact of dual earthquake situations from both distant and local sources. Furthermore, the study implemented the latest available earthquake data to perform the probabilistic seismic hazard assessment for Dubai. The estimated PGA for Dubai was 0.16g corresponding to 10% probability of exceedance and 0.22g for 2% exceedance probability. The given PGA values were evaluated taking into consideration the existence of the west coast fault as a source of seismic activities that has an impact on Dubai [15].

In 2008, Abdalla et al. [16] investigated the impact of the November 27th , 2005 earthquake that was generated from Qeshm island, Iran. The study highlights that UAE, and particularly Dubai is susceptible to long period earthquakes from Iran that will have a significant impact on high rise buildings especially those built on soft or reclaimed soils [16]. The recorded earthquake had a 6.2 body wave magnitude, 10km focal depth and 185Km epicentral distance to Dubai, UAE. The authors stated that high rise buildings in Dubai were the most significantly affected structures by the event. This is attributed to their flexibility and the amplification from the soft local site conditions as well as their deep foundation systems [16]. The Study was concluded with emphasis on the increased seismicity from distant sources affecting Dubai especially the Makran subduction zone and Zagros thrust fault. Finally, it recommended the installation of earthquake monitoring devices on important skyscrapers and called for the development of national seismic design code [16].

UAE seismic hazard is affected by both earthquakes originating from local as well as distant sources [15] , [17]. In addition to the large magnitude earthquakes originating from Zagros fault or Makran subduction zone, the north eastern part of UAE exhibits moderate level of seismicity and might be a source of future moderate magnitude events. For example, on March 10, 2007 two moderate earthquakes took place in the eastern part of UAE [17]. The two events were recorded by Dubai broadband stations and were used to study the seismicity of the eastern part. It was

mainly used to investigate the source parameters, focal depth and mechanisms. The two events had 3.66 and 3.94 moment magnitudes and no structural damage was reported. However, these events resulted in significant shaking that alarmed residents in northern parts of UAE and Oman [17]. Such moderate events are not expected to cause that level of shaking. This case could be attributed to the magnification of ground motion that took place in the sedimentary deposits soil that is beneath many high rise buildings located close to the shore in UAE [17]. The focal mechanism of these two events was approximated using waveform inversion and compression wave polarity as normal fault with minor right-lateral strike. These recorded earthquakes have raised awareness that the region might be susceptible to damaging events and that a better understanding of the region tectonics and seismic hazard is urgently needed [17].

In 2008, Barakat et al. [18] reported a comparative earthquake risk assessment approach applied to the UAE. The vast development in UAE and the major investments in high rise buildings increased its vulnerability to earthquakes. In addition, UAE holds a unique location opposite to the subduction boundary [18]. Historically, the UAE was thought of as a place with very low seismicity until an earthquake with body wave magnitude of 5 happened in Masafi in 2002 and other smaller magnitude earthquakes were recorded in several locations. This created a shift in the view of UAE seismicity that a moderate seismic activity might be present [18]. There are several sources that contribute towards the claimed seismicity in UAE. Additionally, there are several faults that were mapped intersecting UAE, and its seismic activity level is not known [18]. For instance, Zagros thrust belts affects UAE seismicity and is considered to be one of the most active seismic sources in the world. Furthermore, the UAE territory makes it close to the Arabian plate boundary where significant stresses are accumulated. Another possible source is the oceanic crust in Makran subduction zone which is a very active zone for strong ground motions. The authors of that study noted that despite the vast development occurring in UAE, many high rise building were not designed following proper seismic design guidelines. Moreover, the developed codes and guidelines are not based on a thorough study of the possible seismic hazard in UAE [18].

In 2008, a comprehensive seismic hazard assessment for the Arabian Peninsula region was conducted by Pascucci et al. [19]. The authors stated that Dubai and Abu Dhabi were classified by the UBC'97[2] and other researches to be in zone 0 with no

requirements for seismic design. However, after Masafi earthquake in 2002 and the GSHAP map, it became necessary to revisit this classification.

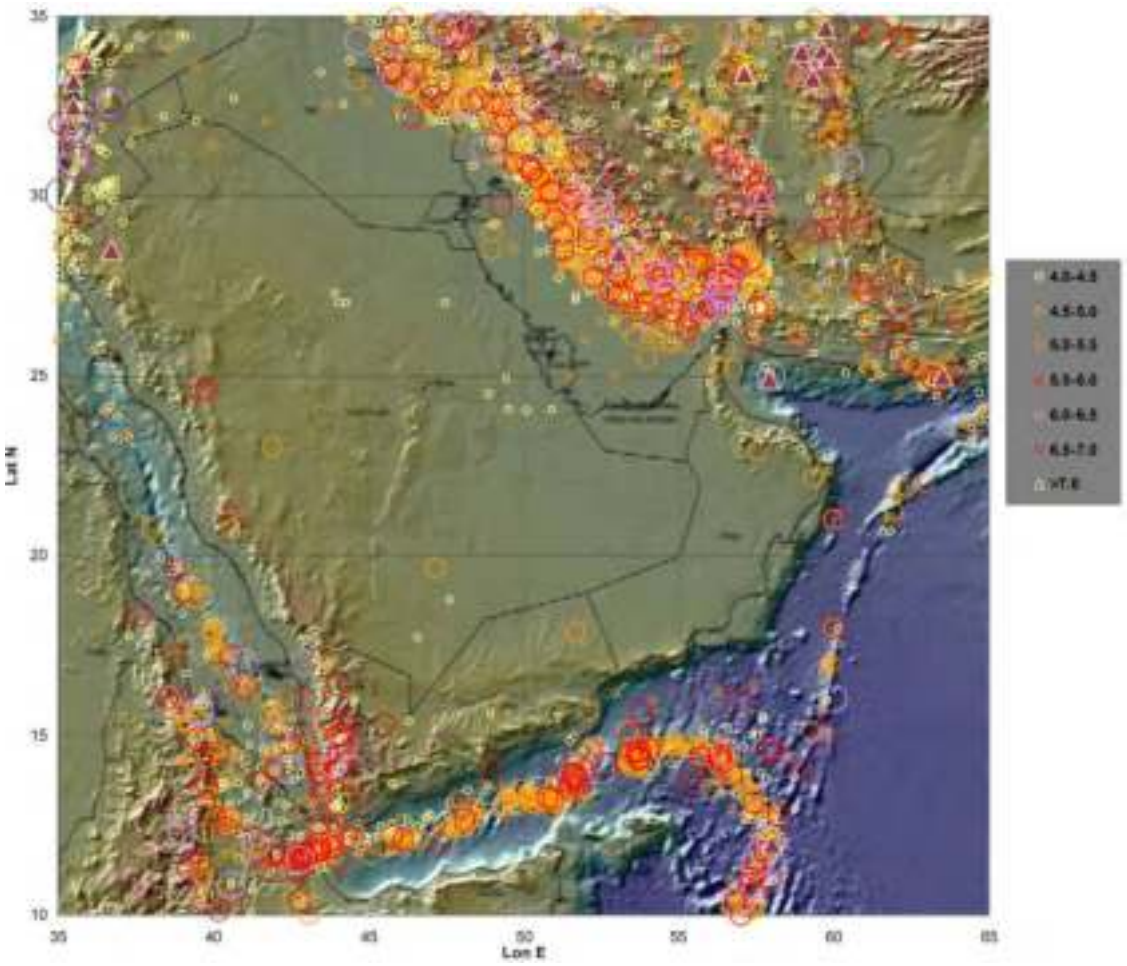

Figure 3: Earthquake Catalogue for Arabian Peninsula by Pascucci et al. [19]

Moreover, there is no unified seismic design code that is applicable for structures in the Arabian Peninsula region. For instance, Dubai local authorities require applying zone 2A according to UBC'97 [2] for buildings that have more than four stories and 2B for buildings with more than nine stories, while Abu Dhabi municipality has adapted IBC. In this study, the authors used appropriate attenuation functions relative to the tectonic features of each source zone, such as the next generation attenuation equation for sources characterized by shallow crustal earthquakes, to provide ground motion parameters for the Arabian Peninsula region. Although the Arabian plate is considered stable, it is surrounded by very active source zones such as the Markan subduction zone and Zagros fold belt [19]. The results of this seismic hazard assessment was presented in terms of PGAs and uniform hazard response spectrums for 2% and 10%exceedance

probability in 50 years. Furthermore, the authors assembled an earthquake catalogue that spans the region back for 2000 years. Figure 3 shows the earthquake catalogue which presents a clear image of the significant amount of earthquake events taking place around the Arabian plate boundaries. The scale on the right of the catalogue represents the moment magnitude of the recorded events.

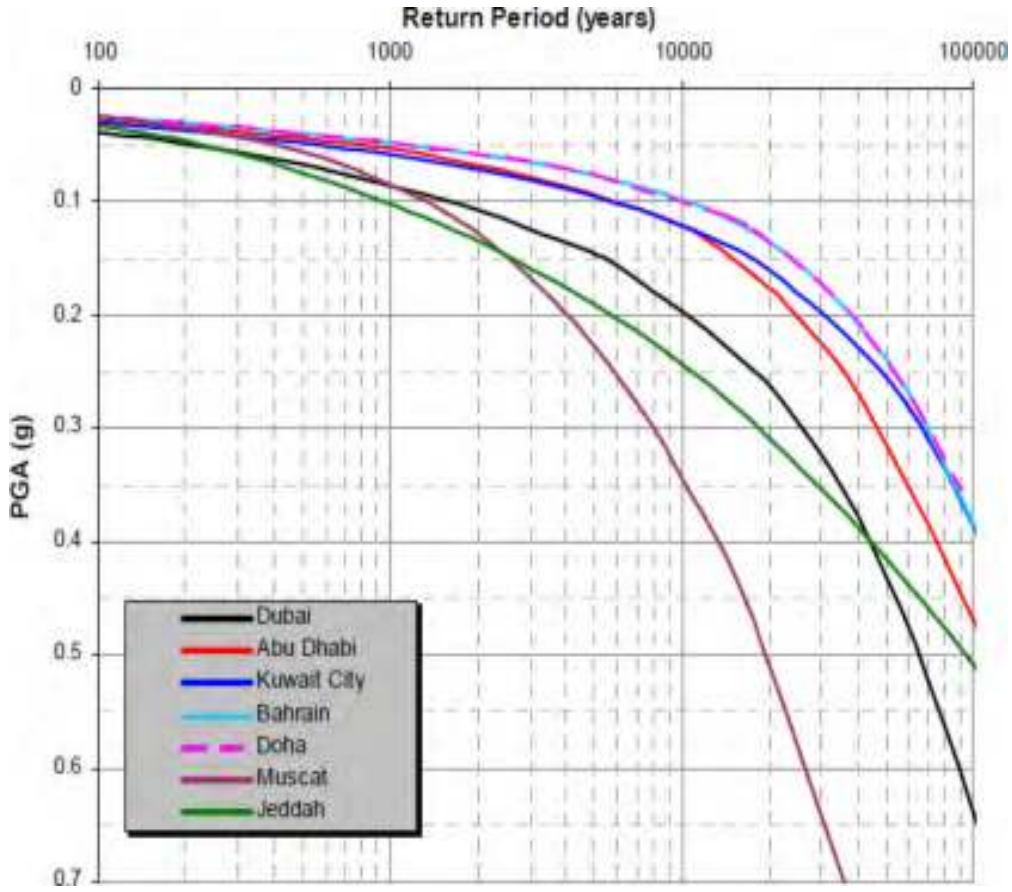

Figure 4: PGA for Rock Sites by Pascucci et al. [19]

The peak ground acceleration and spectral accelerations for major cities in the Arabian Peninsula are summarized in Figure 4 and Table 1 [19].

Table 1: Spectral Accelerations for Major Cities in Arabian Peninsula by Pascucci et al. [19]

Location	PGA (g)		0.2s SA (g)		1.0s SA (g)		2.0s SA (g)	
	475year	2475year	475year	2475year	475year	2475year	475year	2475year
Dubai	0.06	0.11	0.160	0.277	0.056	0.097	0.022	0.041
Abu Dhabi	0.04	0.07	0.102	0.173	0.039	0.068	0.015	0.028
Kuwait City	0.05	0.08	0.113	0.186	0.044	0.070	0.017	0.028
Bahrain	0.04	0.06	0.092	0.149	0.037	0.057	0.013	0.023
Doha	0.04	0.06	0.090	0.145	0.045	0.056	0.013	0.022
Muscat	0.05	0.15	0.125	0.338	0.045	0.118	0.017	0.054
Jeddah	0.07	0.15	0.182	0.374	0.041	0.102	0.020	0.049

Aldama et al. [13] provided a probabilistic seismic hazard assessment study for Abu Dhabi, Dubai and Ras Al Khaimah in 2009. In their study, the authors examined the amount of diversity in the results of the seismic hazard assessment studies for the UAE and Arabian Peninsula. Furthermore, they noted that there are no less than seven hazard studies that have been published showing a wide range of PGAs for 475 years return period ranging from 0.05g to 0.16g [13]. Additionally, it was mentioned that Dubai and Abu Dhabi were classified as per UBC'97 [2] to be in zone 0 with no seismic requirements. As a result of the substantial amount of development in the construction sector, the municipalities have raised their requirements for buildings more than five stories to zone 2A. The study started with a detailed review of the UAE tectonics and the major seismic source zones as shown in Figure 5. Furthermore, the authors highlighted the uncertainties in previous hazard studies in terms of source zones, recurrence parameters and ground motion prediction equations. They have used 20 source zones presented in Figure 6 with logic-tree frame-work in their probabilistic hazard assessment study. The results of this study were presented in form of uniform hazard response spectra as well as hazard curves for rock sites in Abu Dhabi, Dubai and Ras Al Khaimah. The conclusion of this study supports UBC'97 classification of Dubai as zone 0 without any seismic design requirements [13].

Figure 5: UAE Tectonics Settings by Aldama et al. [13]

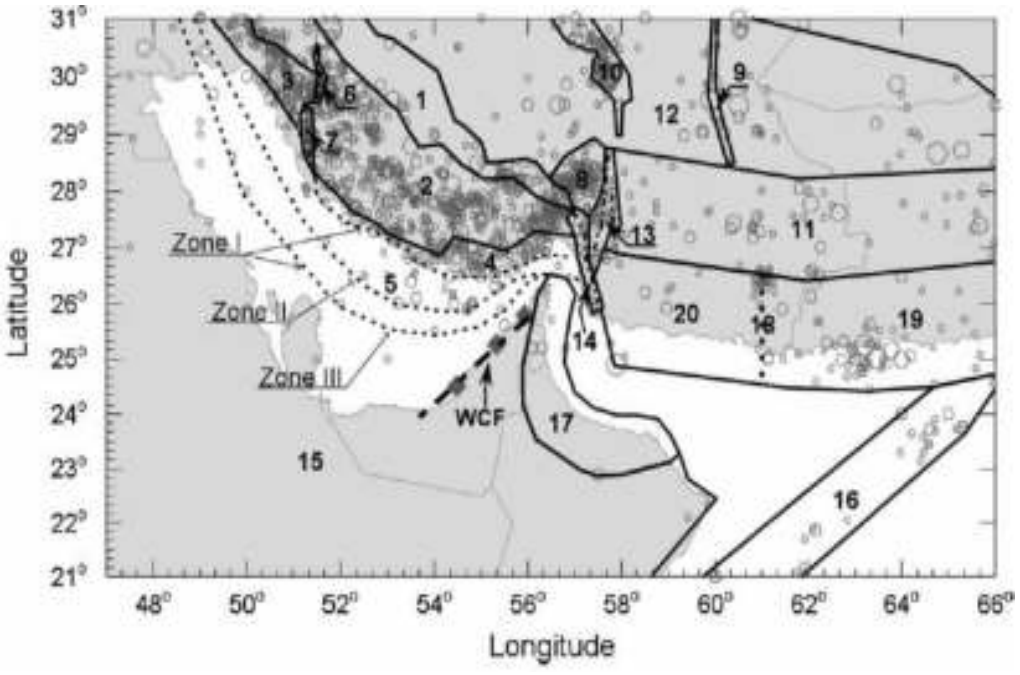

Figure 6: Seismic Source Zones for Aldama et al. Study [13]

One of the more recent probabilistic seismic hazard assessments was done in 2011 for a specific site near Dubai creek by Shama [20]. The study considered all possible seismic source zones affecting Dubai which were:

1- Zagros fold-thrust region.
2- Makran subduction zone.
3- Zendan-Minab-Palami fault system.
4- Local crustal faults in UAE, such as Dibba, Wadi El Fay, Wadi Ham, Wadi-Shimal, Oman and West Coast fault.

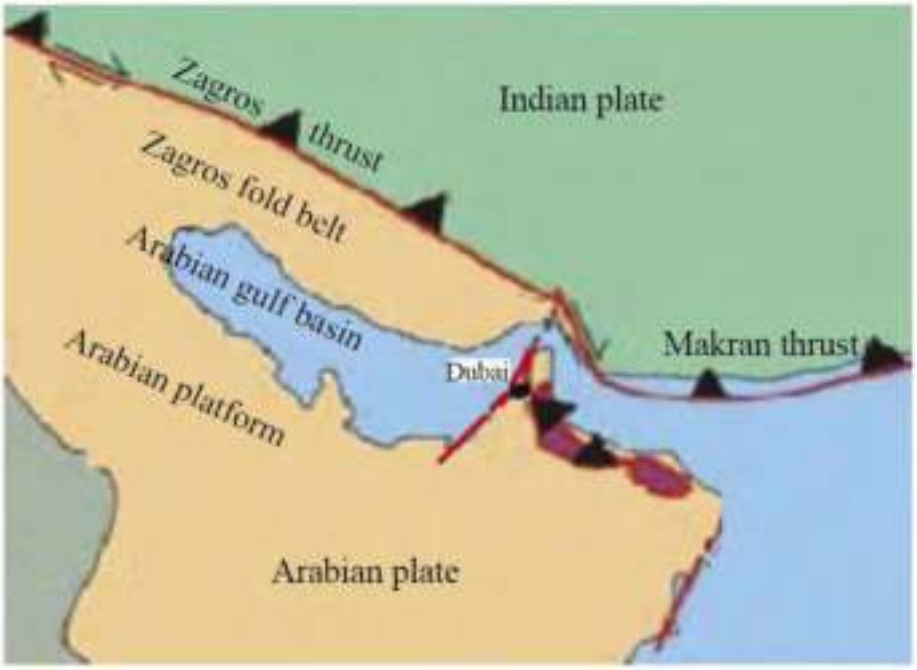

Figure 7: Seismic Source Zones Used by Shama for Dubai [20]

The seismic source zones were mapped as shown in Figure 7. Furthermore, due to the absence of specific attenuation relations for UAE, the author used relations from earthquake records having similar attenuation features to those affecting Dubai. Additionally, the earthquakes catalogue implemented in this study was obtained from Incorporated Research Institutions for Seismology (IRIS) database [21]. Using logic-trees to reduce uncertainties, the author has produced higher PGAs for Dubai compared to previous hazard studies. It was concluded that Dubai has PGA of 0.17g for 475years return period and 0.33g for 2475year return period. The resulting spectrums are shown in Figure 8 [20]. The author highlighted that the seismic hazard of Dubai was governed

by local faults, especially the west coast fault. He recommended the need for further investigation about the seismicity of west coast fault and other local faults in UAE [20].

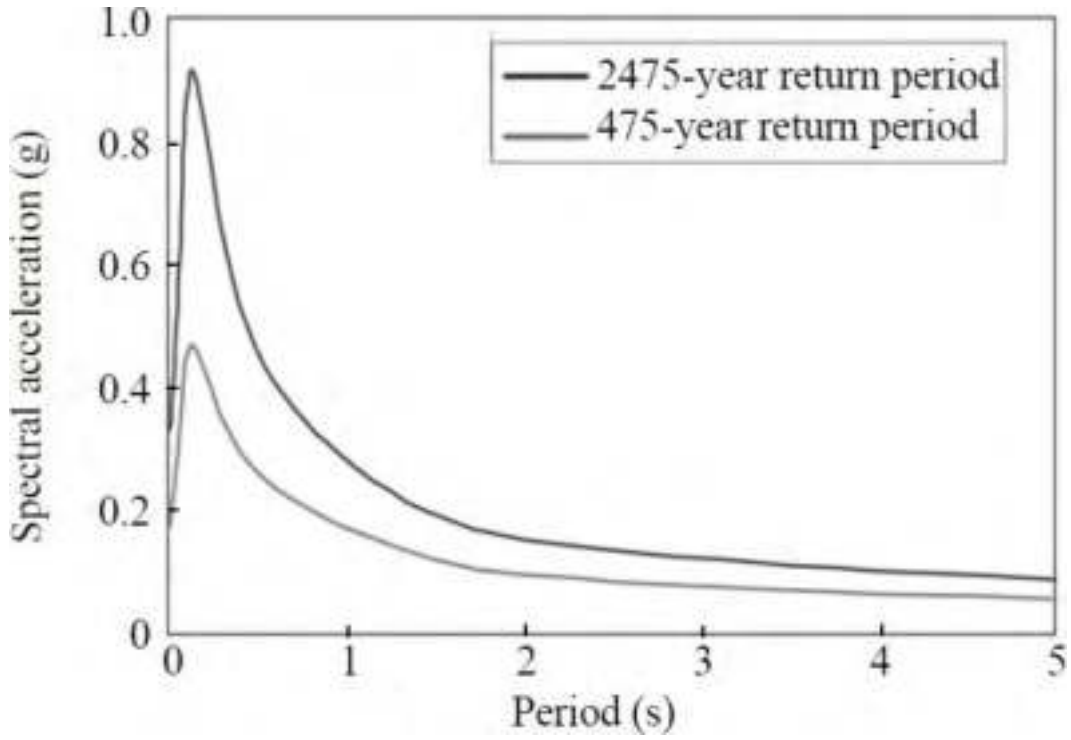

Figure 8: Uniform Hazard Response Spectrum for Dubai by Shama [20]

The latest seismic hazard study for UAE available to the author during this research was published in 2013 by Khan et al. [22]. The study provided a comprehensive probabilistic seismic hazard assessment and spectral accelerations for the entire UAE. Furthermore, it implemented a standardized earthquakes catalogue for UAE compiled from United States Geological Survey (USGS) [23], National Geosciences of Iran [24] and the National Center of Meteorology and Seismology of UAE (NCMS) [25] that dates back to 110 years. Figure 9 shows the used earthquake catalogue.

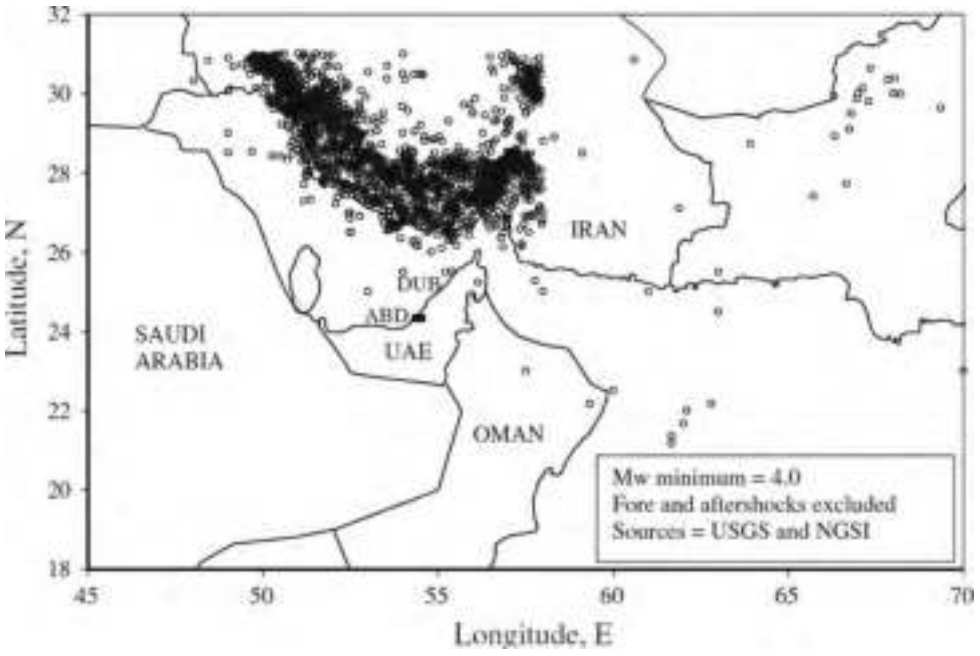

Figure 9: Earthquake Catalogue for UAE by Khan et al. [22]

Furthermore, the authors have used seven different ground motion prediction equations incorporating three next generation attenuation equations due to the lack of specific equations for UAE. The seismic source zones included in this study are shown in Figure 10. Finally, the study was concluded with producing contour seismic hazard maps for UAE with PGAs, short and long period spectral accelerations and uniform hazard spectra corresponding to 2% probability of being exceeded in 50 years which complies with latest building codes. For Dubai corresponding to 2475years return period, the recommended PGA was 0.12g, spectral acceleration at 0.2 sec. was 0.25g and spectral acceleration at 1 sec. was 0.1g [22].

Reviewing the previous probabilistic seismic hazard studies conducted for UAE and Dubai, it is clearly noted that there are significant variations in the estimated seismicity levels. In fact, results vary from no seismic hazard to very high seismicity as shown in Table 2. This is attributed to the differences in the used source zonation, recurrence parameters, earthquake catalogues and ground motion prediction equations. The differences are mainly due to the lack of detailed seismological measurement and data in this region and such data is required to provide a comprehensive and sound seismic hazard study [1].

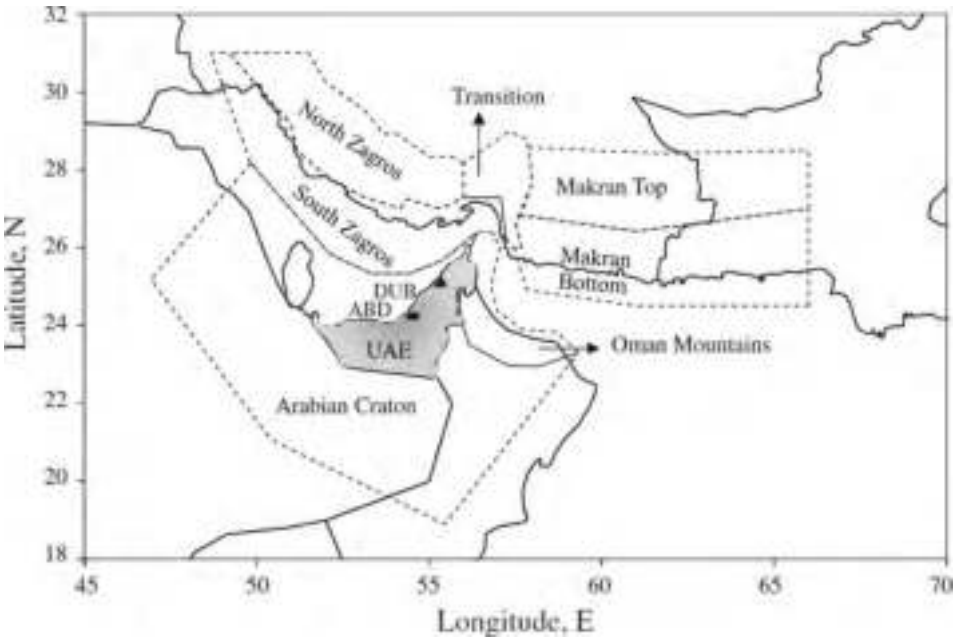

Figure 10: Seismic Source Zones implemented in Khan et al. Study [22]

Table 2: PGA for Dubai from Several Hazard Studies [22]

Study	PGA (return period = 475 years) (g)
Al-Haddad et al. (1994)	<0.05
Grunthel et al. (1999)	0.32
Abdalla and Al Homoud (2004)	0.14
Sigbjornsson and Elnashai (2006)	0.16
Peiris et al. (2006)	0.06
Musson et al. (2006)	0.05
Aldama-Bustos et al. (2009)	<0.05
Shama (2011)	0.17

In 2006 Dubai Municipality has initiated Dubai Seismic Network (DSN) with four remote seismic stations intended to monitor local and distant seismic sources that might affect Dubai Seismicity [26]. This network was upgraded in 2012 with five strong motion stations placed in areas closer to Dubai [26]. Furthermore, the recordings by DSN for the period from 2006 to 2013 suggest three local seismicity clusters affecting Dubai which are; (1) Masafi-Bani Hamid, (2) Northern Huwaylat and (3) Wadi-Nazwa as shown in Figure 11. The establishment of DSN shows that Dubai Seismicity is not

only a concern to researchers but it also shows the efforts of local authorities in mitigating possible hazards.

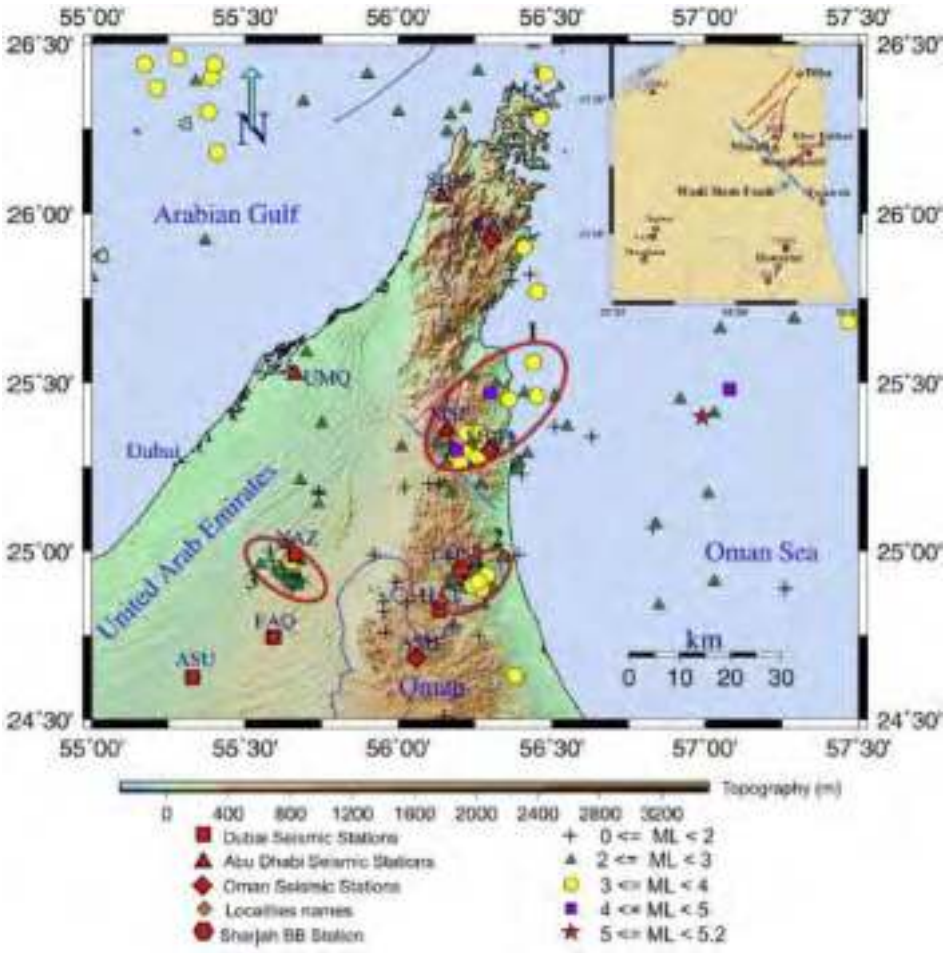

Figure 11: Local Seismic Sources Recorded by DSN [26]

2.2 Effects of Seismicity on Design of Buildings in Dubai

As a result of the diverse estimates of Dubai Seismic hazard, several researches have been conducted to examine the implications of the different hazard estimates on design of buildings in Dubai. For instance in 2011, AlHamaydeh et al. [27] studied the seismic design factors for RC special moment resisting frames in Dubai, UAE. This research study assessed the Response Modification Factor (R), Deflection Amplification Factor (C_d) and the System Over-strength Factor (Ω_o) defined in the International Building Code (IBC'09) for three buildings designed in Dubai. The buildings were four, sixteen and thirty two stories. The authors utilized non-linear

analyses, such as pseudo static and incremental dynamic, with two sets of ground motion corresponding to 475 and 2475 return periods to quantify the seismic response factors of the buildings. It was concluded that the seismic design levels had a great impact on the seismic response factors for RC special moment resisting frames buildings. Furthermore, the study highlighted the effect of the buildings' natural time period on the response factors. It was noted that the increase in the natural period of the structure was associated with substantial reduction in the response modification factor (R). Based on their findings, the authors advised a resolution to the diverse estimates of Dubai seismicity and recommended a period dependent response modification factor (R) and deflection amplification factor (C_d) [27].

Another example of the impact of the controversial seismicity estimates in UAE is the research by Mwafy in 2011 [11]. In this research the author investigated the seismic design response factors for high-rise buildings with RC shear walls located in UAE. It was highlighted that due to the increased concern about UAE seismicity and the implementation of IBC'09 in Abu Dhabi, there is a necessity for studying the seismic design factors based on standard procedures. To achieve the objective of verifying the seismic design response factors for high-rise RC shear wall buildings in UAE, five buildings with stories varying from 20 to 60 were designed following UBC'97 zone 2A seismic design requirements. The response factors R, Ω_o and C_d for the buildings were inspected using inelastic push-over analysis and incremental dynamic collapse analysis. It was found that the initial stiffness and lateral capacity of the buildings can be conservatively approximated using push-over analysis with uniform loading profile. Furthermore, the over-strength factor (Ω_o) was estimated using push-over analysis and the results were verified by the incremental dynamic analysis. It was noted that Ω_o values exhibit inverse relationship with the fundamental time period of structures and the IBC'09 values are considered conservative estimates. Nevertheless, it was recommended to possibly increase the over-strength by approximately 20% for buildings with 20-stories or lesser. Additionally, incremental dynamic analysis was performed employing two groups of ground motion records, 10 natural and 10 artificial acceleration records, representing events from both local and distant sources. The results were used to verify Ω_o factor and to estimate Rand C_d. It was also concluded that the code values are conservative for the response reduction factor as well as the deflection amplification factor. However, incremental dynamic

analysis results suggested higher values for the over-strength factor compared to the results obtained from the inelastic push-over analysis [11].

In 2012, AlHamaydeh et al. [28] provided a quantifiable evaluation for four different lateral force resisting systems that can be applied for tall buildings in Dubai without any restrictions on their height for seismic design category D as per IBC'09. This research study was driven by the diversity in seismic hazard assessment results in Dubai. Therefore, the authors used the conservative seismic hazard estimate by Sigbjornsson and Elnashai in 2006 [15] to design four buildings with different lateral force resisting systems and construction materials according to IBC'09 requirements. Furthermore, the proposed buildings were 20-story RC building with Special Moment Resisting Frames (SMRF), 20-story RC building with dual system (SMRF with Special Shear Wall), 20-story steel building with Special Moment Resisting Frames (SMRF), and 20-story steel building with dual system (SMRF with Special Steel Plate Shear Wall). It was concluded that buildings with dual systems will have marginally higher weights which will not considerably affect their construction cost. Nevertheless, the steel buildings had the lightest weight but were expected to have higher construction cost due to the skilled labor requirements. Finally, stiffer systems such as the dual systems will be subjected to higher accelerations and forces compared to softer system such as the SMRF which will exhibit higher drift and inelastic damage when subjected to earthquake events [28].

More recently in 2013 the performance and cost of tall buildings with different lateral systems in Dubai were quantified by AlHamaydeh et al. [1]. The study considered four practical lateral force resisting systems that can be used in Dubai, which are Concrete SMRF, Steel SMRF, Concrete Dual System (SMRF with Special Shear wall), and Steel Dual System (SMRF with Special Steel Plate Shear Wall). It quantified the seismic performance and construction cost of the four lateral system. The authors of the study highlighted the urgent need for consensus regarding the UAE seismic hazard. Furthermore, they noted that the variations in UAE seismic hazard estimates are due to lack of in -depth seismological data and measurements. The buildings considered in this study were 20-story buildings designed as per IBC'12 requirements for seismic design category D as suggested in Dubai seismic hazard study by Sigbjornsson and Elnashai in 2006 [15]. Moreover, the buildings' performance was investigated using linear elastic Time History Analysis (THA). The THA was done

using 22-Farfield earthquake records specified in FEMA-P695[6] and scaled according to ASCE7-10 [29] guidelines. The THA results showed that the four systems are having acceptable levels of performance between Immediate Occupancy (IO) Life Safety (LS). Additionally, it was concluded that the SMRF systems have higher inter-story drift compared to the dual systems and hence it is expected to have more damage. The steel dual system is expected to have the best performance with respect to inter-story drift. However, the steel systems were estimated to have higher initial construction cost compared to the concrete systems, but faster revenue generation due to their shorter construction duration. The conclusions of this study serve as guidelines for designers and developers to choose the suitable lateral force resisting system based on their preferred selection criteria [1].

2.3 Performance Based Earthquake Engineering

Performance Based Earthquake Engineering (PBEE) is the promising future of seismic design and evaluation of structures. Generally, most advances in earthquake engineering arise as a result of lessons learned from severe and damaging earthquakes. The earliest version of PBEE came in the 90s as a response to the lack of code design guidelines that are applicable to existing buildings. In addition, after Northridge earthquake in 1994, it was very clear that significant damages might happen to code compliant structures. This raised the awareness that damages that might happen to structures designed satisfying code requirements might not be acceptable to the society expectations [30]. PBEE aims in making a complete shift in traditional design approaches. It suggests designing, evaluating and constructing structures that satisfy a pre-set performance objectives that meet owners and society needs. Several publications presented an outline for the PBEE procedures, such as SEAOC Vision 2000 [31], ATC 40 [32] and FEMA 273 [33]. The intent of ATC 40 and FEMA 273 was to provide guidelines for the application of PBSD in evaluating and retrofitting existing buildings. The outlined framework for PBEE in these documents did not differ in concept, only the details were different [34]. Furthermore, PEER has developed a systematic global framework for second generation PBEE. As shown in Figure 12, PEER PBEE proposed framework is based on four stages; hazard estimation, structural analysis, damage analysis and finally loss assessment. Furthermore, a more recent publication which outlines the next generation PBSD guidelines is given by FEMA 445

[30]. The main goal of using PBSD techniques for new structures is to be able to predict the seismic performance with more sensible measures to the society, such as maintenance cost, human losses and downtime cost (loss of use). Additionally, it ensures that the structures are satisfying the set performances objectives. The process of PBSD exhibits several sources of uncertainties, such as the estimation of seismic capacities and demands. It also depends mainly on the set performance objectives which consist of the specified damage limit state at each seismic hazard level. The seismic capacity of structures can be evaluated using either nonlinear static procedures (e.g. Push-Over Analysis) or nonlinear dynamic procedures (e.g. Incremental Dynamic Analysis). The following subsections present some of the analyses that are used in evaluating seismic capacities and expected performance.

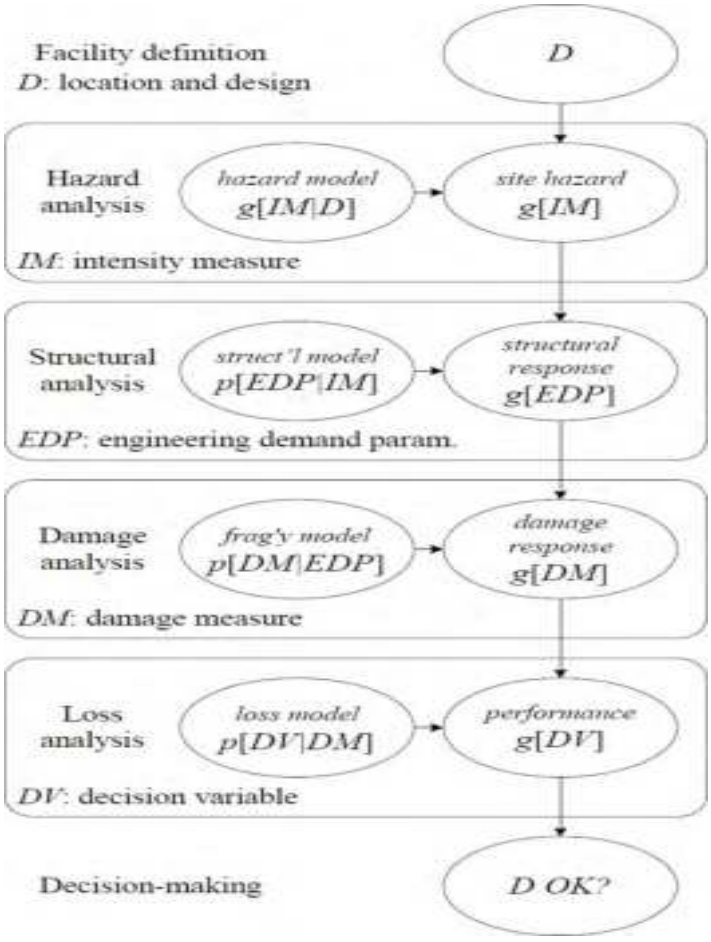

Figure 12: PEER's PBEE Framework Flowchart [35]

2.3.1 Nonlinear Analyses. Push-over analysis is a static nonlinear analysis in which the structure is pushed with a profile of forces or displacements distributed along

the height of the structure. The profile should imitate the inertial forces of the structure. The intensity of the pushing function is increased monotonically until the ultimate capacity of the structure is reached, but without causing the building to start shaking. Furthermore, there are several types of the push-over analysis. For example, if the structure is pushed with a constant function throughout the analysis, it is called conventional push-over. On the other hand, it is an adaptive push-over when the profile of the forcing function changes during the analysis to account for the different mode shapes. Although push-over is a static analysis, it is capable of providing a reasonably good estimate of the capacity and ductility of the structure. Additionally, it gives an insight view of the structure behavior and highlights the design flaws which cannot be noticed in a conventional elastic analysis [4]. The capacity curves developed using push-over analysis are generally independent of any seismic demand and can be used to assess the structure performance against the set performance objectives [36]. However, push-over analysis provides its best estimate for the structural response of structures vibrating predominantly in their fundamental mode of vibration. Additionally, the triggered modes of deformations and design weaknesses depend to a high extent on the selected load or displacement pattern [37]. Therefore, engineering judgment should be used in choosing the pattern of loading and in elaborating push-over analysis results [37].

Dynamic analyses offer higher accuracy in capturing the earthquake response of structures. However, it is computationally expensive and mandates special attention in interpreting the results. The use of dynamic analyses is becoming more popular in both research and industry as the computational power of computers is increasing and more verified software are easily available. In dynamic nonlinear analysis, the solution of the governing equation of motion varies with time. Hence, the solution cannot be obtained analytically, but it requires numerical methods [4]. The equation of motion for a Multi-Degree of Freedom System (MDFS) subjected to ground motion is expressed as follows [4]:

$$mu^{\cdot\cdot} + cu^{\cdot} + ku = -mu_g^{\cdot\cdot}(t) \qquad (1)$$

in which *m, c* and *k* are mass, damping and stiffness matrices, respectively. $u^{\cdot\cdot}$ is absolute accelerations vector, $u^{\cdot}$ is relative velocity vector, u is the displacement vector, and $u_g^{\cdot\cdot}$ is the ground acceleration. There are several dynamic analysis

methods, such as spectral analysis, modal analysis and response history analysis. Incremental Dynamic Analysis (IDA) is an inelastic response history [4]. It is a very powerful nonlinear dynamic analysis which gives an enhanced estimate for the capacity of the structure when subjected to ground shaking. Furthermore, it monitors the behavior of the structure under seismic loading starting from the elastic range to the formation of plastic hinges and finally to the collapse of the structure. IDA is performed by applying a suite of ground motion records on the structure and increasing the intensity of each record until collapse occurs using multiple scale factors at small increments to capture a fine picture of the structural behavior. The results obtained from IDA gives advanced details of the structural behavior and capacity compared to the conventional static push-over analysis results [4]. In addition, IDA shows the expected response of the structure with respect to the changes in ground motion intensity and allows for evaluation of the performance using the fragility curves [4].

2.3.2 Performance Investigations. In this research, the performance investigation procedures are adopted from Federal Emergency Management Agency (FEMA) publication "Quantification of Seismic Performance Factors" P695 [6]. FEMA P695 was established to develop a standard methodology that can be used to quantify the structural systems performance and response parameters (i.e. R, C_d, Ω_o). The established procedure can be used to evaluate the seismic response parameters for new structural systems, verify and improve values for structural systems in current design codes. It can also be used to investigate the expected seismic performance of buildings designed using PBSD techniques. The main performance objective implemented in FEMA P695 is to reduce probabilities of structural collapse at Maximum Considered Earthquake (MCE) demand. The collapse evaluation procedures outlined in FEMA P695 has been successfully implemented by some researchers to test several lateral force resisting systems. For instance, it was used to evaluate the expected seismic performance of Steel Plate Shear walls (SPSWs) with two different design approaches for the infill panels [38]. Additionally, the seismic performance of residential buildings with core walls having three different configurations for the lateral system (i.e. all shear walls, all columns except core wall and columns and shear walls combined) was tested using FEMA P695 methodology [39]. Furthermore,Gogus and Wallace [40] applied FEMA P695 procedures to investigate the seismic performance and response factors of Reinforced Concrete (RC) shear walls designed as per current design codes. The study

investigated the current seismic design factors given for RC shear walls in codes. It concluded that the code specified C_d & Ω_o factors are satisfactory and recommended larger values for the response modification factors (R) for buildings with high (3 or more) height/length ratios.

FEMA P695 offers systematic, standardized and well-established procedures for collapse evaluation of structures. It starts with choosing the analysis software, creating nonlinear analysis models, and then, selecting and scaling the ground motion records that will be used in performing the IDA. FEMA P695 adapted two sets of ground motion record from PEER NGA database [7]. PEER NGA database was chosen due to the large number of ground motion records available there. It has more than 3,550 time history records from 160 earthquake events with varying magnitudes between 4.2 and 7.9. For all the records, the two horizontal components (fault normal and fault parallel) are available and for most of them the vertical component is obtainable. The two record sets implemented in FEMA P695 methodology were classified according to their epicentre distance as far-field and near-field sets. The main reason for this classification is to allow the investigation of collapse fragility and sensitivity to directionality and pulse effects. Far-field record set consists of 22 records; each has two components, obtained from 14 seismic events with magnitudes ranging from 6.5-7.6. The distance from fault rapture (source distances) for all far-field records is more than 10 km. On the other hand, the near-field record set contains 28 records; each has two components, which are also obtained from 14 events with magnitudes between 6.5 and 7.9. The source distance for all the near-field records is less than 10 km and half of the records include pulses. The selected records have to be scaled up since most available records are not strong enough to cause failure in modern structures. The scaling method consists of two steps; normalization and scaling. First, all records are normalized using the geometric mean of the two horizontal components of their Peak Ground Velocity (PGV). Normalizing records with their PGVs removes variations due to the event magnitude, epicentre distance, site conditions and source type. However, it maintains the record-to-record variability required to estimate collapse fragility accurately. Far-field records normalization factors are available in FEMA P695, Appendix A, Table A-4D. Similarly normalization factors for near-field records are given in FEMA P695, Table A-6D. The second step is calculating the scaling factor for the records. All normalized records are scaled up using a single scaling factor to

ensure that 50% of the scaled records cause the structure to collapse. The scaling method implemented in FEMA P695 is similar to the scaling procedure of ASCE7-10 [29]. However, FEMA P695 scales the records such that the median spectral acceleration of the records matches the MCE level spectral acceleration at the fundamental time period of the structure. Figure 13 shows an example of anchoring the median spectral acceleration of far-field records set to FEMA P695 MCE response spectrums at a fundamental period of 1 second.

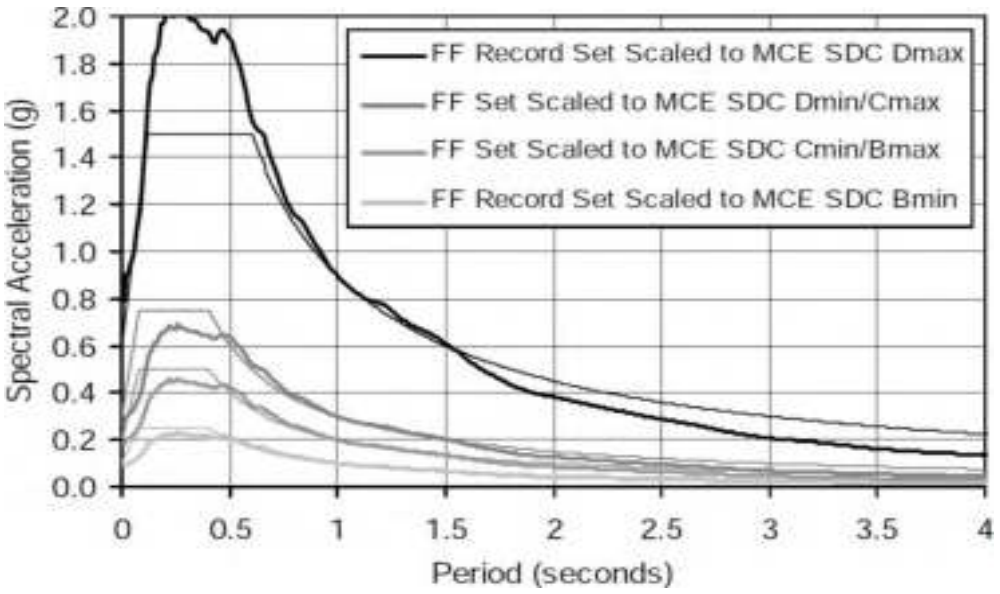

Figure 13: FEMA P695 Scaled far-field Records Set to Match MCE Response Spectrums [6]

On the other hand, ASCE7-10 scaling method matches the spectral accelerations of the records to the MCE demand over a range of time periods. FEMA P695 Scale Factor (SF) is calculated following Eq. (2) and then applied for all records. C_{3D} is the three dimensional analysis coefficient; it should be 1 for 2-D analysis and 1.2 for 3-D analysis. S_{NRT} is the normalized records median spectral acceleration at the structure's fundamental time period, given in FEMA P695 Table A-3.

$$SF = \frac{ACMR_{10\%}}{C_{3D}SSF}\left(\frac{S_{MT}}{S_{NRT}}\right) \quad (2)$$

The IDA is then performed using the scaled records. The intensity of each ground motion is incrementally increased until the structure collapses or reaches a code specified collapse limit. The maximum story drift ratio at each increment should be

extracted and the IDA (maximum story drift ratio versus intensity measure) curves are plotted. Using the IDA results, the median collapse intensity ($\hat{S}_{CT}$) is estimated as the spectral acceleration at which half of the records used (i.e. 22 records for far-field set and 28 records for bear-field set) causes the structure to collapse. Then the corresponding MCE spectral acceleration, 5% damped, at the structure's fundamental period is calculated (S_{MT}). Subsequently, the Collapse Margin Ratio (CMR) is estimated as the ratio between $\hat{S}_{CT}$ and S_{MT}. Then the CMR is modified to consider the frequency content of the records and the increase in the structure's fundamental period before collapse. This is incorporated indirectly using Spectral Shape Factors (SSF) rather than choosing the analysis ground motion records based on the natural period of each structure. SSF are given in FEMA P695 Tables 7-1a & 7-1b based on ductility of the structures, fundamental time period, and seismic design category. The period based ductility (μ_T) is the ratio between ultimate roof deformation (δ_u) and effective yield roof deformation ($\delta_{y,eff}$). δ_u and $\delta_{y,eff}$ should be estimated as per the procedures given in FEMA P695, Appendix B and is shown in Figure 14.

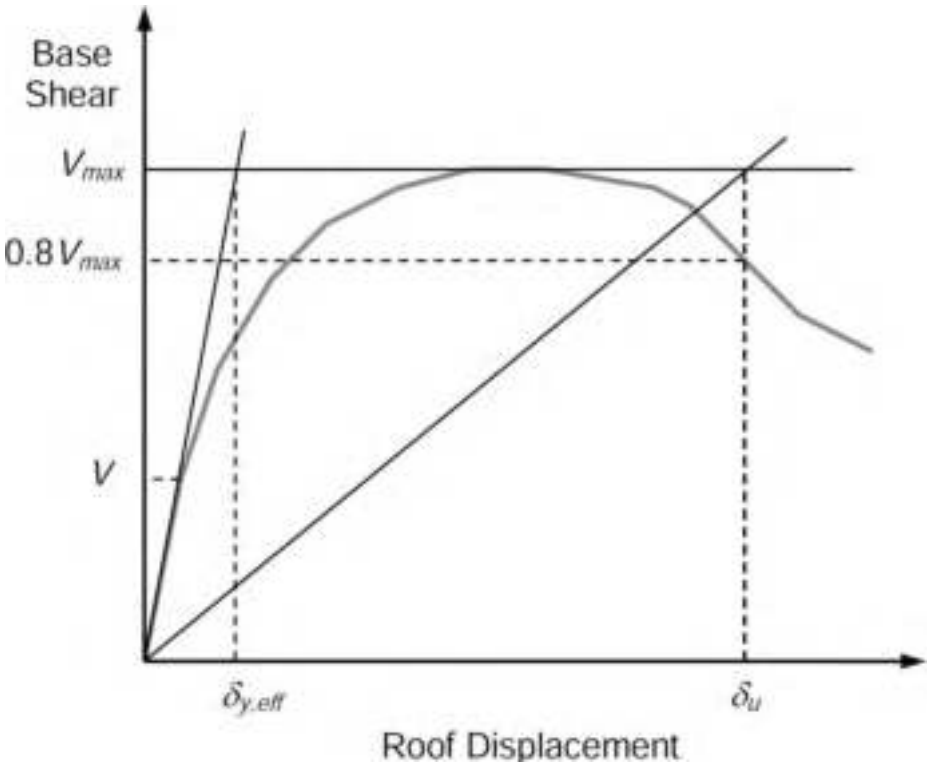

Figure 14: Estimating Effective and Ultimate Yield Deformations [6]

Furthermore, the IDA results shall account for the different sources of uncertainties which are: Record-to-record uncertainty (β_{RTR}); Design basis uncertainty (β_{DR}); Testing data uncertainty (β_{TD}) and Nonlinear simulation uncertainty (β_{MDL}). The collapse fragility of the structures is defined using a random variable (S_{CT}) which is calculated using Eq. (3).

$$S_{CT} = \hat{S}_{CT}\lambda_{TOT} \tag{3}$$

S_{CT} depends on λ_{TOT} which is a log normally distributed random variable with a unity median and lognormal standard deviation that is equal to (β_{TOT}). λ_{TOT} and β_{TOT} are calculated as shown in Eq. (4) and Eq. (5), respectively.

$$\lambda_{TOT} = \lambda_{RTR}\lambda_{DR}\lambda_{TD}\lambda_{MDL} \tag{4}$$

$$\beta_{TOT} = \sqrt{\beta_{RTR}^2 + \beta_{DR}^2 + \beta_{TD}^2 + \beta_{MDL}^2} \tag{5}$$

The parameters λ_{RTR}, λ_{DR}, λ_{TD}, and λ_{MDL} are also log normally distributed with lognormal standard deviations β_{RTR}, β_{DR}, β_{TD}, and β_{MDL}, respectively. Moreover, the uncertainty parameters β_{RTR}, β_{DR}, β_{TD}, and β_{MDL} are obtained from FEMA P695. Record to record uncertainty (β_{RTR}) is given a fixed value of 0.4 in FEMA P695 chapter 7 for systems with high ductility ($\mu_T > 3$) and can be calculated using Eq. (6) for systems with limited ductility.

$$\beta_{RTR} = 0.1 + 0.\,\mu_T \leq 0.4 \tag{6}$$

Moreover, the quality of design requirements uncertainty (β_{DR}) is obtained from Table 3-1 in FEMA P695. It generally depends on the completeness and robustness of design requirement as well as the level of confidence in the design criteria. The uncertainty related to quality of test data (β_{TD}) depends on completeness and robustness of the test results in evaluating performance and failure mechanisms of materials, members, connections, assemblies and systems. It also depends on the level of confidence in the test results. The values can be found in FEMA P695, Table 3-1. Finally, the quality of nonlinear models uncertainty (β_{MDL}) is provided in Table 5-3 in FEMA P695. It is related to the accuracy of modeling and capability of representing structural collapse mechanisms. The three uncertainty parameters, β_{DR}, β_{TD}, and β_{MDL}, range from superior with a numerical value of 0.1 to poor with a value of 0.5. Once IDA results are modified to consider uncertainty, the calculated CMR is then adjusted to account for the spectral

shape of the records used in the analysis. The Adjusted Collapse Margin Ratio (ACMR) is obtained by multiplying the SSF by CMR (i.e. ACMR = SSF x CMR). ACMR is an essential factor in evaluating the collapse safety and expected seismic performance of structures. FEMA P695 provides values for acceptable ACMRs in Table 7-3. The values depend on the total system collapse uncertainty (β_{TOT}) and the allowed probability of collapse at MCE level. Higher total system uncertainty and lower collapse probability increase allowable ACMRs. As per FEMA P695, for any single structural system to have an acceptable seismic performance, the calculated ACMR should be higher than acceptable ACMR for 20% collapse probability. This means that the system should have a probability of collapse at the MCE spectral accelerations level that it less than 20%. However, on average for a group of archetypes, the calculated ACMR should be higher than acceptable ACMR for 10% probability of collapse. This indicates that the average system collapse probability at MCE spectral accelerations should be less than 10%.

Chapter 3: Buildings Description and Design

3.1 Buildings Description

Twelve reference buildings with stories varying from 6 to 12 are selected to target the main inventory of buildings in Dubai, UAE. The selected buildings are office buildings made up of Reinforced Concrete (RC). The number of floors is varied to represent the majority of common buildings in Dubai. For the twelve buildings, the same plan consisting of five 20ft (6m) bays and total dimensions of 100ftx100ft (30mx30m) is implemented. The typical floor plan view is shown in Figure 15.

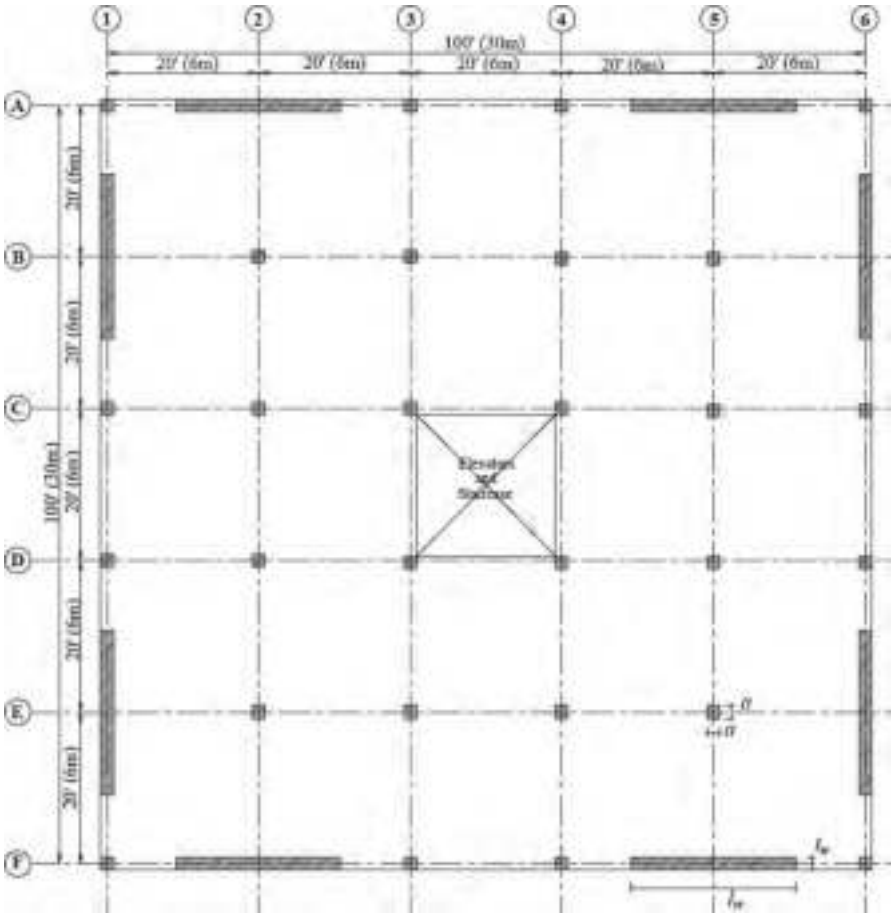

Figure 15: Typical Floors Plan View

Furthermore, the overall structural height varies between 78ft to 156ft (24m to 48m); with a typical floor height of 13ft (4m). The lateral force resisting system consists of special or ordinary reinforced concrete shear walls depending on the seismic hazard level. The shear walls are placed along the perimeter of the building which increases

the building torsional resistance and makes it symmetrical in both directions. In addition, the gravity system consists of RC square columns, while the floor system comprises of 8in (200mm) cast-in-situ flat slab without beams. However, the gravity system is not designed to be part of the lateral force resisting system. It is only designed for vertical loads and to satisfy the deformation compatibility requirement. For design purposes, concrete compressive strength ($f_c^{'}$) is assumed to be 4.0 Ksi (28Mpa) for columns and slabs, and 5.0Ksi (38Mpa) for shear walls. Additionally, the yield strength (f_y) of reinforcement is assumed to be 60Ksi (420Mpa). Super Imposed Load (SDL) is 75 psf (3.6KPa), excluding the self-weight of the concrete slabs. Curtain wall (cladding) load on the perimeter of each floor is 15 psf (0.72 KPa). Moreover, for office buildings the typical floors live load is 50 psf (2.4Kpa) and the roof live load is 20 psf (1 Kpa) as per ASCE7-10 [29]. The buildings are designed and detailed according to International Building Code 2012 (IBC'12) [5] requirements for three different seismic hazard levels representing high, moderate and low levels of seismicity in Dubai. The highest seismicity level represents the upper bound, and it is obtained from USGS [41] intermediate estimate for Dubai, as illustrated in Figure 16. Moreover, the moderate seismic design level represents Abu Dhabi International Building Code 2011 (AIBC'11) [42] estimate for Dubai, and the lowest level is representing the lower bound given by Aldama's et al. [13] seismic hazard study. The elastic design response spectrums for the three considered seismicity levels along with the proposed twelve buildings are presented in Figure 17. As shown, at every seismic design level, three buildings with 12-stories, 9-stories and 6-stories are designed with special RC shear walls. However, at the lowest seismic design level, six buildings are designed. Three of them have special RC shear walls and the other three have ordinary RC shear walls. Summary of all buildings details including response modification factors (R), design spectral accelerations and elastic fundamental time periods are given in Table 3. As per IBC'12 [5], since no sufficient information is available about soil properties at the proposed buildings site, a site class D is assumed for the 12 reference buildings.

Figure 16: USGS Seismic Hazard Estimate for Dubai [41]

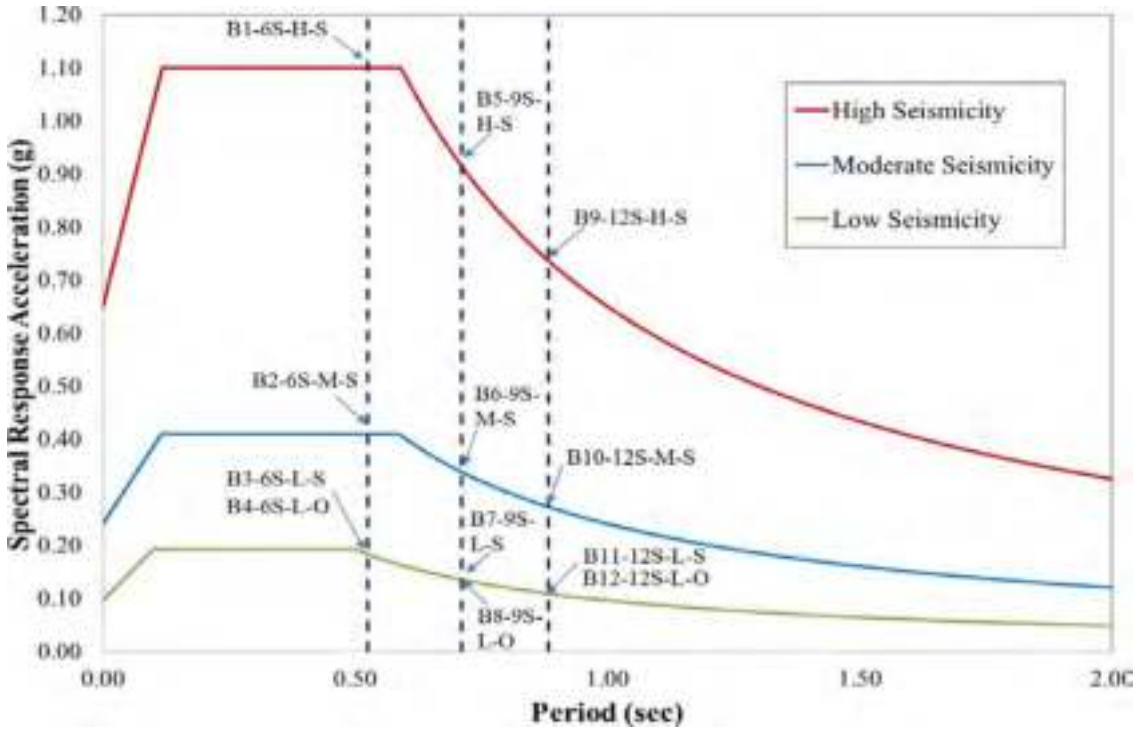

Figure 17: Elastic Design Response Spectrums & Proposed Reference Buildings

Table 3: Buildings Characteristics

Building No.	No. of Floors	Shear Wall Type	R	C_d	Design S_s (g)	Design S_1 (g)	Natural Period (sec)	Approx. Period (C_u*T_a) (sec)
1	6	Special	6	5	1.65	0.65	1.03	0.73
2	6	Special	6	5	0.42	0.17	2.21	0.77
3	6	Special	6	5	0.18	0.06	2.92	0.89
4	6	Ordinary	5	4.5	0.18	0.06	2.92	0.89
5	9	Special	6	5	1.65	0.65	1.45	1
6	9	Special	6	5	0.42	0.17	2.92	1.04
7	9	Special	6	5	0.18	0.06	3.51	1.21
8	9	Ordinary	5	4.5	0.18	0.06	3.51	1.21
9	12	Special	6	5	1.65	0.65	1.8	1.24
10	12	Special	6	5	0.42	0.17	3.13	1.29
11	12	Special	6	5	0.18	0.06	3.97	1.5
12	12	Ordinary	5	4.5	0.18	0.06	3.97	1.5

3.2 Buildings Design Details

The twelve reference buildings are designed and detailed according to IBC'12 [5] standards which refers to ASCE7-10 for minimum design loads [29] and ACI318-11 for structural concrete requirements [43]. The designs implement the state of the art practices in design and construction followed in Dubai, UAE. For the design purposes, elastic analysis is done using 3D models on CSI ETABS commercial package [8]. To fix the majority of the seismic mass, the gravity system is designed first and fixed for all buildings. The following two subsections outline the design process of the gravity system and lateral force resisting system of the twelve buildings.

3.2.1 Gravity System Design. The gravity system is designed to resist axial forces from all vertical loads in addition to the moments and shears induced from deformation compatibility requirements. In order to ensure the structural stability of gravity columns, they are designed to resist the induced actions (bending moments and shear forces) from the deformations that will be imposed by earthquake excitations on the building. The bending moments and shear forces are estimated based on the maximum allowable inter-story drift by IBC'12 [5] which is 2%. The stiffness of the columns is estimated using ETABS by applying a force at the top and bottom of the considered story and by getting the corresponding displacement. The shear forces are

then calculated by multiplying the maximum allowable displacement by the stiffness for each column. Then from the shear force, the moment is calculated as shown in Equations (7) and (8).

$$V = K \times d \tag{7}$$

$$M = \frac{L}{2} \times V \tag{8}$$

Where V is shear force, d is displacement (evaluated from ETABS), M is moment and L is column height. It should be noted that the calculated deformation compatibility shear can actually be resisted by concrete only. Therefore, minimum lateral reinforcement is provided in columns according to clause 7.10 in ACI318-11 [43].

The gravity columns and flat slabs are design using in-house verified spreadsheets according to ACI318-11[43] requirements. Columns cross section and reinforcement are changed every three floors to optimize the design and match with common design trends in Dubai. The gravity system is common for all buildings with the same number of floors. A summary of the design details for all buildings is given in Tables 4-7.

Table 4: 12-Story Buildings Gravity Columns Design Summary

Floors	Column Type	Column Size (inxin)	Reinforcement	Ties in X and Y
10, 11 & 12	Corner	28x28	16#10	2 Legs #4 @14in
	Edge	28x28	12#10	2 Legs #4 @14in
	Opening	28x28	20#10	2 Legs #4 @12in
	Interior	28x28	16#10	2 Legs #4 @14in
7, 8 & 9	Corner	30x30	8#10	2 Legs #4 @18in
	Edge	30x30	8#10	2 Legs #4 @18in
	Opening	30x30	8#10	2 Legs #4 @18in
	Interior	30x30	8#10	2 Legs #4 @18in
4, 5 & 6	Corner	32x32	12#9	2 Legs #4 @16in
	Edge	32x32	12#9	2 Legs #4 @16in
	Opening	32x32	12#10	2 Legs #4 @16in
	Interior	32x32	12#9	2 Legs #4 @16in
1, 2 & 3	Corner	34x34	12#9	2 Legs #4 @16in
	Edge	34x34	12#9	2 Legs #4 @16in
	Opening	34x34	12#10	2 Legs #4 @16in
	Interior	34x34	12#9	2 Legs #4 @16in

Table 5: 9-Story Buildings Gravity Columns Design Summary

Floors	Column Type	Column Size (inxin)	Reinforcement	Ties in X and Y
7, 8 & 9	Corner	28x28	16#10	2 Legs #4 @14in
	Edge	28x28	12#10	2 Legs #4 @14in
	Opening	28x28	20#10	2 Legs #4 @12in
	Interior	28x28	16#10	2 Legs #4 @14in
4, 5 & 6	Corner	30x30	8#10	2 Legs #4 @18in
	Edge	30x30	8#10	2 Legs #4 @18in
	Opening	30x30	8#10	2 Legs #4 @18in
	Interior	30x30	8#10	2 Legs #4 @18in
1, 2 & 3	Corner	32x32	12#9	2 Legs #4 @16in
	Edge	32x32	12#9	2 Legs #4 @16in
	Opening	32x32	12#10	2 Legs #4 @16in
	Interior	32x32	12#9	2 Legs #4 @16in

Table 6: 6-Story Buildings Gravity Columns Design Summary

Floors	Column Type	Column Size (inxin)	Reinforcement	Ties in X and Y
4, 5 & 6	Corner	28x28	16#10	2 Legs #4 @14in
	Edge	28x28	12#10	2 Legs #4 @14in
	Opening	28x28	20#10	2 Legs #4 @12in
	Interior	28x28	16#10	2 Legs #4 @14in
1, 2 & 3	Corner	30x30	8#10	2 Legs #4 @18in
	Edge	30x30	8#10	2 Legs #4 @18in
	Opening	30x30	8#10	2 Legs #4 @18in
	Interior	30x30	8#10	2 Legs #4 @18in

Table 7: Typical Floors Slab Reinforcement Schedule

Thickness	Top Reinforcement	Bottom Reinforcement	Remarks
8 in	#5 @ 6in o.c.	#5 @ 6in o.c.	Additional #6 @ 5in 6.7ft long provided over columns in both directions

3.2.2 Lateral Force Resisting System Design. After finalizing the gravity system design, the lateral system is designed to resist the seismic lateral loads. Linear static analysis is performed for the 12 buildings using ETABS [8].The seismic forces are determined using the Static Equivalent Lateral Force method (SELF). SELF is

permitted for all the 12 buildings with seismic design categories B and D. This is because the total height is not exceeding 160ft and no structural irregularities exist according to ASCE7-10, Table 12.6-1 [29]. The design of the lateral force resisting system satisfies both drift and strength requirements. Inter-story drift is controlled within code limits using ETABS by varying the shear wall stiffness (by changing the in-plan length). Figure 18 depicts sample 3D analysis models representing each group, 12-story, 9-story and 6-story, of the reference buildings. On the other hand, strength requirements are satisfied by designing the shear walls for the induced bending moments and shear forces by the seismic actions using Quickwall software [9]. Shear walls thickness and reinforcement are changed every three floors to optimize the design and to match common design practices in Dubai. However, walls in-plan length is kept constant throughout the buildings height to avoid any vertical structural irregularities. Boundary elements vertical extent is checked every three floors. For practical constructability, it is designed to have the same wall thickness. Additionally, to avoid having slender shear walls cross sections and to eliminate warping effects, an aspect ratio of at least 1:12 is maintained between wall length and thickness. Shear walls cost optimized design summary is shown in Tables 8-10.

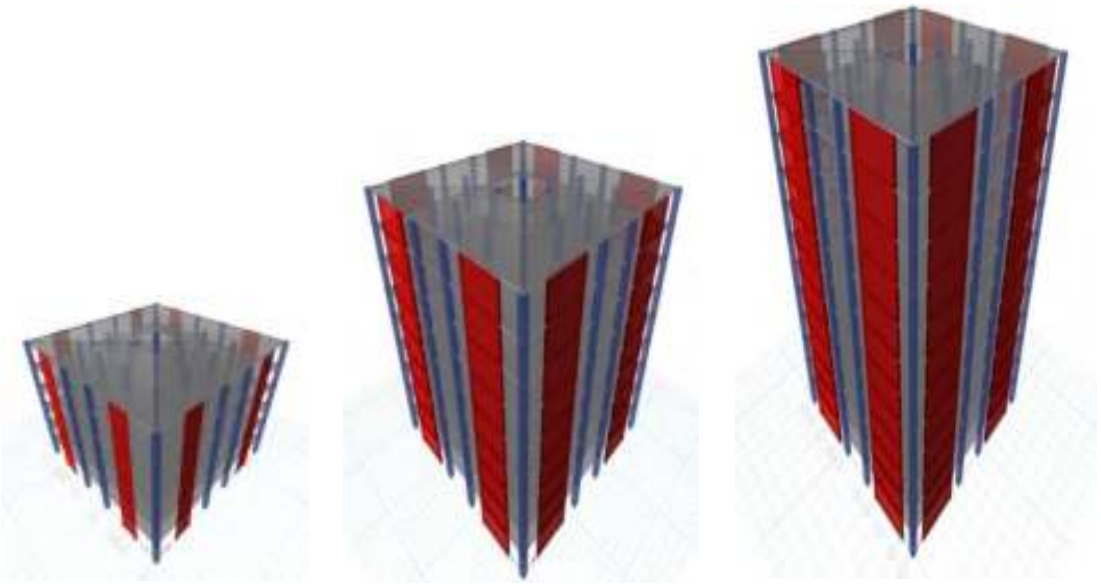

(a) (b) (c)

Figure 18: Sample ETABS 3D Analysis Models: (a) 6-Story Buildings, (b) 9-Story Buildings, (c) 12-Story Buildings

Table 8: 12-Story Buildings RC Shear walls Cost Optimized Design Summary

Floors	Parameter	B9-12S-H-S	B10-12S-M-S	B11-12S-L-S	B12-12S-L-O
	L	23ft	17ft	15ft	15ft
10, 11 & 12	**T**	18in	12in	10in	10in
	L_{BE}	-	-	-	-
	R_{BE}	-	-	-	-
	$C_{BE,w}$	6#4 @ 4in	3#4 @ 4in	3#4 @ 4in	-
	$C_{BE,L}$	3#4 @ 4in	3#4 @ 4in	2#4 @ 4in	-
	R_{HW}	#5 @ 16in	#5 @ 18in	#4 @ 18in	#4 @ 18in
	R_{VW}	#5 @ 16in	#5 @ 16in	#4 @ 18in	#4 @ 18in
7, 8 & 9	**T**	20in	14in	12in	12in
	L_{BE}	-	-	-	-
	R_{BE}	-	-	-	-
	$C_{BE,w}$	6#4 @ 4in	3#4 @ 4in	3#4 @ 4in	-
	$C_{BE,L}$	3#4 @ 4in	3#4 @ 4in	2#4 @ 4in	-
	R_{HW}	#6 @ 16in	#5 @ 18in	#5 @ 18in	#5 @ 18in
	R_{VW}	#7 @ 8in	#7 @ 16in	#5 @ 18in	#5 @ 18in
4, 5 & 6	**T**	22in	16in	14in	14in
	L_{BE}	-	-	-	-
	R_{BE}	-	-	-	-
	$C_{BE,w}$	6#4 @ 4in	3#4 @ 4in	3#4 @ 4in	-
	$C_{BE,L}$	3#4 @ 4in	3#4 @ 4in	2#4 @ 4in	-
	R_{HW}	#6 @ 12in	#6 @ 16in	#5 @ 18in	#5 @ 16in
	R_{VW}	#7 @ 4in	#7 @ 8in	#5 @ 16in	#5 @ 12in
1, 2 & 3	**T**	24in	18in	16in	16in
	L_{BE}	4ft	2ft	2ft	-
	R_{BE}	26 #9	14 #9	5 #6	-
	$C_{BE,w}$	6#5 @ 4in	3#4 @ 4in	3#4 @ 4in	-
	$C_{BE,L}$	3#5 @ 4in	3#5 @ 4in	2#5 @ 4in	-
	R_{HW}	#6 @ 10in	#6 @ 14in	#6 @ 14in	#6 @ 14in
	R_{VW}	#9 @ 4in	#7 @ 8in	#6 @ 8in	#6 @ 6in

T: wall thickness; L_{BE}: boundary element length; R_{BE}: boundary element reinforcement; R_{VW}: shear wall vertical reinforcement; $C_{BE,w}$: boundary element confinement reinforcement perpendicular to wall; $C_{BE,L}$: boundary element confinement reinforcement parallel to wall; R_{HW}: shear wall horizontal reinforcement.

Table 9: 9-Story Buildings RC Shear Walls Cost Optimized Design Summary

Floors	Parameter	B5-9S-H-S	B6-9S-M-S	B7-9S-L-S	B8-9S-L-O
	L	19ft	13ft	12ft	12ft
7, 8 & 9	**T**	16in	10in	8in	8in
	L_{BE}	-	-	-	-
	R_{BE}	-	-	-	-
	$C_{BE,w}$	5#3@4in	4#4 @ 4in	3#4 @ 4in	-
	$C_{BE,L}$	3#3 @ 4in	2#5 @ 4in	2#4 @ 4in	-
	R_{HW}	#6 @ 18in	#5 @ 18in	#4 @ 18in	#4 @ 18in
	R_{VW}	#6 @ 16in	#5 @ 18in	#4 @ 18in	#4 @ 18in
4, 5 & 6	**T**	18in	12in	10in	10in
	L_{BE}	-	-	-	-
	R_{BE}	-	-	-	-
	$C_{BE,w}$	5#3 @ 4in	4#4 @ 4in	3#4 @ 4in	-
	$C_{BE,L}$	3#3 @ 4in	2#5 @ 4in	2#4 @ 4in	-
	R_{HW}	#6 @ 14in	#5 @ 18in	#4 @ 18in	#4 @ 16in
	R_{VW}	#9 @ 8in	#8 @ 12in	#4 @ 18in	#4 @ 16in
1, 2 & 3	**T**	20in	14in	12in	12in
	L_{BE}	3.5ft	2.5ft	1.5ft	-
	R_{BE}	22 #10	12 #9	8 #6	-
	$C_{BE,w}$	5#4 @ 4in	4#4 @ 4in	3#4 @ 4in	-
	$C_{BE,L}$	3#5 @ 4in	2#5 @ 4in	2#5 @ 4in	-
	R_{HW}	#6 @ 10in	#5 @ 10in	#5 @ 18in	#5 @ 18in
	R_{VW}	#9 @ 4in	#9 @ 6in	#6 @ 8in	#6 @ 9in

Table 10: 6-Story Buildings RC Shear Walls Cost Optimized Design Summary

Floors	Parameter	B1-6S-H-S	B2-6S-M-S	B3-6S-L-S	B4-6S-L-O
	L	15ft	10ft	8ft	8ft
4, 5 & 6	**T**	14in	8in	8in	8in
	L_{BE}	-	-	-	-
	R_{BE}	-	-	-	-
	$C_{BE,w}$	4#4 @ 4in	4#3 @ 4in	2#3 @ 4in	-
	$C_{BE,L}$	2#5 @ 4in	4#3 @ 4in	2#3 @ 4in	-
	R_{HW}	#5 @ 14in	#5 @ 18in	#4 @ 18in	#4 @ 18in
	R_{VW}	#7 @ 8in	#5 @ 8in	#4 @ 18in	#4 @ 18in
1, 2 & 3	**T**	16in	10in	10in	10in
	L_{BE}	3ft	2.6ft	1ft	-
	R_{BE}	16 #10	14 #9	6 #6	-
	$C_{BE,w}$	4#4 @ 4in	4#4 @ 4in	2#4 @ 4in	-
	$C_{BE,L}$	2#5 @ 4in	2#5 @ 4in	2#4 @ 4in	-
	R_{HW}	#6 @ 9in	#6 @ 10in	#5 @ 16in	#5 @ 12in
	R_{VW}	#9 @ 4in	#9 @ 4in	#6 @ 8in	#8 @ 8in

T: wall thickness; L_{BE}: boundary element length; R_{BE}: boundary element reinforcement; R_{VW}: shear wall vertical reinforcement; $C_{BE,w}$: boundary element confinement reinforcement perpendicular to wall; $C_{BE,L}$: boundary element confinement reinforcement parallel to wall; R_{HW}: shear wall horizontal reinforcement.

Shear walls reinforcement details for sample buildings are illustrated in Figures 19-26. However, all shear walls reinforcement details are presented in Appendix A.

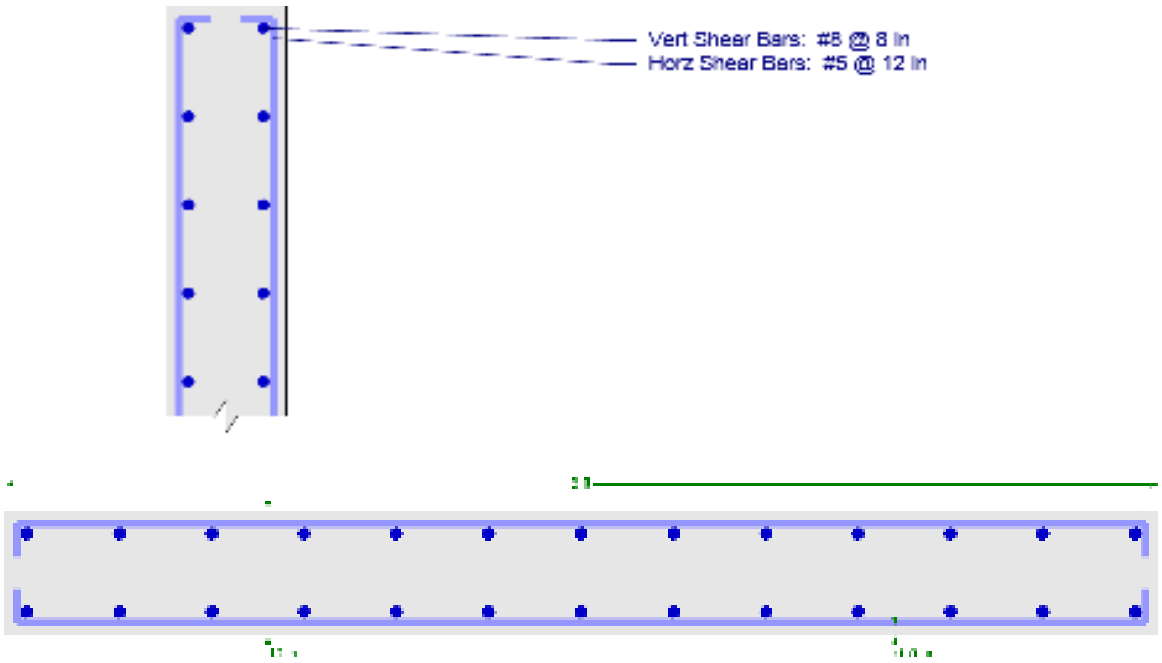

Figure 19: Sample Ordinary RC Shear wall Reinforcement Details for 6-Story Buildings (B4-6S-L-O); Wall Section for Floors 1-3

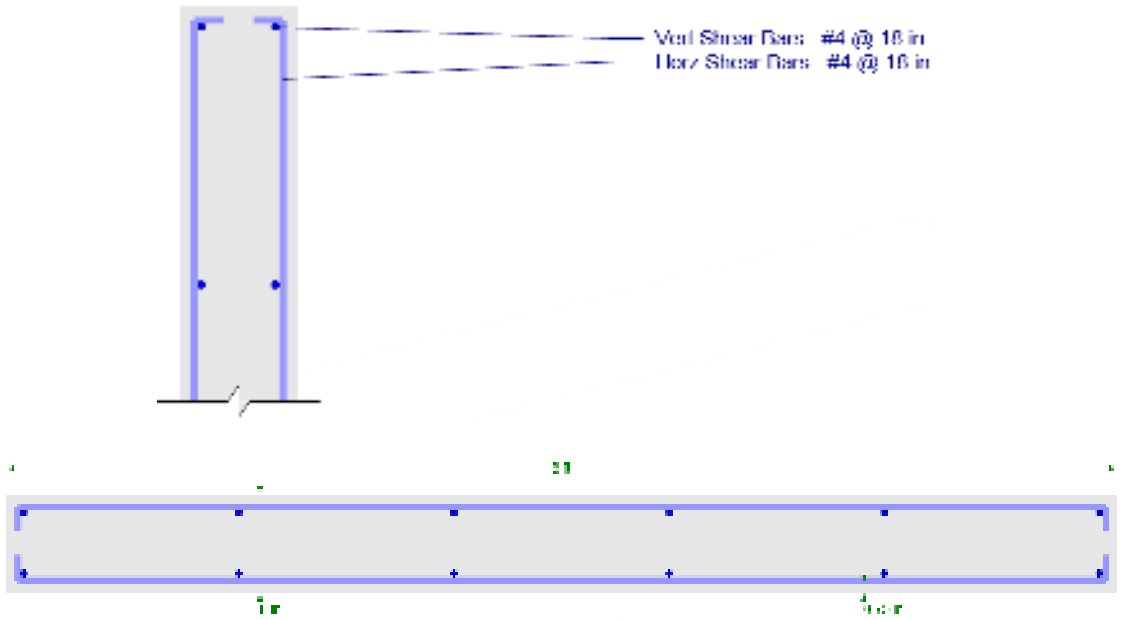

Figure 20: Sample Ordinary RC Shear wall Reinforcement Details for 6-Story Buildings (B4-6S-L-O); Wall Section for Floors 4-6

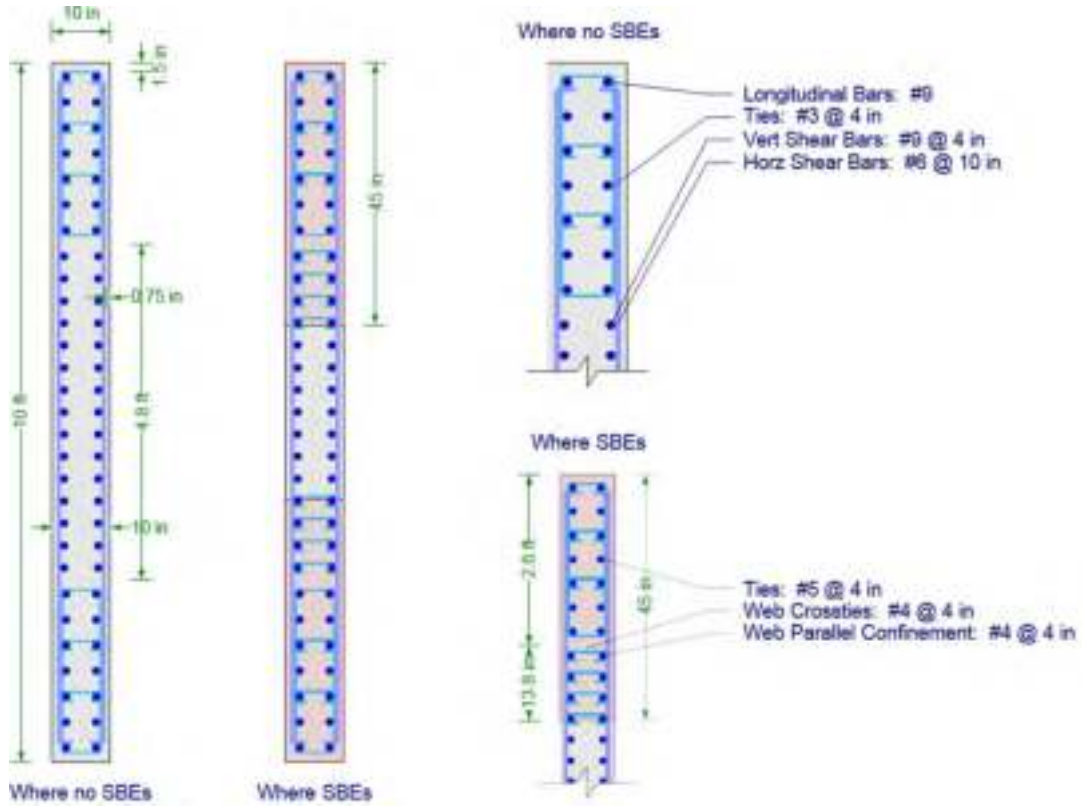

Figure 21: Sample Special RC Shear wall Reinforcement Details for 6-Story Buildings (B2-6S-M-S); Wall Section for Floors 1-3

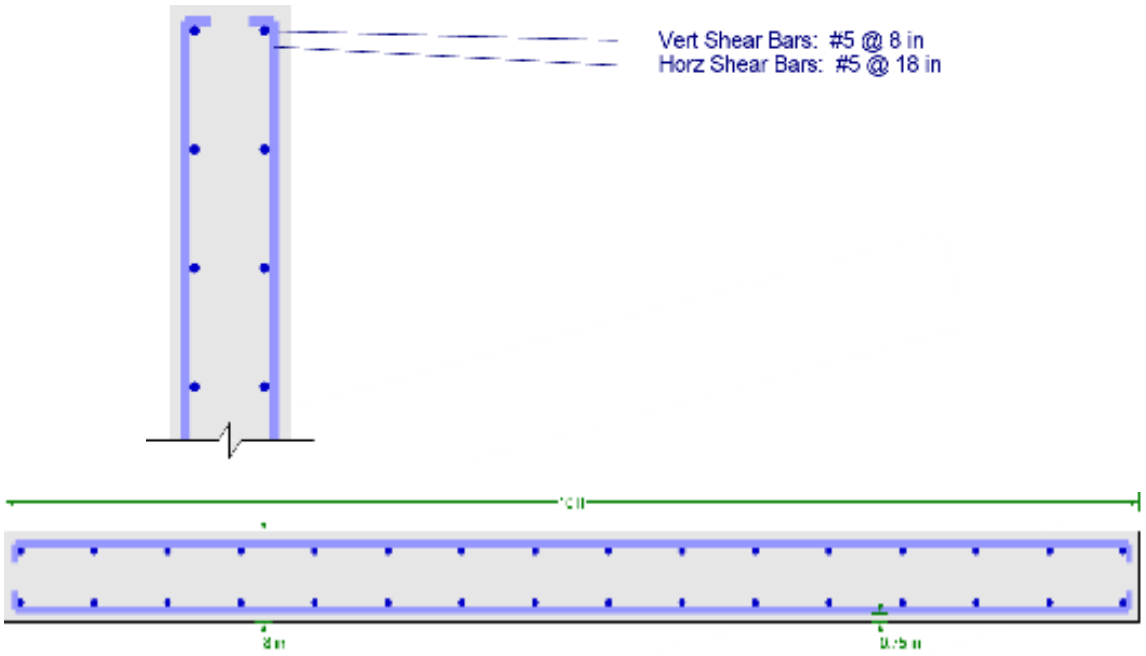

Figure 22: Sample Special RC Shear wall Reinforcement Details for 6-Story Buildings (B2-6S-M-S); Wall Section for Floors 4-6

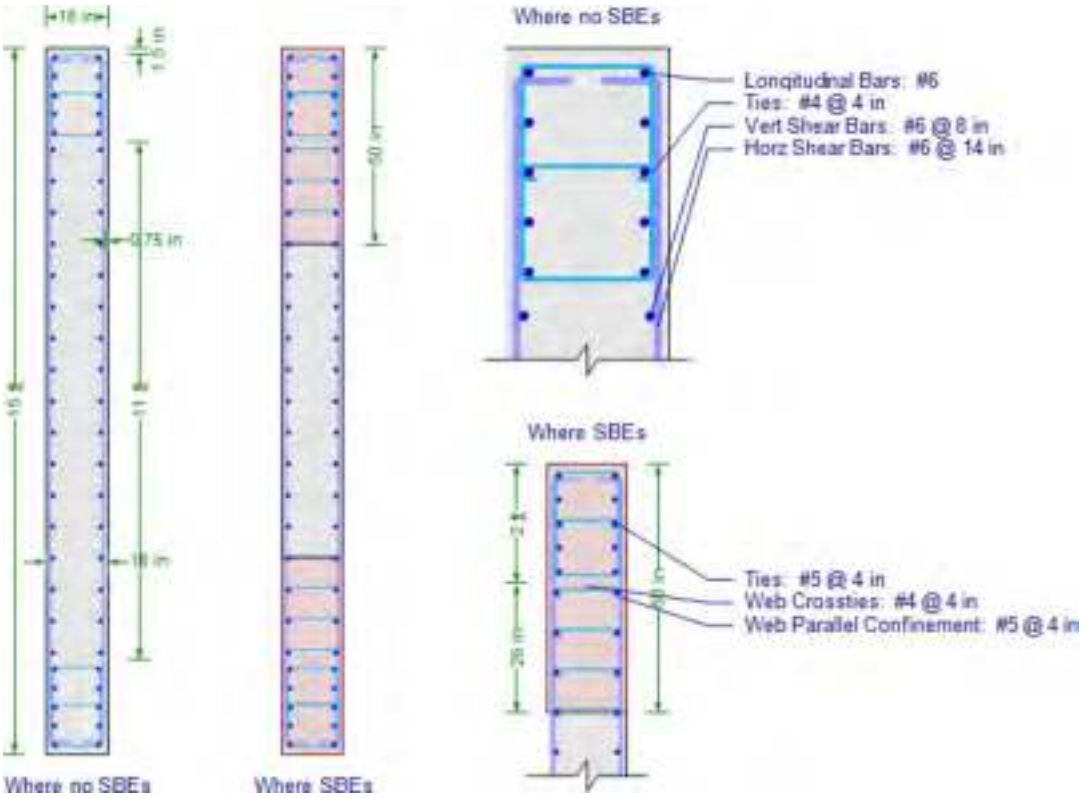

Figure 23: Sample Special RC Shear wall Reinforcement Details for 12-Story Buildings (B11-12S-L-S); Wall Section for Floors 1-3

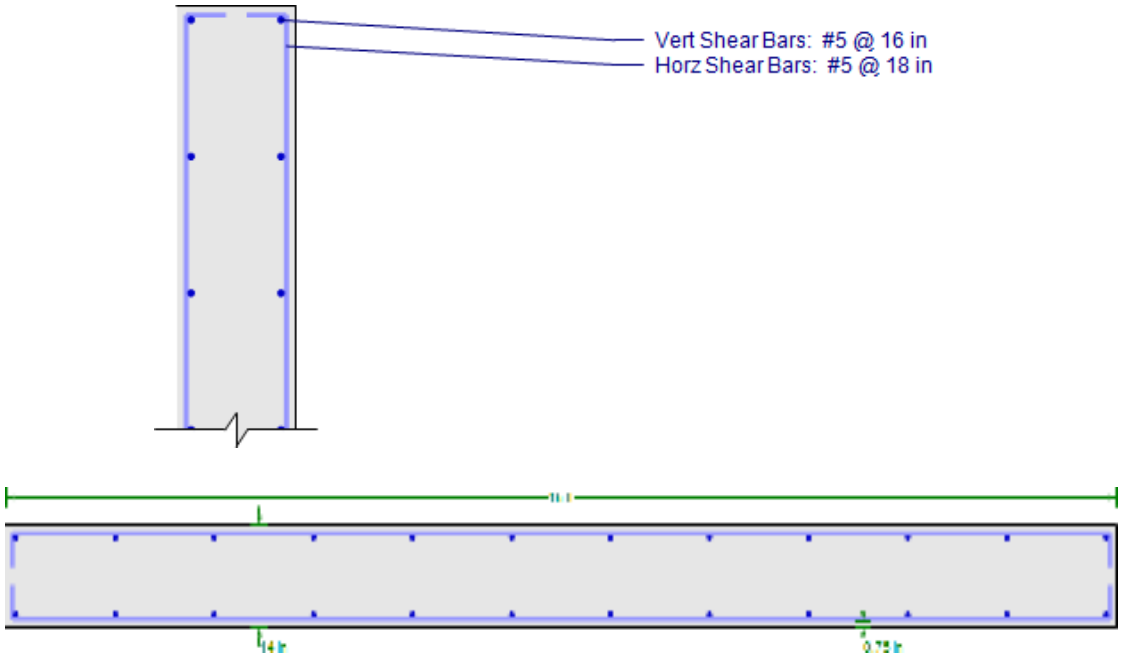

Figure 24: Sample Special RC Shear wall Reinforcement Details for 12-Story Buildings (B11-12S-L-S); Wall Section for Floors 4-6

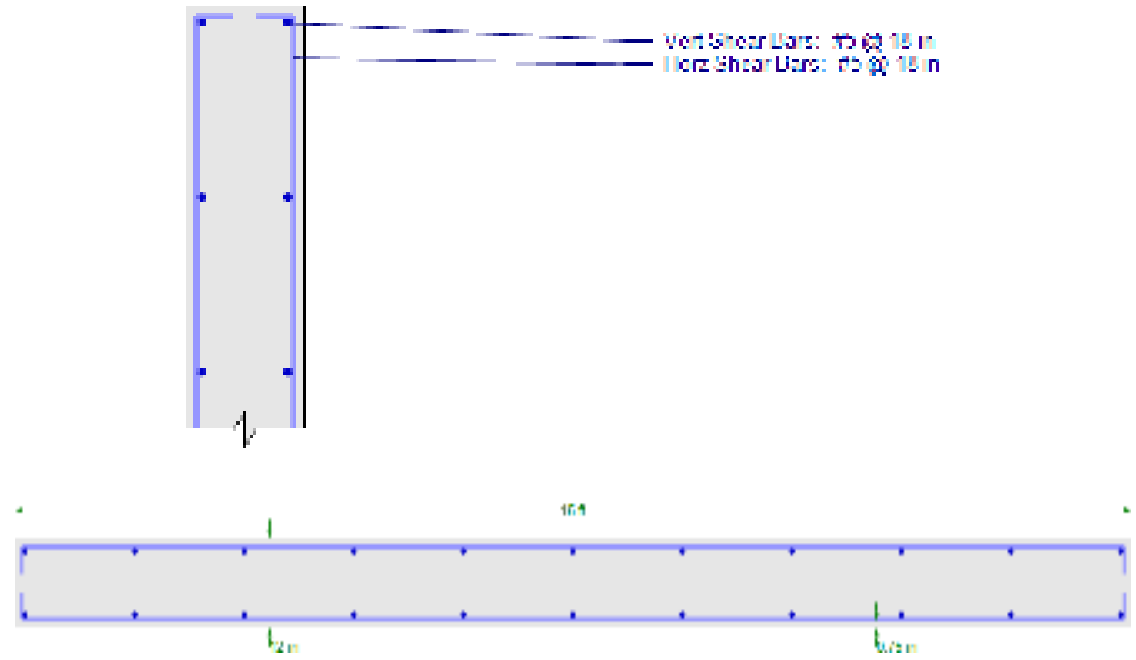

Figure 25: Sample Special RC Shear wall Reinforcement Details for 12-Story Buildings (B11-12S-L-S); Wall Section for Floors 7-9

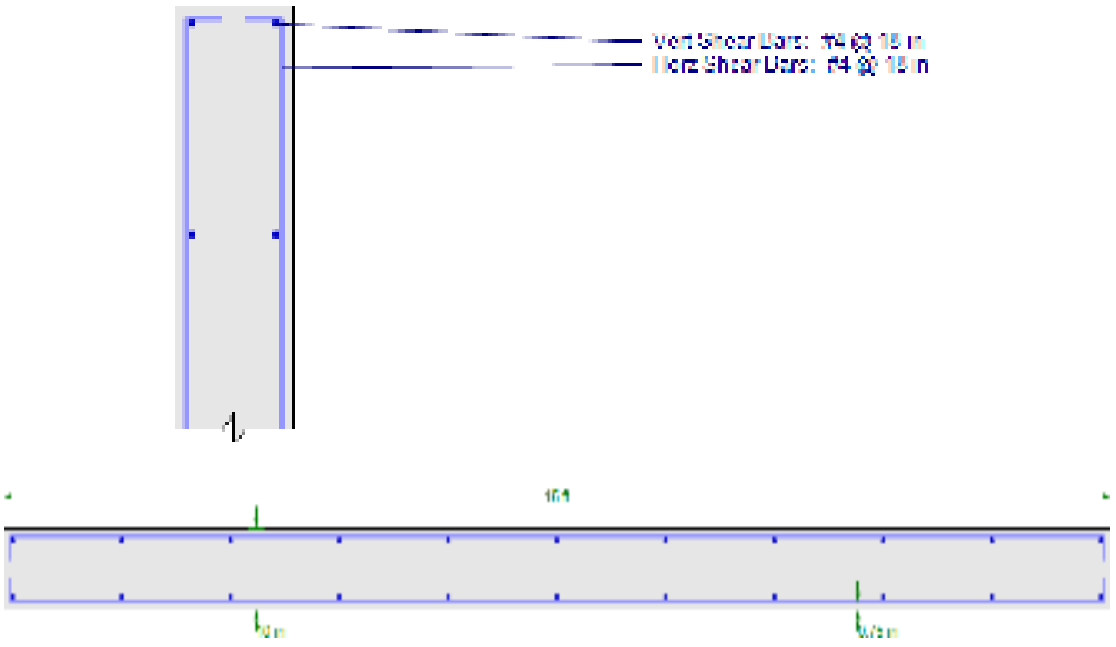

Figure 26: Sample Special RC Shear wall Reinforcement Details for 12-Story Buildings (B11-12S-L-S); Wall Section for Floors 10-12

Chapter 4: Buildings Seismic Performance Evaluation

4.1 Nonlinear Analysis

The seismic performance of the 12 reference buildings is investigated using two types of nonlinear analyses (i.e. Pseudo Static Push-Over Analysis and IDA). The nonlinear simulations are implemented following FEMA P695 [6] collapse evaluation procedures. The following subsections describe the nonlinear modeling and analyses assumptions.

4.1.1 Modeling Assumptions. The 12 reference buildings are idealized using nonlinear fiber finite-element based models on IDARC-2D software [10]. IDARC-2D is capable of performing two dimensional nonlinear analysis and damage analysis of structures. The reference buildings are symmetrical in both directions, hence the 2D analysis is deemed sufficient. In fact, the study focused on a typical building plan without structural irregularities to target a generic group of buildings, instead of just studying a specific special case. Furthermore, IDARC-2D allows modeling of frame structures incorporating the connection rigidity with beams, shear walls, columns and edge elements. Its nonlinear formulation is based on macro-modeling of the structural members by an equivalent element that includes all nonlinear characteristics. The members' characteristics depend on formulation and distribution of plasticity with yield penetration. Properties are evaluated using fiber-based models or mechanics formulations. The nonlinear solution is obtained by using Newmark beta method to integrate equations of motions. IDARC-2D supports most types of pseudo-static push-over analysis, time-history dynamic analysis and quasi-static analyses [10].

In modeling the reference structures, a concentrated plasticity distribution is assumed to represent the actual expected propagation of plastic hinges in shear walls. Similarly the flexibility distribution is presumed to be uniform. Although the tallest reference building is 12-story, P-Delta effects are included in nonlinear dynamic analyses for all buildings, since the lateral system is on the perimeter and largest axial forces act on gravity columns. Second order P-Delta effects are idealized by explicitly modeling the gravity system. However, all lateral force resisting elements (i.e. shear walls) were fixed at the base while gravity columns were hinged at the base to isolate their contribution in resisting lateral loads. Nodal weights are provided in IDARC to

allow the computation of story masses needed for calculating the dynamic properties of structures. The material characteristics used in the nonlinear models are:

- Unconfined Compressive Strength = 5.0 Ksi
- Initial Young's Modulus of Concrete =$57 \times \sqrt{5.0 \times 1000} = 4030.5$ Ksi
- Strain at Max Strength of Concrete = 0.2%
- Stress at Tension Cracking = 0.12 x 5.0 = 0.6 Ksi
- Reinforcement Yield Strength = 60 Ksi
- Reinforcement Ultimate Strength = 1.4 x 60 = 84 Ksi
- Reinforcement Modulus of Elasticity = 29,000 Ksi
- Modulus of Strain Hardening = $\frac{29{,}000}{60} = 483.3$ Ksi
- Strain at Start of Hardening = 3.0%

In addition to geometry and material properties, a very crucial input in any nonlinear model is the hysteretic behavior of the structural members. When structures are subjected to dynamic loads, materials dissipate energy through behaving in an inelastic manner. Yet, the cyclic repeated nature of the dynamic loading causes deterioration in the characteristics (strength and stiffness) of the structural members. The inelasticity and deterioration that happen have to be taken care of in any nonlinear analysis model to capture an accurate representative behavior [44]. There are several models developed to idealize the hysteretic behavior, such as the Polygonal Hysteretic Model (PHM) and the Smooth Hysteretic Model (SHM). For the reference structures, PHM, sometimes referred to as multi-linear models, is adopted. PHM models the actual changes in behavior stages of the structural element. For instance, it captures the initial elastic behavior, cracking, yielding, strength and stiffness deterioration. An example of PHM used in IDARC is the tri-linear (three parameter) model developed by Park et al. [45]. The tri-linear hysteretic modeling allows controlling the stiffness degradation, strength deterioration due to ductility and energy and models slipping. IDARC-2D manual [10] provides recommended values for the hysteretic parameters to achieve severe, moderate, mild or no degrading behavior. Figure 27 presents sample hysteresis developed using the tri-linear model by park et al. [10].

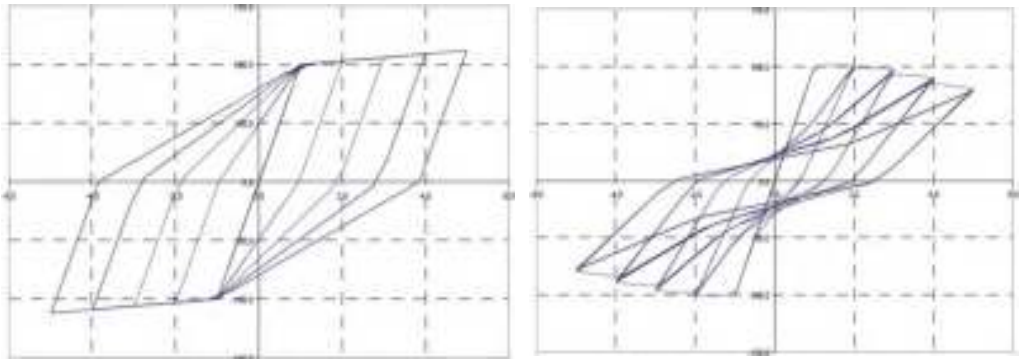

(a) (b)

Figure 27: Tri-Linear Hysteresis: (a) No Degradation, (b) Combined Degradation [10]

Since no specific experimental data are available for the cyclic behavior of the proposed buildings shear walls, IDARC-2D recommended values are selected based on literature recommendations for special and ordinary RC shear walls. Special RC shear walls with proper seismic detailing will have no considerable strength degradation or stiffness deterioration [46].Therefore, a multi-linear hysteretic model with mild degradation will be used to account for that performance. The mild degradation modeling parameters are obtained by averaging mild and no degradation parameters given by IDARC-2D manual [10]. On the other hand, ordinary reinforced concrete shear walls, with lower seismic detailing requirements, are expected to have considerable strength degradation and stiffness deterioration [47]. The degrading behavior will be accounted for, using a tri-linear hysteretic model with average degradation. The average degradation parameters are calculated by averaging IDARC recommended values for severe and mild degradation. Table 11 summarizes the shear walls hysteretic rules modeling parameters. Furthermore, the damping is taken as 5% of critical and is assumed to follow Rayleigh's formulation.

All reference buildings nonlinear models are created using a free format compatible with IDARC-2D. The structures are modeled as two dimensional frames that include columns and shear walls. Slabs are idealized as a rigid horizontal diaphragm with lumped mass. The performance of the buildings is evaluated using nonlinear analyses, namely Pseudo-static push-over analysis and IDA.

Table 11: Shear Walls Hysteresis Rules Modeling Parameters, Calculated from [10]

Parameter	Estimated Value	
	Special RC shear Walls	Ordinary RC Shear Walls
Stiffness Degrading Parameter (α)	130	7
Ductility-Based Strength Degrading Parameter (β_1)	0.035	0.45
Energy-Controlled Strength Degrading Parameter (β_2)	0.03	0.375
Slip or Crack -Closing Parameter (γ)	0.5	0.15

4.1.2 Nonlinear Pseudo-Static (Push-Over) Analysis. The monotonic push-over analysis implemented is displacement based. The buildings are subjected to a linear, inverted triangle, displacement profile. The applied displacement profile is monotonically increased until the structures either collapse or achieve a 20% loss in base shear capacity. The back-bone, or capacity curve, is established as the relationship between normalized base shear and roof drift ratio. The capacity curve is used to obtain reasonable estimates of the buildings' base shear capacity, maximum roof displacement, and period-based ductility.

4.1.3 Nonlinear Incremental Dynamic Analysis (IDA). IDA is performed for all reference buildings to further investigate the expected seismic performance under the random nature of earthquake excitations. It provides a more reliable estimate of the structures' seismic demand and capacities. Furthermore, it is performed using a suite of 22 far-field earthquake records which are multiply scaled up. This simulates the complete response of structures from elasticity through softening and hardening until the dynamic global instability and collapse occur. The selected 22 far-field records are given by FEMA P695 [6] for collapse evaluation which is available at PEER Ground Motion Database [7]. These records are a standard set accepted globally in the earthquake engineering field to be representative of strong ground motion associated with far-fields (typical UAE scenario). They have been carefully selected to cover wide range of PGA/PGV ratios which makes the ensemble critical for low, mid, and high-rise buildings. Furthermore, their number [22 records with 44 combinations of horizontal and vertical components suitable for 2D analysis], inherently possesses the record-to-record variability ensuring statistically-appropriate results. Consequently, the

results are not expected to significantly vary if the records are changed. These natural records are obtained from earthquake events having large magnitudes ranging from 6.5 to 7.6 and originated from distant sources more than 10 km away from fault rupture. A summary of the selected records details is given in Table 12.

Table 12: Far-Field Earthquake Records [7]

No.	Magnitude	Event Name	Station	PGA (g)	PGV (cm/s)	PGA/PGV (g.s/m)
1	6.7	1994 Northridge	Beverly Hills-Mulhol	0.52	63	0.83
2	6.7	1994 Northridge	Canyon Country-WLC	0.48	45	1.07
3	7.1	1999 Duzce, Turkey	Bolu	0.82	62	1.32
4	7.1	1999 Hector Mine	Hector	0.34	42	0.81
5	6.5	1979 Imperial Valley	Delta	0.35	33	1.06
6	6.5	1979 Imperial Valley	El Centro Array #11	0.38	42	0.90
7	6.9	1995 Kobe, Japan	Nishi-Akashi	0.51	37	1.38
8	6.9	1995 Kobe, Japan	Shin-Osaka	0.24	38	0.63
9	7.5	1999 Kocaeli, Turkey	Duzce	0.36	59	0.61
10	7.5	2000 Kocaeli, Turkey	Arcelik	0.22	40	0.55
11	7.3	1992 Landers	Yermo Fire Station	0.24	52	0.46
12	7.3	1992 Landers	Cool Water	0.42	42	1.00
13	6.9	1989 Loma Prieta	Capitola	0.53	35	1.51
14	6.9	1990 Loma Prieta	Gilroy Array #3	0.56	45	1.24
15	7.4	1990 Manjil, Iran	Abbar	0.51	54	0.94
16	6.5	1987 Superstition Hills	El Centro Imp. Co.	0.36	46	0.78
17	6.5	1987 Superstition Hills	Poe Road (temp)	0.45	36	1.25
18	7	1992 Cape Mendocino	Rio Dell Overpass	0.55	44	1.25
19	7.6	1999 Chi-Chi, Taiwan	CHY101	0.44	115	0.38
20	7.6	2000 Chi-Chi, Taiwan	TCU045	0.51	39	1.31
21	6.6	1971 San Fernando	LA - Hollywood Stor	0.21	19	1.11
22	6.5	1976 Friuli, Italy	Tolmezzo	0.35	31	1.13

The choice of far-field records simulates the possible seismic hazard scenario in Dubai of earthquakes originating from distant sources such as zagros thrust or makran subduction zone [20]. In the performed IDA, all the three components of the records; two horizontal and one vertical, are considered. The inclusion of the vertical component in the IDA increases the accuracy of estimating expected damages caused by earthquakes. The ground motion vertical component is generally attributed to the arrival

of the vertical compression waves (P-Waves). Naturally, compression waves have shorter wave length, higher frequency and lower energy compared to shear waves (S-Waves). Most of P-waves energy is stored in high frequency ranges and thus it is proven to be damaging to buildings with vertical periods close to those ranges [4]. Additionally, many researches, such as [48] and [49], emphasized on the damaging effect of ground motions vertical component and recommended including it in the design of earthquake resistant structures. The main concern of vertical component is its effect on axial loads in vertical elements, and its impact on the shear capacity. This affects the structural performance, collapse mechanism and probability [50].The records are scaled up using FEMA P695 [6] methodology, which is described in Section 2.3.2, such that at the structure's natural fundamental period, the median spectral acceleration of the far-field record set matches the Maximum Considered Earthquake (MCE) response spectrum of the highest seismicity level in Dubai. Additionally, the selected records have varying PGA/PGV ratios from 0.38g.s/m to 1.51g.s/m. This makes it critical for both flexible (high-rise) buildings and rigid (low-rise) buildings. To represent a realistic possible scenario, all reference buildings' performance is tested using the same level of scaling, matching highest level of seismic hazard in Dubai. In IDA, it is very vital to choose illustrative intensity measure (IM) as well as Damage Measure (DM). First mode, 5% damped spectral acceleration, $S_a(T_1,5\%)$, is chosen as the IM because of its competency in reducing results scatter and hence it will reduce the number of required runs [51] and [52]. Spectral accelerations also provide a complete characterization of the response. In Addition, the reference buildings heights make them more susceptible to higher PGAs rather than higher PGVs. The DM could be a local response parameter such as beam rotations. It can also be a global response parameter, such as peak drift ratios, story shear force, or story acceleration. In this study, maximum inter-story drift ratio is selected as DM to capture global dynamic instabilities [51] and [52]. IDA results are summarized and used in preparing IDA curves which can be used in defining the expected seismic performance of structures. Figure 28 depicts a typical IDA for a multi-story building. IDA curves capture the behavior of the structure under the increased intensity of ground motion records. It shows the structural response over the intensity range starting from behaving in a linear elastic manner until damages accumulation rate becomes very high and the structure suffers from global dynamic instability. It can be seen in Figure 28 that the structure's response and capacity depends highly on the characteristics of each particular ground motion record. Therefore, for an accurate

estimation of the seismic capacity, a sufficient number of ground motion records are used.

In IDARC, at least 924 (22 records x 2 components x 21 scale factors) IDA runs are performed for each of the 12 reference buildings. IDARC uses Peak Ground Acceleration (PGA) as the IM. Therefore, for each run the target spectral acceleration of each ground motion record is converted to PGA. This is done using the response spectrum of each record to obtain a conversion ratio of PGA to spectral acceleration at the structure's fundamental period. The ratio is multiplied by the target spectral acceleration to obtain the PGA input value to be used in the analysis model.

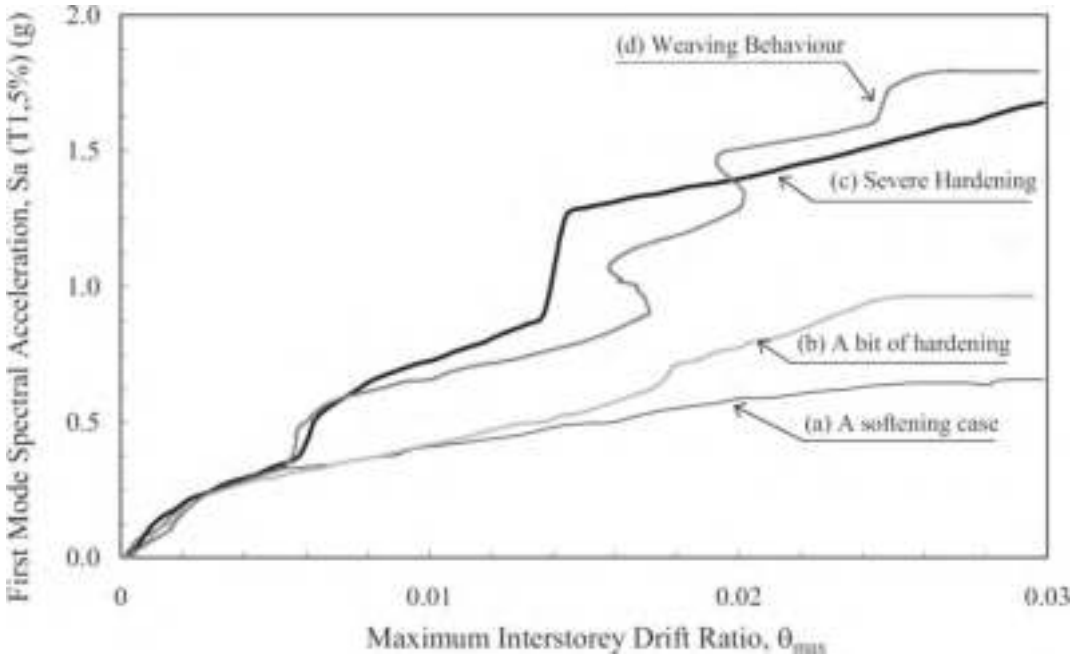

Figure 28: Typical IDA Curves Developed using four earthquake records [4]

4.1.4 Fragility Analysis. Fragility curves provide the probability of exceeding a specific damage state or performance level for a range of chosen IMs. They are very popular effective tools in assessing the seismic vulnerability of structures. The IM could be PGA, PGV or spectral accelerations. It is chosen in this study to be the 5% damped first mode spectral acceleration S (T_1, 5%). The performance limit states are usually classified based on exceeding a specific inter-story drift ratio. This research adapts performance levels specified by ASCE41[53], which are also used by other researchers

in assessing seismic performance of buildings in Dubai, such as [54] and [55]. The three structural performance levels or damage states included in this study are [53]:

I. Immediate Occupancy (IO): indicates minor structural damages without significant yielding and hairline cracking in non-structural elements. The structure's strength and stiffness are retained which limits transient inter-story drift ratios to 0.5% for concrete walls. This limit state is affected mainly by the stiffness of the structural system.

II. Life Safety (LS): indicates major damages occurred to the structure and the lateral force resisting system. Non-structural elements are completely damaged, but not collapsed. Transient drift ratio is limited to 1% and permanent is limited to 0.5% for concrete walls. This performance level is primarily controlled by the strength of the structural system.

III. Collapse Prevention (CP): designates severe damages to the structure and its lateral force resisting system. Non-structural elements have completely collapsed. Drift ratios are limited to 2% transient or permanent for concrete walls. This damage state is governed by the structural system ductility.

The fragility functions are derived using the IDA results at the three damage states. Estimating the fragility functions is one of the main challenges in producing fragility curves. Analytical fragility curves can be illustrated through log-normal distribution function, as shown in Eq. (9).

$$P(C\backslash IM = x) = \emptyset\left(\frac{\ln\left(\frac{x}{\theta}\right)}{\beta}\right) \quad (9)$$

The fragility function is described using the median of IMs (θ) and the IMs standard deviation or dispersion (β). These parameters can be approximated using one of the two popular statistical approaches; method of moments or maximum likelihood method. In method of moments, fragility parameters are evaluated such that the produced fragility distribution has moments (i.e. mean and standard deviation) similar to those of the analytical data. Alternatively, using maximum likelihood method, fragility parameters are estimated to produce a fragility distribution that would most likely re-produce observed data. In this study, maximum likelihood method is

implemented in estimating fragility functions since it provides better representation of the phenomenon and works with truncated IDA and Multiple Stripe Analysis (MSA) [56]. The fitted fragility functions are then adjusted to account for the different sources of uncertainty as per FEMA P695 approach described in section 2.3.2. In this case, record to record uncertainty (β_{RTR}) is given a fixed value of 0.4 for the chosen far-field record set. From Table 3-1 in FEMA P695 [6], a value of 0.2 is chosen for the design basis uncertainty (β_{DR}). This is based on a medium completeness and robustness since the buildings are designed and detailed to resist lateral loads. Additionally, the confidence in the basis of design requirements is high as the buildings are designed according to IBC'12 requirements. The materials, components, assembly and system behaviour are well understood and documented for special and ordinary RC shear walls. Therefore, the test data uncertainty (β_{TD}) is given a value of 0.2 from Table 3-2 in FEMA P695 [6] corresponding to a medium completeness and robustness and high confidence in test results. Finally, nonlinear modeling uncertainty (β_{MDL}) is also equal to 0.2, from Table 5-3 in FEMA P695 [6], which corresponds to medium representation of collapse characteristics, high accuracy and robustness of nonlinear analysis models. This is since the nonlinear modeling is done using IDARC-2D which accounts for plastic hinge and crack formation in all structural elements. It also accounts for shear and flexural deformation in structural members. However, IDARC-2D analysis is limited to 2-Dimensions. Combining the different uncertainty parameters gives a total system collapse uncertainty (β_{TOT}) of 0.525. The total system collapse uncertainty is used to adjust the fragility curves.

4.2 Performance of High Seismicity Designs

The seismic vulnerability of the three reference buildings designed for highest seismicity estimate is assessed using nonlinear static push-over analysis, nonlinear IDA and fragility analysis. Referring to Figure 17, buildings B1-6S-H-S, B5-9S-H-S and B9-12S-H-S represents the highest seismicity designs for 6-story, 9-story and 12-story buildings, respectively. The initial cost optimized design for the special RC shear walls presented in section 3.2.2 is based on the static equivalent lateral force approach. This static method is allowed by ASCE7-10 [29] for regular buildings with heights up to 160ft, the tallest 12-story building is only 156ft. Following the static analysis, the

assumed critical design section for cantilevered shear walls is located at the base, based on the assumption of having a single plastic hinge formed at the bottom. However, before proceeding to any further performance investigations, dynamic analysis is performed using selective records for sample representative buildings of each number of floors to test the designs. For 12-story buildings, dynamic analysis resulted in a critical section different from the one suggested by the code, based on the static analysis. The code critical design section is located at the base of first floor shear wall. However, the failure mechanism initiated by dynamic seismic loads was governed by higher-mode effects and the formation of plastic hinges at upper floors. The critical section resulting in the dynamic analysis was actually shifted from the base of first floor to the bottom of the lowest floor in upper quarter of the building (10^{th} floor). The optimization done initially to the design by reducing dimensions and reinforcement for upper floors magnified the impact of higher-mode effects and triggered the failure and plastic hinge formation to be initiated at the reduced cross section. Therefore, the critical section became located at the weak spot. This is not a contradictable observation; it has been highlighted by previous researchers, such as Tremblay et al. [57], Bachmann and Linde [58], and Panneton et al [59]. It was also experimentally proven by shake table tests [60]. The higher-mode effects were most clearly seen in the slender shear walls of 12-story buildings. This resulted in plastic hinge formation at upper quarter of the buildings. Figure 29 presents modal analysis results for B9-12S-H-S initial optimized design. It is clearly noticed that relative modal weights (%) and modal participation factors are relatively high at 7^{th}, 8^{th} and 12^{th} vibration modes which highlights the impact of higher-modes. Therefore upon review of the preliminary IDA results, it was decided to slightly reduce the optimization in design to enhance the structural performance. Instead of Initially cost optimized design where cross section dimensions and reinforcement were reduced every three floors, in the performance optimized design, the upper quarter of the building is given the same cross section. The upper six floors are given the cross section and reinforcement of the sixth floor (lower quarter). Table 13 presents the revised design for 12-story buildings to optimize the seismic performance.

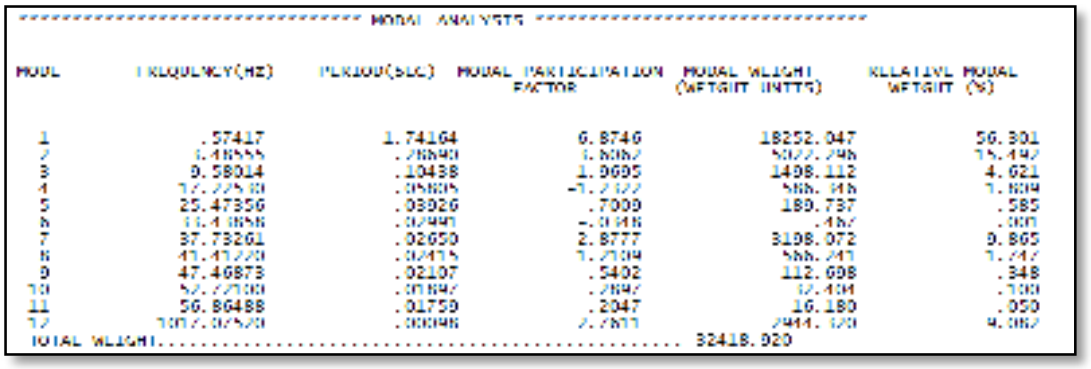

Figure 29: Sample 12-story Building (B9-12S-H-S) IDARC-2D Modal Analysis Output

Table 13: 12-Story Buildings RC Shear walls Performance Optimized Design Summary

Floors	Parameter	B9-12S-H-S	B10-12S-M-S	B11-12S-L-S	B12-12S-L-O
	L	23ft	17ft	15ft	15ft
10, 11 & 12	**T**	20in	14in	12in	12in
	L_{BE}	-	-	-	-
	R_{BE}	-	-	-	-
	$C_{BE,w}$	6#4 @ 4in	3#4 @ 4in	3#4 @ 4in	-
	$C_{BE,L}$	3#4 @ 4in	3#4 @ 4in	2#4 @ 4in	-
	R_{HW}	#6 @ 16in	#5 @ 18in	#5 @ 18in	#5 @ 18in
	R_{VW}	#7 @ 8in	#7 @ 16in	#5 @ 18in	#5 @ 18in
7, 8 & 9	**T**	20in	14in	12in	12in
	L_{BE}	-	-	-	-
	R_{BE}	-	-	-	-
	$C_{BE,w}$	6#4 @ 4in	3#4 @ 4in	3#4 @ 4in	-
	$C_{BE,L}$	3#4 @ 4in	3#4 @ 4in	2#4 @ 4in	-
	R_{HW}	#6 @ 16in	#5 @ 18in	#5 @ 18in	#5 @ 18in
	R_{VW}	#7 @ 8in	#7 @ 16in	#5 @ 18in	#5 @ 18in
4, 5 & 6	**T**	22in	16in	14in	14in
	L_{BE}	-	-	-	-
	R_{BE}	-	-	-	-
	$C_{BE,w}$	6#4 @ 4in	3#4 @ 4in	3#4 @ 4in	-
	$C_{BE,L}$	3#4 @ 4in	3#4 @ 4in	2#4 @ 4in	-
	R_{HW}	#6 @ 12in	#6 @ 16in	#5 @ 18in	#5 @ 16in
	R_{VW}	#7 @ 4in	#7 @ 8in	#5 @ 16in	#5 @ 12in
1, 2 & 3	**T**	24in	18in	16in	16in
	L_{BE}	4ft	2ft	2ft	-
	R_{BE}	26 #9	14 #9	5 #6	-
	$C_{BE,w}$	6#5 @ 4in	3#4 @ 4in	3#4 @ 4in	-
	$C_{BE,L}$	3#5 @ 4in	3#5 @ 4in	2#5 @ 4in	-
	R_{HW}	#6 @ 10in	#6 @ 14in	#6 @ 14in	#6 @ 14in
	R_{VW}	#9 @ 4in	#7 @ 8in	#6 @ 8in	#6 @ 6in

T: wall thickness; L_{BE}: boundary element length; R_{BE}: boundary element reinforcement; R_{VW}: shear wall vertical reinforcement; $C_{BE,w}$: boundary element confinement reinforcement perpendicular to wall; $C_{BE,L}$: boundary element confinement reinforcement parallel to wall; R_{HW}: shear wall horizontal reinforcement.

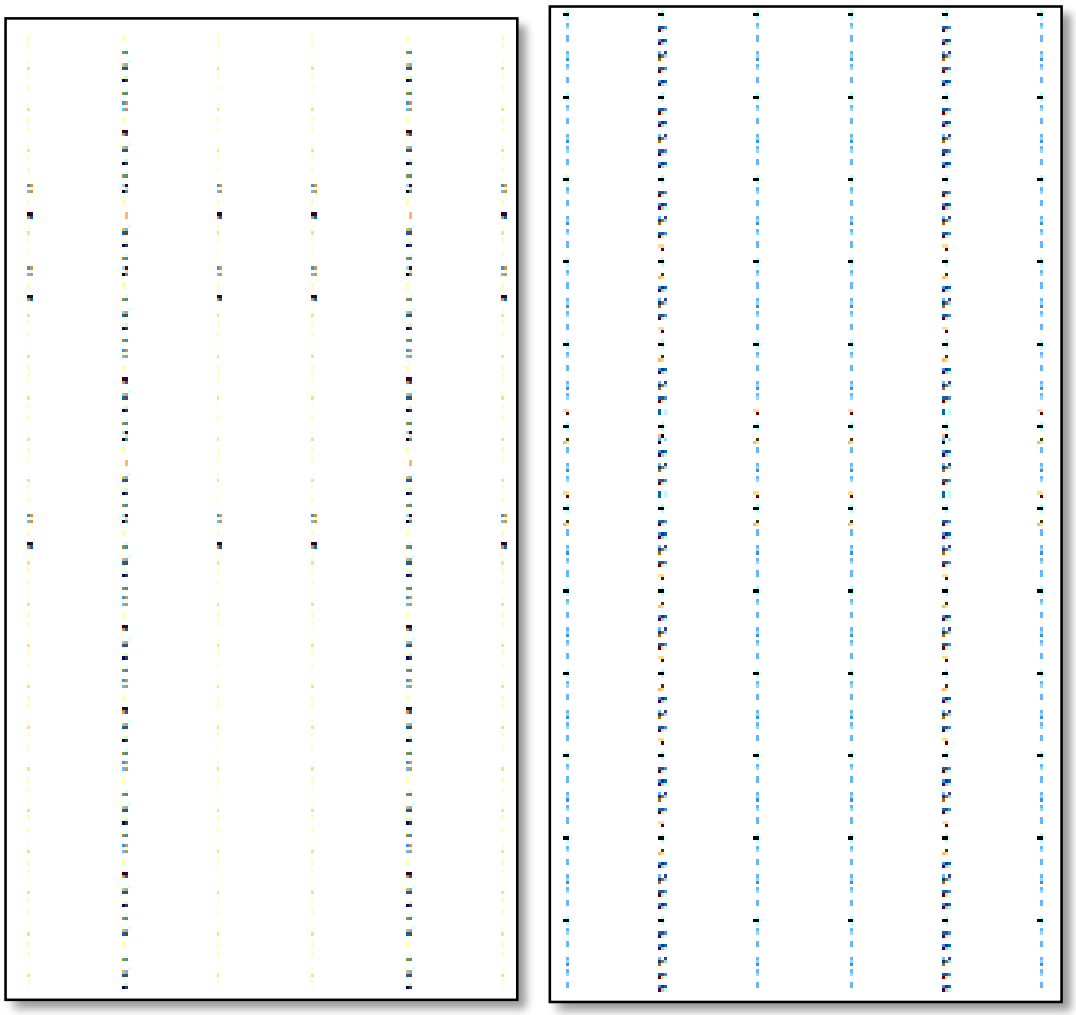

Figure 30: Sample Final Damage State of Perimeter Frame for a 12-story Building (B9-12S-H-S): (a) Initially Cost Optimized Design, (b) Performance Optimized Design

Figure 30 illustrates the collapse mechanism in cost optimized design versus performance optimized design. It is observed that for the cost optimized design, first plastic hinge is formed at the bottom and top of 10^{th} floor and bottom of 11^{th} floor. On the other hand, in performance optimized design, the plastic hinge formation is shifted to lower floors (7^{th} and 8^{th} floors). The minor upgrade in 12-story buildings design

resulted in significant enhancement in performance. For instance, in one particular case the cost optimized design collapsed at a record scaled to match a 0.6g PGA. The total structural damage index reported by IDARC-2D was 0.244 and maximum inter-story drift was 1.82%. Oppositely, the performance optimized design collapsed at a significantly higher scaling factor of 1.6g PGA. The reported overall structural damage index was 0.092 and maximum inter-story drift ratio was 1.56% at 0.6g PGA. There is a clear improvement in performance while the impact on construction cost is very marginal and will be outbalanced by the reduction in life cycle maintenance costs. Figure 30 also shows the final damage state of the gravity columns in the perimeter frame. No local failure is seen in gravity columns which confirm the adequacy of gravity columns design for deformation compatibility.

A similar phenomenon was also observed in the preliminary dynamic analysis results of 9-story buildings. Figure 31 depicts summary of modal analysis of a sample 9-story building (B5-9S-H-S). The impact of higher-modes is lesser compared to 12-story buildings. However, the dynamic analysis results suggested poor performance and pre-mature collapse for the cost optimized design compared to the performance optimized counterpart. The performance optimized design utilized the same cross section dimensions and reinforcement used in 4th floor for floors 7-9. A summary of revised performance optimized design for 9-story buildings is given in Table 14.

******************************** MODAL ANALYSIS ********************************

MODE	FREQUENCY(HZ)	PERIOD(SEC)	MODAL PARTICIPATION FACTOR	MODAL WEIGHT (WEIGHT UNITS)	RELATIVE MODAL WEIGHT (%)
1	.56868	1.75846	6.1883	14789.461	65.677
2	[illegible]	[illegible]	[illegible]	[illegible]	[illegible]
3	9.08915	.11002	2.0480	1621.311	7.200
4	[illegible]	[illegible]	[illegible]	[illegible]	[illegible]
5	24.41317	.04096	1.0294	409.226	1.817
6	[illegible]	[illegible]	[illegible]	[illegible]	[illegible]
7	39.10283	.02557	.5036	97.948	.435
8	[illegible]	[illegible]	[illegible]	[illegible]	[illegible]
9	49.36071	.02026	.2030	16.230	.072
TOTAL WEIGHT				[illegible]	

Figure 31: Sample 9-story Building (B5-9S-H-S) IDARC-2D Modal Analysis Output

Table 14: 9-Story Buildings RC Shear walls Performance Optimized Design Summary

Floors	Parameter	B5-9S-H-S	B6-9S-M-S	B7-9S-L-S	B8-9S-L-O
	L	19ft	13ft	12ft	12ft
7, 8 & 9	**T**	18in	12in	10in	10in
	L_{BE}	-	-	-	-
	R_{BE}	-	-	-	-
	$C_{BE,w}$	5#3 @ 4in	4#4 @ 4in	3#4 @ 4in	-
	$C_{BE,L}$	3#3 @ 4in	2#5 @ 4in	2#4 @ 4in	-
	R_{HW}	#6 @ 14in	#5 @ 18in	#4 @ 18in	#4 @ 16in
	R_{VW}	#9 @ 8in	#8 @ 12in	#4 @ 18in	#4 @ 16in
4, 5 & 6	**T**	18in	12in	10in	10in
	L_{BE}	-	-	-	-
	R_{BE}	-	-	-	-
	$C_{BE,w}$	5#3 @ 4in	4#4 @ 4in	3#4 @ 4in	-
	$C_{BE,L}$	3#3 @ 4in	2#5 @ 4in	2#4 @ 4in	-
	R_{HW}	#6 @ 14in	#5 @ 18in	#4 @ 18in	#4 @ 16in
	R_{VW}	#9 @ 8in	#8 @ 12in	#4 @ 18in	#4 @ 16in
1, 2 & 3	**T**	20in	14in	12in	12in
	L_{BE}	3.5ft	2.5ft	1.5ft	-
	R_{BE}	22 #10	12 #9	8 #6	-
	$C_{BE,w}$	5#4 @ 4in	4#4 @ 4in	3#4 @ 4in	-
	$C_{BE,L}$	3#5 @ 4in	2#5 @ 4in	2#5 @ 4in	-
	R_{HW}	#6 @ 10in	#5 @ 10in	#5 @ 18in	#5 @ 18in
	R_{VW}	#9 @ 4in	#9 @ 6in	#6 @ 8in	#6 @ 9in

T: wall thickness; L_{BE}: boundary element length; R_{BE}: boundary element reinforcement; R_{VW}: shear wall vertical reinforcement; $C_{BE,w}$: boundary element confinement reinforcement perpendicular to wall; $C_{BE,L}$: boundary element confinement reinforcement parallel to wall; R_{HW}: shear wall horizontal reinforcement.

As presented in Figure 32, using the performance optimized design; the building did not pre-maturely collapse before engaging the critical section at the base of the cantilevered shear wall. This is a much preferred failure mechanism compared to the cost optimized design where upper reduced sections cause the structure to collapse. The performance optimized design collapsed at a record scaled to 2g PGA while the cost optimized design collapsed at 0.5g PGA. Furthermore, at the same scale factor of 0.5g PGA cost optimized design reached a peak inter-story drift ratio of 1.35% and total structural damage index of 0.088. On the other hand, performance optimized design reached a peak inter-story drift ratio of 0.73% and total structural damage index of 0.14. Therefore, the upgrade in performance is unquestionable and is totally worth the

slight increase in construction cost. It is also observed from Figure 32 that there are no local failures occurring in gravity columns. This shows that gravity columns design is sufficient for deformation compatibility.

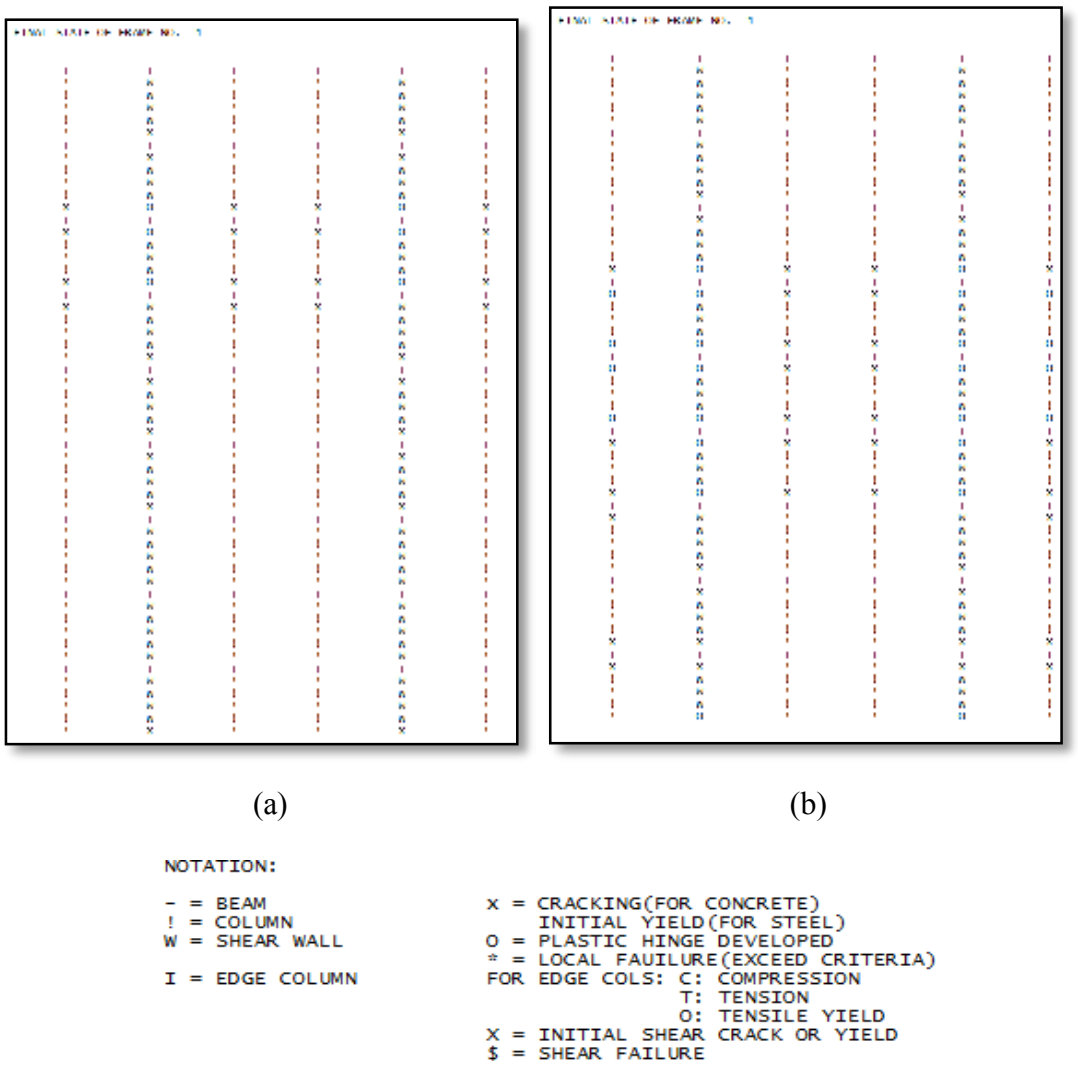

Figure 32: Sample Final Damage State of Perimeter Frame for a 9-story Building (B5-9S-H-S): (a) Initially Cost Optimized Design, (b) Performance Optimized Design

The impact of higher-modes is not very clear in the 6-story buildings. The initially cost optimized design for the shear walls performed satisfactory during initial dynamic analysis. However, significant damage was also observed in fourth floor (first reduced section) and such mechanism is not favorable to most structural engineers. Therefore, for 6-story buildings, a single cross-section was used for all floors with terminating boundary element at third floor. This conforms to the state-of-art design

and construction practices in Dubai, UAE. It also matches the design philosophy adopted in other 12-story and 9-story buildings by keeping the same cross section and reinforcement for upper six floors. Moreover, by utilizing a single cross section, higher-mode effects are totally eliminated and undesirable collapse patterns are avoided. The impact on construction cost is not significant given the reduction in varying formwork sizes and the enhancement in expected performance. The revised performance optimized design for 6-story buildings is summarized in Table 15.

Table 15: 6-Story Buildings RC Shear Walls Performance Optimized Design Summary

Floors	Parameter	B1-6S-H-S	B2-6S-M-S	B3-6S-L-S	B4-6S-L-O
	L	15ft	10ft	8ft	8ft
4, 5 & 6	**T**	16in	10in	10in	10in
	L_{BE}	-	-	-	-
	R_{BE}	-	-	-	-
	$C_{BE,w}$	4#4 @ 4in	4#3 @ 4in	2#3 @ 4in	-
	$C_{BE,L}$	2#4 @ 4in	4#3 @ 4in	2#3 @ 4in	-
	R_{HW}	#6 @ 9in	#6 @ 10in	#5 @ 16in	#5 @ 12in
	R_{VW}	#9 @ 4in	#9 @ 4in	#6 @ 8in	#8 @ 8in
1, 2 & 3	**T**	16in	10in	10in	10in
	L_{BE}	3ft	2.6ft	1ft	-
	R_{BE}	16 #10	14 #9	6 #6	-
	$C_{BE,w}$	4#4 @ 4in	4#4 @ 4in	2#4 @ 4in	-
	$C_{BE,L}$	2#5 @ 4in	2#5 @ 4in	2#4 @ 4in	-
	R_{HW}	#6 @ 9in	#6 @ 10in	#5 @ 16in	#5 @ 12in
	R_{VW}	#9 @ 4in	#9 @ 4in	#6 @ 8in	#8 @ 8in

T: wall thickness; L_{BE}: boundary element length; R_{BE}: boundary element reinforcement; R_{VW}: shear wall vertical reinforcement; $C_{BE,w}$: boundary element confinement reinforcement perpendicular to wall; $C_{BE,L}$: boundary element confinement reinforcement parallel to wall; R_{HW}: shear wall horizontal reinforcement.

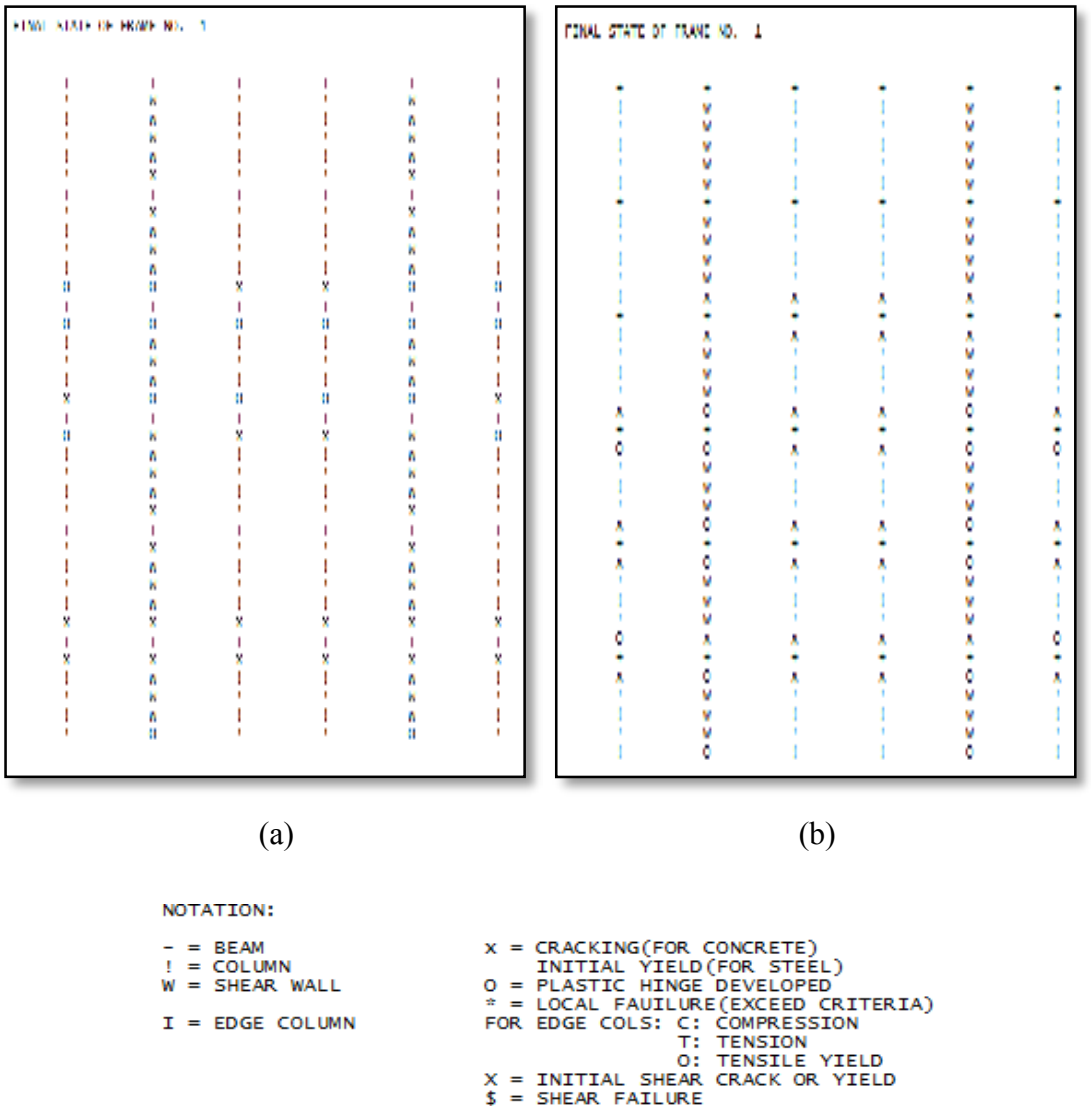

Figure 33: Sample Final Damage State of Perimeter Frame for a 6-story Building (B1-6S-H-S): (a) Initially Cost Optimized Design, (b) Performance Optimized Design

The final damage state of the lateral system of a sample 6-story building (B1-6S-H-S) is shown in Figure 33. It is observed that performance optimized design exhibits a more desirable distribution of plastic hinges and collapse mechanism. In this particular case the two designs collapsed at the same scale factor of 2.0g PGA. The maximum drift ratio and total structural damage index were 4.52% and 0.14, respectively for cost optimized design at 2.0g PGA. Similarly, at the same level of 2.0g PGA, peak drift ratio was 2.8% and structural damage index was 0.071 for performance optimized design. Similar to 12-story and 9-story buildings, the final damage state presented in Figure 33 shows that no local failures are happening in gravity columns.

Therefore, the deformation compatibility requirements are satisfied and the collapse is not resulting from local mechanisms in gravity columns.

The impact of the RC shear walls reinforcement on the overall performance is investigated. This is done to guarantee that the conclusions are not sensitive to a particular design. For each group of buildings, the high seismicity design is chosen to represent the group. The walls' designs are varied by altering the boundary element vertical reinforcement, horizontal and vertical wall reinforcement by +/-15%. Afterwards, the resulting capacity curves from push over analysis are compared as shown in Figure 34.

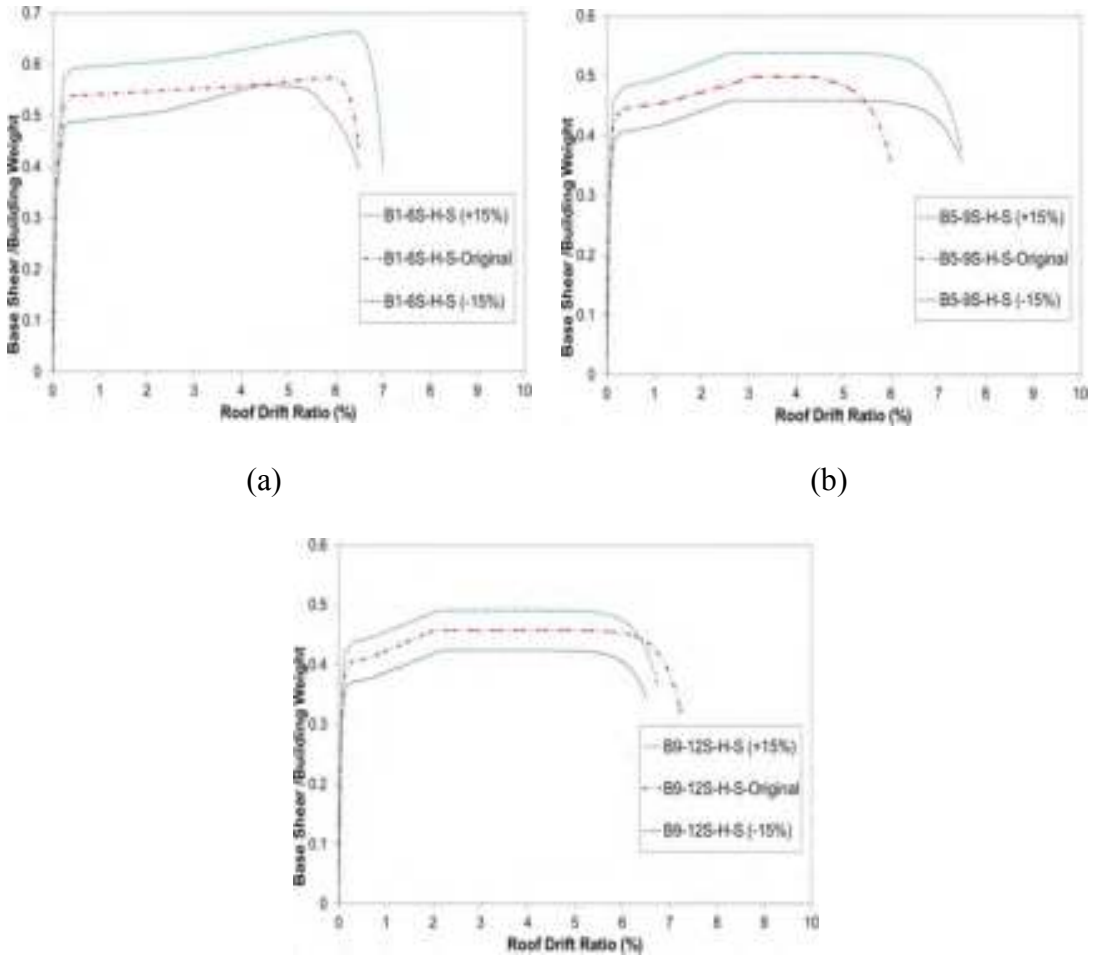

(a) (b)

(c)

Figure 34: Capacity Curves: (a) 6-Story Building, (b) 9-Story Building, (c) 12-Story Building

As expected, there are minor differences in the structural response when some design changes are introduced. This observation is common among the 6-story, 9-story and 12-story buildings. The main differences between the designs are either slight increase or decrease in the yield strength and base shear capacity. However, the overall structural response pattern is conserved. This confirms that the global performance conclusions are not very sensitive to a particular design.

The next three subsections present the performance investigation results for the highest seismicity designs which are B1-6S-H-S, B5-9S-H-S and B9-12S-H-S. The three high seismicity buildings are designed with special RC shear walls. It will be seen that even though the design of 12-story and 9-story buildings has been upgraded, the higher-mode effects are still present. The performance optimized designs showed structural response that is satisfactory to most structural engineers and building officials. However, the failure in 12-story and 9-story buildings is still not resulting from the critical design section at the wall base; instead it is resulting from the damages at upper floors which have weaker reduced sections. As a result, these buildings did not satisfy the performance criteria recommended by FEMA P695 for collapse safety.

4.2.1 Nonlinear Static Push-Over Analysis Results. The expected seismic performance of the buildings is initially evaluated using nonlinear static push-over analysis. Analysis results are used to establish the back-bone curves for each building. Figure 35 depicts capacity curves for buildings B1-6S-H-S, B5-9S-H-S and B9-12S-H-S, respectively. In back-bone curves, the vertical axis represents the base shear capacity normalized by the building seismic weight and the horizontal axis is the roof drift ratio. Normalized base shear capacities are 0.57, 0.5 and 0.46 for B1-6S-H-S, B5-9S-H-S and B9-12S-H-S, respectively. As expected, base shear capacity is higher for the shorter building (6-story). This is attributed to the relatively higher stiffness of squat shear walls compared to their slender counterpart. It is worth mentioning that the seismic capacity estimated using push-over analysis is completely independent of any seismic demand. B1-6S-H-S reached a maximum roof drift ratio of 6.5%, while B5-9S-H-S reached 6% and B9-12S-H-S reached 7.25%. Ultimate roof displacements corresponding to 20% loss of shear capacity, as defined by FEMA P695 [6], are 60.45in, 82.03in and 132.7in for B1-6S-H-S, B5-9S-H-S and B9-12S-H-S, respectively. The three buildings have period-based ductility calculated as recommended by FEMA P695 [6] greater than 8, which represents a ductile behavior.

Additionally, the behavior of the three designs is linear elastic at relatively low drift ratios. The 12-story building (B9-12S-H-S) has a flat slope at the peak base shear capacity; it is approximately behaving in an elastic perfectly plastic manner. Similarly, the 9-story building (B5-9S-H-S) has a less flat slope at the ultimate force. On the other hand, the 6-story building (B1-6S-H-S) has an increasing slope until it reaches the maximum base shear capacity, which then drops sharply. It can also be observed that in the three high seismicity designs, the capacity curves do not experience severe degradation in strength or deterioration in stiffness which matches the expected behavior of well detailed special RC shear walls.

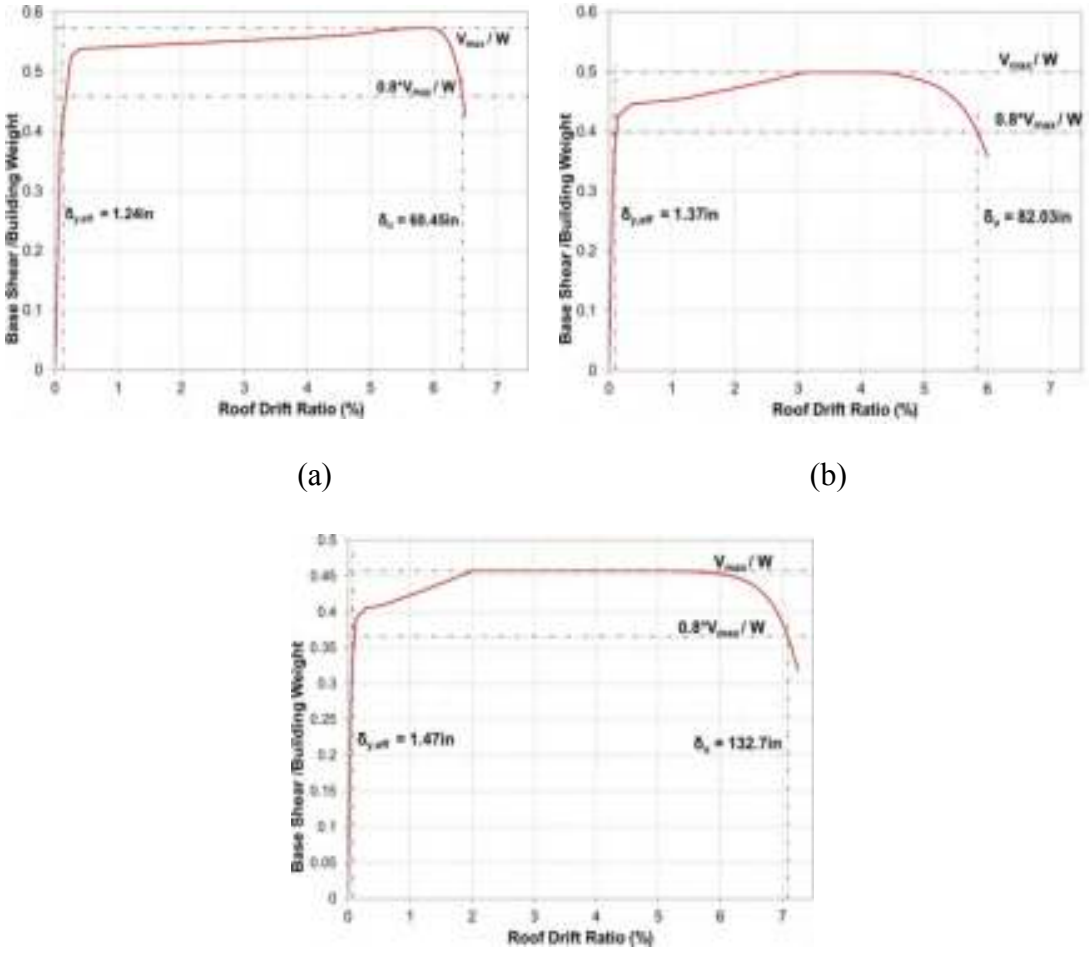

(a) (b)

(c)

Figure 35: Back-Bone Curves: (a) B1-6S-H-S; (b) B5-9S-H-S; (c) B9-12S-H-S

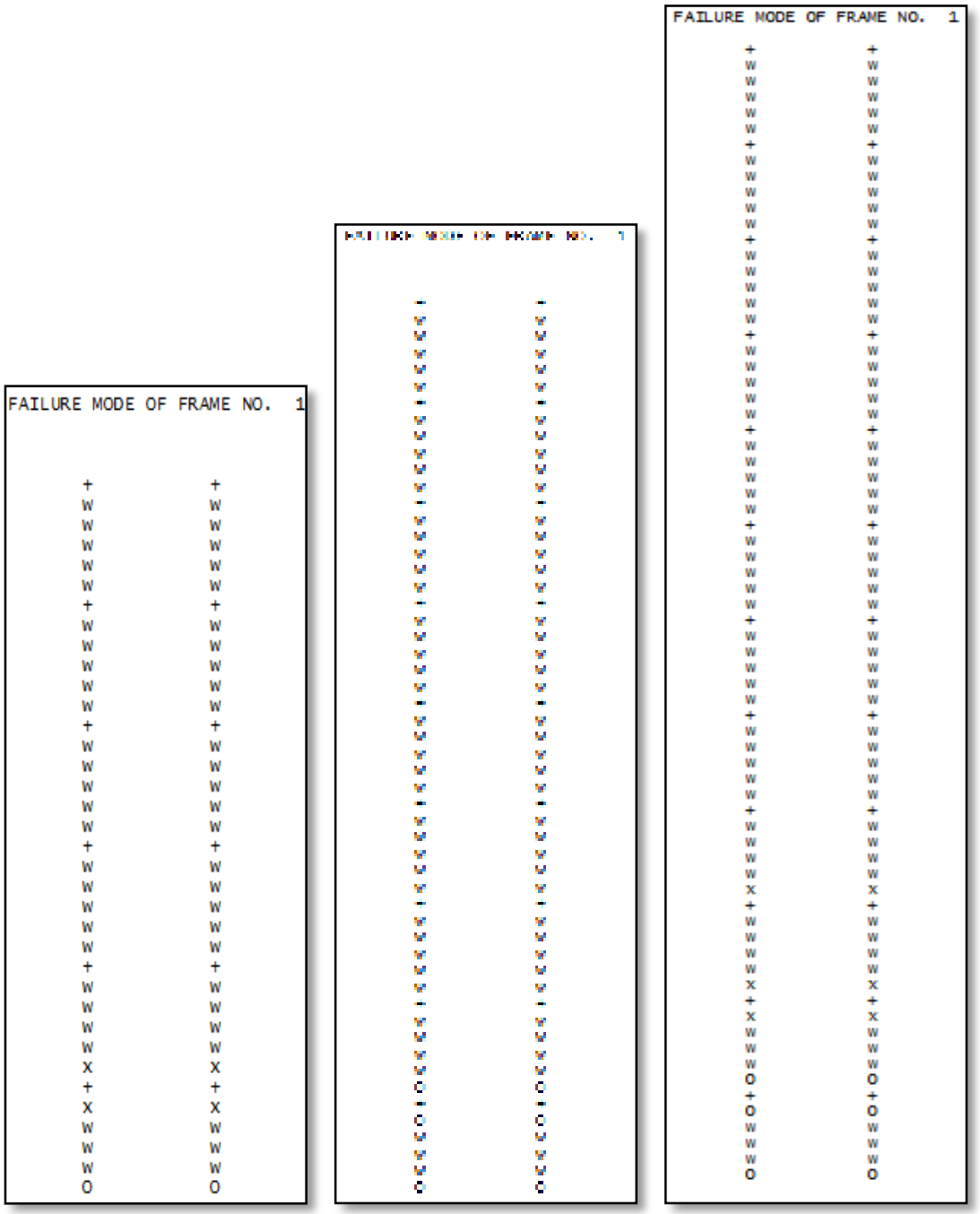

Figure 36: Buildings' Final Damage State: (a) B1-6S-H-S; (b) B5-9S-H-S; (c) B9-12S-H-S

Figure 36 shows the final damage state of the buildings after reaching 20% loss in base shear capacity. B5-9S-H-S and B9-12S-H-S developed plastic hinges at top and bottom of first floor shear walls, while B1-6S-H-S has only plastic hinging at the critical section at the base. It can be noticed that static push-over analysis resulted in a failure mode at the base of the shear walls conforming to the design code assumed critical section. The overall structural damage index reported by IDARC-2D is 0.359, 0.426 and 0.618 for B1-6S-H-S, B5-9S-H-S and B9-12S-H-S. It is worth mentioning that these damages are concentrated at first floor shear walls.

4.2.2 Nonlinear Incremental Dynamic Analysis Results. The expected seismic performance of the high seismicity designs is investigated under the random nature of earthquakes. IDA provides better insight of the expected structural response compared to the static analysis. This is due to its dynamic nature and its ability to capture the response of systems vibrating in any mode, not necessarily the fundamental mode [37]. The IDA in this case is performed using a very fine increment of 0.1g for the spectral accelerations. The increments are increased until all records cause the structures to collapse or exceed the CP maximum drift ratio limit of 2% as specified by ASCE41[53].

It should be noted that the MCE level (S_{MT}), mentioned from this point onwards, refers to the highest seismicity estimate level. This is particularly chosen to achieve the objectives of this research of investigating the performance, construction and life cycle cost of the different designs under the high seismic hazard that might be present in Dubai. This scenario will simulate a conservative possible seismic hazard in Dubai and its consequences on performance of buildings designed for different seismic hazard levels.

Figure 37 presents the resulting IDA curves for high seismicity designs (i.e. B1-6S-H-S, B5-9S-H-S and B9-12S-H-S). The structural response derived from IDA curves can depend to some extent on the characteristics of the particular accelerograms used. Thus, the performance is judged based on the suit of records to segregate this effect. On average, at low drift ratios (approximately up to 1%), the three designs (B1-6S-H-S, B5-9S-H-S and B9-12S-H-S) exhibit a linear behavior. The same linear behavior is resulting from some of the ground motion records up to the MCE spectral acceleration. At higher spectral accelerations, the structural response starts to vary

showing several patterns of nonlinearities, such as softening, hardening and weaving. For only few records, the structure seems to soften and move to large drifts rapidly until it reaches collapse. Collapse in these curves, whether resulting from convergence issues, numerical instabilities, or very large drift ratio, is represented using a drift ratio of 10% and a flat line in IDA curves.

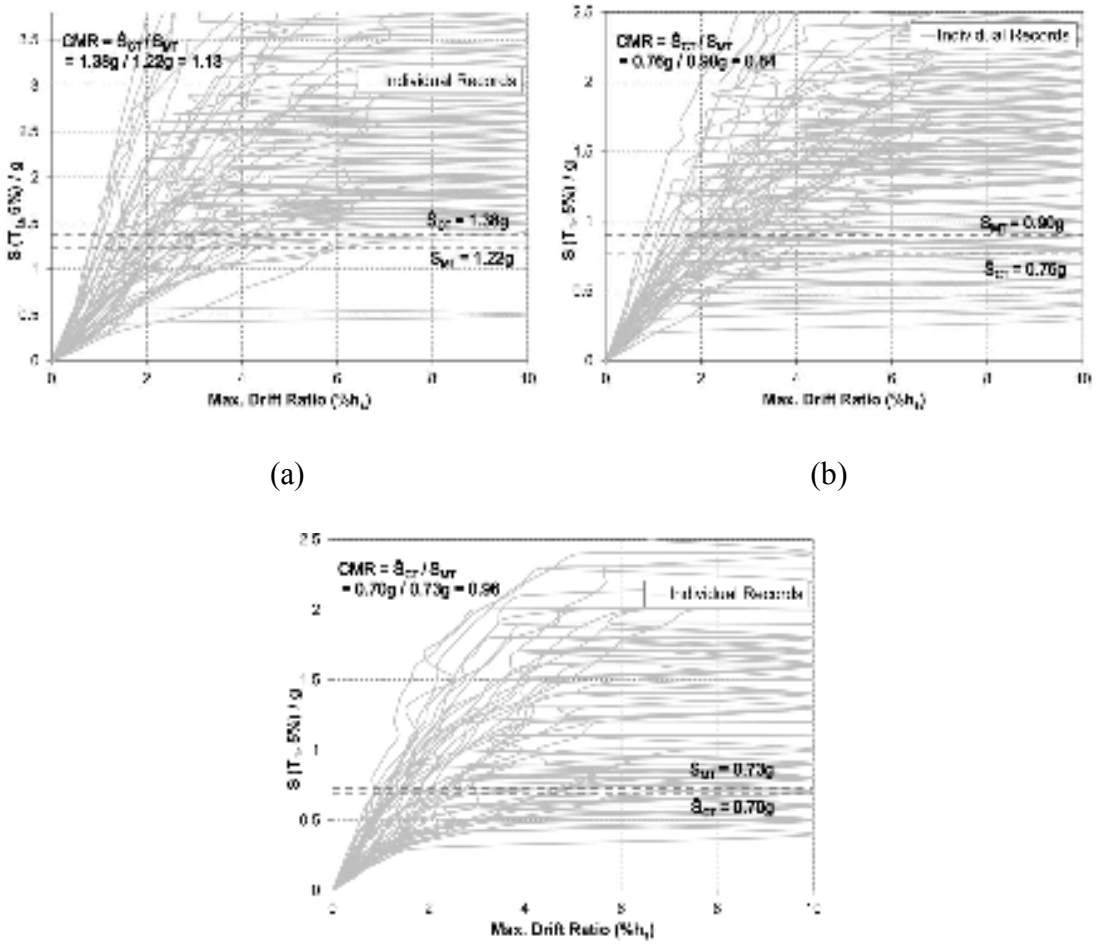

(a) (b)

(c)

Figure 37: Incremental Dynamic Analysis Curves: (a) B1-6S-H-S; (b) B5-9S-H-S; (c) B9-12S-H-S

The majority of the earthquake records caused severe hardening and weaving around the elastic response. The weaving observation conforms to the common equal displacement rule stating that inelastic and elastic displacements are equal for structures with relatively moderate time periods [61]. In addition, for some records, the hardening

phenomena in which the structure seems to perform better at higher intensities is sort of against the common expectation [61]. This is because generally the time and pattern of the time-history governs the response more than just the intensity. Moreover, the upward scaling done to the records makes the less responsive cycles at the beginning of the time-history strong enough to cause damage and yielding of the structural elements. Therefore, some strong ground motion records at some intensity might cause early yielding of a specific floor, usually low floor. This floor acts as a sacrificial fuse which reduces the response of higher floors [61]. Another very interesting observation that is clearly seen in IDA curves shown in Figure 37 is what is called "Structural Resurrection." This phenomenon has been observed by [61] and is defined as a severe hardening behavior. In structural resurrection, the building moves all the way to complete collapse (numerical instability or convergence issues) at some intensity. Then at higher intensities it shows a lower or higher response, but without collapsing. This happens because the time and pattern of the ground motion record at a particular intensity might be more damaging than at a higher intensity. In other words, this intensity causes the structure to resonate [61]. This is observed in the three designs, but more often in shorter buildings; B1-6S-H-S (6-story) and B5-9S-H-S (9-story) compared to the 12-story building (B9-12S-H-S). To capture this phenomenon during the IDA runs, even when the structure collapses at any intensity, the particular record is scaled up again and analysis is re-run. However, after three consecutive failures, it was assumed that the structure has collapsed. From Figure 37 (a), B1-6S-H-S design seems very robust. It reached significantly high spectral accelerations for several records without flattening the IDA curve or indicating high rate of damage accumulation. Furthermore, B1-6S-H-S behaved linearly for few records up to 3.8g. Similar behavior is also noticed for B5-9S-H-S design. It reached up to 2.5g for some records with linear relationship. This is less clear in B9-12S-H-S design which showed more obvious weaving and softening behavior. The median collapse intensity ($\hat{S}_{CT}$); the spectral acceleration at which 50% (22) of the records caused the structure to collapse, is1.38g, 0.76g and 0.70g for B1-6S-H-S, B5-9S-H-S and B9-12S-H-S, respectively. Moreover, it can be observed from Figure 37 that the number of flat lines representing collapse for the three designs is significantly higher above the MCE level (S_{MT}). This indicates that high seismicity designs reach collapse, excessively large drift ratios and global instabilities, at spectral accelerations much higher than MCE level. Furthermore, comparing median collapse intensity ($\hat{S}_{CT}$) to MCE level (S_{MT}), the Collapse Margin

Ratio (CMR) is 1.13, 0.84 and 0.96 for B1-6S-H-S, B5-9S-H-S and B9-12S-H-S, respectively. Based on CMR, only the 6-story building design (B1-6S-H-S) has an acceptable, but low collapse margin. However, the CMR has to be adjusted to account for sources of uncertainties and spectral shape of ground motion records before being used to judge the structural performance. The adjusted values for CMRs are shown in the next subsection.

4.2.3 Fragility Analysis. The seismic vulnerability of the three designs is investigated with the use of fragility curves. Additionally, the performance is quantified at the three limit states given by ASCE41 [53]. Using total system collapse uncertainty (β_{TOT}) of 0.525, calculated in section 4.1.4, IDA results are adjusted. Then the CMR calculated from adjusted results is multiplied by SSF to account for the period elongation and spectral content of the records. SSF is given in Tables 7-1a and 7-1b in FEMA P695 based on seismic design level, fundamental period of the structure and period-based ductility. SSF is 1.39 for B1-6S-H-S, 1.46 for B5-9S-H-S and 1.53 for B9-12S-H-S. Analytical, fitted and adjusted collapse fragility curves are given in Figure 38 for B1-6S-H-S, B5-9S-H-S and B9-12S-H-S. Collapse is defined in FEMA P695 as either when the structure reaches excessive lateral drift (global dynamic instability) or through limit state criteria. In this study, the latter option is adapted in creating collapse fragility curves. Therefore, collapse in this case will be defined as exceeding the drift ratio limit of CP Limit state of ASCE41 which is 2% for concrete walls [53]. In Figure 38 (a), it is observed that building B1-6S-H-S collapse fragility curve is very flat and only approaches plateau at a significantly high spectral acceleration of 3.8g. Similarly, B5-9S-H-S and B9-12S-H-S designs show relatively flat collapse fragility curves presented in Figures 38 (b) and (c). The adjusted median collapse intensity (S_{CT}) is 1.92g, 1.1g and 1.07g for designs B1-6S-H-S, B5-9S-H-S and B9-12S-H-S, respectively. ACMRs are evaluated using the adjusted median collapse intensity (S_{CT}) and S_{MT}. The calculated ACMR is 1.57 for B1-6S-H-S, 1.23 for B5-9S-H-S and 1.47 for B9-12S-H-S. This indicates 57%, 23% and 47% margin of safety against collapse for buildings B1-6S-H-S, B5-9S-H-S and B9-12S-H-S, respectively. With the adjusted IDA results, the fragility curves are constructed for three damage states namely: IO, LS and CP. The three limit states fragility curves are given in Figure 39 for the three designs.

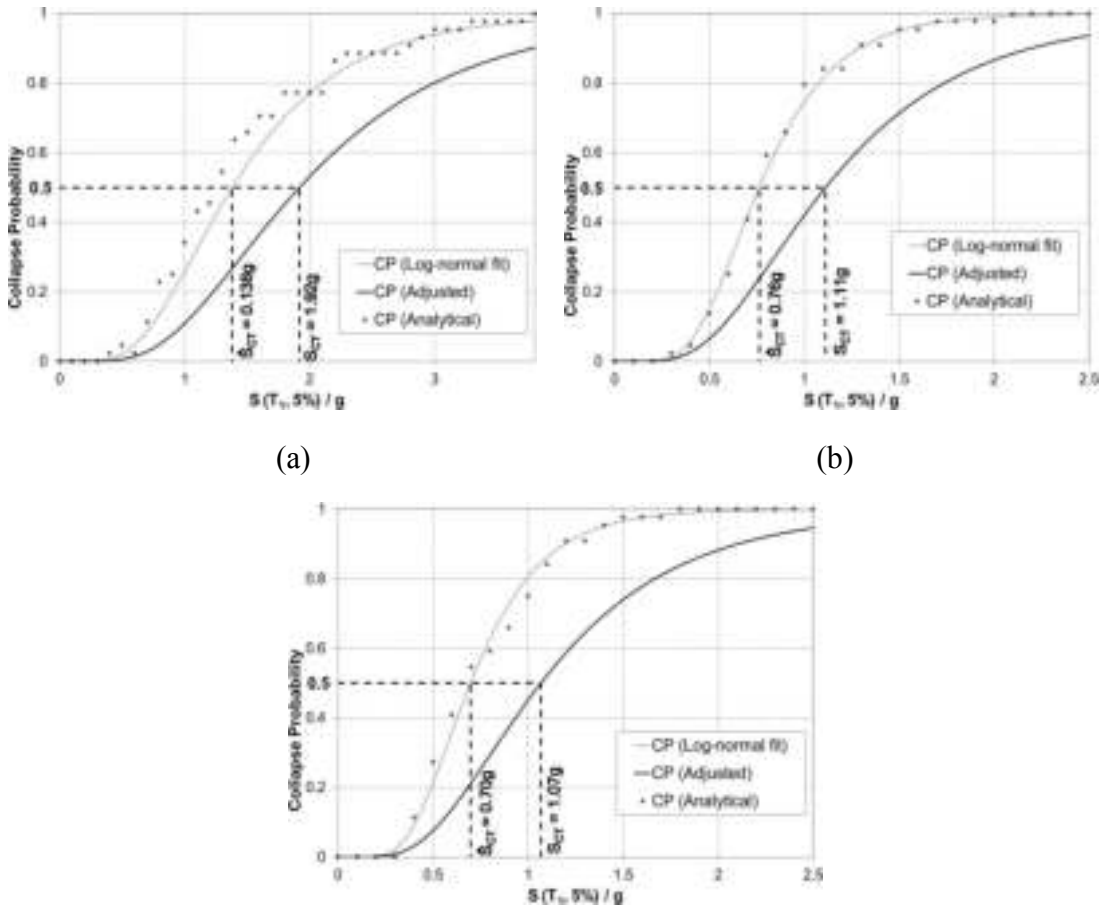

Figure 38: Collapse Fragility Curves: (a) B1-6S-H-S; (b) B5-9S-H-S; (c) B9-12S-H-S

The three buildings (B1-6S-H-S, B5-9S-H-S and B9-12S-H-S) show satisfactory performance, having flatter fragility curves at the three limit states. The steepness of the fragility curve is reduced moving from IO to CP, which indicates higher probabilities of exceeding IO performance level compared to CP. At B1-6S-H-S MCE level (S_{MT}) of 1.22g, there is 20% probability that the design exceeds CP limits state, 66% it exceeds LS limit state and 95% it exceeds IO damage limit. Similarly for B5-9S-H-S at the MCE level (S_{MT}) of 0.90g, the probabilities are 34%, 71% and 97% of exceeding CP, LS and IO, respectively. Finally, B9-12S-H-S has a 23% probability of exceeding CP, 64% of exceeding LS and 94% of exceeding IO at the MCE level of 0.73g. Therefore, only the 6-story building (B1-6S-H-S) satisfies the performance criteria recommended by FEMA P695 to have a collapse probability of 20% or less at the MCE level. As mentioned earlier at the beginning of this section, higher-mode effects are still present in the slender shear walls of 12-story and 9-story buildings. This

resulted in failure happening in the weak reduced sections instead of the design section. However, the structural performance of these buildings (B5-9S-H-S and B9-12S-H-S) is seen satisfactory to most structural/earthquake engineers and building officials. They have reasonable margin of safety against collapse (i.e. 23% for B9-12S-H-S and 34% for B5-9S-H-S, respectively).

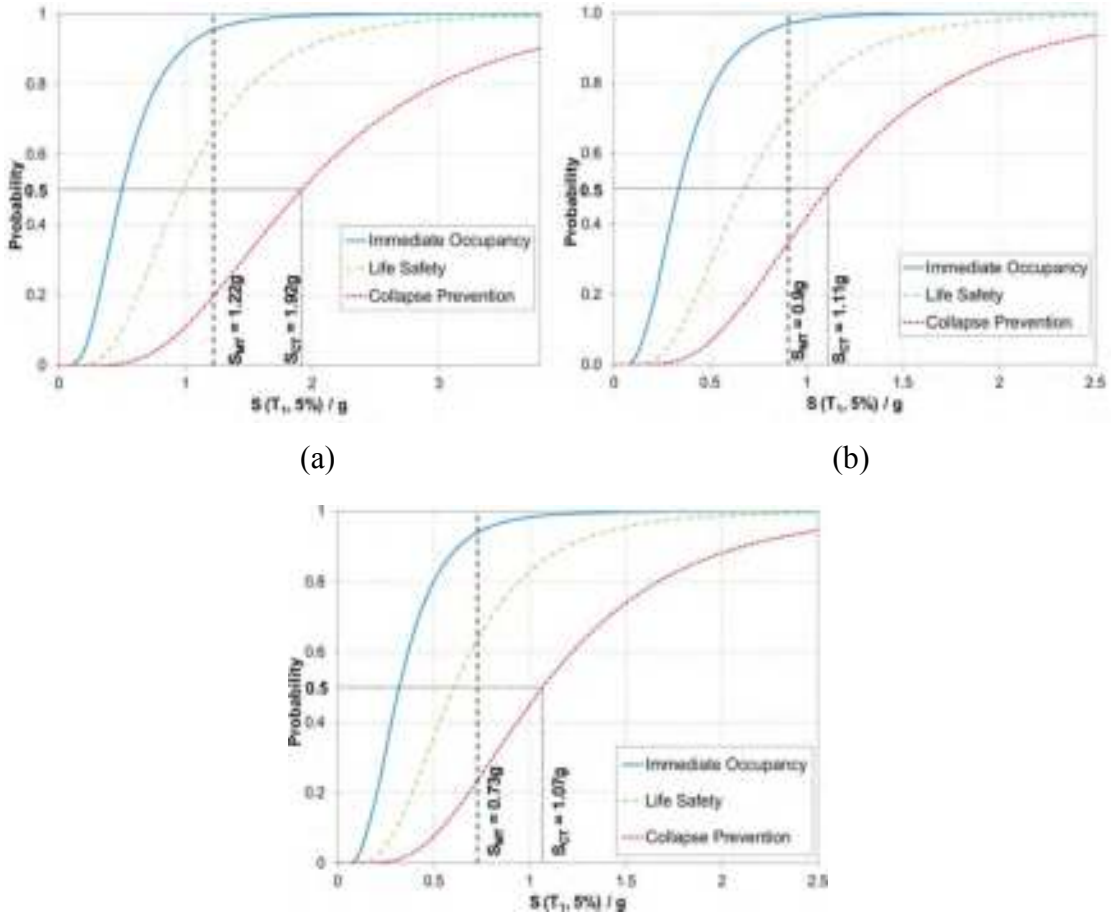

Figure 39: IO, LS and CP Fragility Curves: (a) B1-6S-H-S; (b) B5-9S-H-S; (c) B9-12S-H-S

4.3 Performance of Moderate Seismicity Designs

The following three subsections present the performance investigation results of the buildings designed for moderate seismicity estimate of Dubai. Referring to Figure 17, buildings B2-6S-M-S, B6-9S-M-S and B10-12S-M-S represent moderate

seismicity designs. The lateral force resisting system for moderate seismicity designs is special RC shear walls.

4.3.1 Nonlinear Static Push-Over Analysis Results. Initial investigation of structural response is done using nonlinear static push-over analysis. Back-bone curves are established for each design. Established capacity curves are presented in Figure 40 for buildings B2-6S-M-S, B6-9S-M-S and B10-12S-M-S.

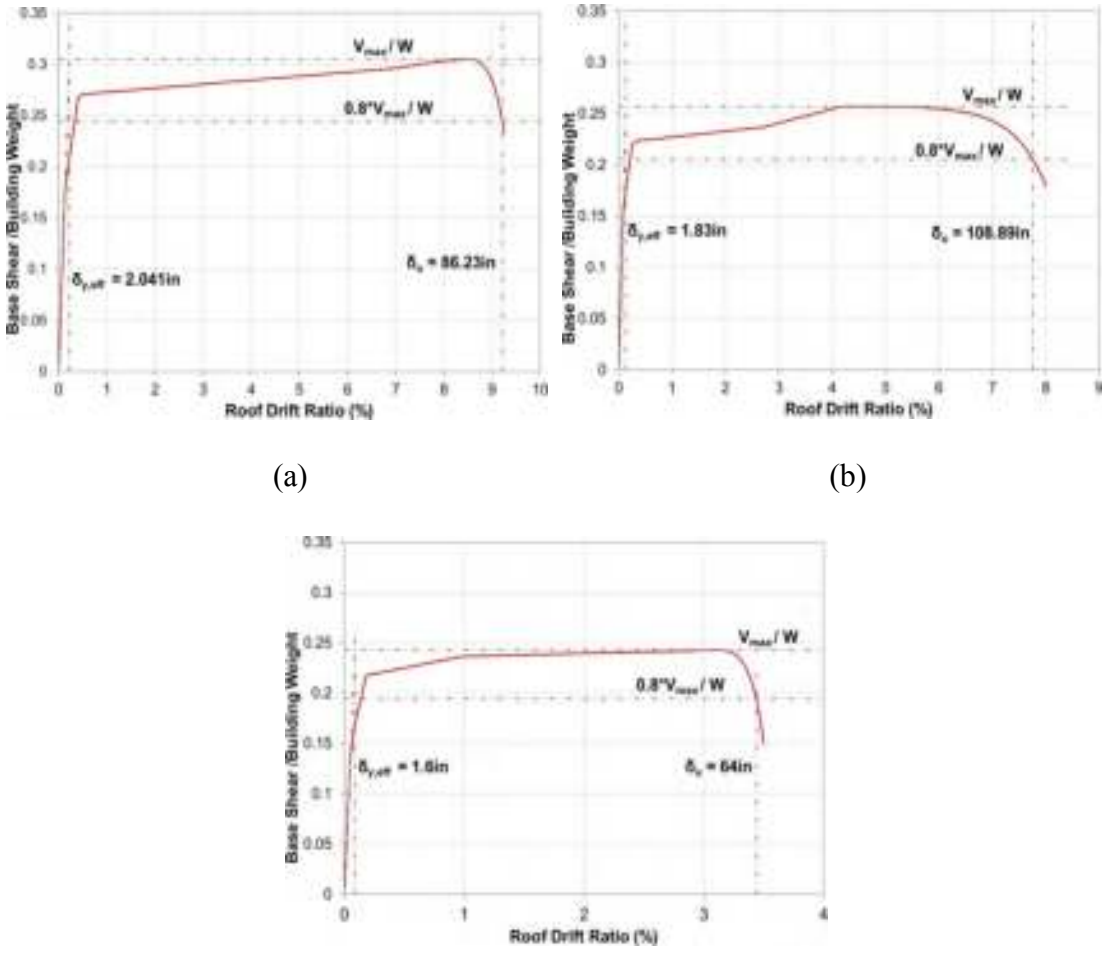

(a) (b)

(c)

Figure 40: Back-Bone Curves: (a) B2-6S-M-S; (b) B6-9S-M-S; (c) B10-12S-M-S

From shown capacity curves, normalized base shear capacities are 0.31, 0.26 and 0.24 for buildings B2-6S-M-S, B6-9S-M-S and B10-12S-M-S, respectively. The 6-story building has the highest normalized base shear capacity due to its lateral system (shear walls) relatively higher stiffness. Maximum drift ratios achieved by B2-6S-M-S,

B6-9S-M-S and B10-12S-M-S are 9.25%, 8% and 3.5%, respectively. As defined by FEMA P695, ultimate roof displacements corresponding to 20% reduction in shear capacity are 86.23in, 108.89in and 64in for B2-6S-M-S, B6-9S-M-S and B10-12S-M-S. The three designs have period-based ductility greater than 8 calculated as recommended by FEMA P695. Moreover, B2-6S-M-S, B6-9S-M-S and B10-12S-M-S designs behave linearly at low drift ratios. At the peak base shear, buildings B6-9S-M-S and B10-12S-M-S have a flat slope, while B2-6S-M-S has a positive increasing slope until it achieves maximum base shear capacity which then drops suddenly. Additionally, it is clear from the back-bone curves that the special RC shear walls designed for moderate seismicity are experiencing mild strength degradation and stiffness deterioration.

Final Damage states, at 20% reduction in base shear capacity, of the three buildings are illustrated in Figure 41. In building B6-9S-M-S, plastic hinges are developed at top and bottom of first floor shear walls. However, B2-6S-M-S and B10-12S-M-S share a similar mechanism at the bottom of first floor walls. The overall structural damage index reported by IDARC-2D is 0.371 for B2-6S-M-S, 0.455 for B6-9S-M-S and 0.359 for B10-12S-M-S. It should be noted that these damages are triggered at the first floor shear walls only. Therefore, similar to high seismicity designs, the pseudo static push-over analysis results of moderate seismicity designs is suggesting a single critical section at the base of the wall. This conclusion matches with design code recommendation for regular buildings permitted to be designed following the static method (SELF) by ASCE7-10 [29].

4.3.2 Nonlinear Incremental Dynamic Analysis Results. Moderate seismicity designs performance is further investigated using IDA to capture the dynamic response and the impact of higher-modes. The analysis is performed using 0.1g increments of spectral accelerations until all records collapse the structure or cause drift ratios that exceed CP drift limit. Figure 42 depicts IDA curves for moderate seismicity designs (B2-6S-M-S, B6-9S-M-S and B10-12S-M-S). IDA curves show that, on average, the three designs exhibit a linear behavior at low drift ratios except for some ground motion records in which the structure remains linear up to significantly high spectral accelerations. At higher spectral accelerations, most records show nonlinear structural response, such as softening, hardening and weaving.

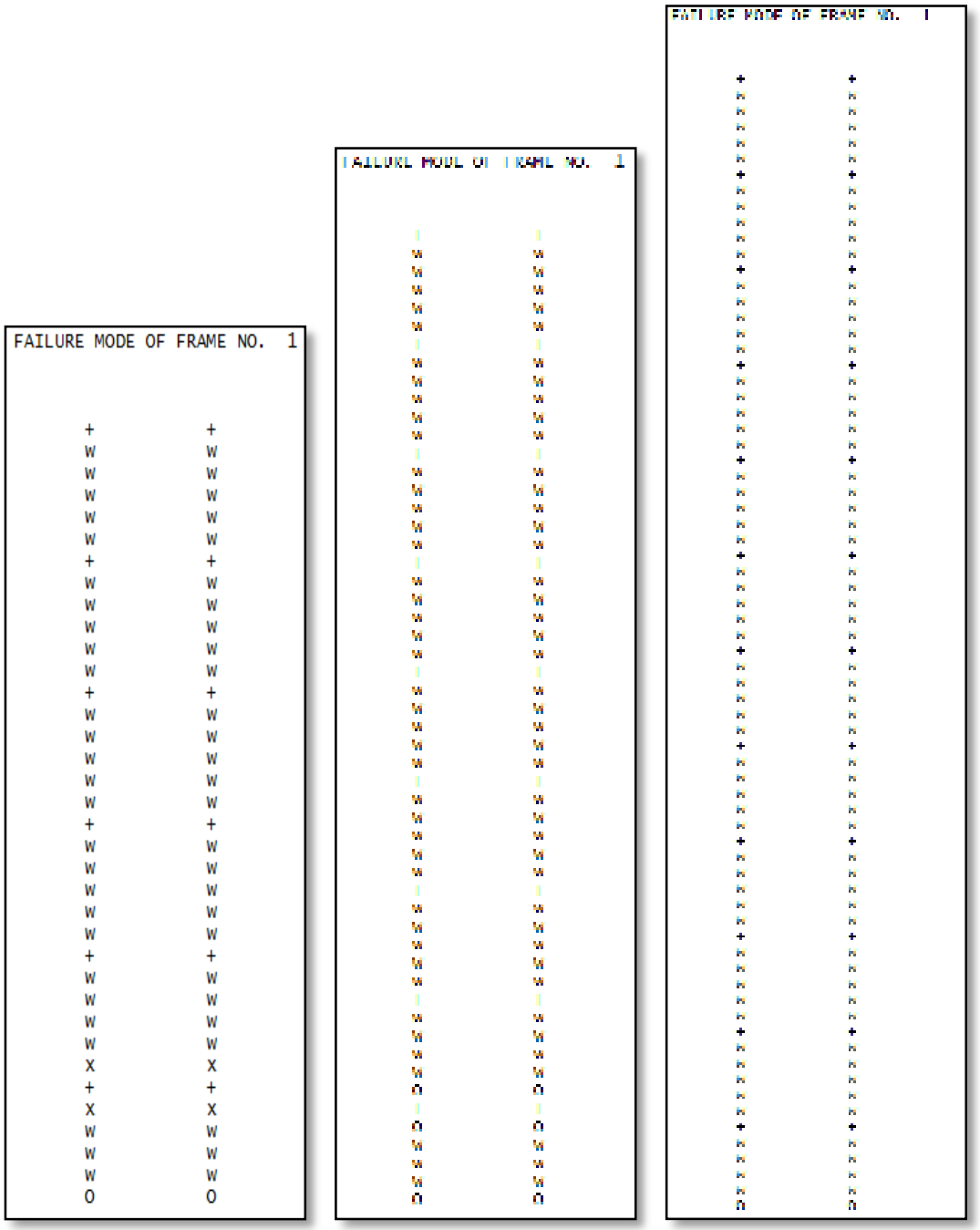

Figure 41: Buildings' Final Damage State: (a) B2-6S-M-S; (b) B6-9S-M-S; (c) B10-12S-M-S

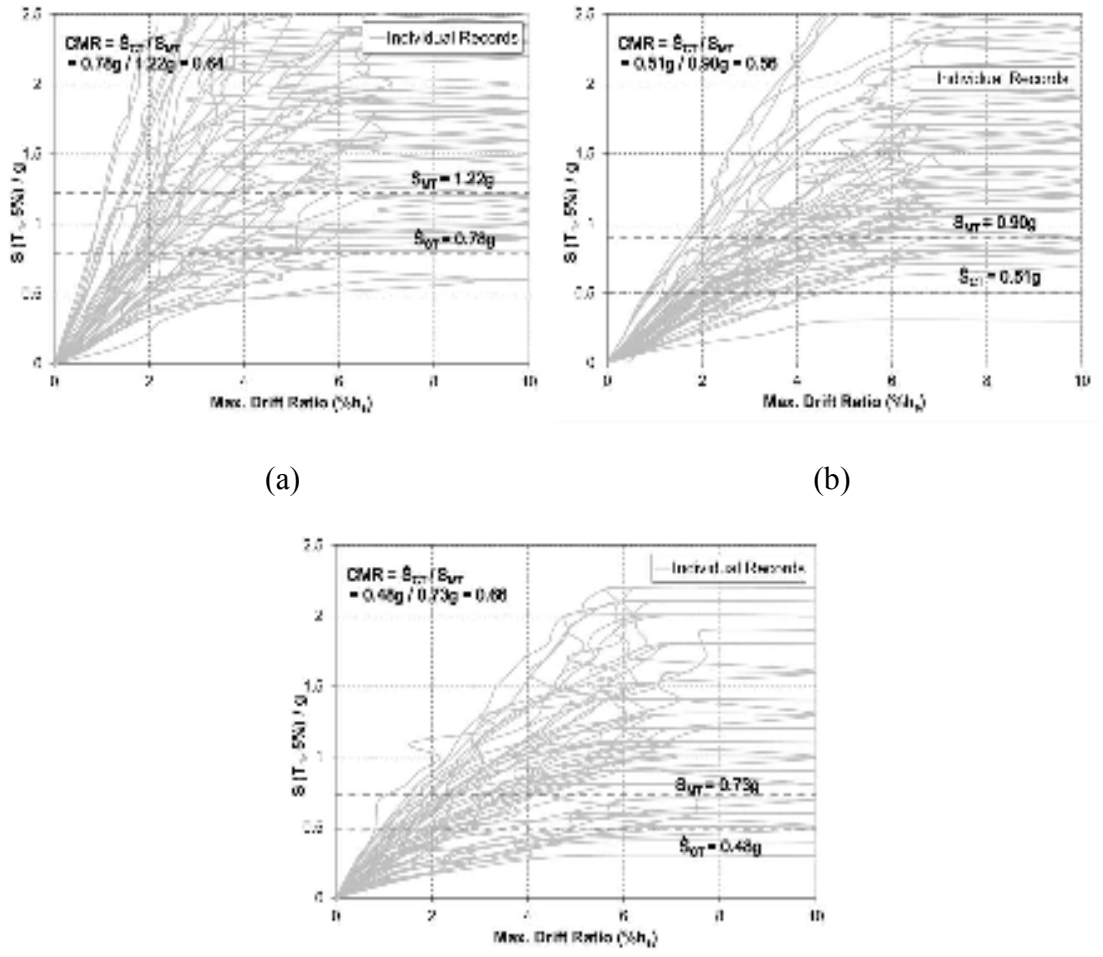

Figure 42: Incremental Dynamic Analysis Curves: (a) B2-6S-M-S; (b) B6-9S-M-S; (c) B10-12S-M-S

Mainly significant weaving is observed in the three designs and in some cases structural resurrection is noticed. It is interesting to highlight that structural resurrection is most observed in the 6-story building (B2-6S-M-S) and least observed in the 12-story building (B10-12S-M-S). It is clear from Figure 42 that the 6-story building design (B2-6S-M-S) shows a much better performance than 9 and 12 story buildings. The IDA curve of B2-6S-M-S shows some records which have reached 2.5g spectral acceleration without reaching collapse. This is less observed in B6-9S-M-S building. However, for B10-12S-M-S design all ground motion records caused the structure to collapse at 2.5g. This is indicated with the flat lines in the IDA curves. Furthermore, B10-12S-M-S design is showing the most obvious weaving and hardening patterns compared to B2-6S-M-S and B6-9S-M-S. Median collapse intensity ($\hat{S}_{CT}$) is 0.78g for B2-6S-M-S,

0.51g for B6-9S-M-S and 0.48g for B10-12S-M-S. Additionally, it is observed in Figure 42 that for the three buildings, the number of flat lines representing collapse is higher above the MCE level (S_{MT}). This shows that moderate seismicity designs reach collapse, excessively large drift ratios and global instabilities, at spectral acceleration higher than MCE level. Furthermore, calculated CMRs are 0.64, 0.56 and 0.66 for B2-6S-M-S, B6-9S-M-S and B10-12S-M-S, respectively. None of the three designs have any margin of safety against structural collapse based on CMRs. However, decision about performance cannot be made completely based on CMRs without doing the proper adjustments. The adjusted CMRs are presented in following section.

4.3.3 Fragility Analysis. IDA results are adjusted to account for uncertainty sources using β_{TOT} of 0.525, as calculated in section 4.1.4. Adjusted results are used to construct fragility curves for the three moderate seismicity designs. CMRs are adjusted using SSFs to account for frequency content of records. From FEMA P695, SSF is 1.39, 1.46, and 1.53 for B2-6S-M-S, B6-9S-M-S and B10-12S-M-S designs, respectively. Figure 43 shows analytical, fitted and adjusted collapse fragility curves for B2-6S-M-S, B6-9S-M-S and B10-12S-M-S designs. Building B2-6S-M-S has the flattest collapse fragility curve compared to B6-9S-M-S and B10-12S-M-S which have much steeper curves. The 6-story building (B2-6S-M-S) collapse fragility curve approaches plateau at a lower rate unlike the 9-story building (B6-9S-M-S) and 12-story building (B10-12S-M-S). Adjusted median collapse intensity (S_{CT}) is 1.09g, 0.75g and 0.69g for buildings B2-6S-M-S, B6-9S-M-S and B10-12S-M-S, respectively. Moreover, ACMR, ratio between S_{CT} and S_{MT}, is 0.89 for B2-6S-M-S, 0.82 for B6-9S-M-S and 0.95 for B10-12S-M-S. This reflects that the three moderate seismicity designs have no margin of safety against collapse. To further asses the designs' seismic vulnerability at other performance levels, Figure 44 presents CP, LS and IO fragility curves for B2-6S-M-S, B6-9S-M-S and B10-12S-M-S. It is observed that fragility curves steepness is reduced moving from IO to CP performance levels, indicating higher probabilities of exceeding IO compared to CP. From Figure 44 (a), it can be seen that B2-6S-M-S at the MCE level (S_{MT}= 1.22g) has 58% probability of exceeding CP performance level, 96% probability of exceeding LS and 100% probability of exceeding IO.

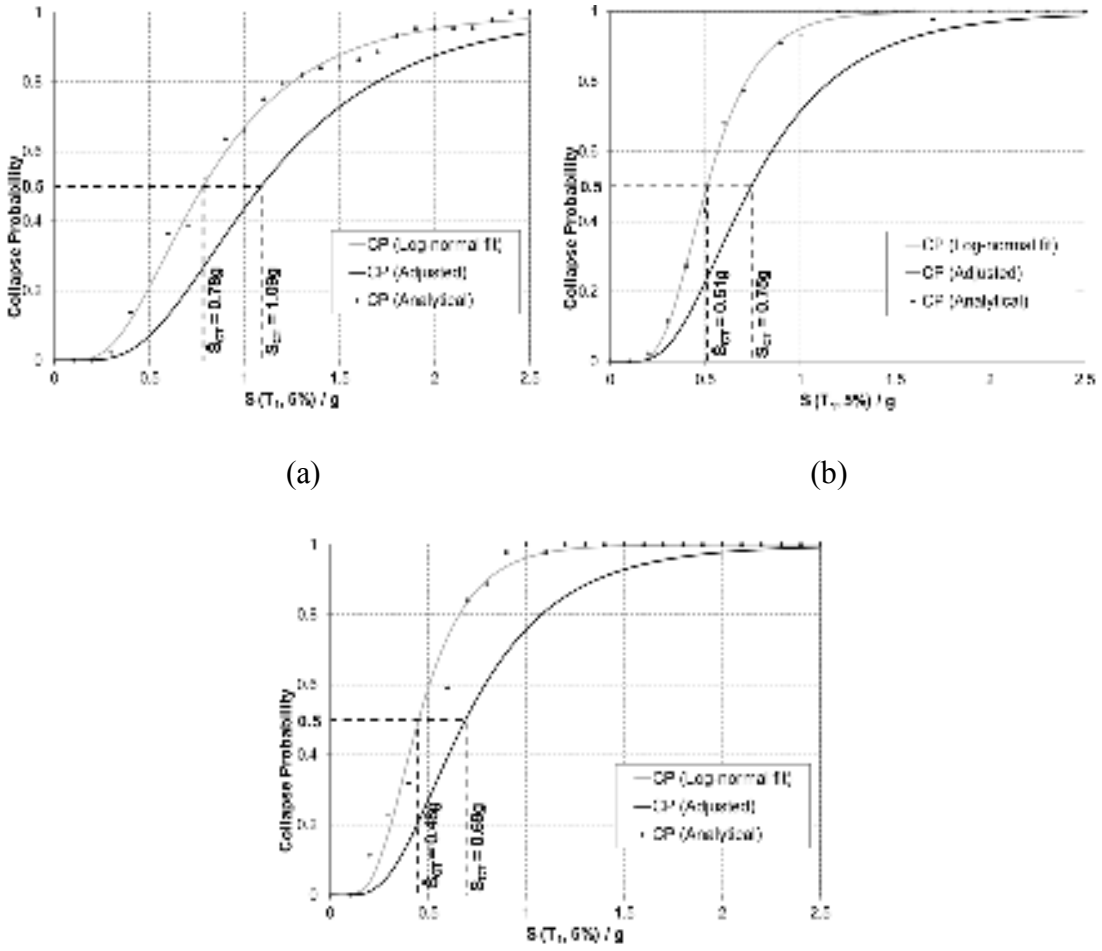

(a) (b)

(c)

Figure 43: Collapse Fragility Curves: (a) B2-6S-M-S; (b) B6-9S-M-S; (c) B10-12S-M-S

Similarly as shown in Figure 44 (b), B6-9S-M-S at MCE level (S_{MT}= 0.90g) has 64%, 97% and 100% probabilities of exceeding CP, LS and IO damage states, respectively. Finally for B10-12S-M-S, Figure 44 (c) shows that at MCE level (S_{MT}= 0.73g) there is 54% probability it exceeds CP, 85% probability it exceeds LS and 99% probability of exceeding IO. Therefore, none of the three moderate seismicity designs satisfies the performance recommendations by FEMA P695.

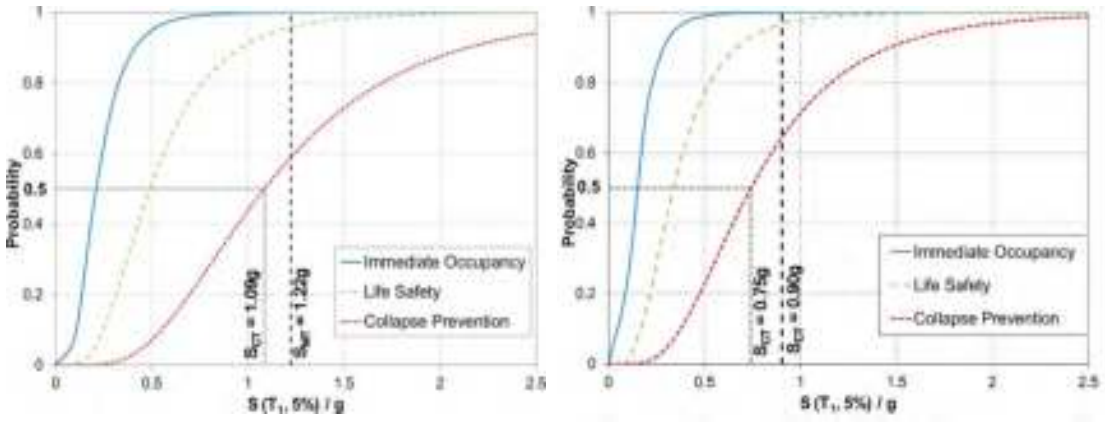

(a) (b)

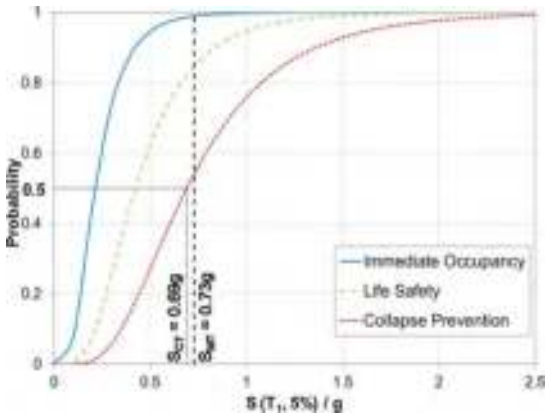

(c)

Figure 44: IO, LS and CP Fragility Curves: (a) B2-6S-M-S; (b) B6-9S-M-S; (c) B10-12S-M-S

4.4 Performance of Low Seismicity Designs

The performance of buildings designed for low seismicity will be shown in the following three subsections. As shown in Figure 17, at the lowest design response spectrum, six buildings are designed. Three buildings have special RC shear walls (B3-6S-L-S, B7-9S-L-S and B11-12S-L-S) and the other three have ordinary RC shear wall (B4-6S-L-O, B8-9S-L-O and B12-12S-L-O).

4.4.1 Nonlinear Static Push-Over Analysis Results. Capacity curves of the buildings with special RC shear walls (i.e. B3-6S-L-S, B7-9S-L-S and B11-12S-L-S) are shown in Figure 45.

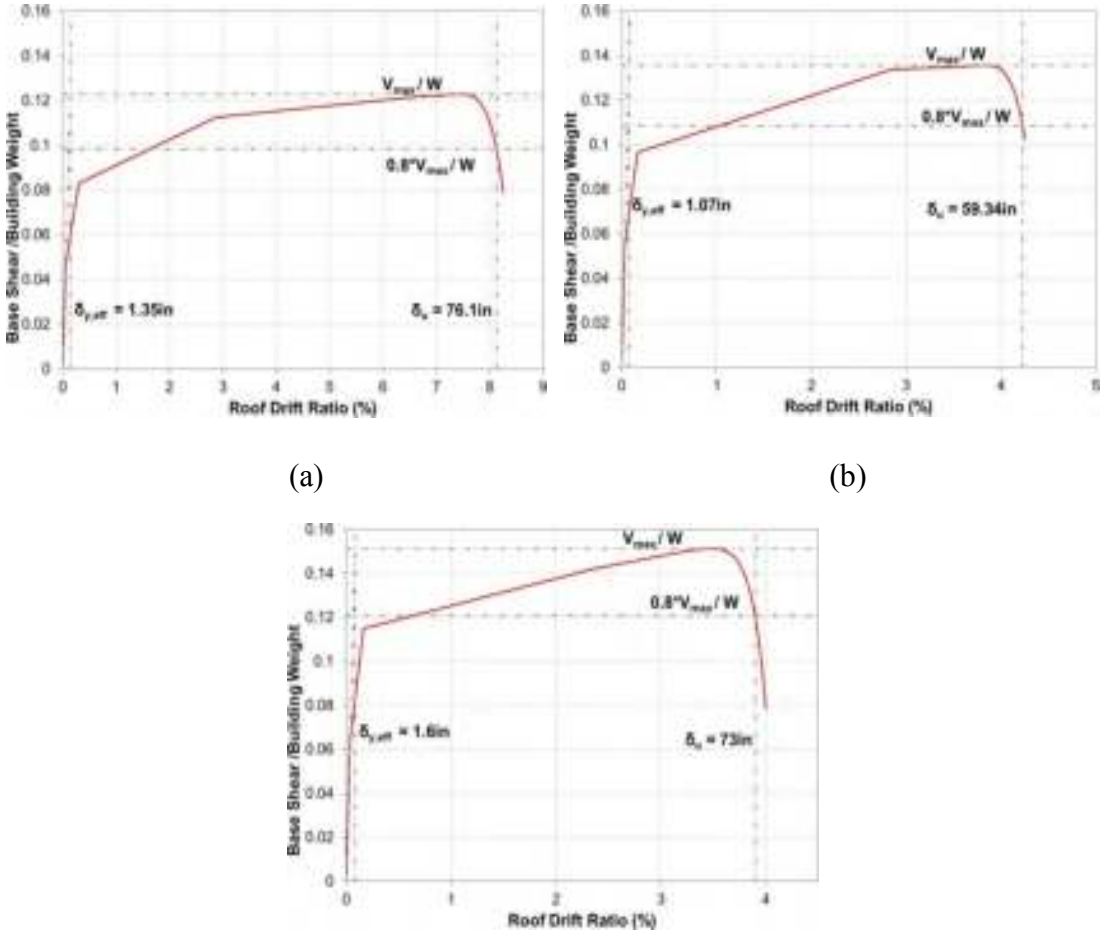

(a) (b)

(c)

Figure 45: Back-Bone Curves: (a) B3-6S-L-S; (b) B7-9S-L-S; (c) B11-12S-L-S

The backbone curves presented in Figure 45 reflect that the three buildings are behaving linearly at very low drift ratios. It is also very clear that the capacity curves are multi-linear. Although, buildings B3-6S-L-S, B7-9S-L-S and B11-12S-L-S are designed with special RC shear walls, the back- bone curves indicate obvious degradation in stiffness and sudden drop in strength after reaching the peak shear strength. This could be attributed to the very low seismic design criteria adapted in these buildings design. Furthermore, the normalized base shear capacity is 0.12 for B3-6S-L-S, 0.14 for B7-9S-L-S and 0.15 for B11-12S-L-S. Maximum roof drift ratios are 8.25%, 4.25% and 4% for B3-6S-L-S, B7-9S-L-S and B10-12S-M-S, respectively. Additionally, the ultimate roof displacement calculated as per FEMA P695 is 76.1in for B3-6S-L-S, 59.3in for B7-9S-L-S and 73in for B11-12S-M-S.

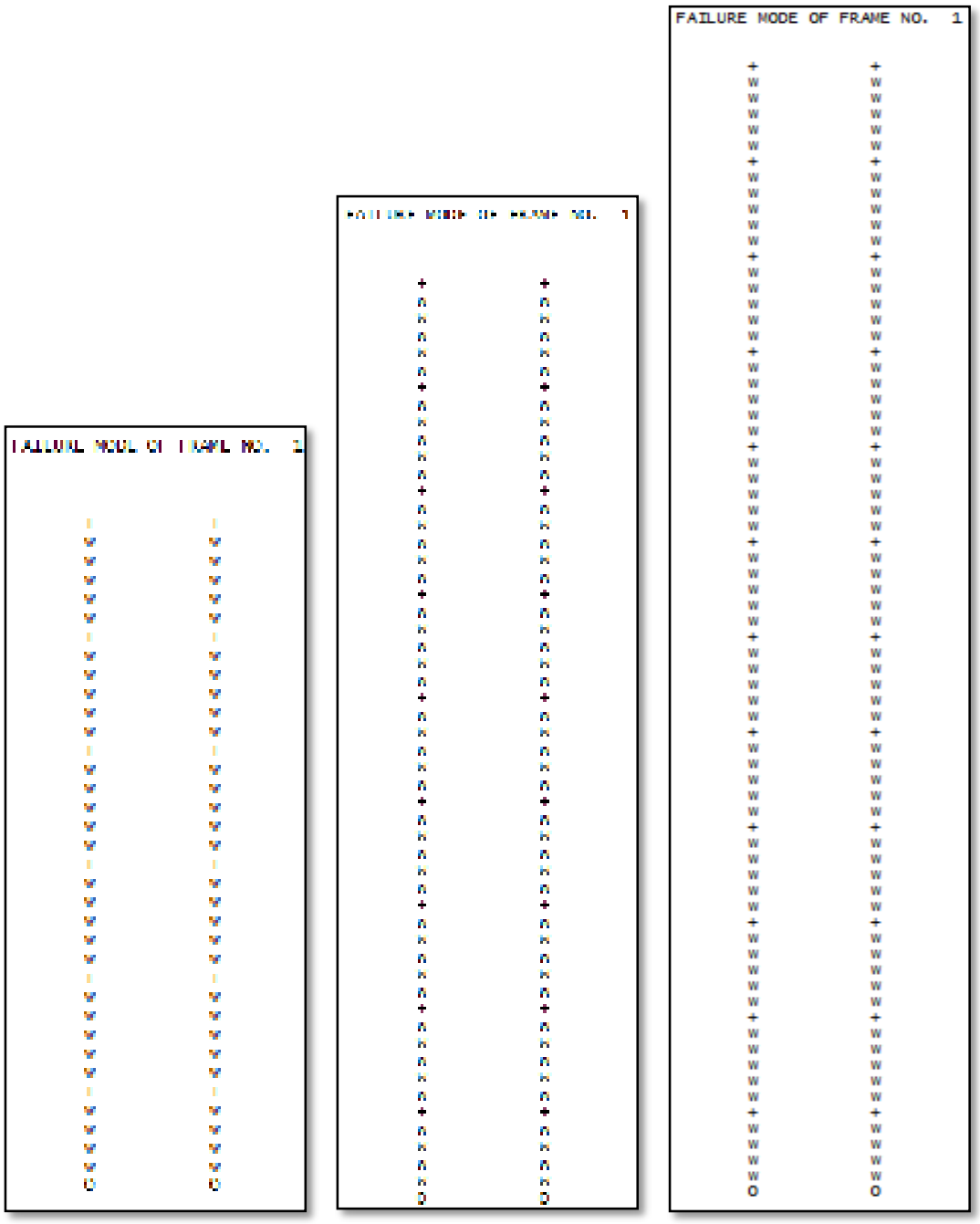

Figure 46: Buildings' Final Damage State: (a) B3-6S-L-S; (b) B7-9S-L-S; (c) B11-12S-L-S

Buildings B3-6S-L-S, B7-9S-L-S and B11-12S-M-S exhibit a ductile behavior with period-based ductility, conforming to FEMA P695, greater than 8. In general, the three designs base shear capacities drop sharply after reaching their maximum.

Final damage states of buildings B3-6S-L-S, B7-9S-L-S and B11-12S-M-S are presented in Figure 46. Overall structural damage reported by IDARC-2D is 0.373 for B3-6S-L-S, 0.357 for B7-9S-L-S and 0.356 for B11-12S-M-S. These damages are concentrated in first floor shear walls. The three buildings' failure mechanism is through the development of plastic hinges at the critical section at the shear wall base. This mechanism is matching the design code assumption.

Figure 47 depicts the capacity curves for the three low seismicity designs with ordinary RC shear walls. In the three buildings (B4-6S-L-O, B8-9S-L-O and B12-12S-L-O) there is a clear severe degradation in stiffness and deterioration in strength. The buildings reach their base shear strength and suddenly drop afterwards. This is very clear in the 12-story (B12-12S-L-O) and 9-story (B8-9S-L-O) buildings. In the 6-story building (B4-6S-L-O), the drop in strength is less severe after the peak. The three buildings exhibit a linear behavior at very low drift ratios. Base shear capacities are 0.13, 0.075 and 0.12 for buildings B4-6S-L-O, B8-9S-L-O and B12-12S-L-O, respectively. Additionally, the maximum roof drift ratio is 9.2% for B4-6S-L-O, 2.25% for B8-9S-L-O and 2.75% for B12-12S-L-O. Ultimate roof displacements calculated according to FEMA P695 are 84.55in, 26.73in and 47.62in for B4-6S-L-O, B8-9S-L-O and B12-12S-L-O, respectively. Furthermore, the three designs' estimated ductility is higher than 8. Final damage states after reaching 20% loss in strength are shown in Figure 48 for buildings B4-6S-L-O, B8-9S-L-O and B12-12S-L-O. It is also observed that the final damage state of B4-6S-L-O, B8-9S-L-O and B12-12S-L-O buildings is caused by plastic hinge formation at the code critical section which is at the wall base. The total overall structural damage is 0.629 for B4-6S-L-O, 0.491 for B8-9S-L-O and 0.445 for B12-12S-L-O, as estimated by IDARC-2D. The reported damages are mainly accumulated at first floor shear walls.

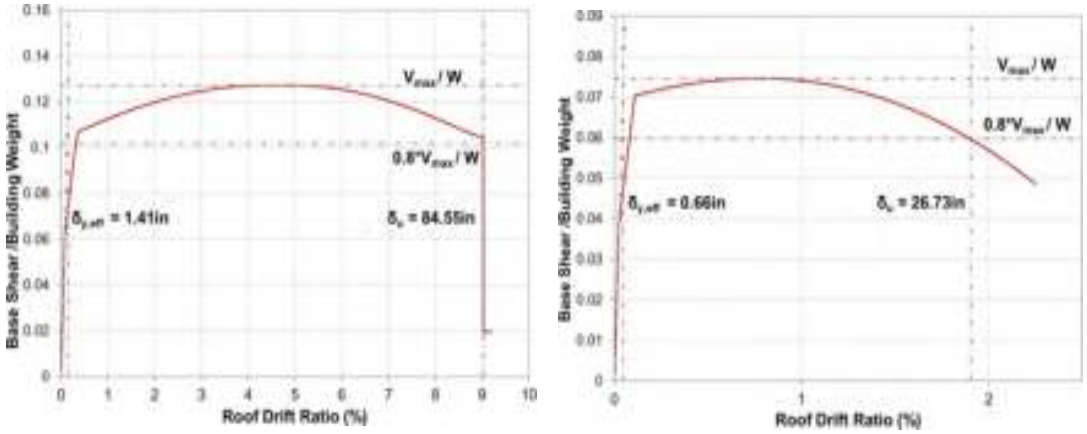

(a) (b)

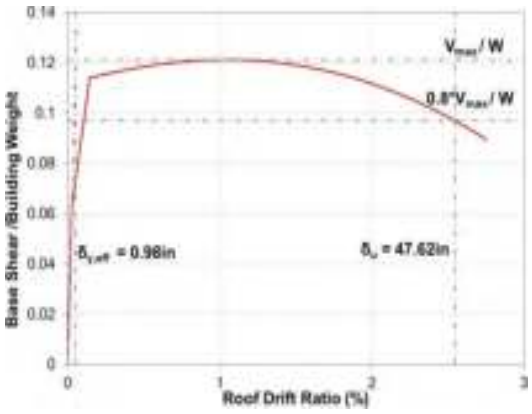

(c)

Figure 47: Back-Bone Curves: (a) B4-6S-L-O; (b) B8-9S-L-O; (c) B12-12S-L-O

4.4.2 Nonlinear Incremental Dynamic Analysis Results. The Impact of dynamic loads and higher-modes on performance of low seismicity designs is investigated using IDA. Figure 49 shows IDA curves of buildings B3-6S-L-S, B7-9S-L-S and B11-12S-L-S designed for low seismicity with special RC shear walls. The three buildings have linear behavior with a sharp slope at low drift ratios. Only for the 6-story building (B3-6S-L-S), few records are causing linear response with a bit of weaving up to high spectral accelerations. Relatively, the 6-story building (B3-6S-L-S) is showing a more robust performance than 9-story (B7-9S-L-S) and 12-story (B11-12S-L-S) buildings.

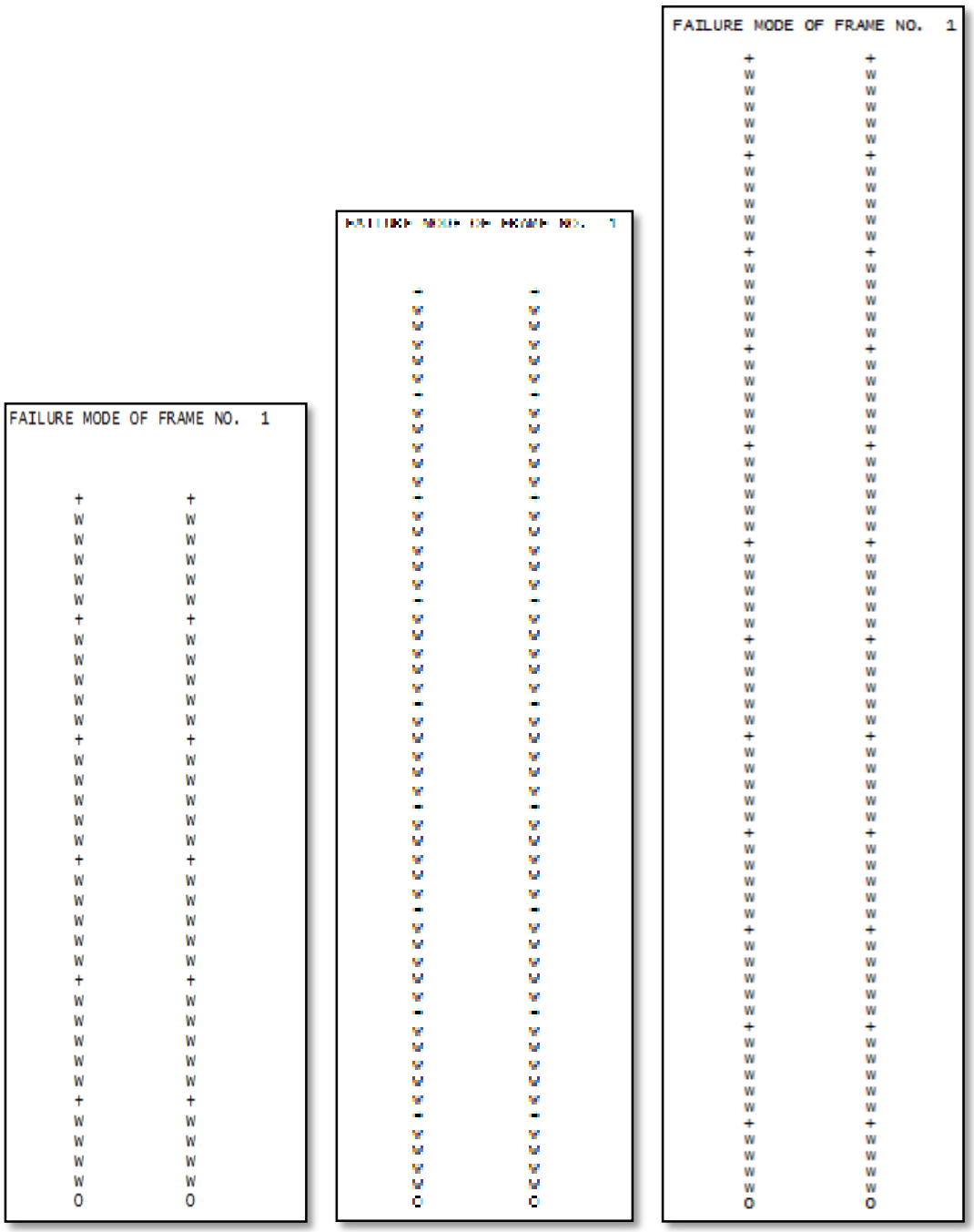

Figure 48: Buildings' Final Damage State: (a) B4-6S-L-O; (b) B8-9S-L-O; (c) B12-12S-L-O

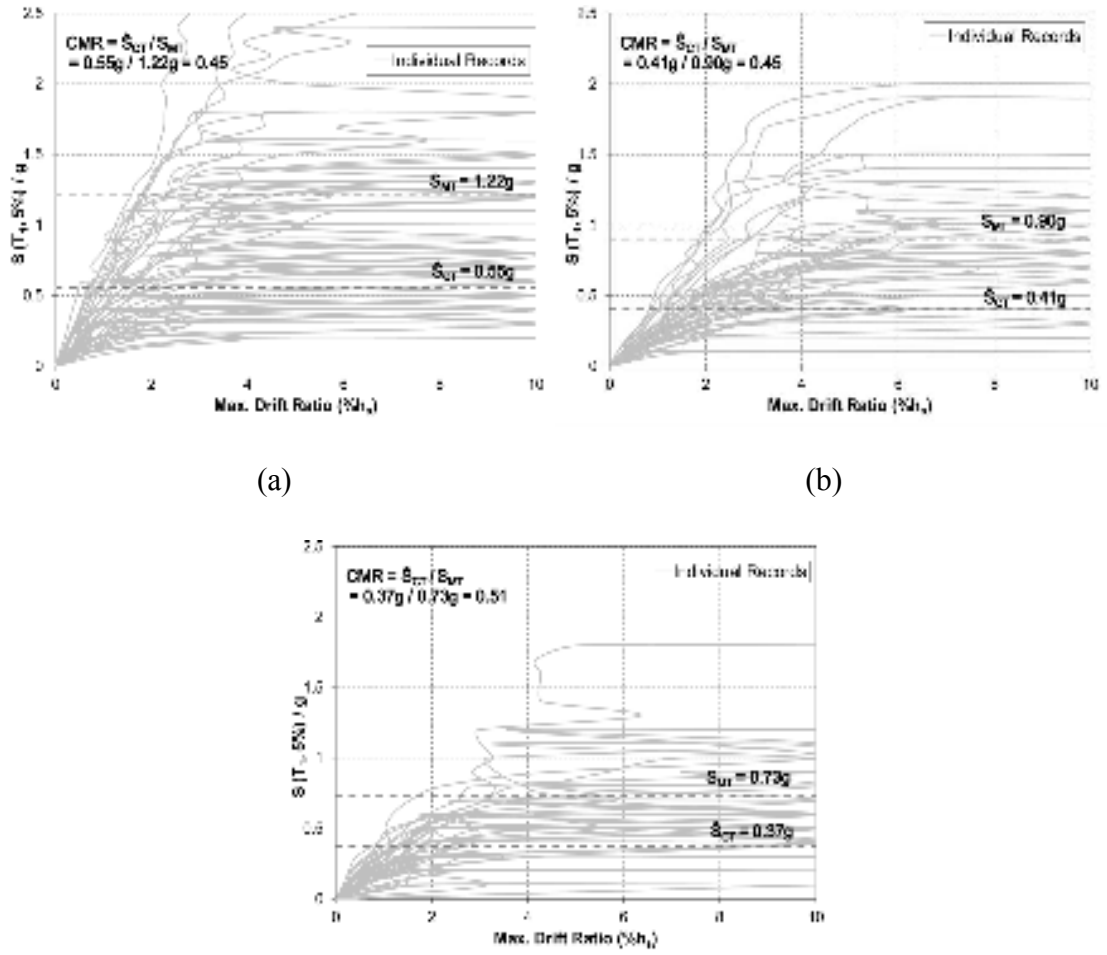

(a) (b)

(c)

Figure 49: Incremental Dynamic Analysis Curves: (a) B3-6S-L-S; (b) B7-9S-L-S; (c) B11-12S-L-S

The hardening phenomenon is most seen in the 6-story building (B3-6S-L-S), while it is least seen in the 12-story building (B11-12S-L-S), except for some records. Additionally, B3-6S-L-S design showed more structural resurrection incidents than the other two designs; B7-9S-L-S and B11-12S-L-S. In Figure 49 (b) and (c), it can be seen that buildings B7-9S-L-S and B11-12S-L-S are experiencing a clear softening response to ground motion records. The IDA curves for the three designs show that most of the flat lines which represent the collapse of the structure are below the MCE level (S_{MT}). This indicates an expected poor performance and collapse at spectral accelerations lower than S_{MT}. Additionally, in general the low seismicity designs (B3-6S-L-S, B7-9S-L-S and B11-12S-L-S) are collapsing at low drift ratios except for some records in

the 6-story building (B3-6S-L-S). The median collapse intensity ($\hat{S}_{CT}$) is 0.55g for B3-6S-L-S, 0.41g for B7-9S-L-S and 0.37g for B11-12S-L-S. Furthermore, the CMRs are 0.45, 0.45 0.51 for buildings B3-6S-L-S, B7-9S-L-S and B11-12S-L-S, respectively. The performance of the low seismicity designs, based on the CMRs without uncertainty and spectral content adjustments, is very poor. The adjusted CMRs are given in the next section for a better evaluation of the performance.

Similarly, IDA curves are given for the low seismicity designs with ordinary RC shear walls in Figure 50. It is observed that at very low drift ratios, the buildings B4-6S-L-O, B8-9S-L-O and B12-12S-L-O are experiencing a linear behavior with a very steep slope. This reflects the expected stiffness degradation of ordinary RC shear walls without any special reinforcement detailing. In all the three buildings, collapse is occurring before spectral accelerations of 2g. The 6-story building (B4-6S-L-O) has few flat lines above MCE level, but more lines below indicating higher probability of collapse at spectral accelerations lower than MCE level. On the other hand, the other two buildings (B8-9S-L-O and B12-12S-L-O) have most of the flat lines below MCE level. This highlights more structural collapse incidents at levels below MCE. As shown in Figure 50, the three designs experience a bit of weaving and softening in most records. However, in some cases few records show hardening and structural resurrection. Building B4-6S-L-O (6-story) design has the most number of structural resurrections compared to B8-9S-L-O and B12-12S-L-O designs. In most cases, collapse is seen for the three low seismicity designs with ordinary RC shear walls at low drift ratios. The median collapse intensity ($\hat{S}_{CT}$) is 0.43 for B6-9S-M-S, 0.25 for B8-9S-L-O and 0.24 for B12-12S-L-O. Moreover, CMRs are 0.35, 0.28 0.33 for buildings B4-6S-L-O, B8-9S-L-O and B12-12S-L-O, respectively. From the shown IDA curves and calculated CMRs, the expected performance of low seismicity designs with ordinary RC shear walls is clearly very low. The ACMRs for low seismicity designs are presented in the next section.

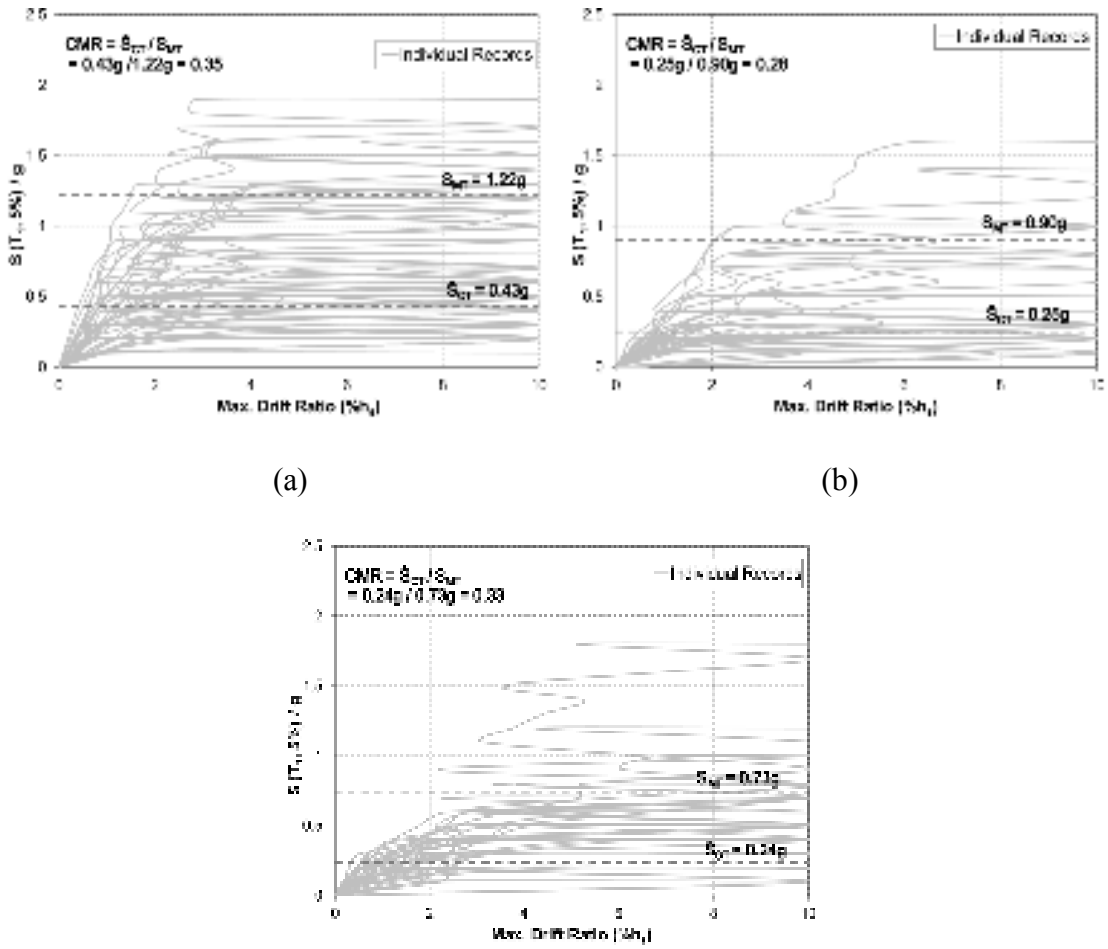

(a) (b)

(c)

Figure 50: Incremental Dynamic Analysis Curves: (a) B4-6S-L-O; (b) B8-9S-L-O; (c) B12-12S-L-O

4.4.3 Fragility Analysis. Fragility analysis results are used to investigate the low seismicity designs earthquake vulnerability. Fragility curves are constructed using IDA results after they are adjusted to consider the different sources of uncertainties and the spectral content of the records. The spectral content is accounted for using SSF given in FEMA P695 Tables 7-1a and 7-1b. SSF is 1.39 for B3-6S-L-S and B4-6S-L-O, 1.46 for B7-9S-L-S and B8-9S-L-O, 1.53 for B11-12S-L-S and B12-12S-L-O. Figure 51 depicts observed, fitted and adjusted collapse fragility curves for low seismicity designs with special RC shear walls (i.e. B3-6S-L-S, B7-9S-L-S and B11-12S-L-S). It is very clear that the collapse fragility curves are very steep for the three buildings with special RC shear wall. This reflects a sharp increase in collapse probability with any small increase in spectral accelerations for the three buildings.

However, the 6-story building (B3-6S-L-S) shows a relatively flatter curve compared to buildings B7-9S-L-S and B11-12S-L-S.

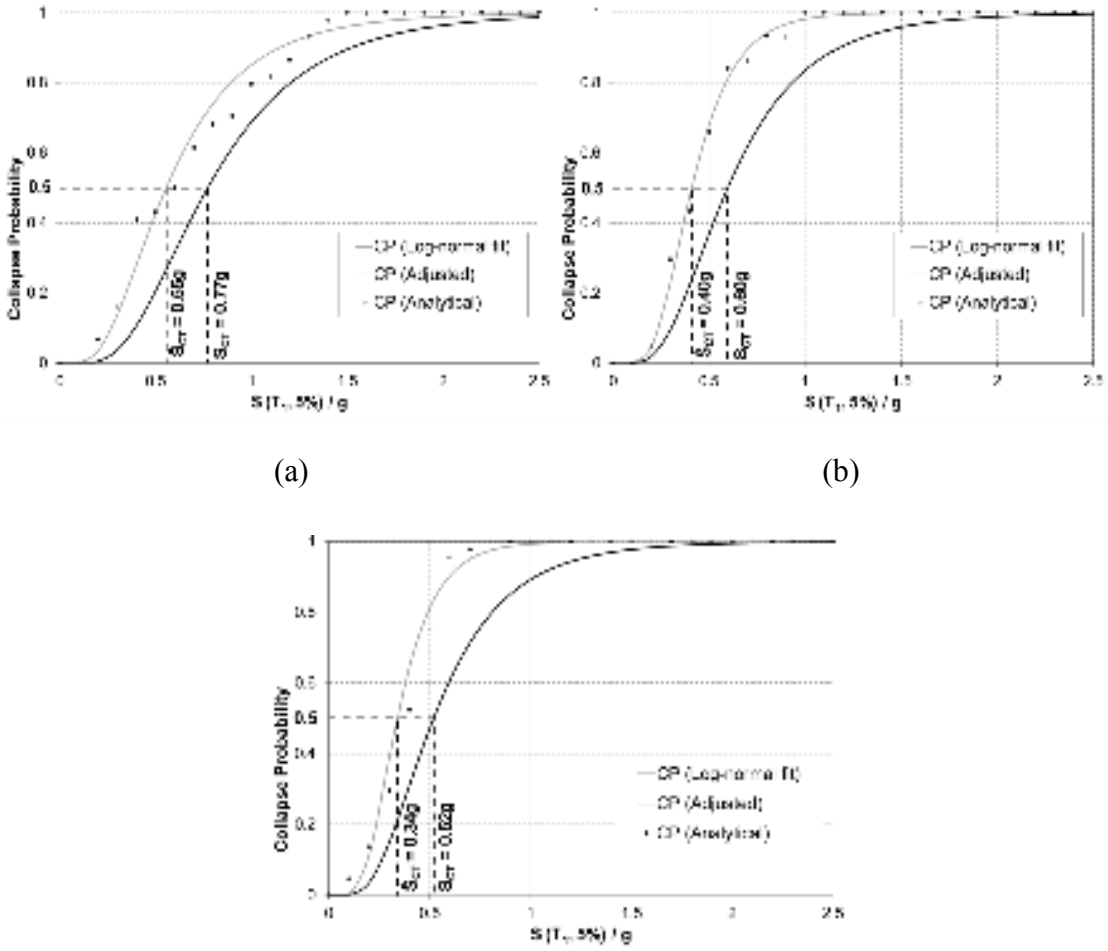

Figure 51: Collapse Fragility Curves: (a) B3-6S-L-S; (b) B7-9S-L-S; (c) B11-12S-L-S

The adjusted median collapse intensity (S_{CT}) is 0.77g, 0.60g and 0.52g for buildings B3-6S-L-S, B7-9S-L-S and B11-12S-L-S, respectively. Therefore, ACMR is 0.63 for B3-6S-L-S, 0.66 for B7-9S-L-S and 0.71 for B11-12S-L-S. This reflects no safety margin against collapse for low seismicity designs with special RC shear walls. CP, LS and IO adjusted fragility curves are shown in Figure 52 for buildings B3-6S-L-S, B7-9S-L-S and B11-12S-L-S.

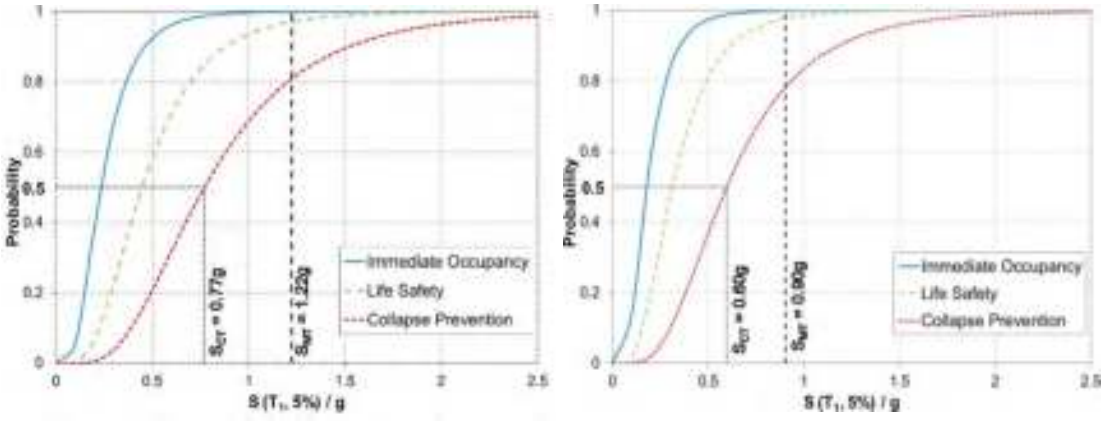

(a) (c)

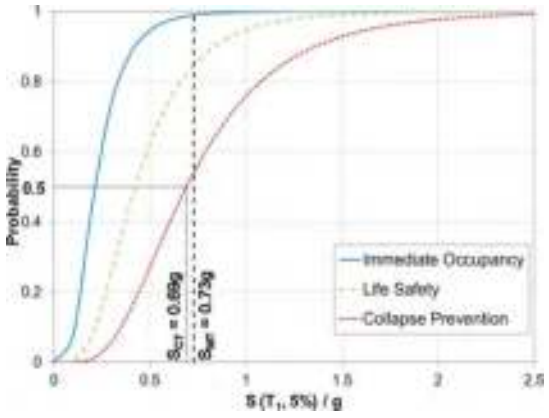

(c)

Figure 52: IO, LS and CP Fragility Curves: (a) B3-6S-L-S; (b) B7-9S-L-S; (c) B11-12S-L-S

As observed in Figure 52 (a), the 6-story building (B3-6S-L-S) shows a slight flatness in CP and LS fragility curves. However, from Figure 52 (b) and (c), the 12-story (B11-12S-L-S) and 9-story (B7-9S-L-S) buildings have very steep fragility curves in all performance levels indicating poor response and high limit states probabilities of exceedance. Furthermore, at the MCE level (S_{MT}) of each design, B3-6S-L-S and B7-9S-L-S have 100% probability of exceeding IO damage state, while B11-12S-L-S has 99% exceedance probability. B3-6S-L-S (6-story) design has 81% probability of exceeding CP and 97% probability of exceeding LS at MCE level. Similarly, the 12-story building (B11-12S-L-S) has 73% probability of exceeding CP and 96% probability of exceeding LS. Additionally, the 9-story building (B7-9S-L-S) has 98% probability of exceeding LS and 78% probability of exceeding CP. Consequently, the

performance of low seismicity designs with special RC shear walls is confirmed to be poor and none of the buildings satisfies FEMA P695 performance objectives.

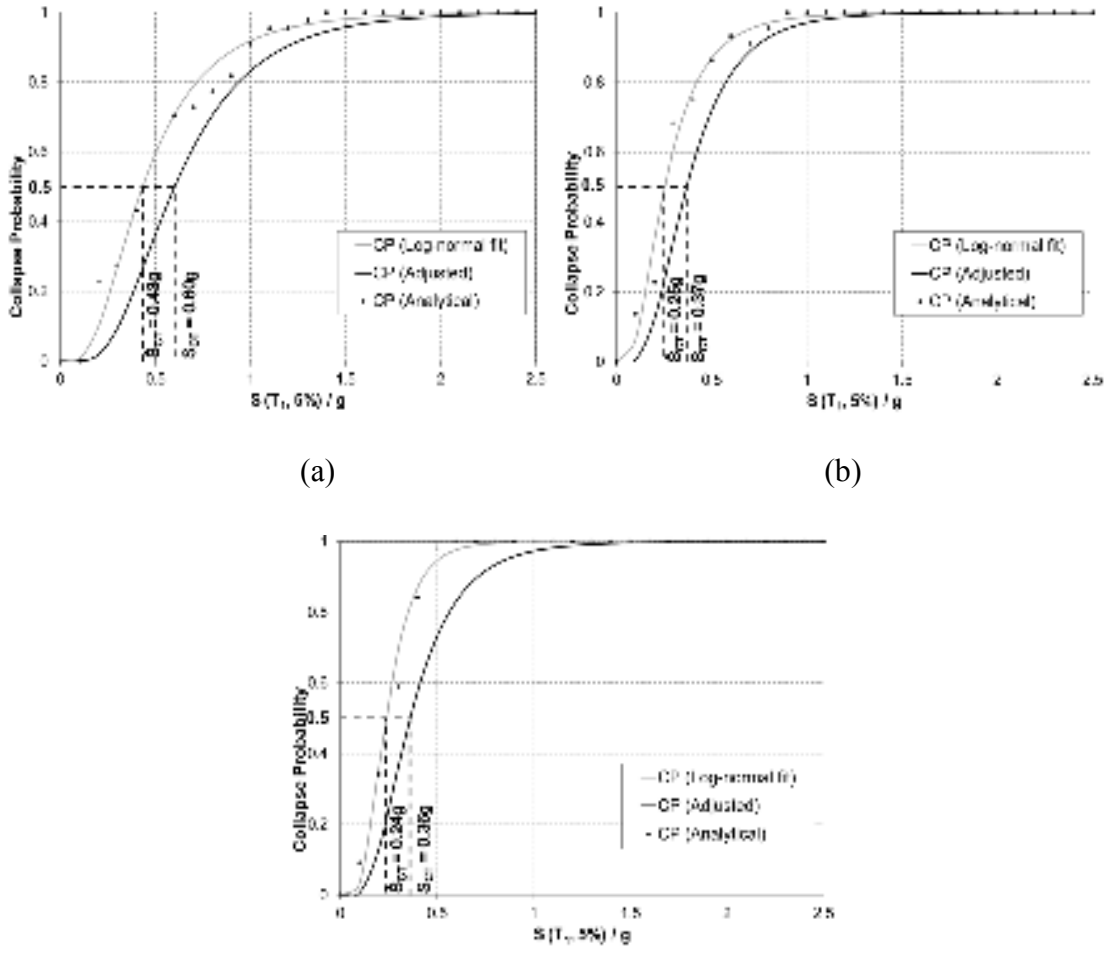

(a) (b)

(c)

Figure 53: Collapse Fragility Curves: (a) B4-6S-L-O; (b) B8-9S-L-O; (c) B12-12S-L-O

Collapse fragility curves for low seismicity designs (i.e. B4-6S-L-O, B8-9S-L-O and B12-12S-L-O) with ordinary RC shear walls are given in Figure 53. These curves are very sharp showing high collapse probabilities at low spectral accelerations for buildings B4-6S-L-O, B8-9S-L-O and B12-12S-L-O. However, B4-6S-L-O has slight flatness in its collapse fragility curve relative to B8-9S-L-O and B12-12S-L-O buildings. The adjusted median collapse intensity (S_{CT}) is 0.60g for B4-6S-L-O, 0.37g for B8-9S-L-O and 0.36g for B12-12S-L-O. Furthermore, the ACMRs are 0.49, 0.41and 0.50 for buildings B4-6S-L-O, B8-9S-L-O and B12-12S-L-O, respectively.

This reflects no collapse margin of safety for the low seismicity designs with ordinary RC shear walls. Figure 54 presents the three performance levels (CP, LS and IO) fragility curves for the three designs.

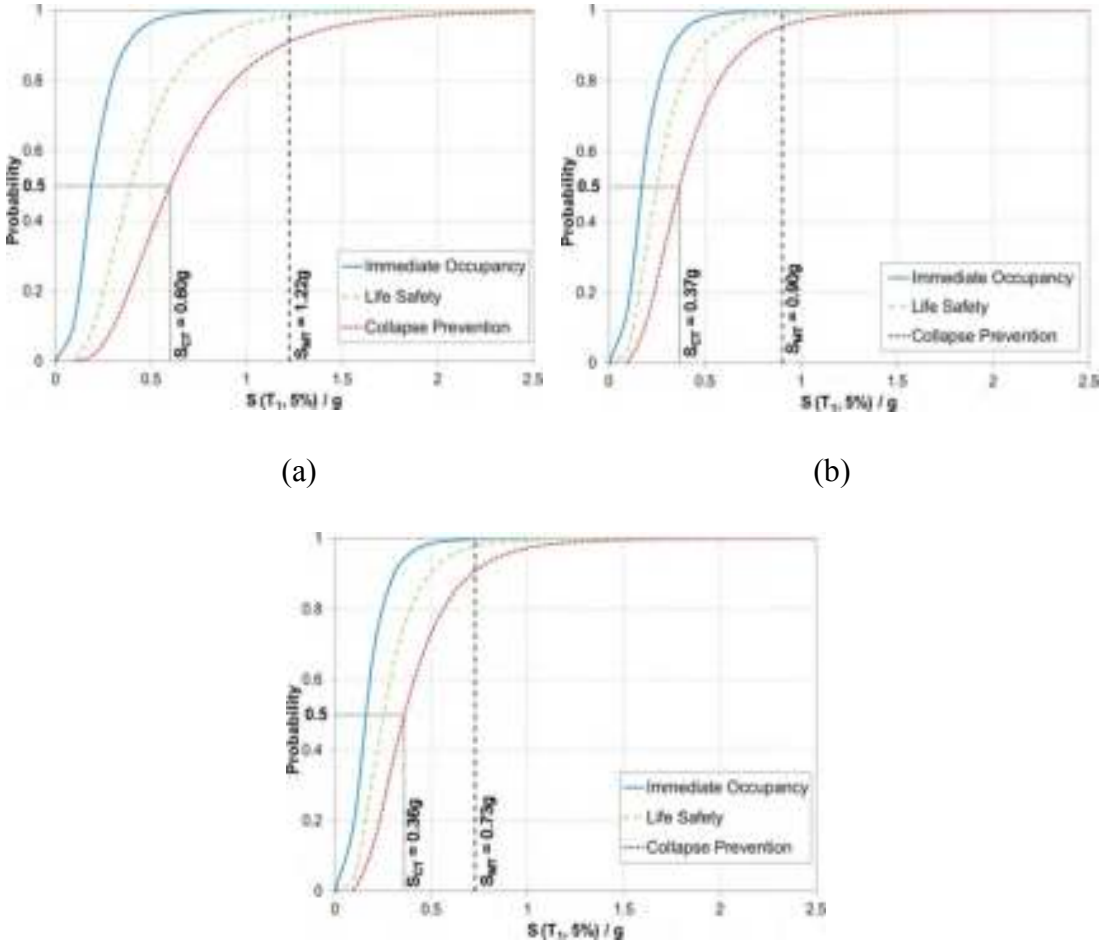

(a) (b)

(c)

Figure 54: IO, LS and CP Fragility Curves: (a) B4-6S-L-O; (b) B8-9S-L-O; (c) B12-12S-L-O

The presented fragility curves show very steep, almost vertical, curves for buildings B8-9S-L-O and B12-12S-L-O. It is marginally flatter for building B4-6S-L-O (6-story). For buildings B8-9S-L-O and B12-12S-L-O, the probability of exceeding all limit states approached 100% at approximately 1.0g spectral acceleration. However, for building B4-6S-L-O this happened at 1.5g. At MCE (S_{MT} = 1.22g) level B4-6S-L-O design has 91%, 98% and 100% of exceeding CP, LS and IO, respectively. Furthermore, building B8-9S-L-O has 100% probability of exceeding IO, 99%

probability of exceeding LS and 95% probability of exceeding CP at MCE (S_{MT} = 0.90g) level. Similarly, at MCE (S_{MT} = 0.73g) level B12-12S-L-O design has 91%, 98% and 100% probabilities of exceeding CP, LS and IO, respectively. Accordingly, the performance of low seismicity designs with ordinary RC shear walls can be labeled very poor. This is due to the high collapse probabilities which do not satisfy FEMA P695 performance criteria.

4.5 Comparison of Results

The seismic vulnerability of the twelve reference buildings is assessed by comparing the designs in two different patterns. The adjusted collapse probabilities and fragility curves are used to compare the resulting performance of buildings with the same number of floors, but having different seismic design levels. Additionally, the comparison is made among buildings with different number of stories, but designed for the same seismicity level.

4.5.1 Seismicity Level-to-Level. This section covers the comparison between buildings with the same number of floors designed for different seismicity levels. The objective is to investigate the impact of the seismic design criteria on the seismic performance of buildings. The comparison is made for the three different numbers of stories, 6-story, and 9-story and 12-story buildings. Table 16 summarizes the Main seismic performance indicators for 6-story buildings designed for the three seismicity levels (high, moderate and low).

Table 16: 6-Story Buildings Performance Indicators

Ref. Buildings	Seismic Design Level	Normalized Base Shear Capacity	S_{CT}	S_{MT}	ACMR
B1-6S-H-S	High	0.57	1.92	1.22	1.57
B2-6S-M-S	Moderate	0.31	1.09	1.22	0.89
B3-6S-L-S	Low	0.12	0.77	1.22	0.63
B4-6S-L-O	Low	0.13	0.6	1.22	0.49

It can be seen that the 6-story building (B1-6S-H-S) designed for highest seismicity level has the highest performance among other buildings. ACMR of B1-6S-H-S is 1.57

which reflects a 57% margin of safety against collapse at MCE level. However, ACMRs for other buildings (B2-6S-M-S, B3-6S-L-S and B4-6S-L-O) is below 1, reflecting that collapse will occur below MCE level. Moreover, as illustrated in Figure 55 B1-6S-H-S has significantly higher base shear capacity compared to other designs.

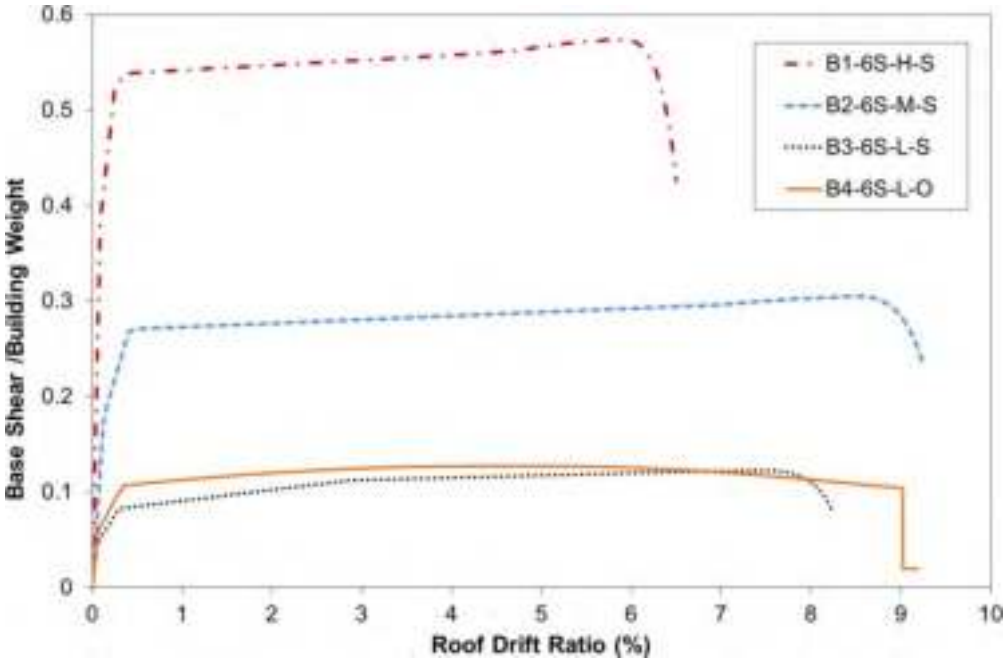

Figure 55: 6-Story Buildings Capacity Curves

Moderate seismicity design (B2-6S-M-S) also has a much higher base shear capacity compared to low seismicity designs. It is interesting to note that the 6-story building with ordinary RC shear walls (B4-6S-L-O) has marginally better performance than the building designed with special RC shear walls (B3-6S-L-S). As shown in Figure 55, B4-6S-L-O has higher yielding strength and base shear capacity compared to B3-6S-L-S. According to IBC'12, ordinary RC shear walls are designed for higher forces (smaller response modification factor, R=5) compared to special RC shear walls (R=6). Furthermore, for the squat shear walls, the design is governed by strength requirements. Therefore, the ordinary RC shear walls cross section required more shear and flexural reinforcement compared to the special RC shear walls. This resulted in a slightly higher capacity for the ordinary walls. However, this is only seen in the static analysis results. As shown in Table 16, B3-6S-L-S has ACMR of 0.63 while B4-6S-L-O has ACMR of 0.49.

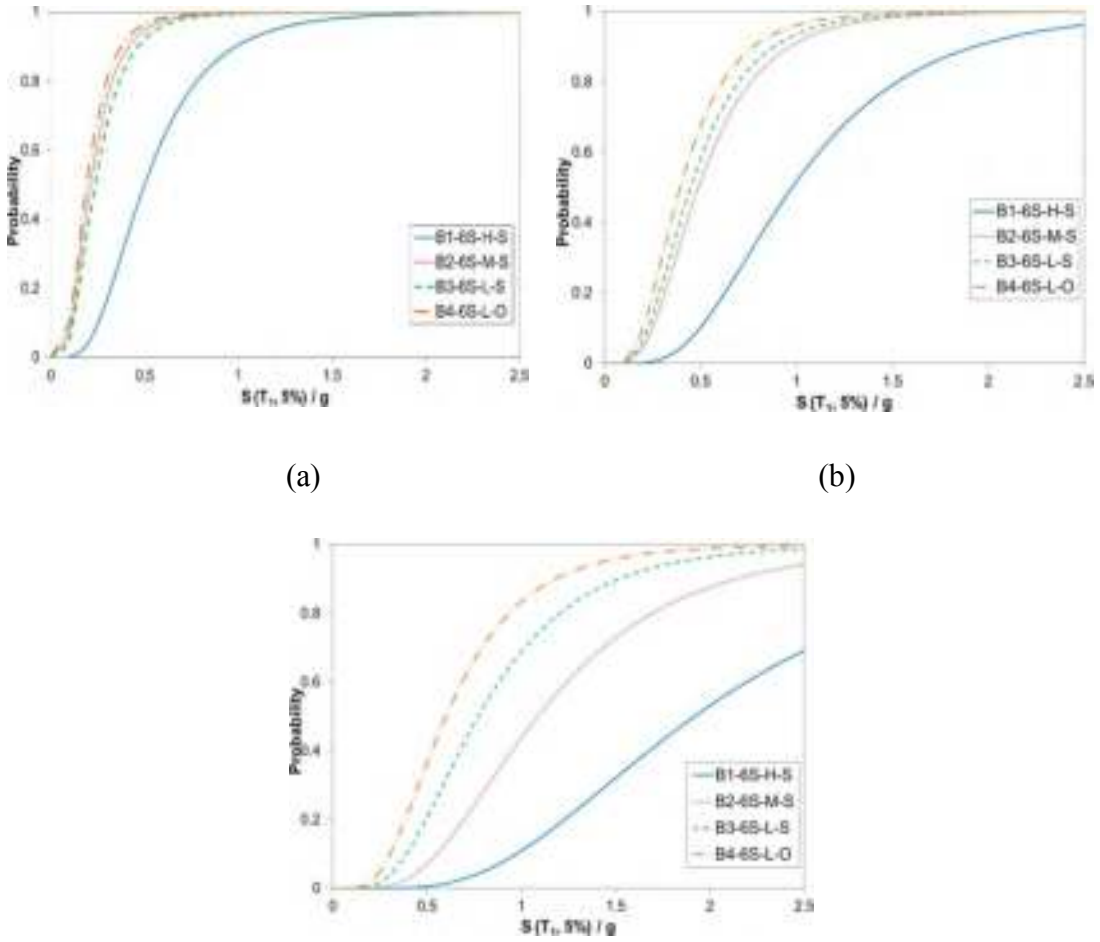

(a) (b)

(c)

Figure 56: 6-Story Buildings Adjusted Fragility Curves: (a) IO Limit State; (b) LS Limit State; (c) CP Limit State

The adjusted fragility curves of the four 6-story buildings are shown in Figure 56 for the three performance levels. Figure 56 (a) shows that moderate and low seismicity designs experience very similar probabilities of exceeding IO performance level. The difference in performance between moderate and low seismicity designs is clearer in LS and CP limit states, as shown in Figure 56 (b) and (c). B1-6S-H-S designed for highest seismicity has the flattest fragility curve in the three performance limit states, reflecting a robust design with low collapse probabilities at high spectral accelerations.

Figure 57 depicts limit states probabilities of exceedance at MCE level. B1-6S-H-S has the lowest probability of exceeding the three limit states at MCE level. On the other hand, B4-6S-L-O has the highest limit states probabilities of exceedance. It is noteworthy to mention that although B4-6S-L-O was expected to perform better than B3-6S-L-S based on the static analysis; the fragility analysis shows higher probabilities of exceeding LS and CP at MCE for B4-6S-L-O, which reflects poor performance.

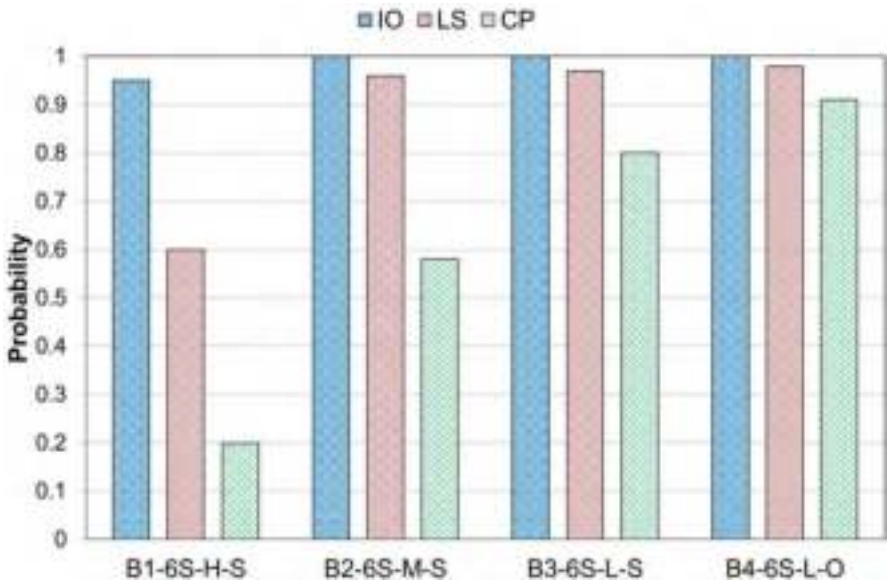

Figure 57: 6-Story Buildings Limit States Probabilities of Exceedance at MCE Level

Summary of the key performance indicators for 9-story buildings designed for the three seismic hazard levels is given in Table 17. Only B5-9S-H-S has 23% margin of safety against collapse while other designs collapse at spectral accelerations lower than MCE level. This highlights a poor performance for moderate and low seismicity designs of the 9-story buildings.

Table 17: 9-Story Buildings Performance Indicators

Ref. Buildings	Seismic Design Level	Normalized Base Shear Capacity	S_{CT}	S_{MT}	ACMR
B5-9S-H-S	High	0.5	1.1	0.9	1.23
B6-9S-M-S	Moderate	0.26	0.75	0.9	0.82
B7-9S-L-S	Low	0.14	0.6	0.9	0.66
B8-9S-L-O	Low	0.075	0.37	0.9	0.41

Based on the static analysis results, B5-9S-H-S and B6-9S-M-S have significantly higher base shear capacities than low seismicity designs (B7-9S-L-S and B8-9S-L-O). This can be clearly seen in the capacity curves shown in Figure 58.

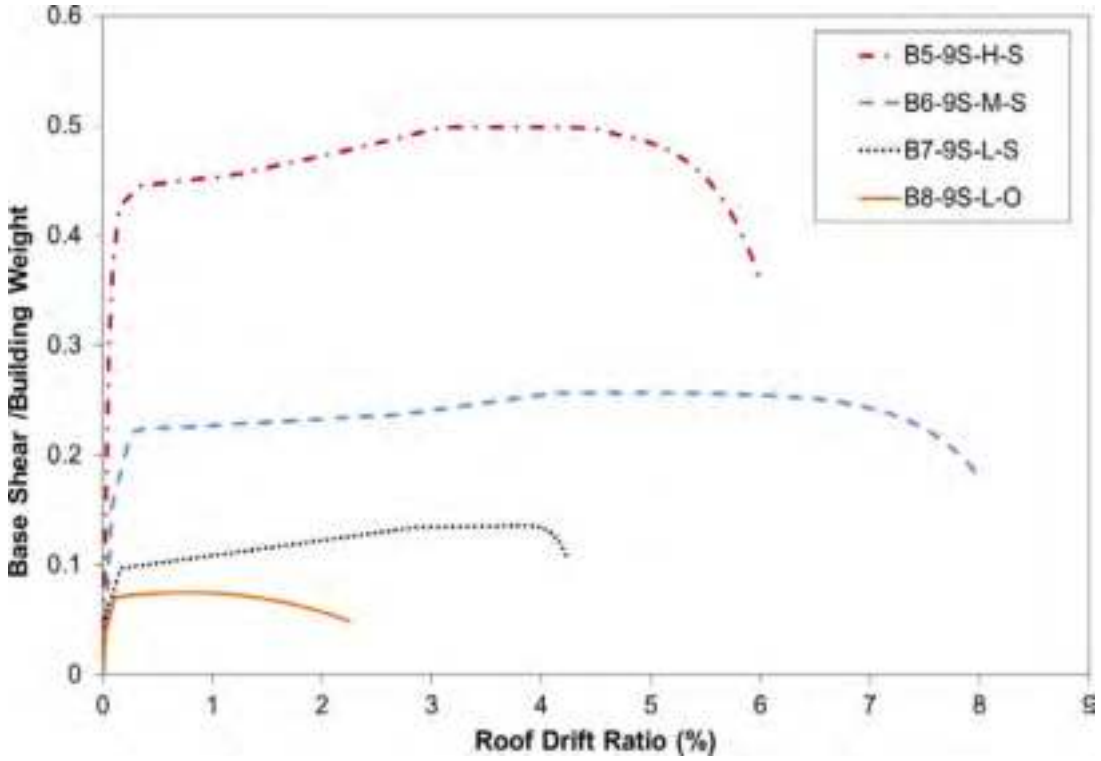

Figure 58: 9-Story Buildings Capacity Curves

It is observed that B5-9S-H-S, B6-9S-M-S and B7-9S-L-S have flat slopes at the maximum base shear capacity and the drop in strength is gradual afterwards, except for B7-9S-L-S which has a sharp drop. However, B8-9S-L-O (Ordinary RC shear wall building) capacity curve reaches its maximum strength and then drops sharply. Unlike the 6-story buildings (B3-6S-L-S and B4-6S-L-O), in 9-story buildings the special RC shear walls in B7-9S-L-S had a clear enhanced performance compared to ordinary RC shear walls in B8-9S-L-S. This is because for the taller buildings the shear walls design was governed by drift requirements. Hence, the design resulted in the same cross section for both special and ordinary walls, and the provided reinforcement was based on the minimum code requirements. With the same reinforcement and cross section

dimensions, special shear walls will clearly show an enhanced performance due to its high level of detailing and the presence of the confined boundary elements.

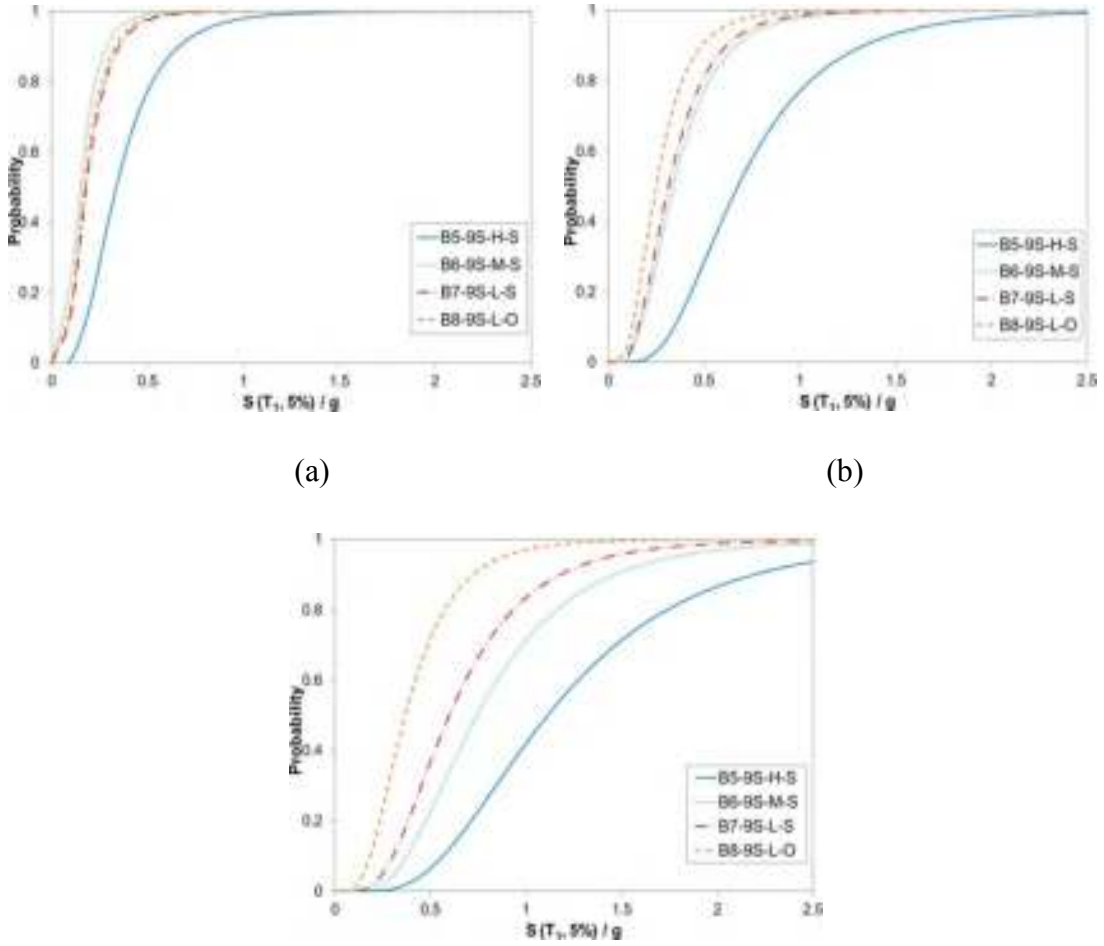

Figure 59: 9-Story Buildings Adjusted Fragility Curves: (a) IO Limit State; (b) LS Limit State; (c) CP Limit State

Figure 59 depicts the adjusted fragility curves for 9-story buildings. The fragility curves for the four buildings are very steep at IO limit state with slightly enhanced performance for B5-9S-H-S. At LS limit state, B5-9S-H-S fragility curve is a bit flatter while the performance of the other three buildings seems poor and similar. However, the difference in performance between the buildings is very clear at CP limit state. As expected, B5-9S-H-S has a clear enhanced performance and B8-9S-L-O has the lowest performance. To capture the performance at MCE level, Figure 60 shows the limit states exceedance probabilities for the four designs.

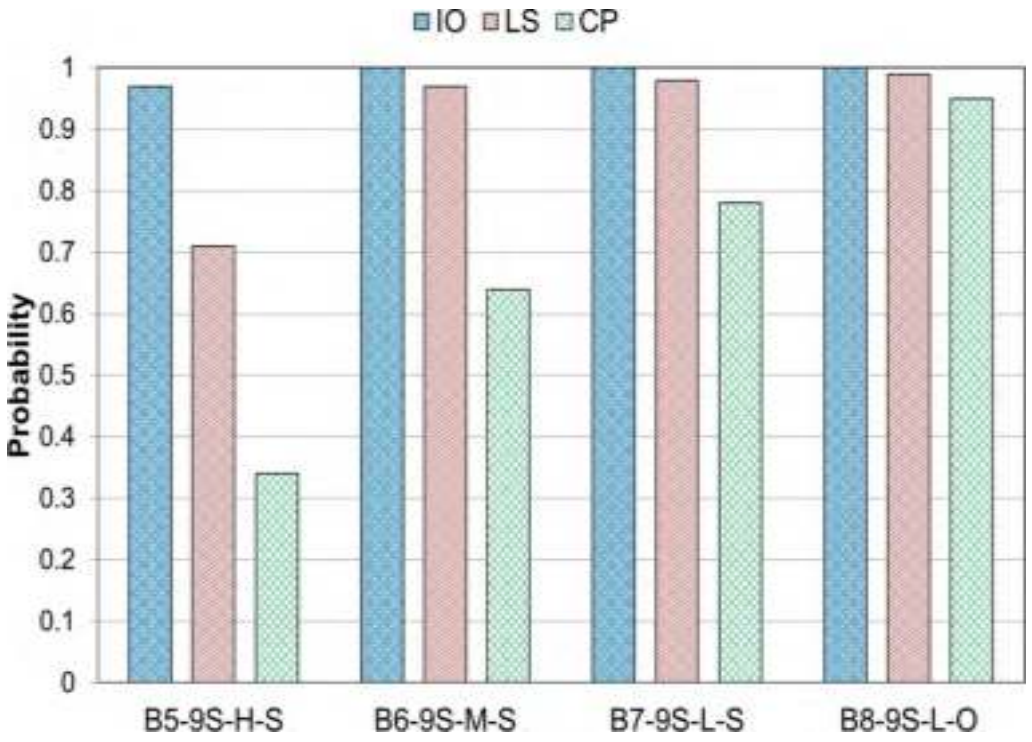

Figure 60: 9-Story Buildings Limit States Probabilities of Exceedance at MCE Level

It is clear that B5-9S-H-S has the lowest probabilities of exceedance at IO, LS and CP compared to B6-9S-M-S, B7-9S-L-S and B8-9S-L-O. Moreover, the 9-story building (B8-9S-L-O) with ordinary RC shear walls is showing higher exceedance probabilities at LS and CP compared to the building (B7-9S-L-S) with special RC shear walls. This reflects the enhanced performance of the well-detailed special RC shear walls compared to their ordinary counterparts when both are designed at the same seismic level.

The 12-story buildings performance indicators are summarized in Table 18. The ACMR of B9-12S-H-S is showing a 47% safety margin against collapse. Conversely, the other three designs have ACMRs below 1 which highlights that these designs collapse below MCE level. However, for the moderate seismicity design (B10-12S-M-S) the ratio is close to 1. As shown in Figure 61, B9-12S-H-S shows a much higher base shear capacity than other buildings. The high and moderate seismicity designs (B9-12S-H-S and B10-12S-M-S) are showing a flat slope at the peak strength and the capacity drops at slower rate.

Table 18: 12-Story Buildings Performance Indicators

Ref. Buildings	Seismic Design Level	Normalized Base Shear Capacity	S_{CT}	S_{MT}	ACMR
B9-12S-H-S	High	0.46	1.07	0.73	1.47
B10-12S-M-S	Moderate	0.24	0.69	0.73	0.95
B11-12S-L-S	Low	0.15	0.52	0.73	0.71
B12-12S-L-O	Low	0.12	0.36	0.73	0.5

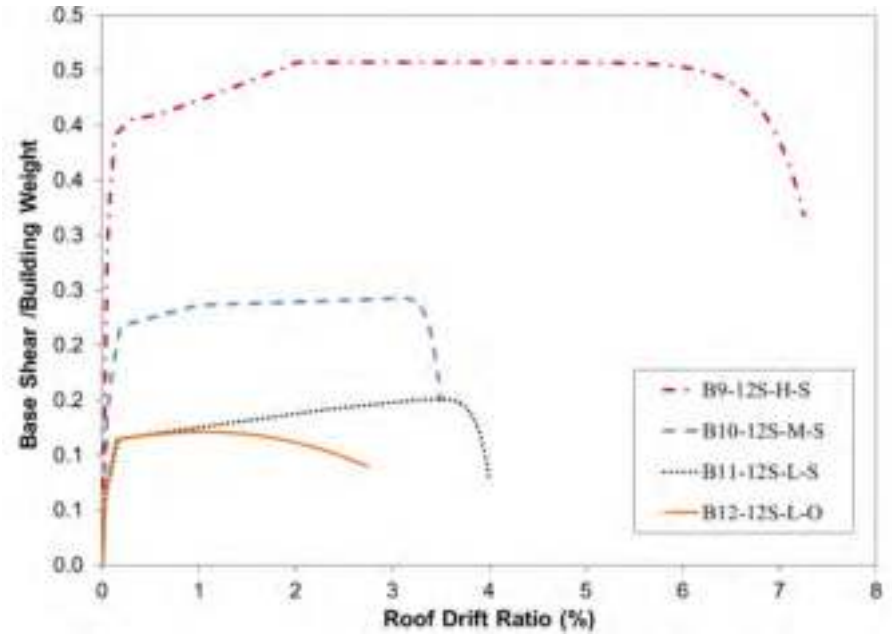

Figure 61: 12-Story Buildings Capacity Curves

Furthermore, buildings B11-12S-L-S and B12-12S-L-O designed for the lowest seismicity design are showing a sudden drop in base shear capacity. As a result, it can be noticed that the special RC shear walls in B11-12S-L-S when designed for low seismicity did not show an enhanced performance as expected. This is particularly seen from static analysis in the 12-story buildings when compared to 6 and 9 story buildings. Figure 62 presents the three limit states fragility curves for buildings B9-12S-H-S, B10-12S-M-S, B11-12S-L-S and B12-12S-L-O.

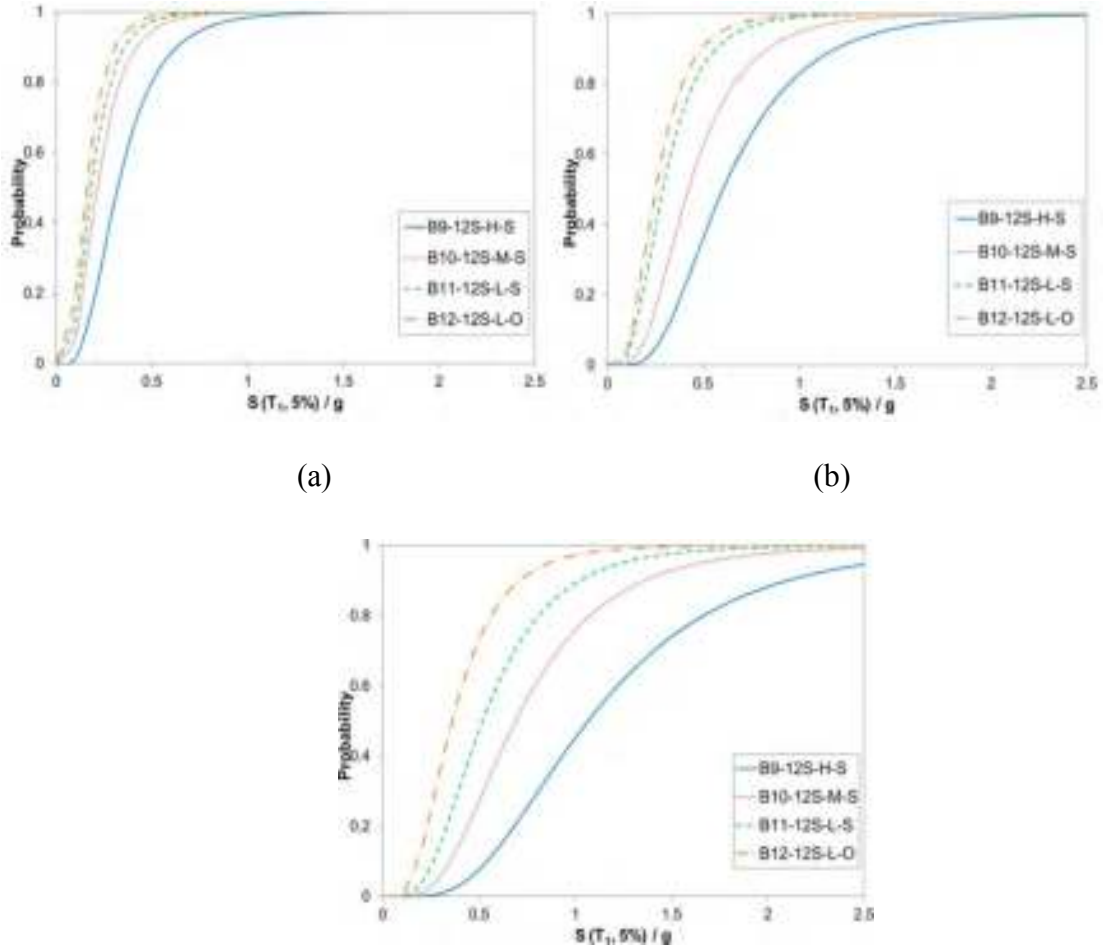

Figure 62: 12-Story Buildings Adjusted Fragility Curves: (a) IO Limit State; (b) LS Limit State; (c) CP Limit State

It is observed from Figure 62 that the low seismicity designs (B11-12S-L-S and B12-12S-L-O) have the lowest performance at the three limit states. This confirms the conclusion that in this case designing special RC shear walls at low seismicity level does not utilize its expected high performance. However, relative to ordinary RC shear walls, the special walls offer a more desirable performance. On the other hand, moderate and high seismicity designs (B9-12S-H-S and B10-12S-M-S) show a better enhanced performance at IO, LS and CP limit states. Comparison between the four 12-story buildings at MCE level is given in Figure 63.

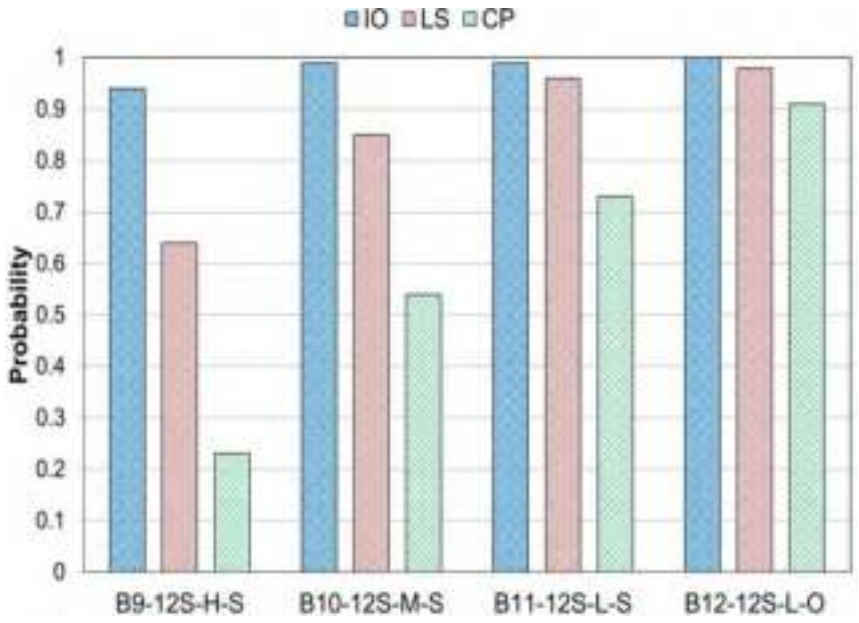

Figure 63:12-Story Buildings Limit States Probabilities of Exceedance at MCE Level

Building B9-12S-H-S has the least probability of exceeding IO, LS and CP limit states at MCE level. On the other hand, B12-12S-L-O has the highest probability of exceedance for the three limit states. Comparing the low seismicity designs (B11-12S-L-S and B12-12S-L-O), the use of special RC shear walls over ordinary RC shear walls offers an enhanced performance. This is shown in the lower limit states probabilities of exceedance for B11-12S-L-S compared to B12-12S-L-O.

4.5.2 Building-to-Building. This section presents the comparison between buildings with different number of floors designed for the same seismicity level. The purpose is to investigate the number of floors impact on the seismic performance of buildings designed for the same seismic hazard level. The comparison is made for the three seismicity levels (high, moderate and low).

It is observed that for high seismicity, the design of 6-story building shear walls was entirely governed by strength requirements which resulted in stronger building with ACMR of 1.57. While the 12-story building shear walls design was governed completely by drift requirements which resulted in an ACMR of 1.47. Hence, for 6 and 12 story buildings the design of all floors was governed by a unique mechanism (strength or drift). This resulted in stronger design for the strength-controlled case (ACMR=1.57) versus the drift-controlled design case (ACMR=1.47). However, 9-story

building design was partially governed by both drift and strength requirements (some floors by strength and others by drift). This variation in mechanism among the floors resulted in a somewhat hybrid-mode reinforcement pattern that was optimized to satisfy the appropriate critical case. In turn, this produced a relatively lower ACMR of 1.23. Highest seismicity designs (B1-6S-H-S, B5-9S-H-S and B9-12S-H-S) adjusted fragility curves for the three limit states are presented in Figure 64.

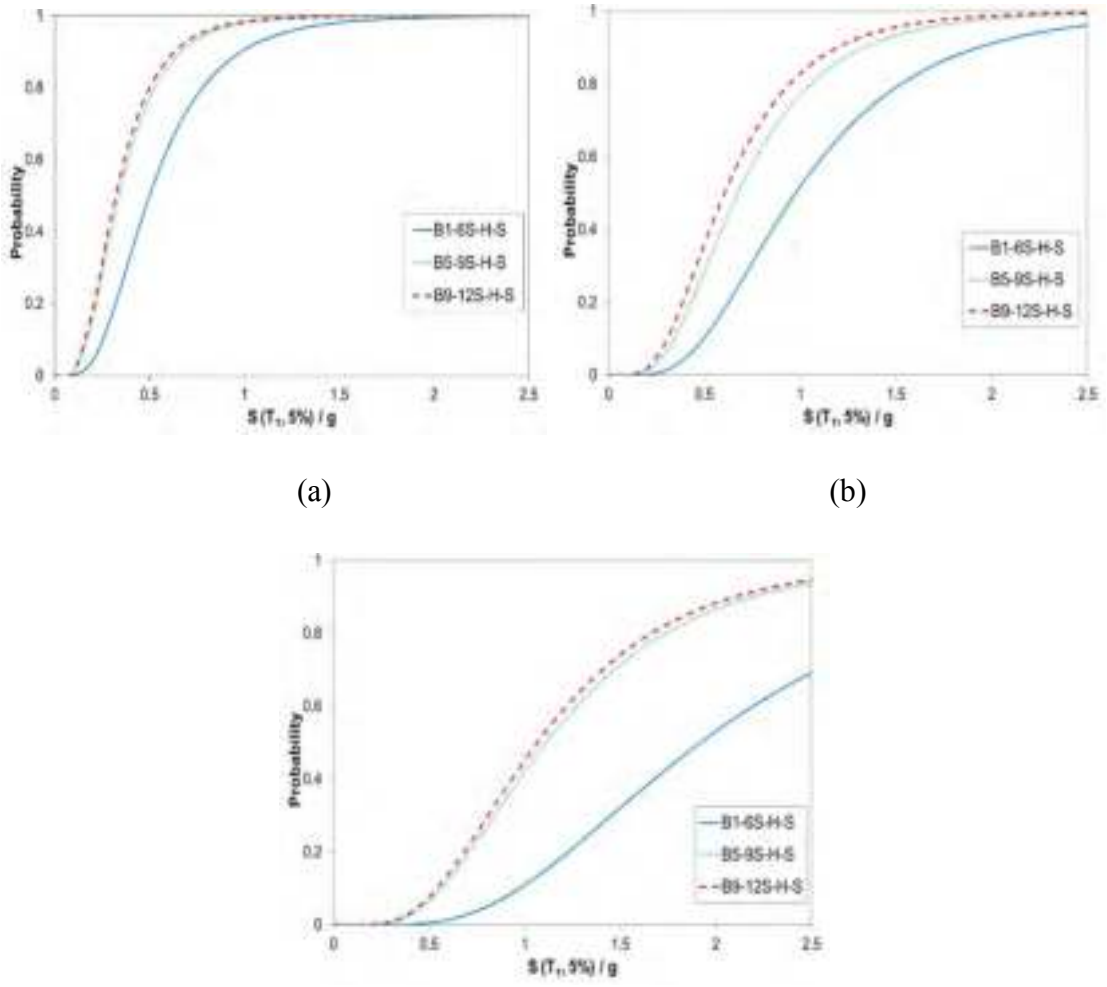

Figure 64: High Seismicity Designs Adjusted Fragility Curves: (a) IO Limit State; (b) LS Limit State; (c) CP Limit State

At IO, LS and CP limit states, the 6-story building (B1-6S-H-S) shows the lowest probabilities of exceedance compared to 9-story building (B5-9S-H-S) and 12-story building (B9-12S-H-S). The fragilities of B5-9S-H-S and B9-12S-H-S are close

with slightly lower exceedance probabilities for B5-9S-H-S. This indicates a better performance at highest seismicity level for shorter buildings (B1-6S-H-S and B5-9S-H-S) and most clearly in the 6-story building (B1-6S-H-S). It is concluded that taller RC shear wall buildings are more seismically vulnerable to earthquakes originating from distant sources than shorter buildings. This could be attributed to the absence of higher-mode effects in the performance optimized design of 6-story buildings. On the other hand, the 9-story and 12-story buildings performance optimized design did not eliminate the impact fully. Instead, the design was balanced to satisfy both the performance and cost constraints. As will be seen, this observation is less clear in moderate and low seismicity designs.

The three limit states probabilities of exceedance at MCE level is shown for the high seismicity designs in Figure 65. Figure 65 shows that the 6-story building (B1-6S-H-S) has the highest performance at its MCE level. This is also reflected in the high ACMR for B1-6S-H-S. Moreover, the 9-story building (B5-9S-H-S) has the least relative performance at its MCE level. However, the three designs (B1-6S-H-S, B5-9S-H-S and B9-12S-H-S) show an overall satisfactory performance and collapse probabilities at their corresponding MCE levels.

Adjusted fragility curves for the three moderate seismicity designs are given in Figure 66. The difference in vulnerability is not very clear among the three designs at IO limit state, except that B6-9S-M-S shows a slightly steeper fragility curve. At LS limit state, the steepness of the fragility curves is reduced and the enhancement in 6-story building (B2-6S-M-S) performance is clearer. The difference in performance is very clear among the three designs at CP limit state. B2-6S-M-S has a relatively flatter fragility curve indicating lower probability of exceeding CP limit state than B6-9S-M-S and B10-12S-M-S. Limit states probabilities of exceedance are shown in Figure 67 for the three designs at MCE level.

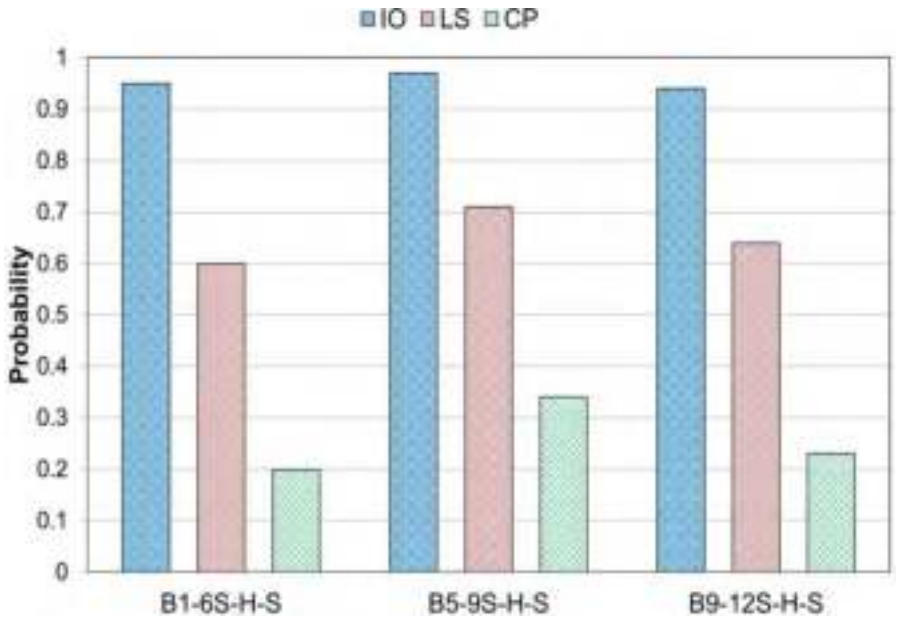

Figure 65: High Seismicity Designs Limit States Probabilities of Exceedance at MCE Level

Building B10-12S-M-S seems to have the best performance at its corresponding MCE level, reflected in the relatively low probabilities of exceeding IO, LS and CP limit states. This conclusion is also supported by its high ACMR compared to B2-6S-M-S and B6-9S-M-S. However, the 6-story building is still also showing a good performance at its MCE level compared to the 9-story building (B6-9S-M-S).

Low seismicity designs consist of six buildings; three of them designed with special RC shear walls and the other three designed with ordinary RC shear walls. Figure 68 depicts the adjusted fragility curves for the low seismicity designs at the IO, LS and CP limit states. At IO limit state, all low seismicity designs have similar steep fragility curves reflecting high probabilities of exceedance. However, the difference in performance is more obvious at LS and CP limit states. In general, 6-story buildings (B3-6S-L-S and B4-6S-L-O) are less seismically vulnerable than 9 and 12 story buildings (B7-9S-L-S, B8-9S-L-O, B11-12S-L-S and B12-12S-L-O). Additionally, low seismicity designs with special RC shear walls (B3-6S-L-S, B7-9S-L-S and B11-12S-L-S) have lower probabilities of exceednace compared to ordinary RC shear wall buildings (B4-6S-L-O, B8-9S-L-O and B12-12S-L-O). This is predominantly seen at LS and CP limit states.

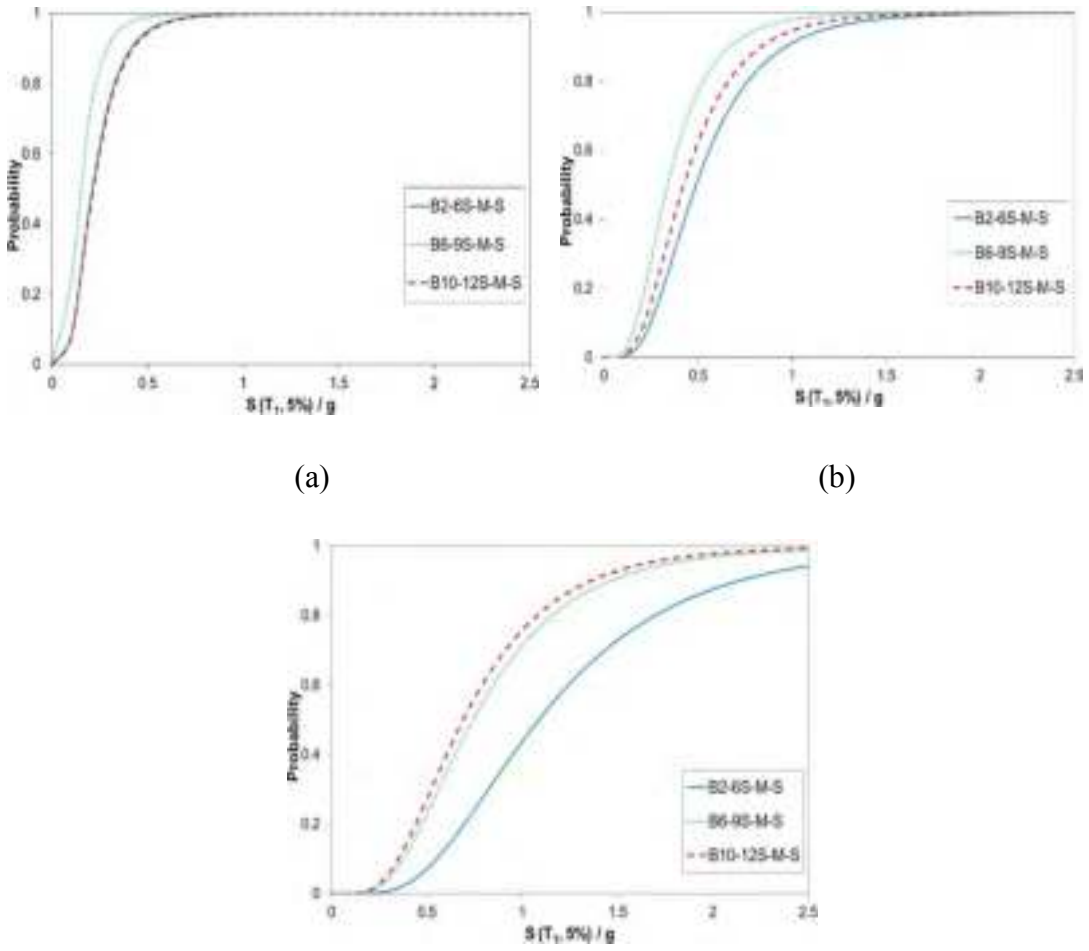

Figure 66: Moderate Seismicity Designs Adjusted Fragility Curves: (a) IO Limit State; (b) LS Limit State; (c) CP Limit State

Figure 69 presents a summary of limit states probabilities of exceedance at MCE level for low seismicity designs. In general, the 12-story building (B11-12S-L-S) has the lowest probabilities of exceeding IO, LS and CP limit states at its MCE level. This is also indicated by its relatively high ACMR. Additionally, it is observed that at the low seismicity, designs with special RC shear walls are showing a much better performance at MCE level compared to ordinary RC shear wall buildings. This conclusion is also observed in the higher ACMRs for special RC shear wall buildings. Therefore, unlike the static analysis results, the dynamic analysis results suggest an enhancement in performance of low seismicity designs with special RC shear walls compared to designs with ordinary RC shear walls.

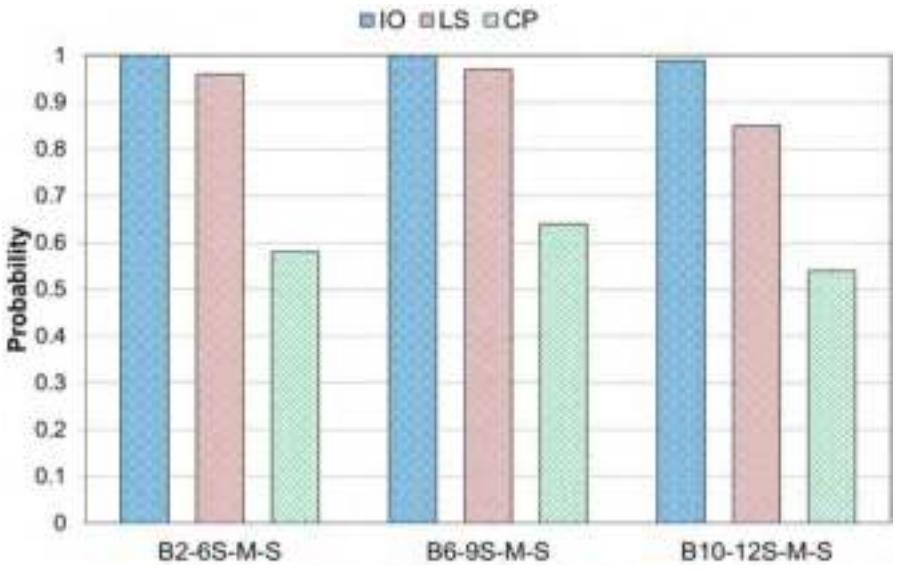

Figure 67: Moderate Seismicity Designs Limit States Probabilities of Exceedance at MCE Level

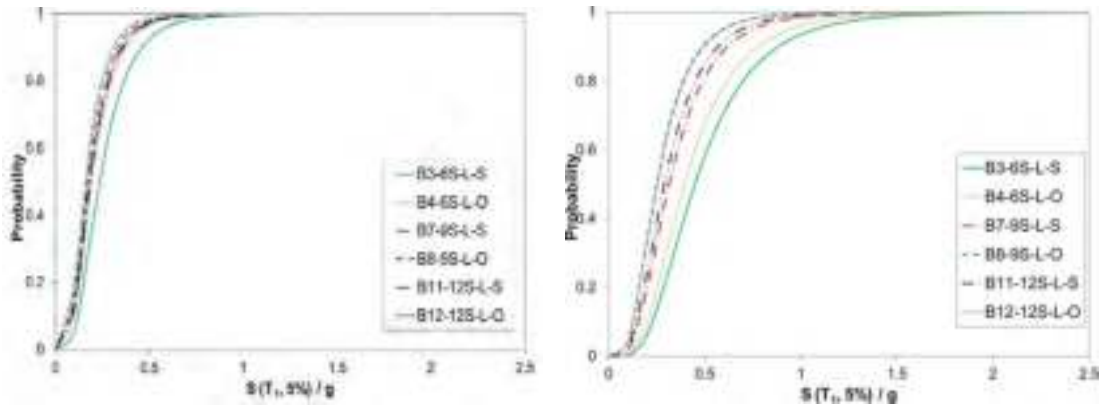

(a) (b)

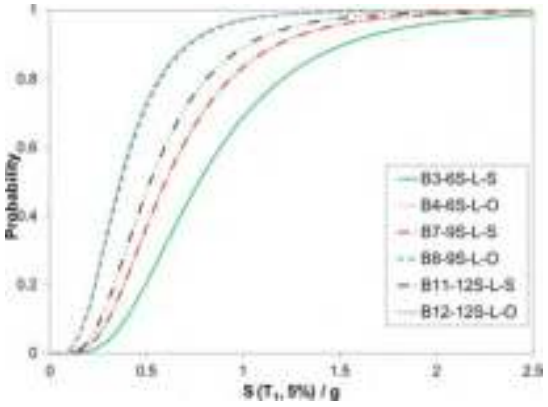

(c)

Figure 68: Low Seismicity Designs Adjusted Fragility Curves: (a) IO Limit State; (b) LS Limit State; (c) CP Limit State

Table 19 summarizes the performance of the twelve reference buildings at their corresponding MCE level. It can be seen that the probabilities of exceeding IO, LS and CP performance levels at MCE is lower for high seismicity designs compared to low seismicity designs. This observation is clearly seen in 6-story, 9-story and 12-story buildings. The lower limit states exceedance probabilities reflect the enhanced performance of high and moderate seismicity designs. The impact of the performance enhancement on the total cost of the buildings will be seen in Chapter 5, particularly in Table 32.

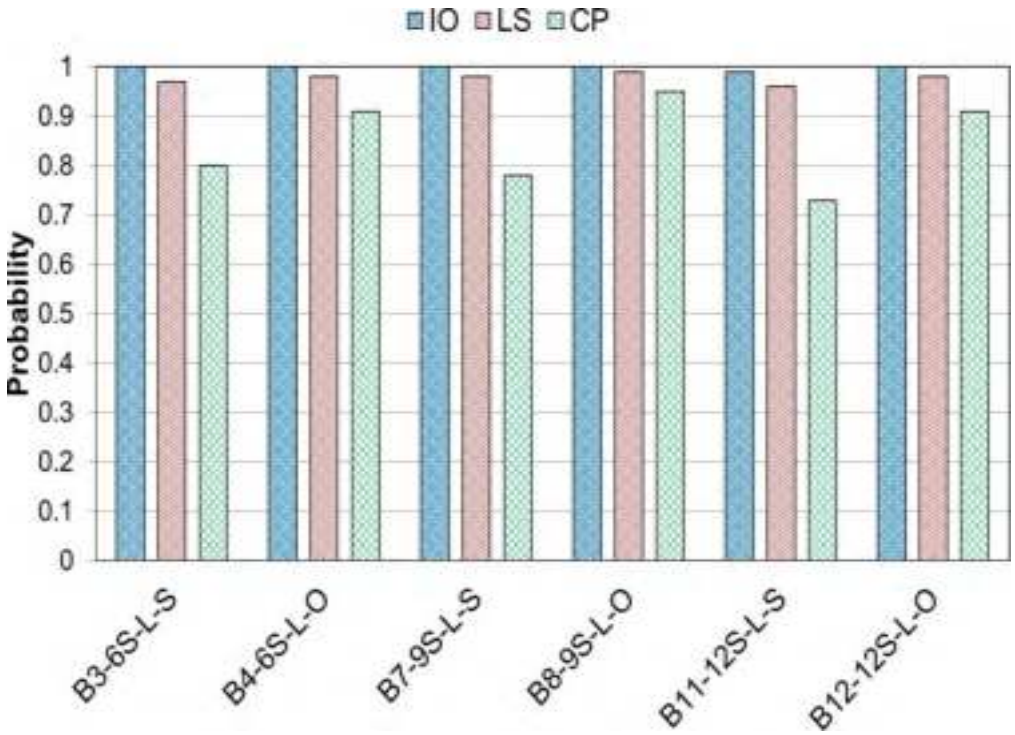

Figure 69: Low Seismicity Designs Limit States Probabilities of Exceedance at MCE Level

Table 19: Summary of the Effects of LFRS Design and Seismic Design level on the exceedance probabilities at MCE level

	Low Seismicity				Moderate Seismicity		High Seismicity	
	Ordinary Shear Wall		Special Shear Wall					
6-Story (B4, B3, B2, B1)	**IO**	100%	**IO**	100%	**IO**	100%	**IO**	95%
	LS	98%	**LS**	97%	**LS**	96%	**LS**	60%
	CP	91%	**CP**	80%	**CP**	58%	**CP**	20%
9-Story (B8, B7, B6, B5)	**IO**	100%	**IO**	100%	**IO**	100%	**IO**	97%
	LS	99%	**LS**	98%	**LS**	97%	**LS**	71%
	CP	95%	**CP**	78%	**CP**	64%	**CP**	34%
12-Story (B12, B11, B10, B9)	**IO**	100%	**IO**	99%	**IO**	99%	**IO**	94%
	LS	98%	**LS**	96%	**LS**	85%	**LS**	64%
	CP	91%	**CP**	73%	**CP**	54%	**CP**	23%

Chapter 5: Construction and Maintenance Cost Comparison

To highlight the significance of the diverse seismic hazard estimates on buildings located in Dubai, the consequences have to be measured and expressed in numbers. For that purpose, the impact of earthquake damages on the economy is investigated to provide more tangible conclusions for decision makers and real estate developers. Performance conclusions are more appealing to consulting engineers and building officials. Generally, earthquakes cause social and economic losses [4]. However, for the objective of this study, focus is given to the direct economic losses in terms of repair costs associated with structural and non-structural damages. Indirect costs and content repair or replacement costs were excluded. Earthquake loss approximation involves; (i) hazard estimation, (ii) assets data (buildings and population) and (iii) seismic vulnerability analysis [4].

The construction cost of each building is divided into two main components; (1) Structural Material Cost and (2) Non-Structural Cost. This cost only represents the skeleton construction cost, considering the superstructure and non-structural elements. It does not account for substructure cost, other construction costs and the contractor's profit. This was done to isolate other factors and focus on the seismic design level impact on construction materials quantities and cost. The structural cost is calculated by estimating the concrete and reinforcing steel quantities and using the market unit price to calculate the total material cost. The concrete unit price used in this estimate is 250 AED/m^3 (68 \$/m^3) and the reinforcement steel unit price is 2500 AED/ton (681 \$/ton). These are average prices obtained through personal communication with major contractors in Dubai. The steel and concrete prices provided by one of the contractors are shown in Appendix B. Table 20 summarizes the bill of quantities and structural cost calculations for the twelve reference buildings. On the other hand, the non-structural cost is calculated using a percentage of the total construction cost estimate in UAE that is provided by Bruce Shaw [62]. The non-structural cost is approximately 55% of the total construction cost for a standard developer finished office building. This percentage was provided through communication with buildings consultants and developers in Dubai. The average total construction cost per unit area in UAE as estimated by Bruce Shaw is given in Table 21. The average value was used in this estimate.

Table 20: Bill of Quantities and Structural Cost Estimation

	Concrete Volume (m^3)			Steel Quantity (ton)			Structural Material Cost		
Ref. Building	Columns	Slabs	Walls	Columns	Slabs	Walls	Concrete	Steel	Total
B1-6S-H-S	334	1087	324	26	263	120	$118,778	$278,721	$397,499
B2-6S-M-S	334	1087	135	26	263	74	$105,915	$247,155	$353,069
B3-6S-L-S	334	1087	108	26	263	19	$104,077	$209,727	$313,804
B4-6S-L-O	334	1087	108	26	263	25	$104,077	$213,621	$317,698
B5-9S-H-S	553	1631	741	35	394	177	$199,174	$412,536	$611,710
B6-9S-M-S	553	1631	345	35	394	115	$172,160	$370,286	$542,446
B7-9S-L-S	553	1631	268	35	394	78	$166,948	$344,812	$511,760
B8-9S-L-O	553	1631	268	35	394	69	$166,948	$338,762	$505,710
B9-12S-H-S	802	2175	1400	43	525	220	$297,904	$536,764	$834,668
B10-12S-M-S	802	2175	747	43	525	90	$253,449	$448,204	$701,654
B11-12S-L-S	802	2175	574	43	525	48	$241,705	$419,679	$661,384
B12-12S-L-O	802	2175	574	43	525	39	$241,705	$413,396	$655,101

Table 21: Total Construction Cost per Unit Area [62]

	Construction Cost Range per m^2		
Building Type	From	To	Average
Low-Medium Rise Office Buildings (Developer Standard)	$1,000	$1,300	**$1,150**

Low-Medium rise buildings are buildings up to 15-story as defined by Brue Shaw [62]. So, this rate will be applicable to the twelve reference buildings.

For the repair costs calculations, structural and non-structural damage percentages are adapted from SEAOC blue book [63]. SEAOC blue book includes five structural and non-structural performance levels. The performance levels, its description and damage percentages are summarized in Table 22. It can be seen that SP2/NP2 corresponds to IO performance level, SP3/NP3 parallels LS performance level and SP4/NP4 is equivalent to CP performance level. From the range of non-structural damage ratios provided by SEAOC blue book, the lower bound was chosen. The selection is based on experience since the reference buildings' lateral system consists of shear walls which are relatively more rigid compared to other structural systems. The structural and non-structural repair costs are calculated using HAZUS economic losses estimation methodology [64] as follows:

Structural Repair Cost ($) = [Structural material cost X Probability of exceeding a limit state at MCE level X Structural damage ratio at the limit state]

Non-Structural Repair Cost ($) = [Non-structural cost X Probability of exceeding a limit state at MCE level X Non-Structural damage ratio at the limit state]

Table 22: SEAOC Blue Book Performance Levels and Damage Percentages

Structural Performance Level	Non-Structural Performance Level	Qualitative Description	Structural Damage Ratio	Non-Structural Damage Ratio
SP1	**NP1**	Operational	0%	0%-10%
SP2	**NP2**	Occupiable	30%	5%-40%
SP3	**NP3**	Life Safe	60%	20%-50%
SP4	**NP4**	Near Collapse	80%	40%-80%
SP5	**NP5**	Collapsed	100%	>70%

It should be noted that damages and associated repair costs are estimated at the highest seismicity MCE level. This is intentionally done to achieve the objectives of this research of comparing the performance and total cost of the twelve different designs under the high seismic hazard. This will represent the worst possible seismic hazard scenario in Dubai and its consequences on buildings designed for different seismicity levels.

The following sections present total construction cost and total repair cost comparison between the different designs.

5.1 6-Story Buildings Cost Comparison

Summary of construction and repair costs is given in Tables 23-25 for 6-story buildings at the three performance levels. The total construction cost is the sum of structural and non-structural costs. Moreover, the total repair cost consists of structural and non-structural repair costs. Figure 70 shows a clear cost comparison between 6-story buildings (B1-6S-H-S, B2-6S-M-S, B3-6S-L-S and B4-6S-L-O) at the three performance levels (IO, LS and CP).

Table 23: Summary of 6-Story Buildings Construction and Repair Costs at IO

	Construction Cost			Immediate Occupancy			
Ref. Buildings	Structural Cost	Non-Structural Cost	Total Construction Cost	Structural Damage Repair Cost	Non-Structural Damage Repair Cost	Total Repair Cost	Total Cost
B1-6S-H-S	$397,499	$364,320	$761,819	$113,287	$17,305	$130,593	**$892,412**
B2-6S-M-S	$353,069	$364,320	$717,389	$105,921	$18,216	$124,137	**$841,526**
B3-6S-L-S	$313,804	$364,320	$678,124	$94,141	$18,216	$112,357	**$790,481**
B4-6S-L-O	$317,698	$364,320	$682,018	$95,309	$18,216	$113,525	**$795,544**

Table 24: Summary of 6-Story Buildings Construction and Repair Costs at LS

	Construction Cost			Life Safety			
Ref. Buildings.	Structural Cost	Non-Structural Cost	Total Construction Cost	Structural Damage Repair Cost	Non-Structural Damage Repair Cost	Total Repair Cost	Total Cost
B1-6S-H-S	$397,499	$364,320	$761,819	$157,410	$48,090	$205,500	**$967,320**
B2-6S-M-S	$353,069	$364,320	$717,389	$203,368	$69,949	$273,317	**$990,707**
B3-6S-L-S	$313,804	$364,320	$678,124	$182,634	$70,678	$253,312	**$931,436**
B4-6S-L-O	$317,698	$364,320	$682,018	$186,807	$71,407	$258,213	**$940,231**

Table 25: Summary of 6-Story Buildings Construction and Repair Costs at CP

	Construction Cost			Collapse Prevention			
Ref. Buildings	Structural Cost	Non-Structural Cost	Total Construction Cost	Structural Damage Repair Cost	Non-Structural Damage Repair Cost	Total Repair Cost	Total Cost
B1-6S-H-S	$397,499	$364,320	$761,819	$63,600	$29,146	$92,746	**$854,565**
B2-6S-M-S	$353,069	$364,320	$717,389	$163,824	$84,522	$248,346	**$965,736**
B3-6S-L-S	$313,804	$364,320	$678,124	$203,345	$118,040	$321,385	**$999,509**
B4-6S-L-O	$317,698	$364,320	$682,018	$231,284	$115,642	$346,926	**$1,028,945**

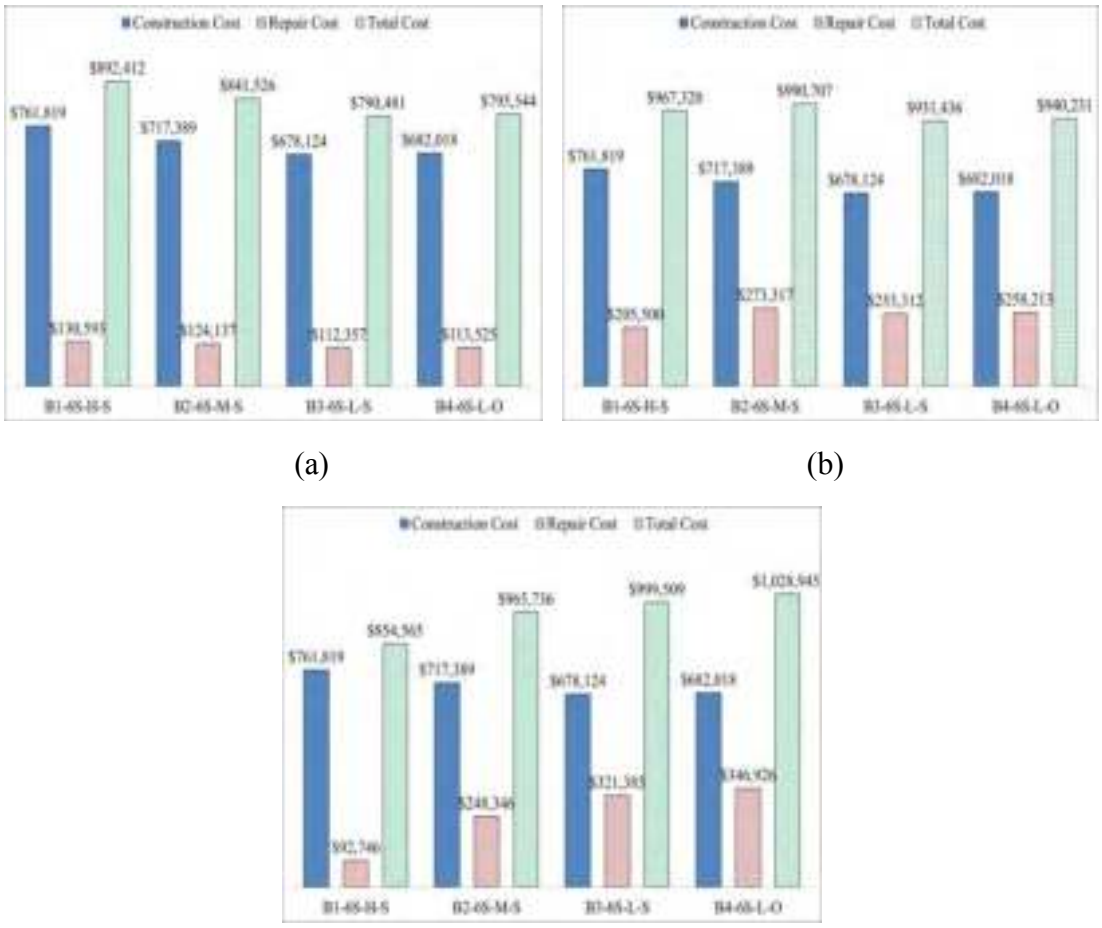

(a) (b)

(c)

Figure 70: 6-Story Buildings Cost Comparison; (a) IO Damage State, (b) LS Damage State, (c) CP Damage State

It can be observed that the 6-story building (B1-6S-H-S) designed for highest seismicity has total construction cost which is 12.3% higher than lowest seismicity design with Special RC shear walls (B3-6S-L-S). It is also 11.7% higher than lowest seismicity design with Ordinary RC shear walls (B4-6S-L-O). Furthermore, the 6-story building (B2-6S-M-S) designed for moderate seismicity has total construction cost of 5.8% higher than lowest seismicity design with Special RC shear walls (B3-6S-L-S). Moreover, it is 5.2% higher than lowest seismicity design with Ordinary RC shear walls (B4-6S-L-O). Therefore, the seismic design level did not significantly affect the initial investment in 6-story buildings. Additionally, lowest Seismicity design (B3-6S-L-S) with special RC shear wall has a lower total construction cost by 0.6% compared to lowest seismicity design (B4-6S-L-O) with ordinary RC shear walls. Hence, in 6-story buildings, the choice of special RC shear walls over ordinary RC shear walls resulted

in minor savings in the initial investment. This conclusion is tied with the findings outlined in section 4.5.1 that the ordinary RC shear walls are designed for higher forces compared to special RC shear walls. As a result, if the design is controlled by strength requirements, the ordinary walls will require more reinforcement compared to the special walls.

From Figure 70 (a) it can be seen that at IO limit state, highest seismicity design (B1-6S-H-S) has the highest repair cost and highest total cost. On the other hand, lowest seismicity design with special RC shear walls (B3-6S-L-S) has the lowest repair and total costs even compared to B4-6S-L-O (designed for low seismicity with ordinary RC shear walls). Furthermore, at LS limit state shown in Figure 70 (b), moderate seismicity design (B2-6S-M-S) has the highest repair cost and highest total cost. On the other hand, lowest seismicity design with special RC shear walls (B3-6S-L-S) has the lowest repair and total costs even compared to B4-6S-L-O. As presented in Figure 70 (c), at CP performance level, lowest seismicity design with ordinary RC shear walls (B4-6S-L-O) has the highest repair cost and highest total cost. The total cost is approximately 20% higher than highest seismicity design (B1-6S-H-S). Additionally, lowest seismicity design with special RC shear walls (B3-6S-L-S) has lower repair and total costs compared to lowest seismicity design with ordinary RC shear walls (B4-6S-L-O) at CP limit state. Total cost of B3-6S-L-S is lower by approximately 3% compared to B4-6S-L-O. It should be noted that high repair costs are associated with an increase in the down time of the structure.

5.2 9-Story Buildings Cost Comparison

Tables 26-28 provide Summary of construction and repair costs for 9-story buildings at the three performance levels. Furthermore, construction and repair costs comparison among 9-story buildings (B5-9S-H-S, B6-9S-M-S, B7-9S-L-S and B8-9S-L-O) is shown in Figure 71 at the three performance levels (IO, LS and CP).

Table 26: Summary of 9-Story Buildings Construction and Repair Costs at IO

Ref. Buildings	Construction Cost			Immediate Occupancy			
	Structural Cost	Non-Structural Cost	Total Construction Cost	Structural Damage Repair Cost	Non-Structural Damage Repair Cost	Total Repair Cost	Total Cost
B5-9S-H-S	$611,710	$546,480	$1,158,190	$178,008	$26,504	$204,512	**$1,362,701**
B6-9S-M-S	$542,446	$546,480	$1,088,926	$162,734	$27,324	$190,058	**$1,278,984**
B7-9S-L-S	$511,760	$546,480	$1,058,240	$153,528	$27,324	$180,852	**$1,239,092**
B8-9S-L-O	$505,710	$546,480	$1,052,190	$151,713	$27,324	$179,037	**$1,231,227**

Table 27: Summary of 9-Story Buildings Construction and Repair Costs at LS

Ref. Buildings	Construction Cost			Life Safety			
	Structural Cost	Non-Structural Cost	Total Construction Cost	Structural Damage Repair Cost	Non-Structural Damage Repair Cost	Total Repair Cost	Total Cost
B5-9S-H-S	$611,710	$546,480	$1,158,190	$260,588	$77,600	$338,188	**$1,496,378**
B6-9S-M-S	$542,446	$546,480	$1,088,926	$315,704	$106,017	$421,721	**$1,510,647**
B7-9S-L-S	$511,760	$546,480	$1,058,240	$300,915	$107,110	$408,025	**$1,466,265**
B8-9S-L-O	$505,710	$546,480	$1,052,190	$300,392	$108,203	$408,595	**$1,460,785**

Table 28: Summary of 9-Story Buildings Construction and Repair Costs at CP

Ref. Buildings	Construction Cost			Collapse Prevention			
	Structural Cost	Non-Structural Cost	Total Construction Cost	Structural Damage Repair Cost	Non-Structural Damage Repair Cost	Total Repair Cost	Total Cost
B5-9S-H-S	$611,710	$546,480	$1,158,190	$166,385	$74,321	$240,706	**$1,398,896**
B6-9S-M-S	$542,446	$546,480	$1,088,926	$277,732	$139,899	$417,631	**$1,506,557**
B7-9S-L-S	$511,760	$546,480	$1,058,240	$319,338	$170,502	$489,840	**$1,548,080**
B8-9S-L-O	$505,710	$546,480	$1,052,190	$384,340	$207,662	$592,002	**$1,644,192**

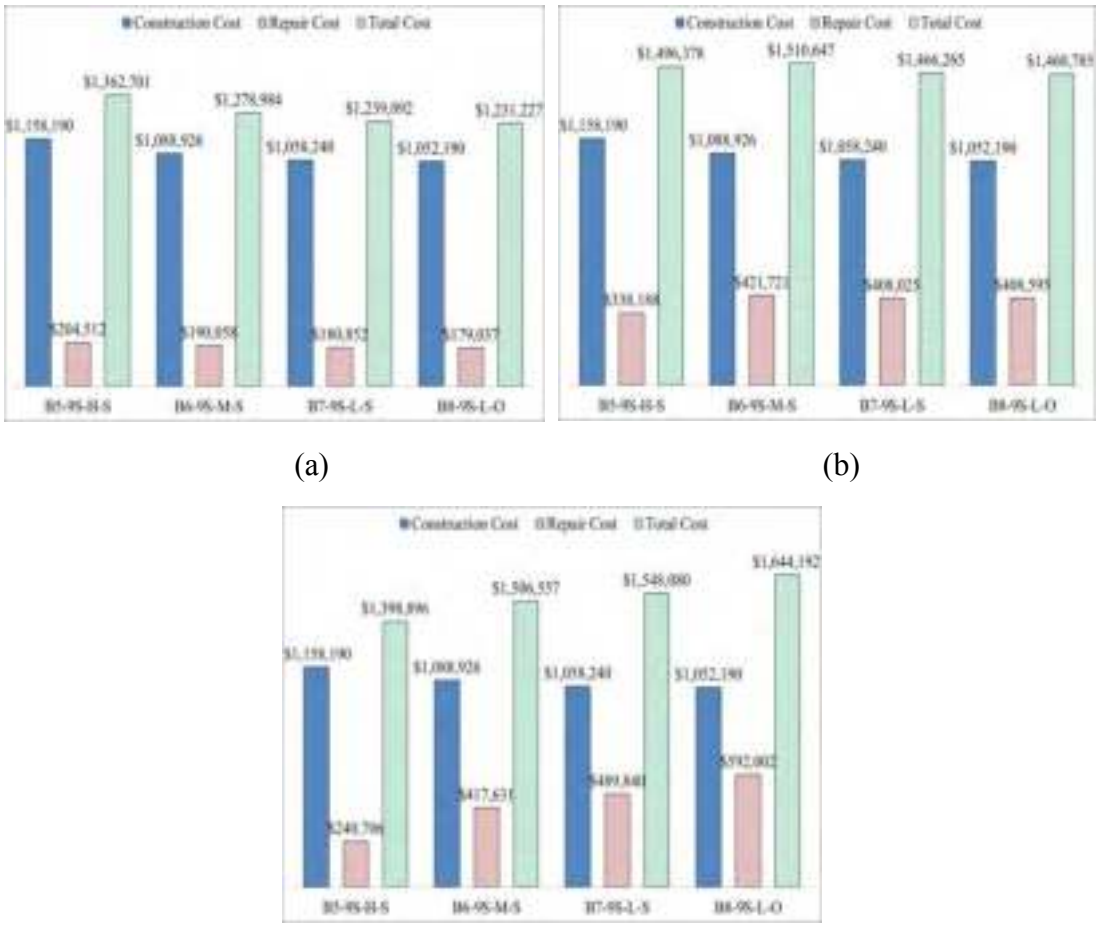

Figure 71: 9-Story Buildings Cost Comparison; (a) IO Damage State, (b) LS Damage State, (c) CP Damage State

It is noted that highest seismicity design (B5-9S-H-S) has a total construction cost of 9.4% higher than lowest seismicity design with Special RC shear walls (B7-9S-L-S). It is also 10% higher than lowest seismicity design with Ordinary RC shear walls (B8-9S-L-O). Furthermore, the 9-story building (B6-9S-M-S) designed for moderate seismicity have a total construction cost which is only 2.9% higher than lowest seismicity design with Special RC shear walls (B7-9S-L-S). Additionally, it is 3.5% higher than lowest seismicity design with Ordinary RC shear walls (B8-9S-L-O). Hence, similar to 6-story buildings, the increase in seismic design level did not severely affect the construction cost of 9-story buildings. Moreover, lowest Seismicity 9-story building (B7-9S-L-S) with special RC shear wall has a higher total construction cost by only 0.6% compared to lowest seismicity design (B8-9S-L-O) with ordinary RC shear walls. The increase in construction cost associated with the choice of special RC shear

walls is negligible. As it was explained in section 4.5.1, 9-story buildings shear walls design was governed by drift requirements. Hence, ordinary and special RC shear walls had the same cross-section while the minimum reinforcement is provided in both. The special shear walls increase in cost is due to the special detailing requirements, such as boundary elements reinforcement and confinement.

From Figure 71 (a), at IO limit state, highest seismicity design (B5-9S-H-S) has the highest repair cost and highest total cost. Lowest seismicity design with ordinary RC shear walls (B8-9S-L-O) has the lowest repair and total costs even when compared to B7-9S-L-S (designed for low seismicity with special RC shear walls). However, the reduction in B8-9S-L-O total cost compared to B7-9S-L-S is very marginal (0.6%). Furthermore, as shown in Figure 71 (b), At LS limit state; moderate seismicity design (B6-9S-M-S) has the highest repair cost and highest total cost. On the other hand, lowest seismicity design with ordinary RC shear walls (B8-9S-L-O) has the lowest repair and total costs. Compared to lowest seismicity building design with special RC shear walls (B7-9S-L-S), B8-9S-L-O only yields 0.4% reduction in total cost. Conversely, Figure 71 (c) shows that at CP limit state, lowest seismicity design with ordinary RC shear walls (B8-9S-L-O) has the highest repair cost and highest total cost. The total cost is approximately 17.5% higher than building (B5-9S-H-S), designed for highest seismicity. Moreover, lowest seismicity design with special RC shear walls (B7-9S-L-S) has 20.8% lower repair cost and 6.2% lower total cost compared to lowest seismicity design with ordinary RC shear walls (B8-9S-L-O) at CP performance level. It is noteworthy to highlight that the higher repair costs are directly linked with higher down time.

5.3 12-Story Buildings Cost Comparison

Construction and repair costs at the three performance levels are summarized in Tables 29-31 for 12-story buildings. Moreover, the comparison of construction and repair costs between 12-story buildings (B9-12S-H-S, B10-12S-M-S, B11-12S-L-S and B12-12S-L-O) is illustrated in Figure 72 at the three performance levels (IO, LS and CP).

Table 29: Summary of 12-Story Buildings Construction and Repair Costs at IO

Ref. Buildings	Construction Cost			Immediate Occupancy			
	Structural Cost	Non-Structural Cost	Total Construction Cost	Structural Damage Repair Cost	Non-Structural Damage Repair Cost	Total Repair Cost	Total Cost
B9-12S-H-S	$834,668	$728,640	$1,563,308	$235,376	$34,246	$269,623	**$1,832,931**
B10-12S-M-S	$701,654	$728,640	$1,430,294	$208,391	$36,068	$244,459	**$1,674,752**
B11-12S-L-S	$661,384	$728,640	$1,390,024	$196,431	$36,068	$232,499	**$1,622,523**
B12-12S-L-O	$655,101	$728,640	$1,383,741	$196,530	$36,432	$232,962	**$1,616,704**

Table 30: Summary of 12-Story Buildings Construction and Repair Costs at LS

Ref. Buildings	Construction Cost			Life Safety			
	Structural Cost	Non-Structural Cost	Total Construction Cost	Structural Damage Repair Cost	Non-Structural Damage Repair Cost	Total Repair Cost	Total Cost
B9-12S-H-S	$834,668	$728,640	$1,563,308	$320,513	$93,266	$413,779	**$1,977,087**
B10-12S-M-S	$701,654	$728,640	$1,430,294	$357,843	$123,869	$481,712	**$1,912,006**
B11-12S-L-S	$661,384	$728,640	$1,390,024	$380,957	$139,899	$520,856	**$1,910,881**
B12-12S-L-O	$655,101	$728,640	$1,383,741	$385,200	$142,813	$528,013	**$1,911,755**

Table 31: Summary of 12-Story Buildings Construction and Repair Costs at CP

Ref. Buildings	Construction Cost			Collapse Prevention			
	Structural Cost	Non-Structural Cost	Total Construction Cost	Structural Damage Repair Cost	Non-Structural Damage Repair Cost	Total Repair Cost	Total Cost
B9-12S-H-S	$834,668	$728,640	$1,563,308	$153,579	$67,035	$220,614	**$1,783,922**
B10-12S-M-S	$701,654	$728,640	$1,430,294	$303,114	$157,386	$460,501	**$1,890,794**
B11-12S-L-S	$661,384	$728,640	$1,390,024	$386,248	$212,763	$599,011	**$1,989,036**
B12-12S-L-O	$655,101	$728,640	$1,383,741	$476,914	$265,225	$742,139	**$2,125,880**

(a) (b)

(c)

Figure 72: 12-Story Buildings Cost Comparison; (a) IO Damage State, (b) LS Damage State, (c) CP Damage State

In general, similar to 6 and 9 story buildings, the seismic design level impact on construction cost is not very severe. For instance, highest seismicity design (B9-12S-H-S) has a total construction cost that is 12.5% higher than lowest seismicity design with Special RC shear walls (B11-12S-L-S). Also, it is 13% higher than lowest seismicity design with Ordinary RC shear walls (B12-12S-L-O). In addition, moderate seismicity design (B10-12S-M-S) total construction cost is only 2.9% higher than lowest seismicity design with Special RC shear walls (B11-12S-L-S). It is also 3.4% higher than lowest seismicity design with Ordinary RC shear walls (B12-12S-L-O). Comparing Lowest Seismicity designs (B11-12S-L-S and B12-12S-L-O), the choice of special RC shear walls over ordinary RC shear walls increases the total construction cost barely by 0.45%.

As shown in Figure 72 (a), at IO limit state, highest seismicity design (B9-12S-H-S) has the highest repair cost and highest total cost. Lowest seismicity design with ordinary RC shear walls (B12-12S-L-O) has the lowest repair and total costs even when compared to B11-12S-L-S (designed for low seismicity with special RC shear walls). However, B12-12S-L-O is only 0.4% lower in total cost compared to B11-12S-L-S. Therefore, choosing special RC shear walls over their ordinary counterpart does not show a significant increase in cost. This conclusion is common among the 6, 9 and 12 story buildings. In fact, cost savings was achieved in 6-story buildings with special RC shear walls. Furthermore, At LS limit state, highest seismicity design (B9-12S-H-S) has the highest total cost. However, lowest seismicity design with ordinary RC shear walls (B12-12S-L-O) has the highest repair cost. Also, B12-12S-L-O design has slightly higher total and repair costs than lowest seismicity design with special RC shear walls (B11-12S-L-S). At CP limit state as presented in Figure 72 (c), lowest seismicity design with ordinary RC shear walls (B12-12S-L-O) has the highest repair cost and highest total cost. The total cost is approximately 19.2% higher than highest seismicity design (B9-12S-H-S). Moreover, lowest seismicity design with special RC shear walls (B11-12S-L-S) has lower repair and total costs compared to lowest seismicity design with ordinary RC shear walls (B12-12S-L-O). B11-12S-L-S total cost is about 6.9% lower than B12-12S-L-O. The higher repair costs also reflect an increase in buildings' downtime.

An overall summary of the impact of Lateral Force Resisting System (LFRS) design and performance level on total cost is illustrated in Table 32. This table can be used to provide guidance for decision makers about the seismic hazard level and LFRS impact on the total cost of 6-story, 9-story and 12-story buildings in Dubai. In Table 32, the total cost of the designs in each group of buildings is normalized by the total cost of low seismicity design with ordinary RC shear walls. This will show the relative impact of the LRFS and seismic design level on total cost at each performance level. For instance, it is noted that at IO and LS performance levels, the choice of special RC shear walls over ordinary RC shear walls does not cause any significant change in overall (construction and repair) cost for 6, 9 and 12-story buildings. However, there is a clear reduction in the overall cost at CP performance level when using special RC shear walls for low seismicity. Furthermore, the overall cost is higher for buildings designed for moderate and high seismicity at IO and LS performance levels compared

to low seismicity designs. On the other hand, at CP performance level, the overall cost is significantly reduced for high and moderate seismicity designs. It is also observed that low seismicity designs have highest overall cost at CP performance level, while for moderate and high seismicity designs the highest overall cost is at LS performance level.

Table 32: Summary of the Effects of LFRS Design and Performance Level on the Total Construction and Repair Cost

	Low Seismicity				Moderate Seismicity		High Seismicity	
	Ordinary Shear Wall		Special Shear Wall					
6-Story	IO	1	IO	-1%	IO	6%	IO	12%
(B4, B3, B2, B1)	LS	18%	LS	17%	LS	25%	LS	22%
[1.0 = $ 795,544]	CP	29%	CP	26%	CP	21%	CP	7%
9-Story	IO	1	IO	1%	IO	4%	IO	11%
(B8, B7, B6, B5)	LS	19%	LS	19%	LS	23%	LS	22%
[1.0 = $ 1,231,227]	CP	34%	CP	26%	CP	22%	CP	14%
12-Story	IO	1	IO	0.4%	IO	4%	IO	13%
(B12, B11, B10, B9)	LS	18%	LS	18%	LS	18%	LS	22%
[1.0 = $ 1,616,704]	CP	31%	CP	23%	CP	17%	CP	10%

The observed change in repair cost with the performance level is due to the probabilistic nature of the calculation. The repair cost at each performance level depends on the probability of exceedance at MCE level and the damage percentage of that corresponding performance level. For example, low seismicity designs have the highest probabilities of exceeding IO performance limit as presented in Table 19 in section 4.5, yet they have the least repair and overall costs as shown in Table 32. This is attributed to the low damage percentage assigned to IO performance level which reflects the minor damages expected.

Chapter 6: Conclusions and Recommendations

6.1 Summary

The research outlined in this thesis investigates the impact of the seismic hazard level on the performance and overall cost of buildings in Dubai. The investigation targets 6-story, 9-story and 12-story buildings located in Dubai and representing the main inventory of buildings. The selected reference buildings are designed and detailed following the state of the art design and construction practices in Dubai based on IBC'12. The buildings' lateral force resisting system consists of special/ordinary RC shear walls. The design of gravity and lateral systems is changed every three floors to optimize the construction cost and match with common practice in Dubai. The 6-story, 9-story and 12-story buildings are designed for the three possible seismicity estimates of Dubai, namely high, moderate and low. At the low seismicity level, the reference buildings are designed using special and ordinary RC shear walls. The highest seismicity design level represents the upper bound of Dubai's seismic hazard as estimated of by USGS [41]. Furthermore, the moderate seismicity design level implemented in this study conforms to AIBC'11 seismic hazard estimate of Dubai. The chosen low seismic design level reflects the lower bound of Dubai's seismic hazard as estimated by Aldama et al. [13]. The seismic performance and collapse safety of the reference buildings are investigated using nonlinear pseudo-static and dynamic analyses, specifically push-over analysis and IDA. Large number of nonlinear analyses is performed to capture the response of the structures due to seismic loads. The nonlinear analyses are performed using a fully detailed fiber-based finite element model developed on IDARC-2D package [10]. The pseudo-static push-over analysis is displacement based and implemented to evaluate the deformations and strength demands of the buildings. Moreover, the IDAs are performed using a suite of 22 far-field earthquake records representing a possible seismic hazard scenario in Dubai. The ground motion records are selected and scaled following FEMA P695 [6] well-established procedures. Over nine hundred nonlinear IDA runs are performed for each reference building to establish reliable IDA curves and derive seismic fragility curves. The first mode, 5% damped, spectral accelerations are used as IMs for IDA and the peak inter-story drift ratios are the DMs. According to Vamvatsikos and Cornell [52], the choice of spectral accelerations as IMs is an efficient way to reduce results' scatter

and provide full characterization of the response. In addition, the reference buildings heights make them more susceptible to higher PGAs rather than higher PGVs. FEMA P695 methodology is implemented to adjust IDA results and account for the different uncertainty sources and records' frequency content. The seismic vulnerability of the buildings is assessed using adjusted fragility functions derived using the maximum likelihood method [56]. The fragility curves are developed for the performance levels outlined in ASCE41 [53], namely IO, LS and CP. Finally, the construction cost of the reference buildings is evaluated and the economic losses are estimated. This is done to highlight the impact of the LFRS, seismic design level and performance level on overall cost of buildings in Dubai. The construction cost only represents the skeleton cost, considering the superstructure and non-structural elements. It does not account for substructure cost, other construction costs and the contractor's profit. This was done to isolate other factors and focus on the seismic design level impact on construction materials quantities and cost.

6.2 Conclusion

This research quantified the impact of the seismic hazard estimate on the performance and overall cost of a group of representative buildings in Dubai, UAE. The preliminary performance investigations of the reference buildings indicated poor structural response due to higher-mode effects. It should be noted that the initial design was based on IBC'12 static method and was mainly driven by cost optimization. However, the dynamic analysis highlighted an undesirable premature collapse mechanism caused by higher-mode effects, which imposed greater demands at upper floors with reduced cross sections. Therefore, designs were revised to consider both enhancing the expected seismic performance and optimizing the construction cost. It is noteworthy that initial designs strictly followed the code design approach. Based on the static method outlined in the design code (IBC'12), cantilevered shear walls should have a single critical section at the base. Yet, the dynamic analysis results showed that the critical section causing the collapse was shifted to upper floors with reduced sections. This is particularly clear in 9-story and 12-story buildings. Hence, following the code recommendations or static analyses, the actual flaws in designs were not fully captured.

The performance of each building is judged based on its capacity curve, ACMR, seismic vulnerability and IO, LS and CP limit states probabilities of exceedance at MCE. Additionally, the impact of the performance enhancement, resulting from the choice of the seismic design level and LFRS, on construction and repair costs is compared among the different designs. This is because the buildings' overall cost is a more practical measure to developers and decision makers reflecting more tangible consequences.

In the 6-story buildings, as expected, designing for the conservative high seismicity estimate yields the highest safety against collapse at MCE level. For instance, the 6-story building designed for high seismicity (B1-6S-H-S) shows 57% margin of safety against collapse at MCE level. On the other hand, the 6-story building designed for moderate and low seismicity (B2-6S-M-S, B3-6S-L-S and B4-6S-L-O) experienced collapse at spectral accelerations below MCE level. Furthermore, high and moderate seismicity designs show the least probabilities of exceeding IO, LS and CP performance levels at MCE. For instance, at IO limit state, choosing to design 6-story buildings for high seismicity instead of low reduces the exceedance probability by 5% at MCE and increases the overall cost by 12%. Similarly, at LS limit state, the exceedance probability is reduced by 39% and the overall cost is increased by only 3%. However, at CP limit state the high seismicity design has a lower exceedance probability at MCE by 78% and a reduction in overall cost by 17%. This reflects the long-term cost savings gained from designing a 6-story building for the high seismicity estimate in Dubai to satisfy the CP performance level. Similarly, moderate seismicity designs compared to low seismicity designs with ordinary RC shear walls show 36% enhancement in performance at CP. This is associated with 5% increase in overall cost at LS limit state and 6% reduction at CP limit state. However, the moderate seismicity design of the 6-story building (B2-6S-M-S) has an ACMR slightly (0.89) below 1. Moreover, designing 6-story buildings for low seismicity estimate, but using special RC shear walls decreases CP exceedance probability at MCE by 12%. This upgrade in performance is also combined with marginal overall cost savings at LS and CP limit states. At IO limit state; although the performance at MCE level is similar between special and ordinary RC shear walls, the overall cost is slightly reduced when using the special walls. Therefore, for the 6-story buildings designed for low seismicity, the

choice of special RC shear walls has improved the performance and reduced overall cost.

Likewise, designing 9-story buildings for the highest seismic hazard estimate (B5-9S-H-S) provides 23% margin of safety against collapse at MCE. On the other hand, collapse occurs below MCE for buildings designed for moderate and low seismicity (B6-9S-M-S, B7-9S-L-S and B8-9S-L-O). Furthermore, high and moderate seismicity designs have lower probabilities of exceeding IO, LS and CP at MCE compared to low seismicity designs. For example, at IO limit state, designing for high seismicity instead of low seismicity with ordinary RC shear walls slightly drops the exceedance probability and increases the overall cost by 11%. Additionally, at LS limit state, the increase in overall cost is negligible while the reduction in exceedance probability is 28%. Nevertheless, there is 15% savings in overall cost and 64% enhancement in probability of exceedance at CP performance level. Hence, similar to 6-story buildings, it is concluded that designing 9-story buildings for the high seismic hazard estimate yields clear savings and enhancement in performance at CP limit state. Moreover, designing the 9-story buildings for moderate seismicity, instead of low seismicity with ordinary RC shear walls, reduces the probability of exceeding CP by 33%. In addition, there is an 8% overall cost savings at CP. Yet, the 9-story building designed for moderate seismicity (B6-9S-M-S) has a low ACMR of 0.82. At the low seismicity level, designing 9-story buildings using special RC shear walls drops CP exceedance probability by 18%. This enhanced performance at MCE comes with almost no impact on overall cost at IO and LS limit states and with 6% reduction in cost at CP. Therefore, designing 9-story buildings for low seismicity using special RC shear walls instead of ordinary RC shear walls improves the structural response and overall cost.

Similarly, the 12-story building (B9-12S-H-S) designed for high seismicity has 47% margin of safety against collapse at MCE. On the other hand, moderate and low seismicity designs (B10-12S-M-S, B11-12S-L-S and B12-12S-L-O) collapse at levels below MCE. Additionally, the buildings designed for higher seismicity exhibit lower IO, LS and CP limit states probabilities of exceedance at MCE. For instance, at IO limit state, high seismicity designs with special RC shear walls experience 6% lesser probabilities of exceedance compared to low seismicity designs with ordinary RC shear walls. This is associated with 13% increase in overall cost. Furthermore, at LS limit

state, the reduction in exceedance probability is 35% and the increase in overall cost is negligible. Conversely, at CP limit state there is 16% savings in overall cost and the probability of exceedance is enhanced by 75%. Therefore, for the three groups of buildings (6-story, 9-story and 12-story), the higher seismicity designs did not cause significant increase in overall cost at IO and LS limit states. However, cost savings are achieved at CP performance level. Similarly, the 12-story building (B10-12S-M-S) designed for moderate seismicity when compared to low seismicity design (B12-12S-L-O) show reduction in probabilities of exceeding LS and CP by 13% and 40%, respectively. The enhanced performance at LS has no impact on overall cost, while at CP there is 11% savings. However, the moderate seismicity design of 12-story buildings has an ACMR of 0.95 which is slightly below 1. This is a borderline case which might be tied to the particulars of this problem and the presence of higher-mode effects in optimized design. Therefore, it is recommended to reduce the optimization in moderate seismicity designs to eliminate the presence of higher-modes and enhance the collapse probability at MCE. Moreover, at low seismicity design level, the special RC shear wall buildings exhibit 20% lower probability of exceeding CP limit state at MCE compared to ordinary RC shear walls. This improvement in performance is associated with almost no influence on overall cost at IO and LS limit states, while overall cost is reduced by 6% at CP limit state. Therefore, it is concluded that the choice of special RC shear walls over ordinary RC shear walls clearly enhances the seismic performance of buildings. This enhancement is combined with almost no additional cost and in some cases with reduction in overall cost. However, it should be noted that designing the special RC shear walls for low seismicity does not fully utilize its high performance. To sum up, the positive impact on overall cost combined with the evident high performance of higher seismicity designs present a possible feasible solution to mitigate the impact of the diverse seismic hazard estimates in Dubai.

It is also noted that the 6-story buildings designs are more robust compared to 9-story and 12-story buildings. Only the 6-story building designed for high seismicity satisfies FEMA P695 performance criteria. This is attributed to the complete absence of higher-mode effects in the squat shear walls and the relatively lesser vulnerability of low rise buildings to earthquakes originating from distant sources. Although 9-story and 12-story buildings designs were optimized to enhance the performance, the higher-mode effects were not completely eliminated to keep the design economical. Therefore,

the higher-mode effects are still present in performance optimized designs of 9 and 12-story buildings. However, these designs are satisfactory to structural engineers and buildings officials based on their relatively low probabilities of exceeding IO, LS and CP limit states at MCE level.

6.3 Recommendations

Based on the outcomes of this research the following recommendations can be made for the selected buildings under the idealized modeling assumptions:

- Medium to relatively high rise RC shear wall buildings should be analyzed and designed considering and accounting for higher-mode effects. Dynamic analyses will clearly highlight the impact of the higher-modes and the formation of plastic hinges in upper floors. Therefore, design optimization should always consider that critical sections might be shifted to upper stories and always trade-off between cost and performance. In case if the high seismicity estimate is adapted in the design, the impact of the higher-modes on the performance will not be very significant. However, following the moderate seismicity estimate, the design will be more sensitive to higher-modes and any optimization in the sections should be done cautiously.
- It is suggested to design buildings for a conservative seismic hazard estimate (high or moderate). This recommendation is supported by the clear enhancement in performance and collapse probability of high seismicity designs. Additionally, designing for the higher seismicity did not yield uneconomical structures. In general, there was a marginal increase in overall cost at IO and LS performance levels, while there was a good reduction in overall cost at CP limit state. Additionally, the performance improvement outweighs the increase in initial investment by reducing repair and downtime costs.
- Even when the use of ordinary RC shear walls is permitted by design code, it is more favorable to choose special RC shear walls. This recommendation is supported by both performance and cost conclusions. The special RC shear walls showed significantly improved structural response compared to the ordinary counterpart with negligible impact on overall cost. In fact, in

some cases the overall cost was reduced for the designs implementing special RC shear walls. However, it is worth mentioning that designing the special RC shear walls for the low seismic hazard estimate does not fully utilize its expected high performance.

6.4 Future Work and Possible Extensions

In light of this research interesting outcomes, it is recommended to extend this investigation to consider the impact of earthquakes originating from near sources. The buildings' downtime cost can also be included in assessing the seismicity impacts on overall cost. Moreover, the impact of other earthquake losses, such as environmental and human losses could be investigated. Furthermore, the effect of seismicity might be investigated on skyscrapers and irregular buildings. Finally, given Dubai's rapid economic growth in the various sectors including transportation, it might be of interest to future researchers to investigate the effect of the seismicity hazard level on performance and overall cost of bridges.

References

[1] M. AlHamaydeh, K. Galal, and S. Yehia, "Impact of lateral force-resisting system and design/construction practices on seismic performance and cost of tall buildings in Dubai, UAE," *Earthq. Eng. Eng. Vib.*, vol. 12, no. 3, pp. 385–397, 2013.

[2] International Conference of Buildings Officials, "Uniform Building Code (UBC)." Whittier, California, 1997.

[3] "Dubai Municipality Survey Department." [Online]. Available: http://www.m1.ae/DSN.html. [Accessed: 02-Nov-2015].

[4] A. S. Elnashai and L. Di Sarno, *Fundemantals of Earthquake Engineering*, 1st ed. John Wiley & Sons, Ltd., 2009.

[5] International Code Council (ICC), "International Building Code." Falls Church, Virginia, 2012.

[6] Federal Emergency Management Agency (FEMA), "Quantification of Building Seismic Performance Factors," *FEMA P695, prepared for the Federal Emergency Management Agency, Prepared by the Applied Technology Council, Redwood City, CA*, no. June. 2009.

[7] "Pacific Earthquake Engineering Research Centre (PEER), 'PEER Ground Motion Database', University of California, Berkeley, California," 2015. [Online]. Available: http://peer.berkeley.edu/nga/. [Accessed: 20-May-2015].

[8] "ETABS." Computers & Structures Inc., Berkeley, California, 2015.

[9] "Quick Concrete Wall." Integrated Engineering Software (IES) Inc., United States of America, Bozeman, 2015.

[10] M. Reinhorn, H. Roh, V. Sivaselvan, S. Kunnath, R. Valles, A. Madan, C. Li, R. Lobo, and Y. Park, "IDARC 2D Version 7.0: A Program for the Inelastic Damage Analysis of Buildings," *New York*. Technical Report MCEER-09-0006, Multidisciplinary Centre for Earthquake Engineering Research, State University of New York at Buffalo, 2009.

[11] A. Mwafy, "Assessment of seismic design response factors of concrete wall buildings," *Earthq. Eng. Eng. Vib.*, vol. 10, no. 01, pp. 115–127, 2011.

[12] G. Grünthal, C. Bosse, S. Sellami, D. Mayer-Rosa, and D. Giardini, "Compilation of the GSHAP regional seismic hazard for Europe, Africa and the Middle East," *Ann. di Geofis.*, vol. 42, no. 6, pp. 1215–1223, 1999.

[13] G. Aldama-Bustos, J. J. Bommer, C. H. Fenton, and P. J. Stafford, "Probabilistic seismic hazard analysis for rock sites in the cities of Abu Dhabi, Dubai and Ra's Al Khaymah, United Arab Emirates," *Georisk Assess. Manag. Risk Eng. Syst. Geohazards*, vol. 3, no. 1, pp. 1–29, 2009.

[14] J. A. Abdalla and A. Al-homoud, "Seismic Hazard Assessment of United Arab Emirates and its surroundings," *J. Earthq. Eng.*, vol. 8, no. 6, pp. 817–837, 2004.

[15] R. Sigbjornsson and A. Elnashai, "Hazard Assessment of Dubai, United Arab Emirates, for Close and Distant Earthquakes," *J. Earthq. Eng.*, vol. 10, no. 5, pp. 749–773, 2006.

[16] J. A. Abdalla, J. T. Petrovski, and Y. E.-A. Mohamedzein, "Vibration Characteristics of a Far Field Earthquake and Its Shaking Effects on Dubai Emerging Skyscrapers," in *14th World Conference on Earthquake Engineering*, 2008.

[17] Y. Al Marzooqi, K. M. Abou Elenean, a. S. Megahed, I. El-Hussain, a. J. Rodgers, and E. Al Khatibi, "Source parameters of March 10 and September 13, 2007, United Arab Emirates earthquakes," *Tectonophysics*, vol. 460, no. 1–4, pp. 237–247, 2008.

[18] S. A. Barakat, A. Shanableh, and A. I. H. Malkawi, "A Comparative Earthquakes Risk Assessment Approach Applied to the United Arab Emirates," *Jordan J. Civ. Eng.*, vol. 2, no. 2, 2008.

[19] V. Pascucci, M. Free, and Z. Lubkowski, "Seismic Hazard and Seismic Design Requirements for the Arabian Peninsula Region," in *14th World Conference on Earthquake Engineering*, 2008.

[20] A. Shama, "Site specific probabilistic seismic hazard analysis at Dubai Creek on the west coast of UAE," *Earthq. Eng. Eng. Vib.*, vol. 10, no. 1, pp. 143–152, 2011.

[21] "Incorporated Research Institutions for Seismology (IRIS)," 2008. [Online]. Available: www.iris.edu. [Accessed: 05-Nov-2015].

[22] Z. Khan, M. El-emam, M. Irfan, and J. Abdalla, "Probabilistic seismic hazard analysis and spectral accelerations for United Arab Emirates - ProQuest," *Natl. Hazards*, vol. 67, pp. 569–589, 2013.

[23] "United States Geological Survey (USGS)." [Online]. Available: http://www.usgs.gov/. [Accessed: 05-Nov-2015].

[24] "National Geosciences of Iran." [Online]. Available: http://www.ngdir.ir/. [Accessed: 05-Nov-2015].

[25] "National Center of Meteorology and Seismology of UAE." [Online]. Available: http://www.ncms.ae/en/. [Accessed: 05-Nov-2015].

[26] E. Al Khatibi, K. M. Abou Elenean, A. S. Megahed, and I. El-Hussain, "Improved Characterization of Local Seismicity Using the Dubai Seismic Network, United Arab Emirates," *J. Asian Earth Sci.*, vol. 90, no. 0, pp. 34–44, 2014.

[27] M. AlHamaydeh, S. Abdullah, A. Hamid, and A. Mustapha, "Seismic design factors for RC special moment resisting frames in Dubai, UAE," *Earthq. Eng. Eng. Vib.*, vol. 10, no. 4, pp. 495–506, 2011.

[28] M. AlHamaydeh, S. Yehia, N. Aly, A. Douba, and L. Hamzeh, "Design Alternatives for Lateral Force-Resisting Systems of Tall Buildings in Dubai, UAE," *Int. J. Civ. Environ. Eng.*, vol. 6, pp. 185–188, 2012.

[29] American Society of Civil Engineers/Structural Engineering Institute (ASCE/SEI), "Minimum design loads for buildings and other structures (ASCE7)." Reston, Virginia, 2010.

[30] Federal Emergency Management Agency (FEMA), "FEMA 445, Next-Generation Performance-Based Seismic Design Guidelines: Program Plan for New and Existing Buildings." Redwood City, CA, 2006.

[31] Structural Engineers Association of California, *SEAOC. Vision 2000, Performance based seismic engineering of buildings, vols I and II: Conceptual framework*. Sacramento (CA), 1995.

[32] Applied Technology Council, "ATC 40, Seismic evaluation and retrofit of existing concrete buildings." 1996.

[33] Federal Emergency Management Agency (FEMA), "FEMA 273, NEHRP Guidelines for The Seismic Rehabilitation of Buildings." Washington, DC, 1997.

[34] A. Ghobarah, "Performance-based design in earthquake engineering: state of development," *Eng. Struct.*, vol. 23, no. 8, pp. 878–884, 2001.

[35] K. A. Porter, "An Overview of PEER's Performance-Based Earthquake Engineering Methodology," *9th Int. Conf. Appl. Stat. Probab. Civ. Eng.*, vol. 273, no. 1995, pp. 973–980, 2003.

[36] F. Naeim, H. Bhatia, and R. Lobo, "Chapter 15: Performance Based Seismic Engineering," in *The Seismic Design Handbook*, no. 2, 2001, pp. 757–792.

[37] H. Krawinkler and G. D. P. K. Seneviratna, "Pros and cons of a pushover analysis of seismic performance evaluation," *Eng. Struct.*, vol. 20, no. 4–6, pp. 452–464, 1998.

[38] R. Purba and M. Bruneau, “Seismic Performance of Steel Plate Shear Walls Considering Two Different Design Philosophies of Infill Plates . II : Assessment of Collapse Potential,” *J. Struct. Eng.*, pp. 1–12, 2014.

[39] J. Lee, S. Han, and J. Kim, “Seismic Performance Evaluation of Apartment Buildings with Central Core,” *Int. J. High-Rise Build.*, vol. 3, no. 1, pp. 9–19, 2014.

[40] A. Gogus and J. Wallace, “Seismic Safety Evaluation of Reinforced Concrete Walls through FEMA P695 Methodology,” *J. Struct. Eng.*, pp. 1–17, 2015.

[41] “United States Geological Survey (USGS),” 2015. [Online]. Available: http://geohazards.usgs.gov/designmaps/ww/. [Accessed: 31-May-2015].

[42] Abu Dhabi Department of Municipal Affair and International Code Council (ICC), “Abu Dhabi International Building Code (AIBC).” Abu Dhabi, UAE, 2011.

[43] “American Concrete Institute.” Code Requirements for Structural Concrete and Commentary (ACI318-11), Farmington Hills, 2011.

[44] V. Sivaselvan and A. M. Reinhorn, “Hysteretic models for deteriorating inelastic structures,” *J. Eng. Mech.*, vol. 126, no. 6, pp. 633–640, 2000.

[45] Y. J. Park, A. H. S. Ang, and Y. K. Wen, “Damage Limiting Aseismic Design of Buildings,” *Earthq. Spectra*, vol. 3, no. 1, pp. 1–26, 1987.

[46] P. Riva, A. Meda, and E. Giuriani, “Cyclic behavior of a full scale RC structural wall,” *Eng. Struct.*, vol. 25, no. 6, pp. 835–845, 2003.

[47] Y. Belmouden and P. Lestuzzi, “Analytical model for predicting nonlinear reversed cyclic behavior of reinforced concrete structural walls,” *Eng. Struct.*, vol. 29, pp. 1263–1276, 2007.

[48] C. J. Collier and A. S. Elnashai, “A Procedure for Combining Vertical and Horizontal Seismic Action Effects,” *J. Earthq. Eng.*, vol. 5, no. 4, pp. 521–539, 2001.

[49] A. J. Papazoglou and A. S. Elnashai, “Analytical and Field Evidence of the Damaging Effect of Vertical Earthquake Ground Motion,” *Earthq. Eng. Struct. Dyn.*, vol. 25, no. October, pp. 1109–1137, 1996.

[50] S. J. Kim, C. J. Holub, and A. S. Elnashai, “Analytical Assessment of the Effect of Vertical Earthquake Motion on RC Bridge Piers,” *J. Struct. Eng.*, vol. 137, no. 2, pp. 252–260, 2011.

[51] D. Vamvatsikos and C. A. Cornell, “The Incremental Dynamic Analysis and Its Application To Performance-Based Earthquake Engineering,” in *12th European Conference on Earthquake Engineering*, 2001.

[52] D. Vamvatsikos and C. A. Cornell, "Applied Incremental Dynamic Analysis," *Earthq. Spectra*, vol. 20, no. 2, pp. 523–553, 2004.

[53] American Society of Civil Engineers/Structural Engineering Institute (ASCE/SEI), "Seismic Rehabilitation of Existing Buildings (ASCE 41)." Reston, Virginia, 2006.

[54] G. A. Al Shamsi, "Seismic Risk Assessment of Buildings in Dubai, United Arab Emirates," M. S. thesis, Dept. of Civil Engineering, American University of Sharjah, 2013.

[55] A. Issa and A. Mwafy, "Fragility Assessment of Pre-Seismic Code Buildings and Emergency Facilities in the UAE," in *Second European Conference On Earthquake Engineering and Seismology*, 2014, pp. 2–4.

[56] J. W. Baker, "Efficient analytical fragility function fitting using dynamic structural analysis," *Earthq. Spectra*, vol. 31, no. 1, pp. 579–599, 2015.

[57] R. Tremblay, P. Leger, and J. Tu, "Inelastic seismic response of concrete shear walls considering P-delta effects," *Can. J. Civ. Eng.*, vol. 24, no. 4, pp. 640–655, 2001.

[58] H. Bachmann and P. Linde, "Dynamic ductility demand and capacity design of earthquake-resistant reinforced concrete walls," *ACI Spec. Publ.*, vol. 157, 1995.

[59] M. Panneton, P. Leger, and R. Tremblay, "Inelastic analysis of a reinforced concrete shear wall building according to the National Building Code of Canada 2005," *Can. J. Civ. Eng.*, vol. 33, no. 7, pp. 854–871, 2006.

[60] H. EL-Sokkary, K. Galal, I. Ghorbanirenani, P. Léger, and R. Tremblay, "Shake Table Tests on FRP-Rehabilitated RC Shear Walls," *J. Compos. Constr.*, vol. 17, no. 1, pp. 79–90, 2013.

[61] D. Vamvatsikos and C. A. Cornell, "Incremental dynamic analysis," *Earthq. Eng. Struct. Dyn.*, vol. 31, no. 3, pp. 491–514, 2002.

[62] "Bruce Shaw Knowledge Centre," 2015. [Online]. Available: http://www.bruceshaw.com/knowledgecentre/chapters/middle-east/uae-average-construction-costs. [Accessed: 11-Nov-2015].

[63] Structural Engineers Association of California (SEAOC), *SEAOC Blue Book, Recommended Lateral Force Requirements and Commentary*, 7th ed. Sacramanti, CA., 1999.

[64] Federal Emergency Management Agency, "Hazus-MH MR5 Technical Manual. Multi-hazard Loss Estimation Methodology: Earthquake Model," Washington, DC, 2010.

Appendix A

RC Shear Walls Reinforcement Details

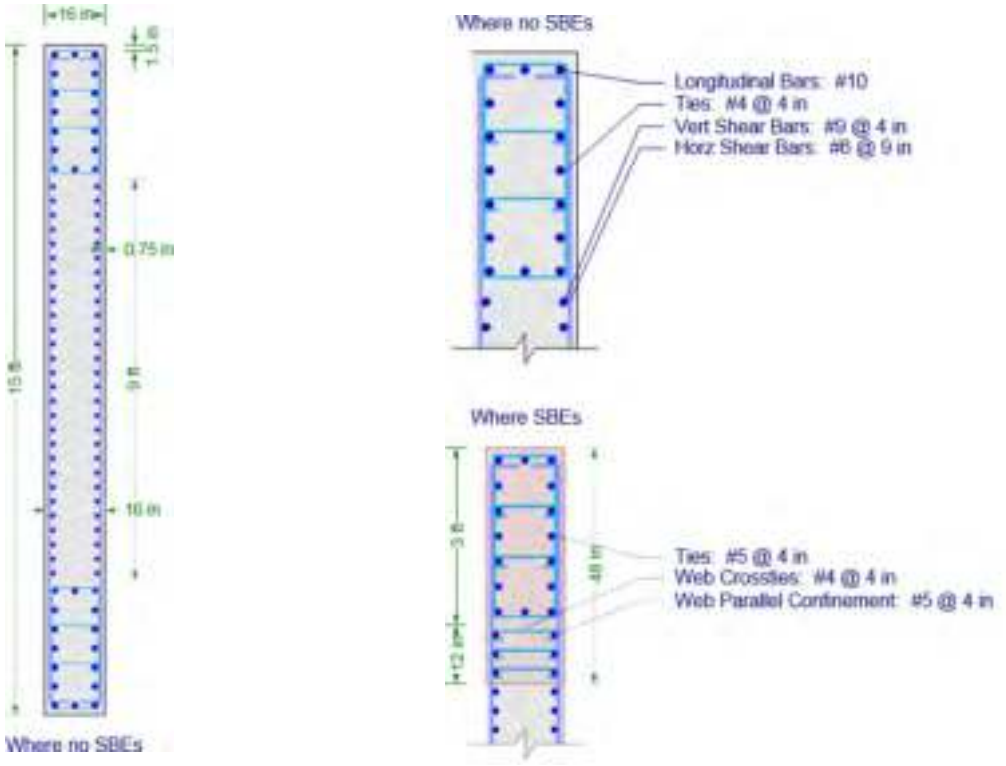

Figure 73: Building (B1-6S-H-S) Special RC Shear Reinforcement Details; Wall Section for Floors 1-3

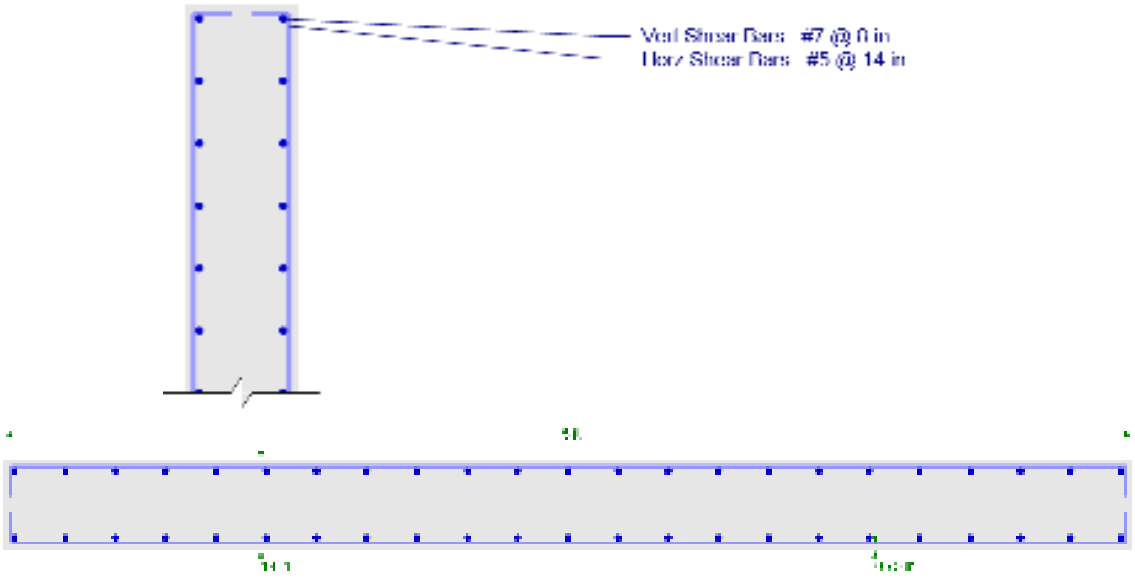

Figure 74: Building (B1-6S-H-S) Special RC Shear Reinforcement Details; Wall Section for Floors 4-6

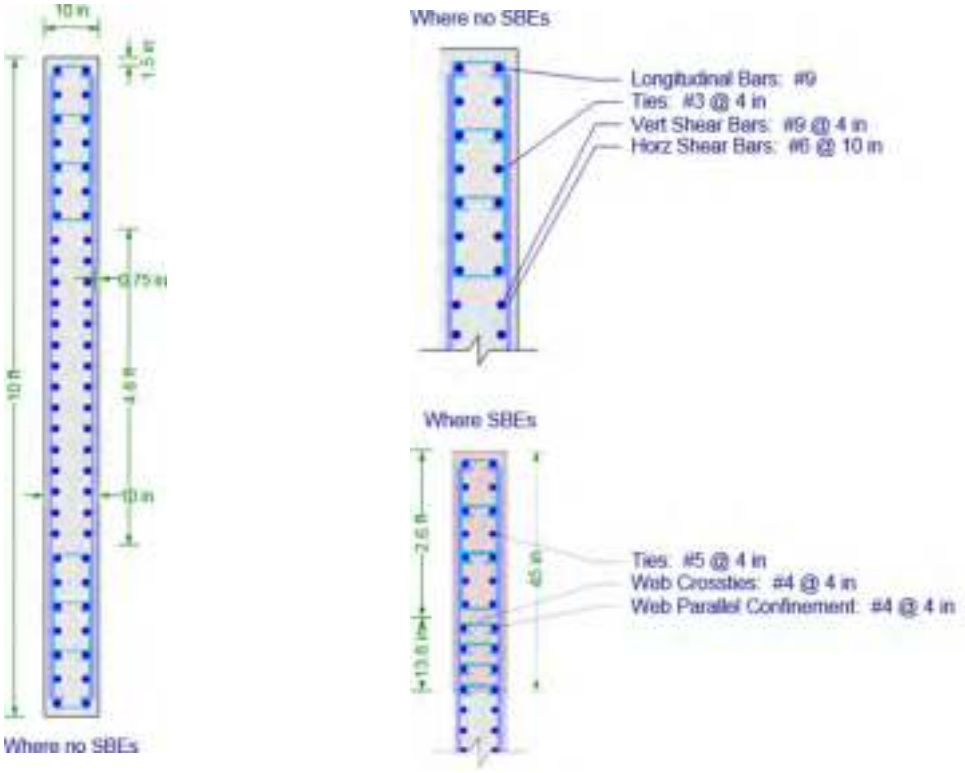

Figure 75: Building (B2-6S-M-S) Special RC Shear Reinforcement Details; Wall Section for Floors 1-3

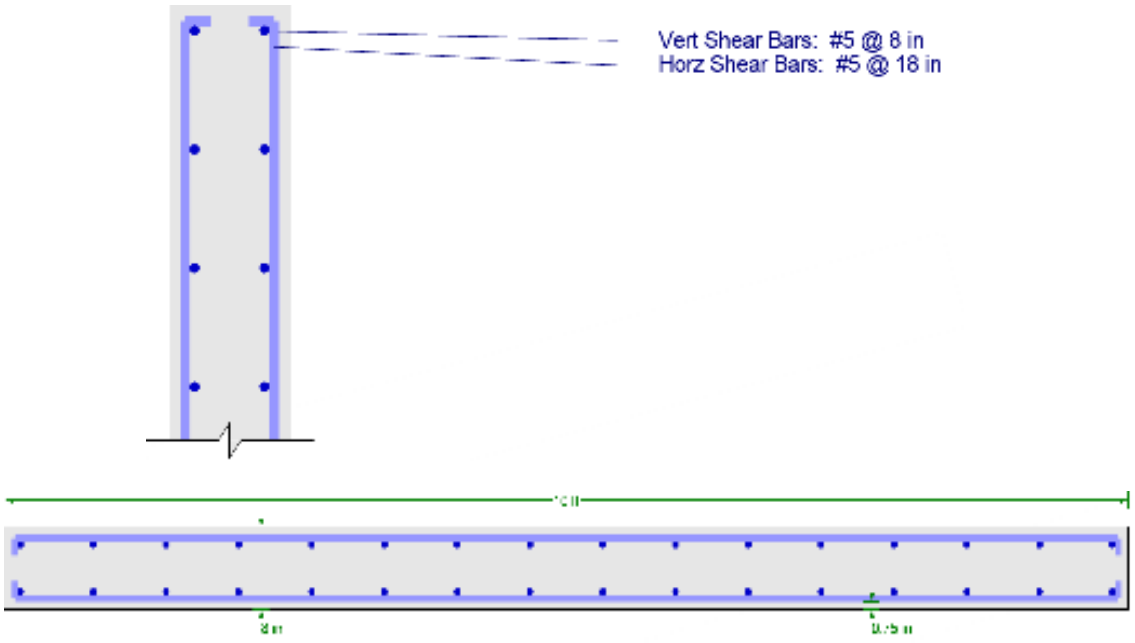

Figure 76: Building (B2-6S-M-S) Special RC Shear Reinforcement Details; Wall Section for Floors 4-6

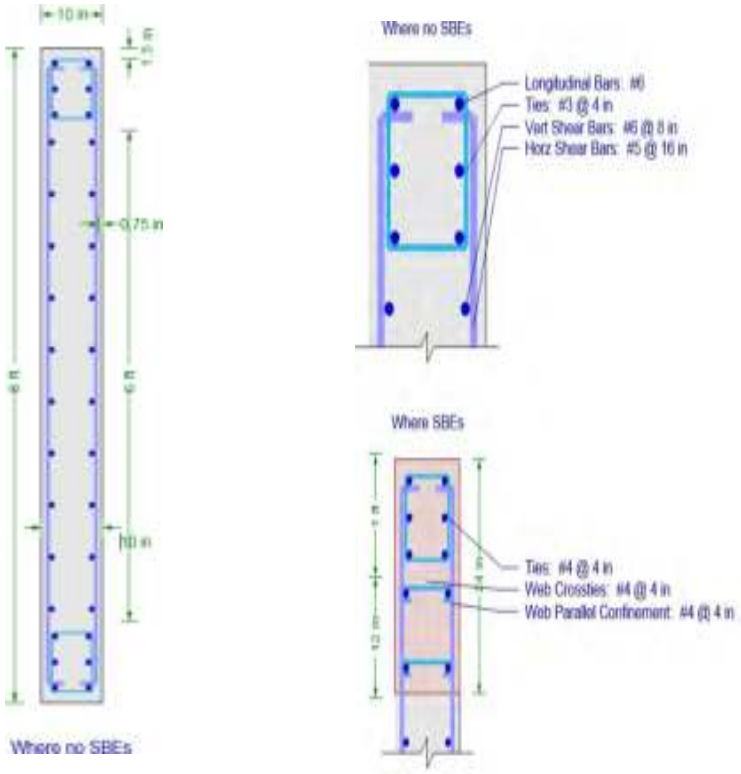

Figure 77: Building (B3-6S-L-S) Special RC Shear Reinforcement Details; Wall Section for Floors 1-3

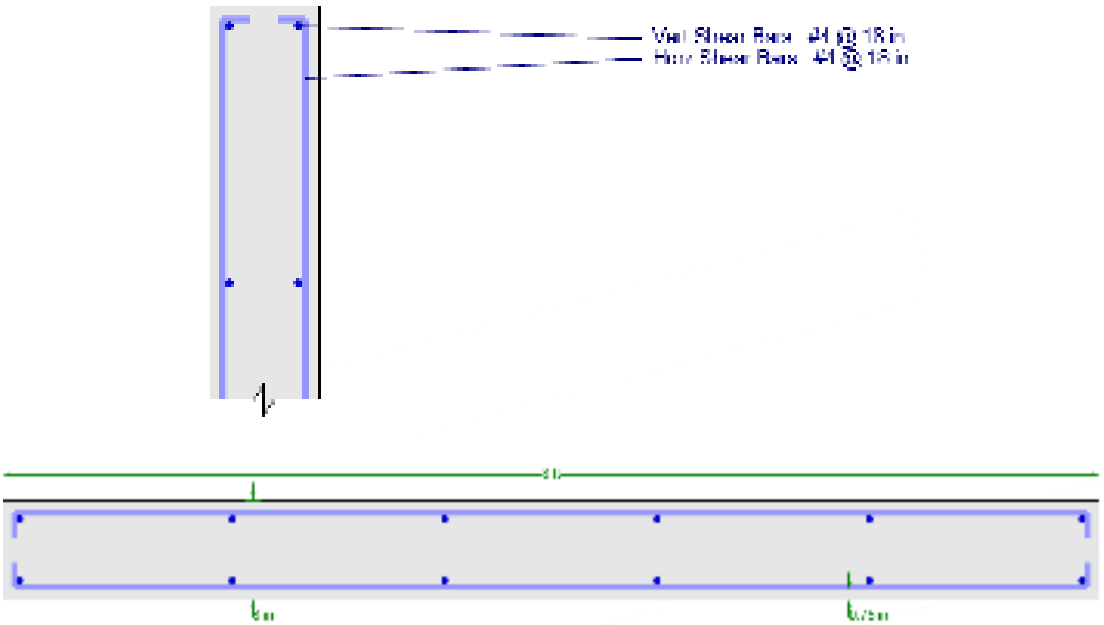

Figure 78: Building (B3-6S-L-S) Special RC Shear Reinforcement Details; Wall Section for Floors 4-6

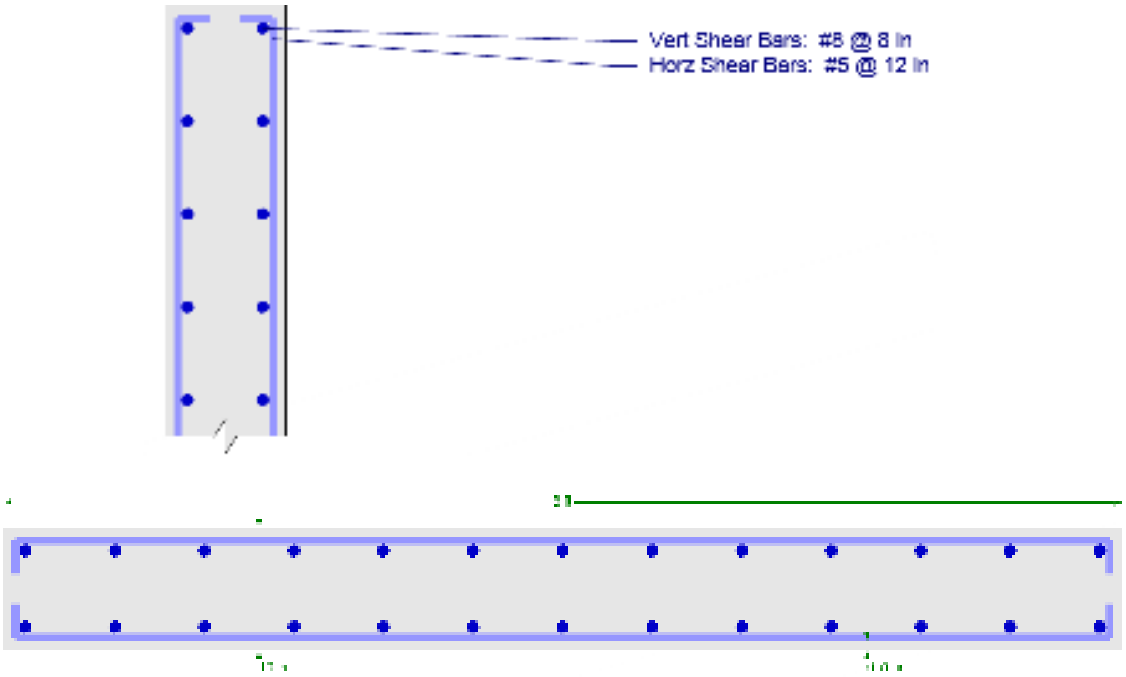

Figure 79: Building (B4-6S-L-O) Ordinary RC Shear Reinforcement Details; Wall Section for Floors 1-3

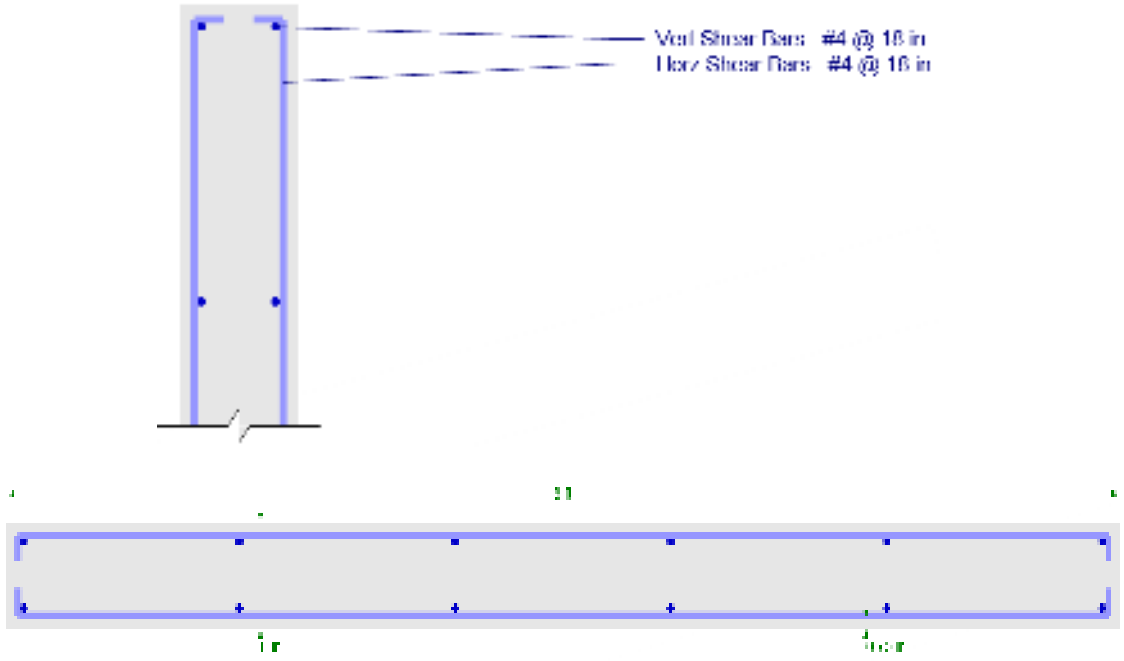

Figure 80: Building (B4-6S-L-O) Ordinary RC Shear Reinforcement Details; Wall Section for Floors 4-6

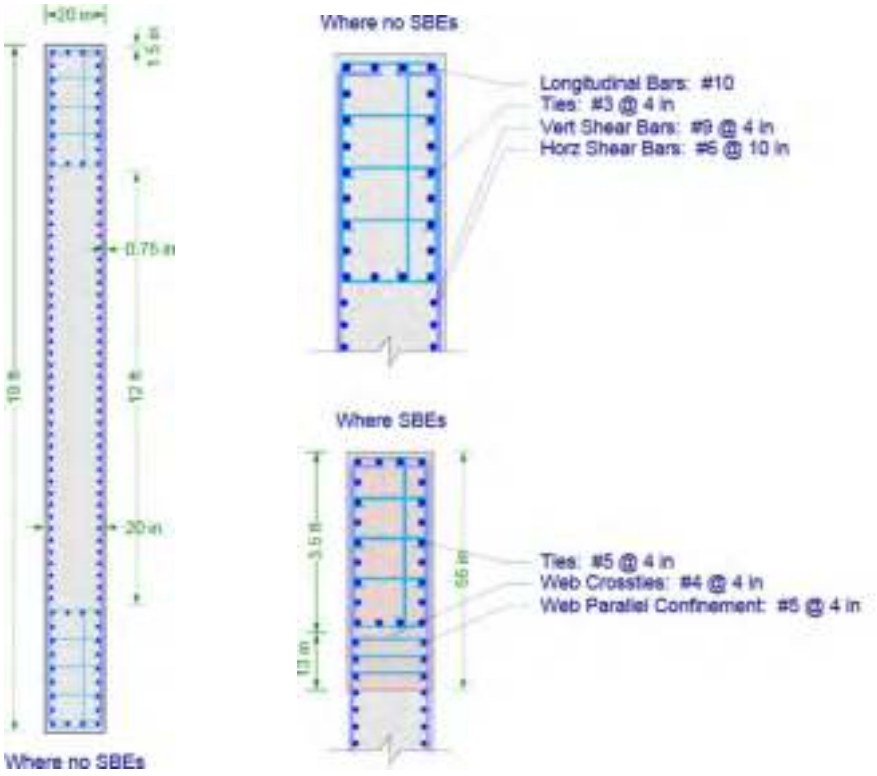

Figure 81: Building (B5-9S-H-S) Special RC Shear Reinforcement Details; Wall Section for Floors 1-3

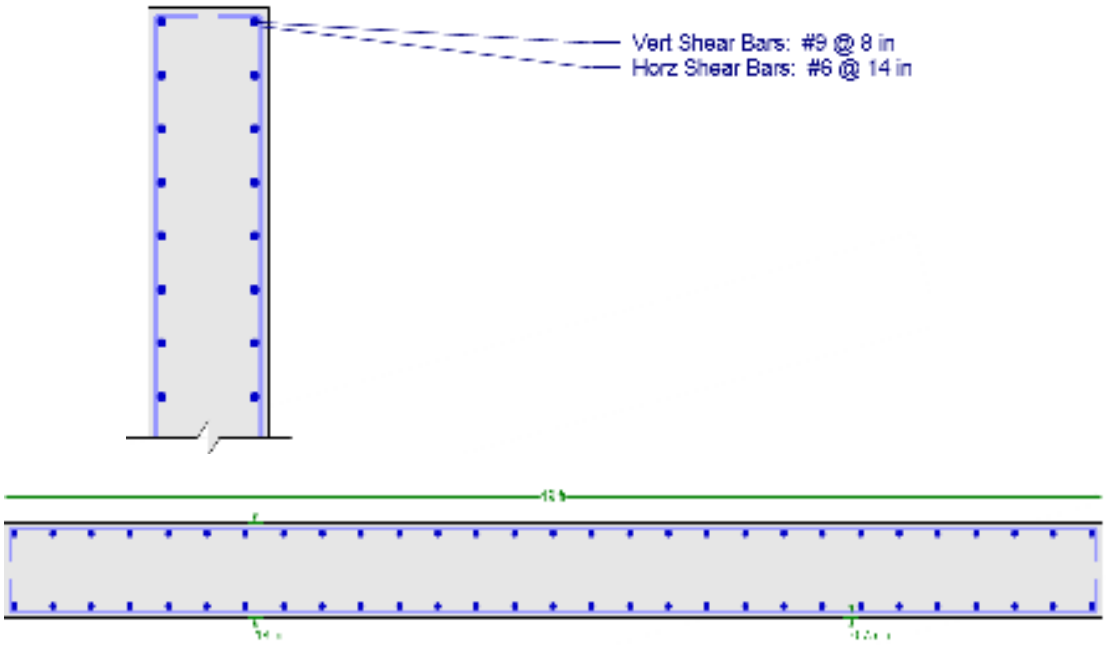

Figure 82: Building (B5-9S-H-S) Special RC Shear Reinforcement Details; Wall Section for Floors 4-6

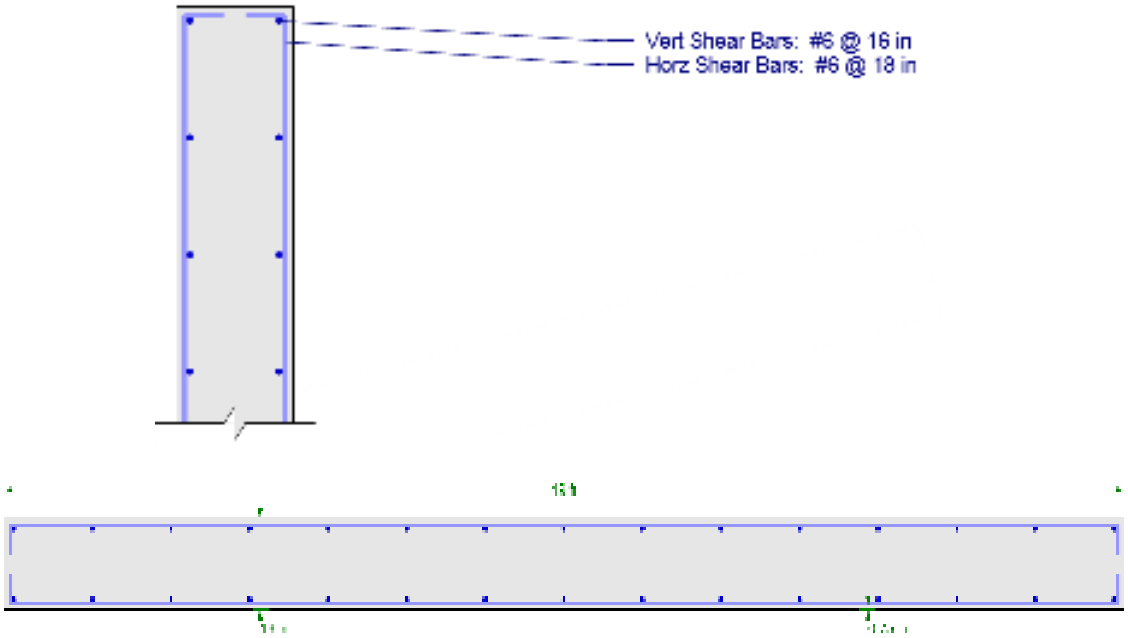

Figure 83: Building (B5-9S-H-S) Special RC Shear Reinforcement Details; Wall Section for Floors 7-9

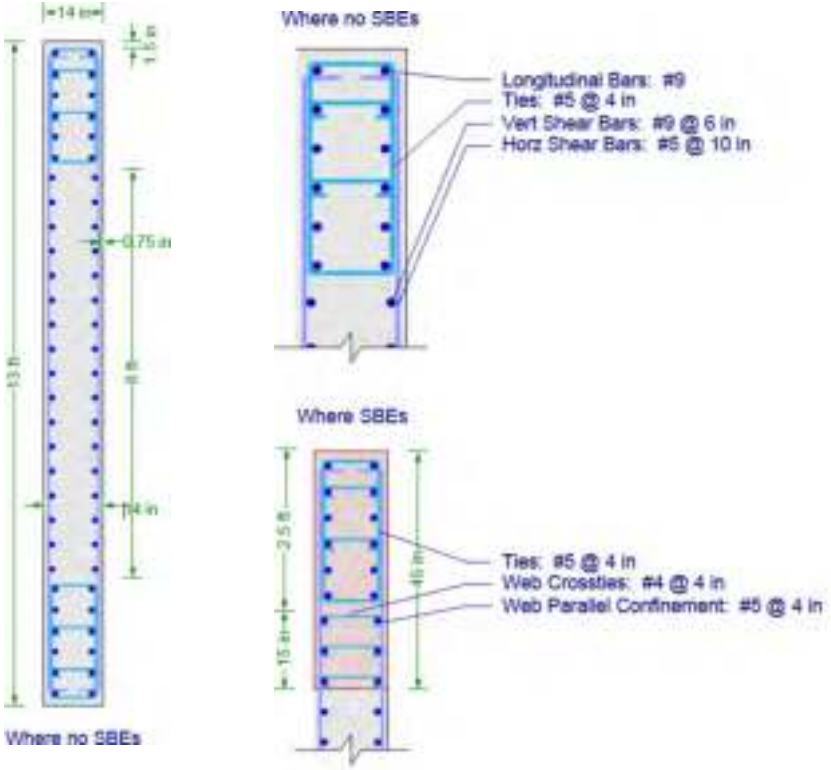

Figure 84: Building (B6-9S-M-S) Special RC Shear Reinforcement Details; Wall Section for Floors 1-3

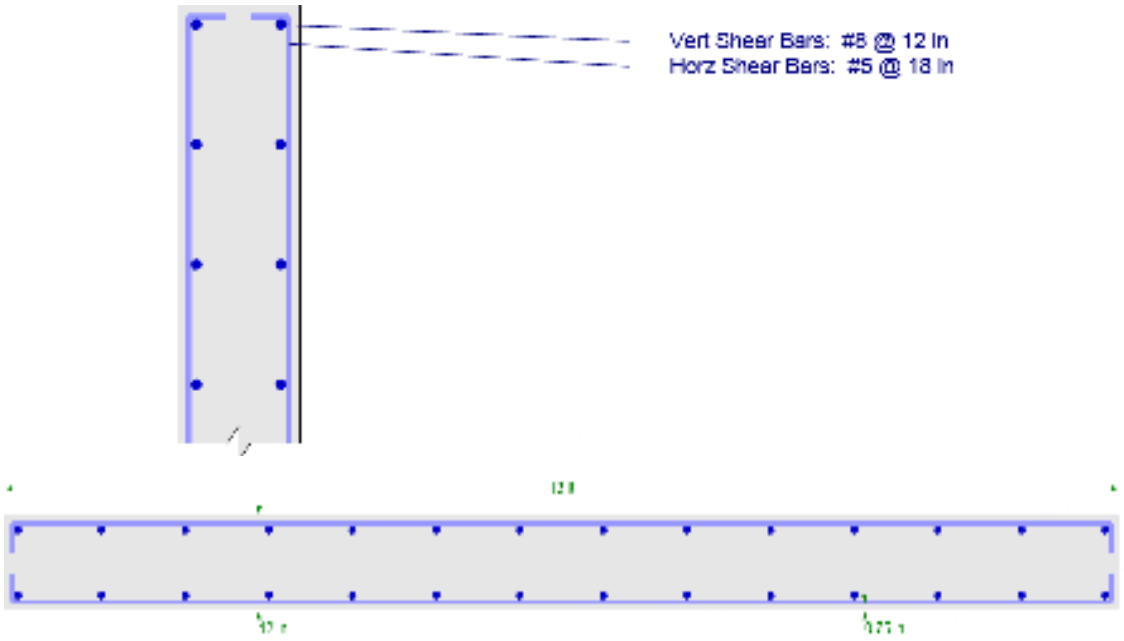

Figure 85: Building (B6-9S-M-S) Special RC Shear Reinforcement Details; Wall Section for Floors 4-6

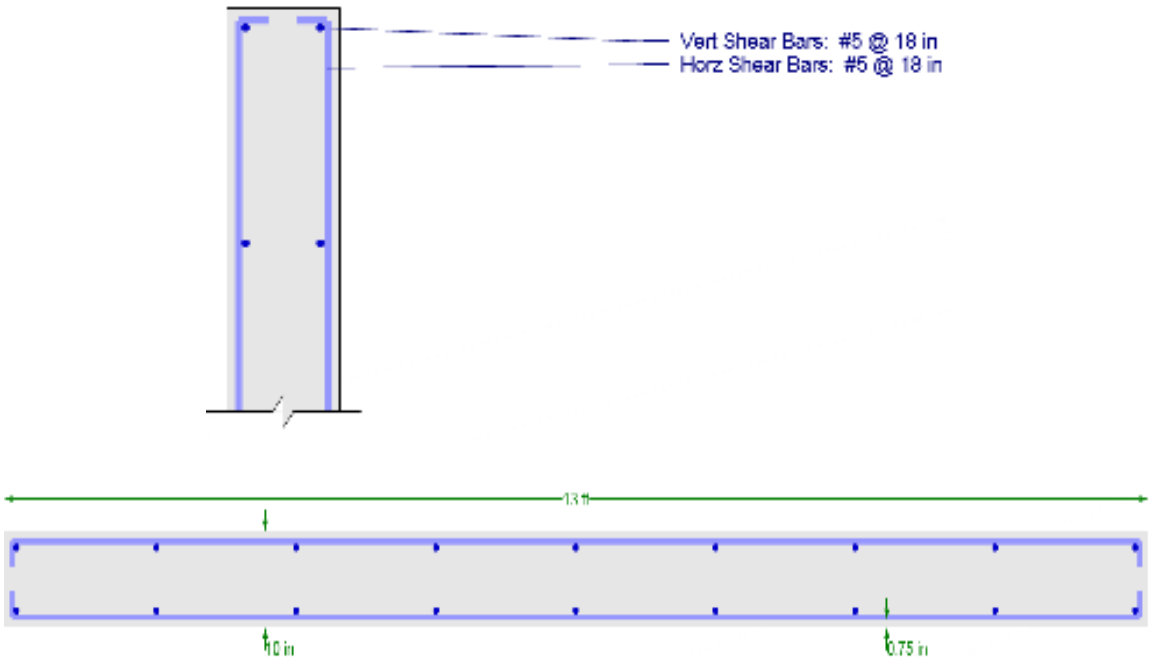

Figure 86: Building (B6-9S-M-S) Special RC Shear Reinforcement Details; Wall Section for Floors 7-9

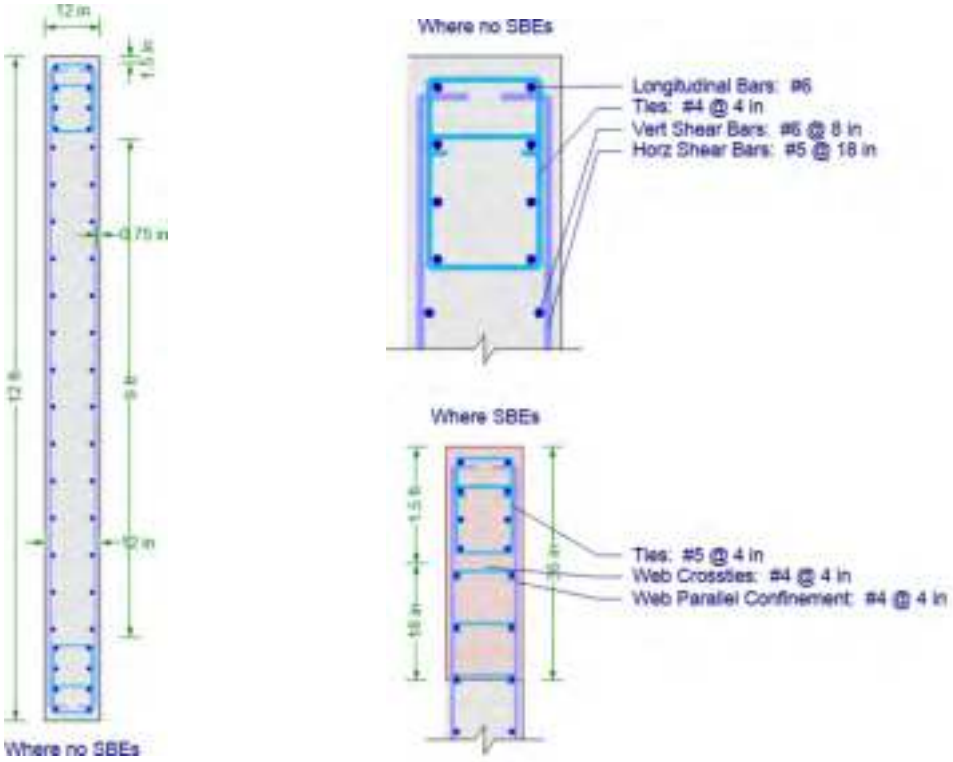

Figure 87: Building (B7-9S-L-S) Special RC Shear Reinforcement Details; Wall Section for Floors 1-3

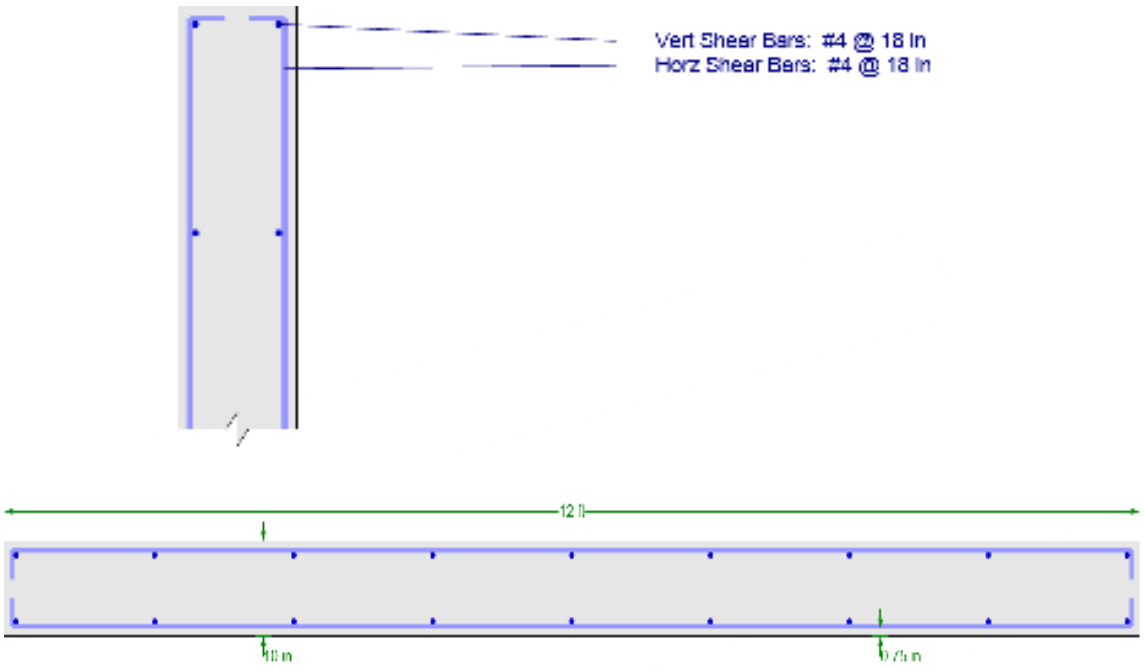

Figure 88: Building (B7-9S-L-S) Special RC Shear Reinforcement Details; Wall Section for Floors 4-6

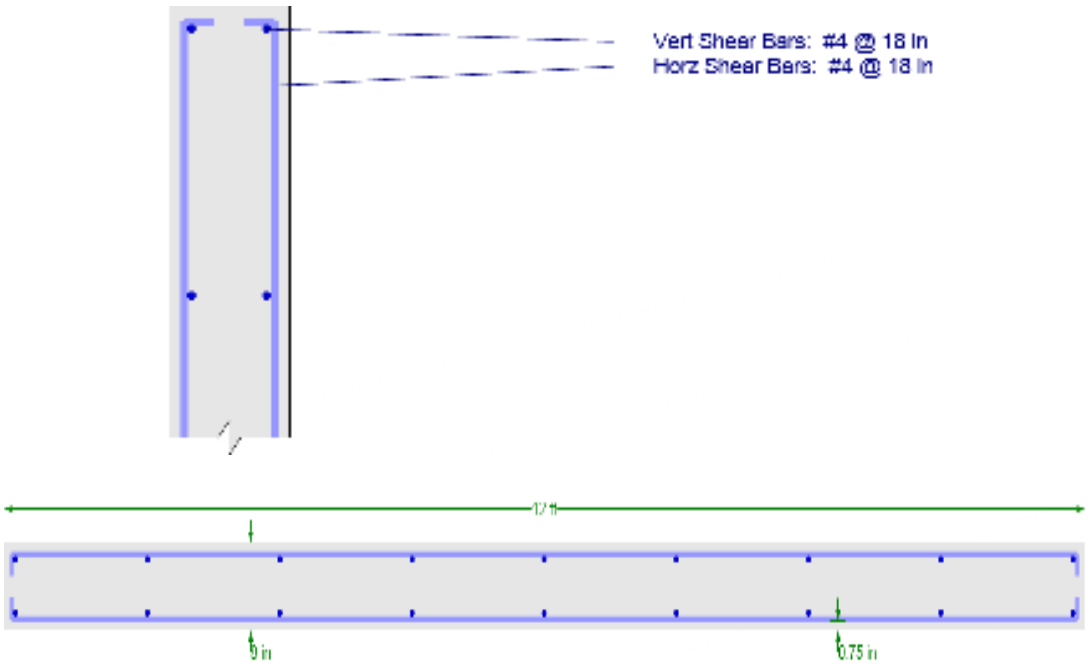

Figure 89: Building (B7-9S-L-S) Special RC Shear Reinforcement Details; Wall Section for Floors 7-9

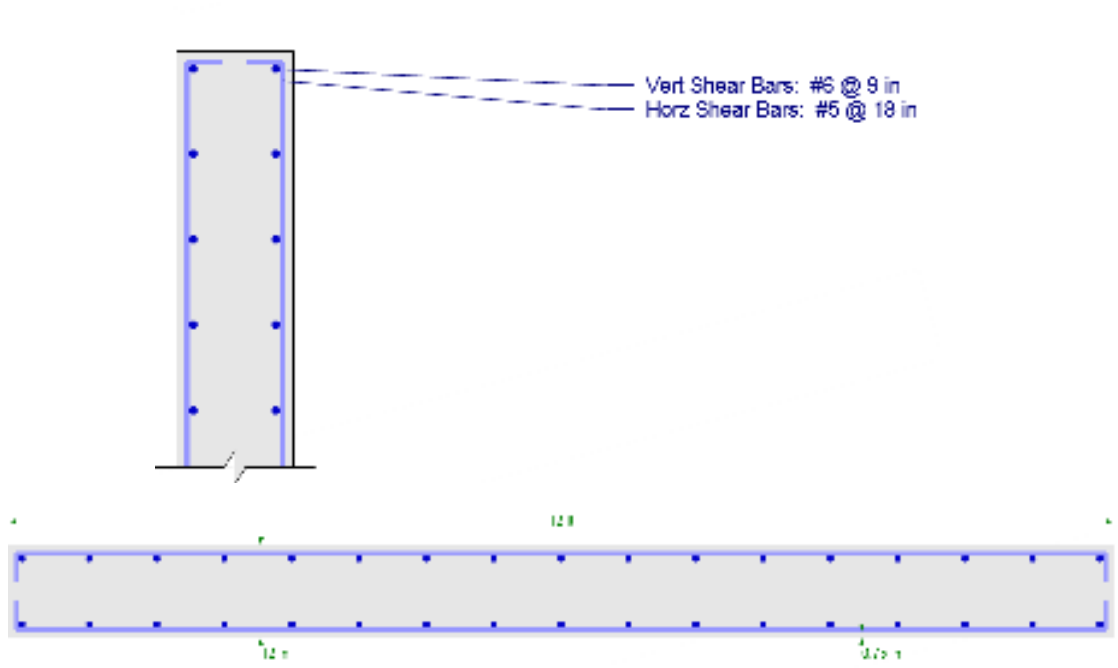

Figure 90: Building (B8-9S-L-O) Ordinary RC Shear Reinforcement Details; Wall Section for Floors 1-3

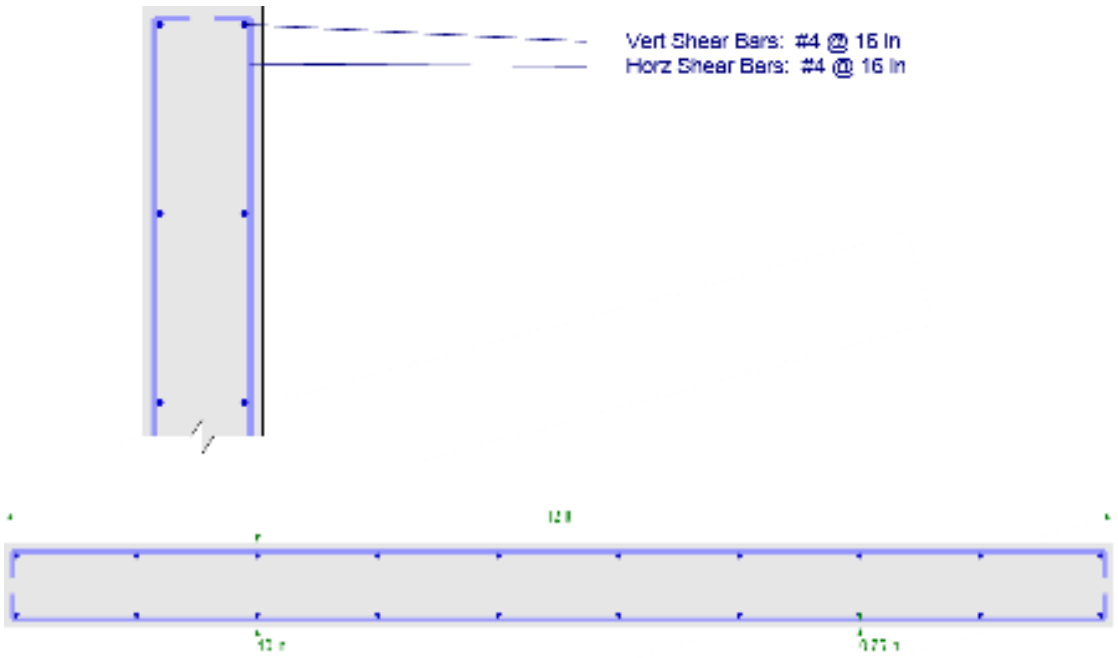

Figure 91: Building (B8-9S-L-O) Ordinary RC Shear Reinforcement Details; Wall Section for Floors 4-6

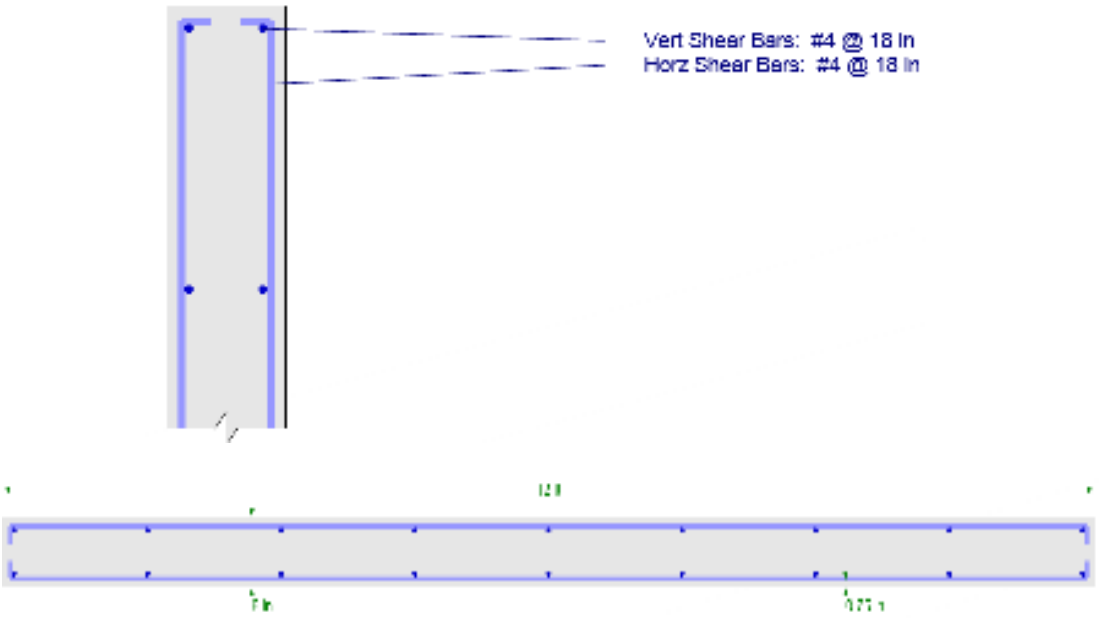

Figure 92: Building (B8-9S-L-O) Ordinary RC Shear Reinforcement Details; Wall Section for Floors 7-9

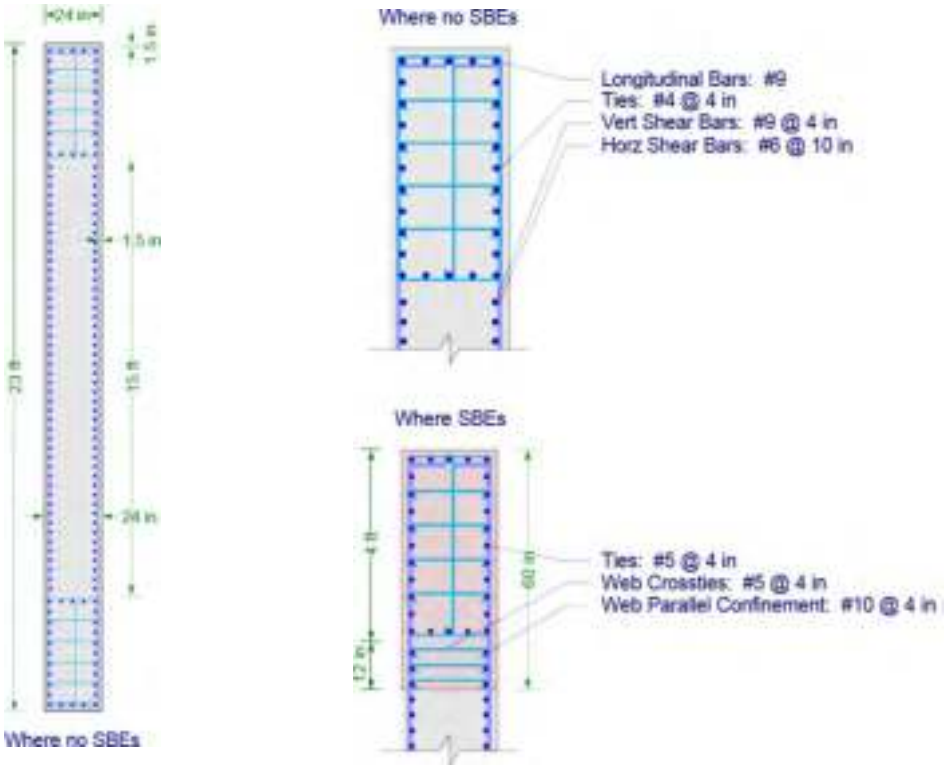

Figure 93: Building (B9-12S-H-S) Special RC Shear Reinforcement Details; Wall Section for Floors 1-3

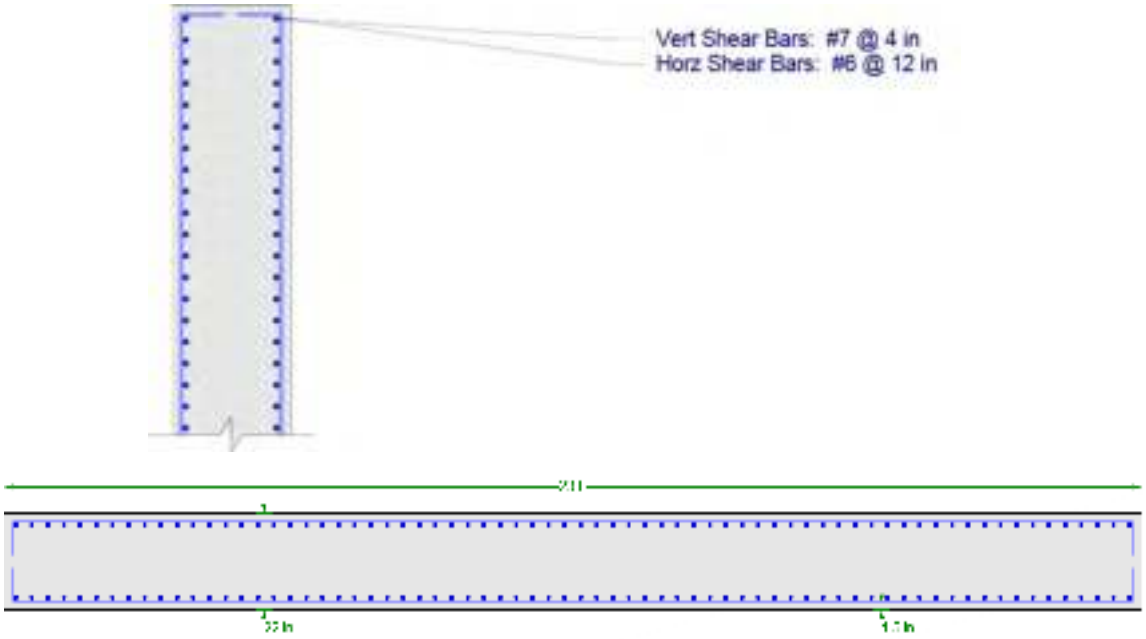

Figure 94: Building (B9-12S-H-S) Special RC Shear Reinforcement Details; Wall Section for Floors 4-6

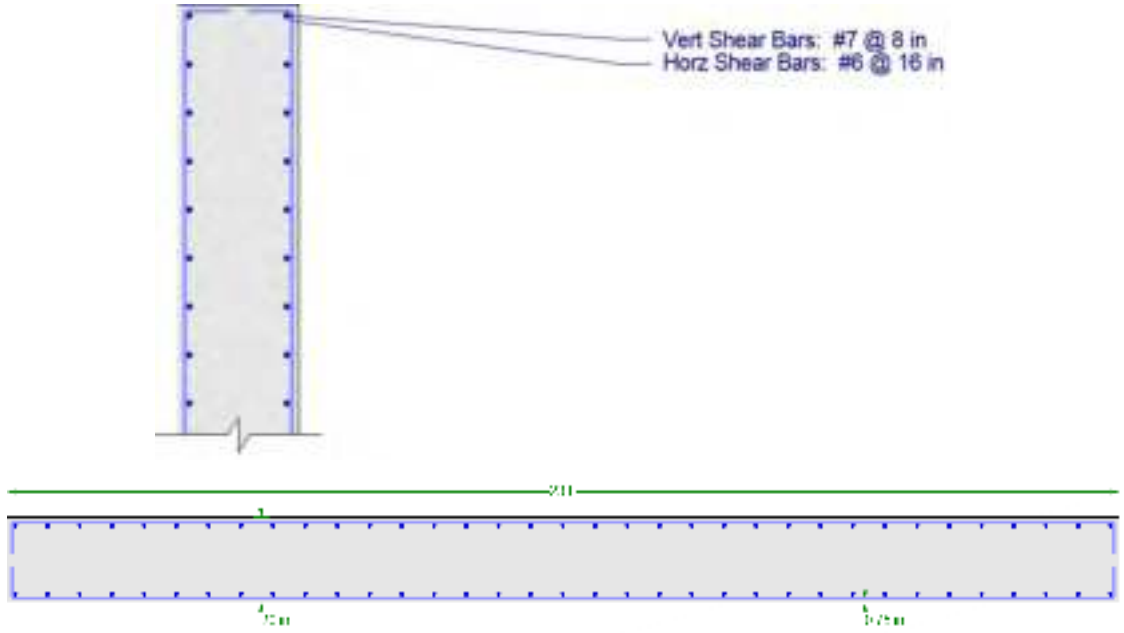

Figure 95: Building (B9-12S-H-S) Special RC Shear Reinforcement Details; Wall Section for Floors 7-9

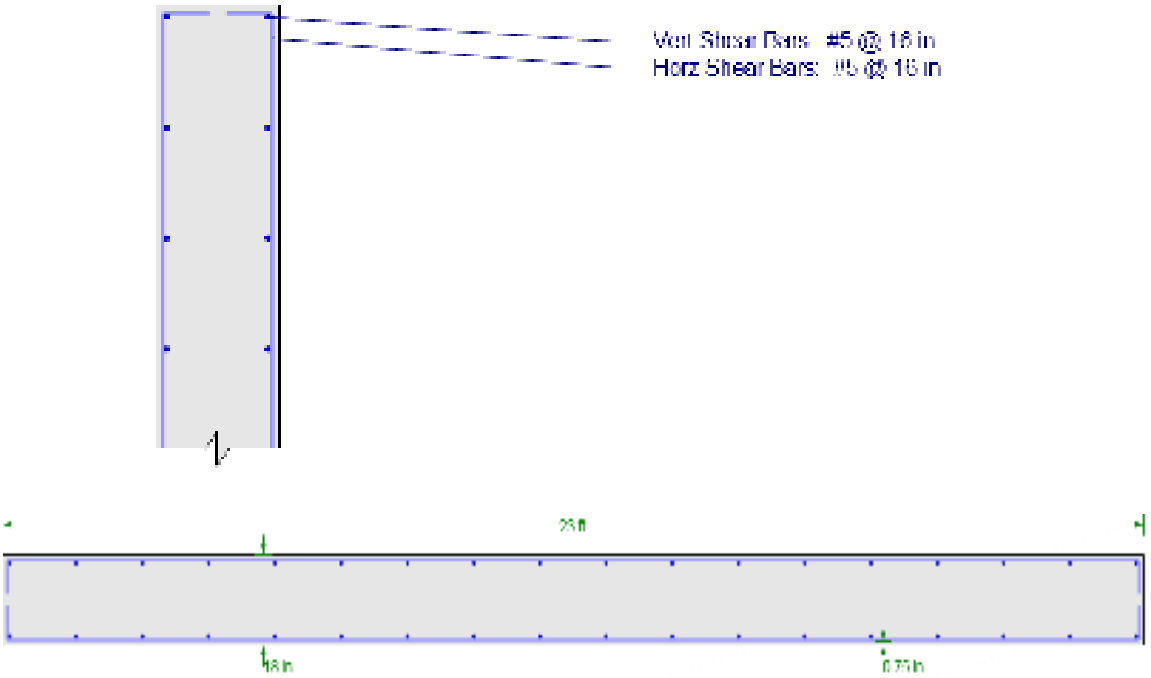

Figure 96: Building (B9-12S-H-S) Special RC Shear Reinforcement Details; Wall Section for Floors 10-12

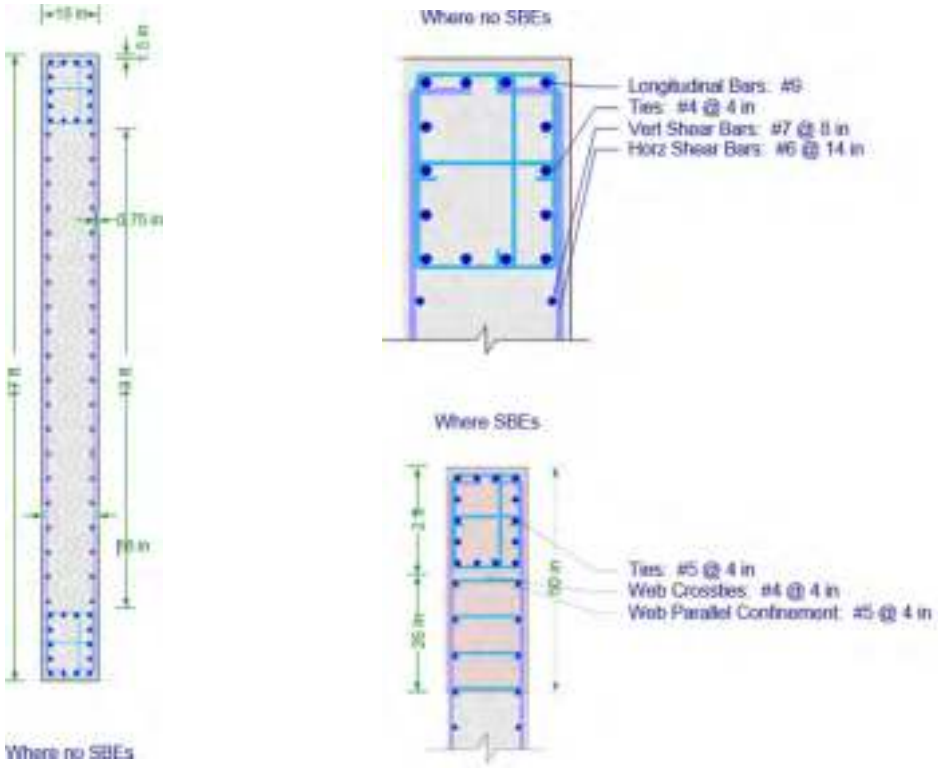

Figure 97: Building (B10-12S-M-S) Special RC Shear Reinforcement Details; Wall Section for Floors 1-3

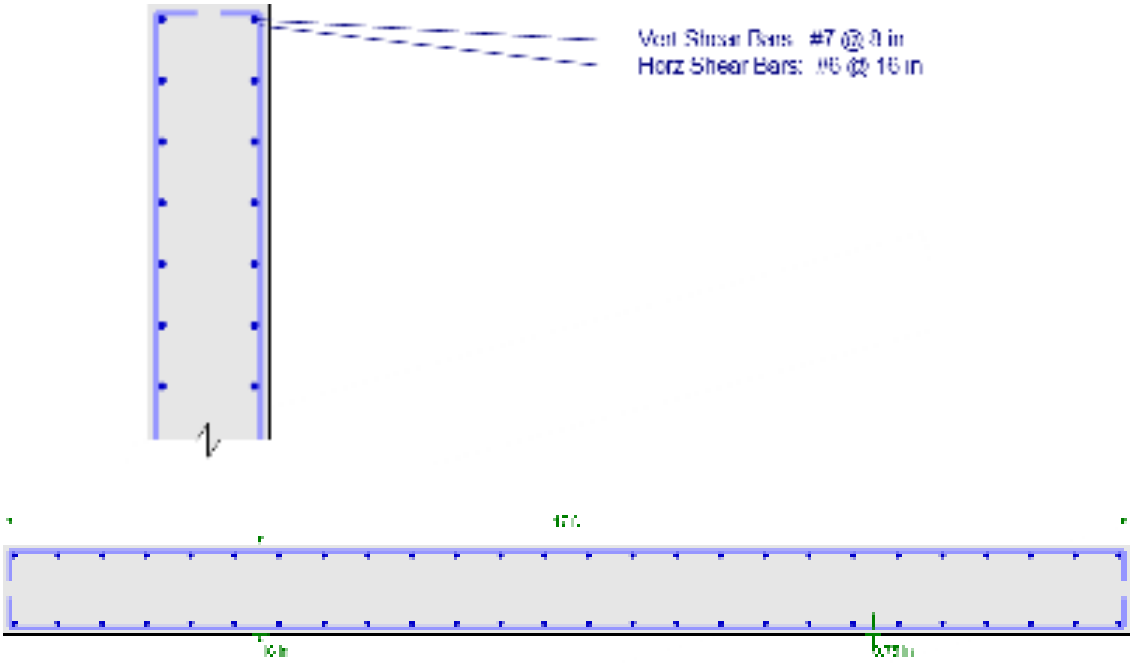

Figure 98: Building (B10-12S-M-S) Special RC Shear Reinforcement Details; Wall Section for Floors 4-6

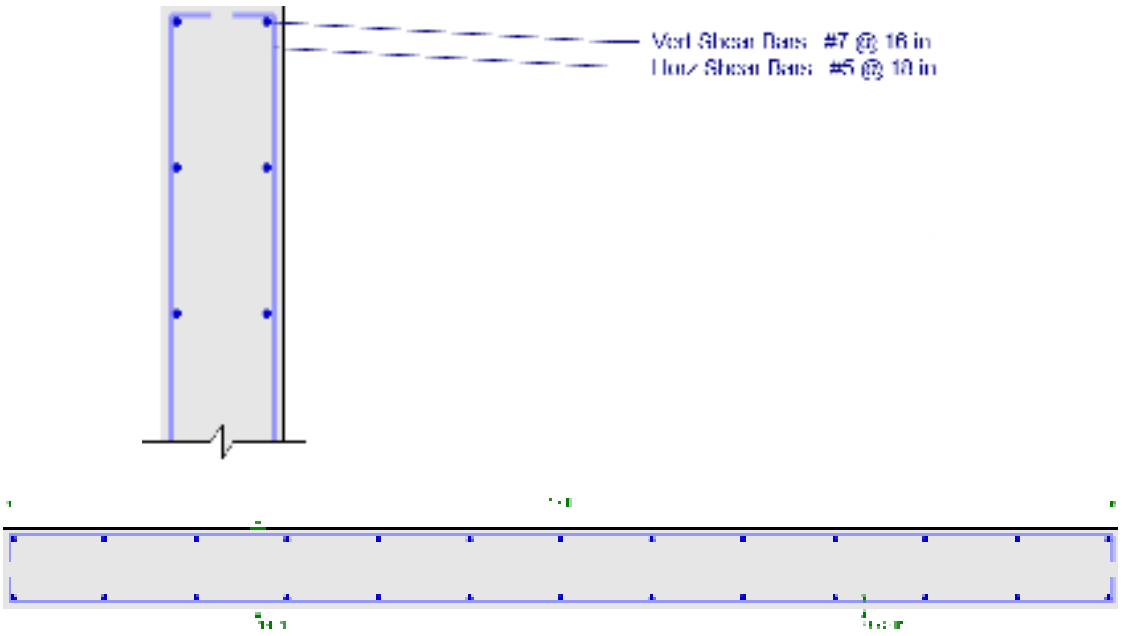

Figure 99: Building (B10-12S-M-S) Special RC Shear Reinforcement Details; Wall Section for Floors 7-9

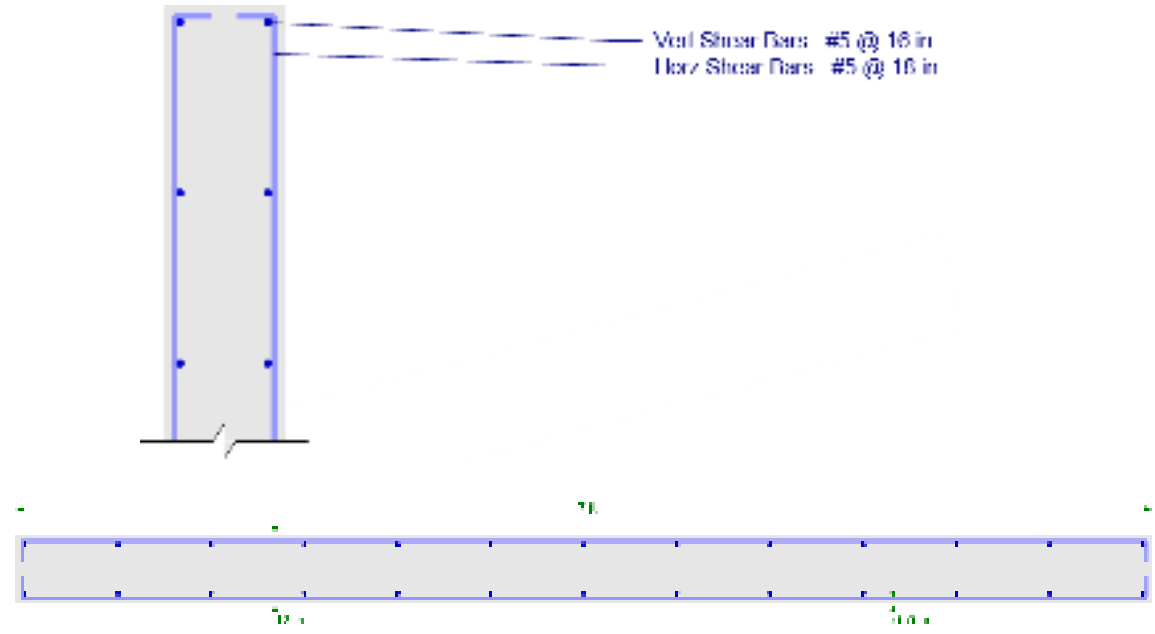

Figure 100: Building (B10-12S-M-S) Special RC Shear Reinforcement Details; Wall Section for Floors 10-12

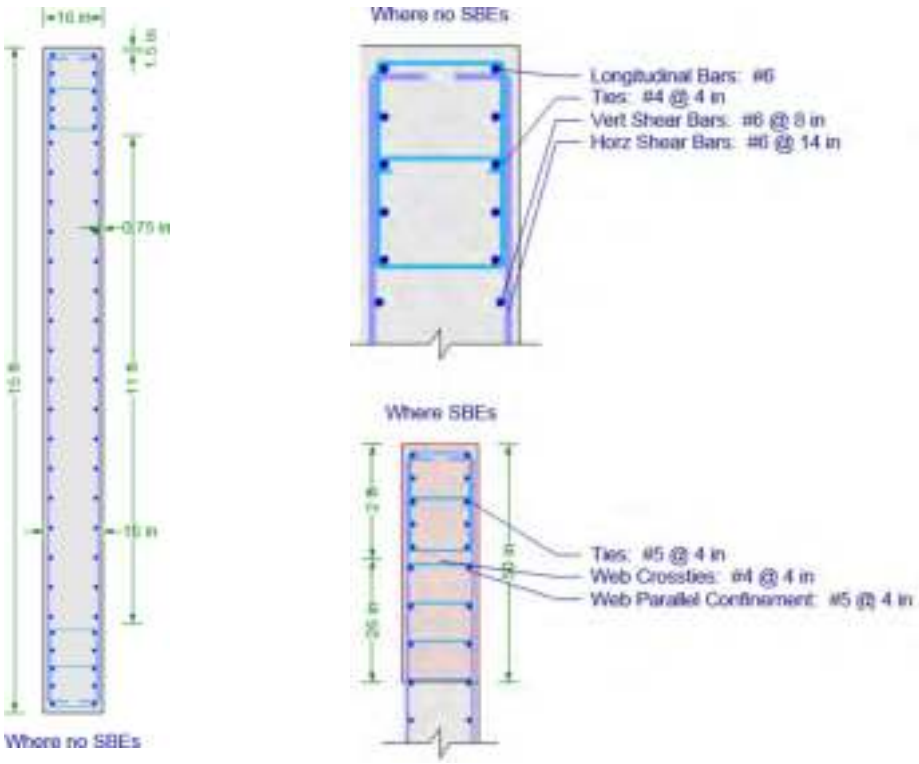

Figure 101: Building (B11-12S-L-S) Special RC Shear Reinforcement Details; Wall Section for Floors 1-3

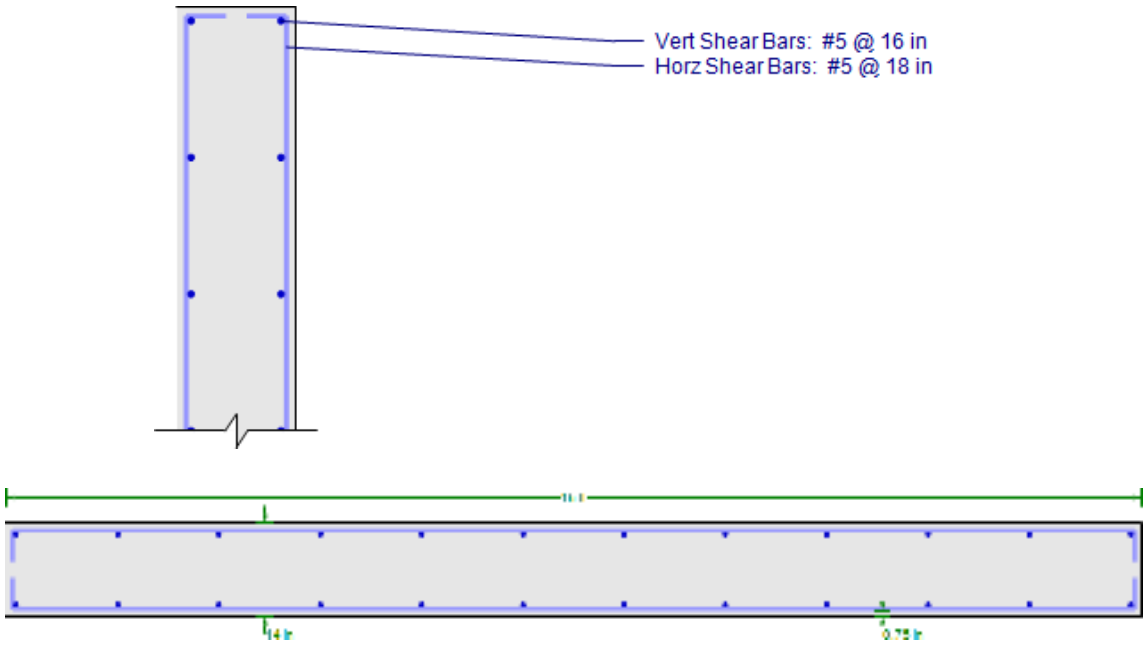

Figure 102: Building (B11-12S-L-S) Special RC Shear Reinforcement Details; Wall Section for Floors 4-6

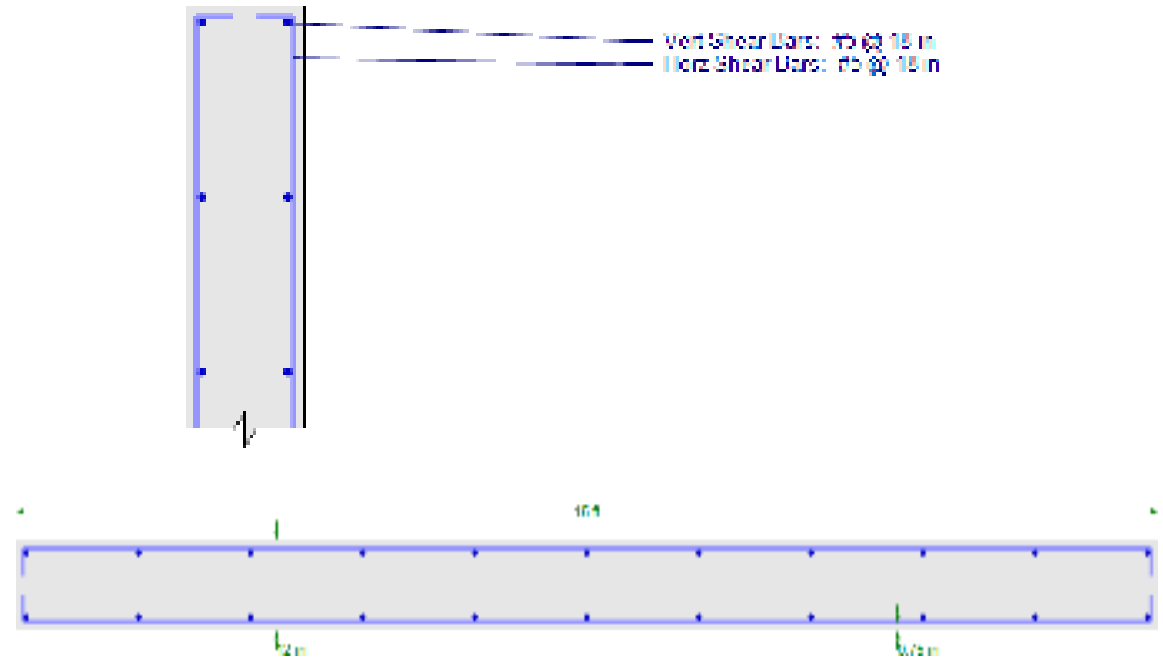

Figure 103: Building (B11-12S-L-S) Special RC Shear Reinforcement Details; Wall Section for Floors 7-9

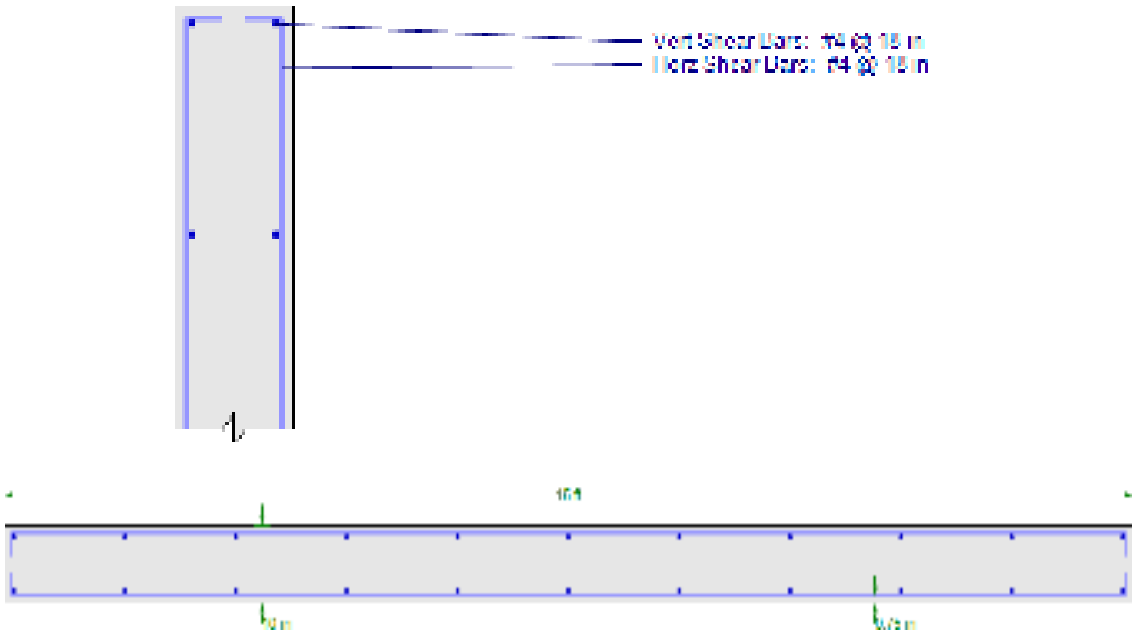

Figure 104: Building (B11-12S-L-S) Special RC Shear Reinforcement Details; Wall Section for Floors 10-12

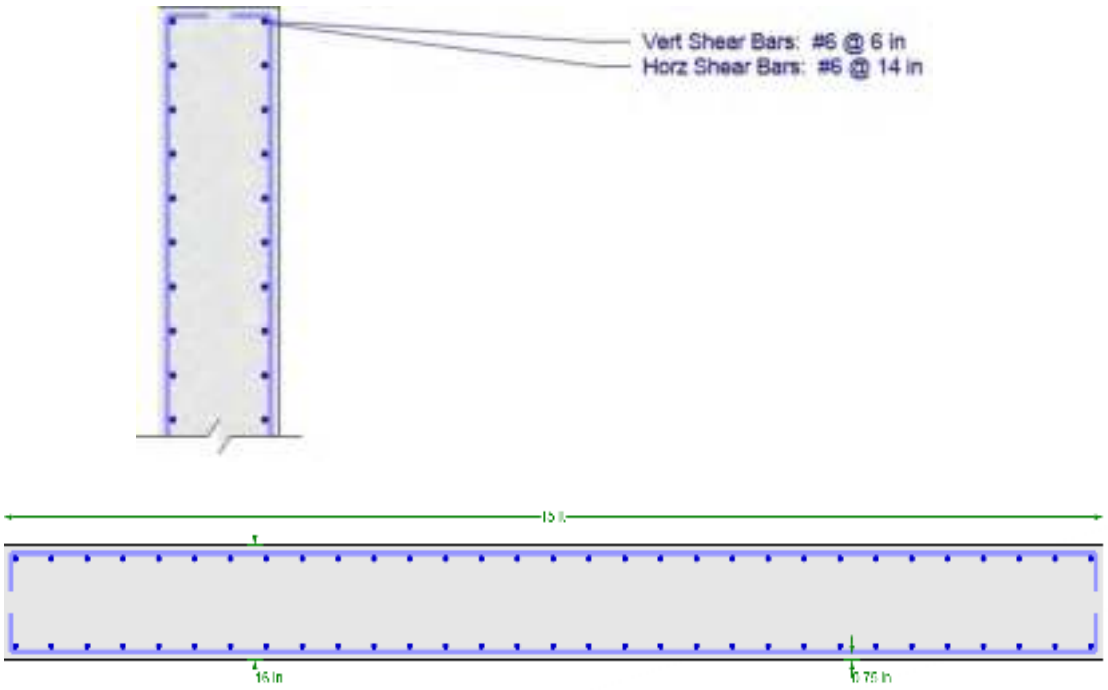

Figure 105: Building (B12-12S-L-O) Ordinary RC Shear Reinforcement Details; Wall Section for Floors 1-3

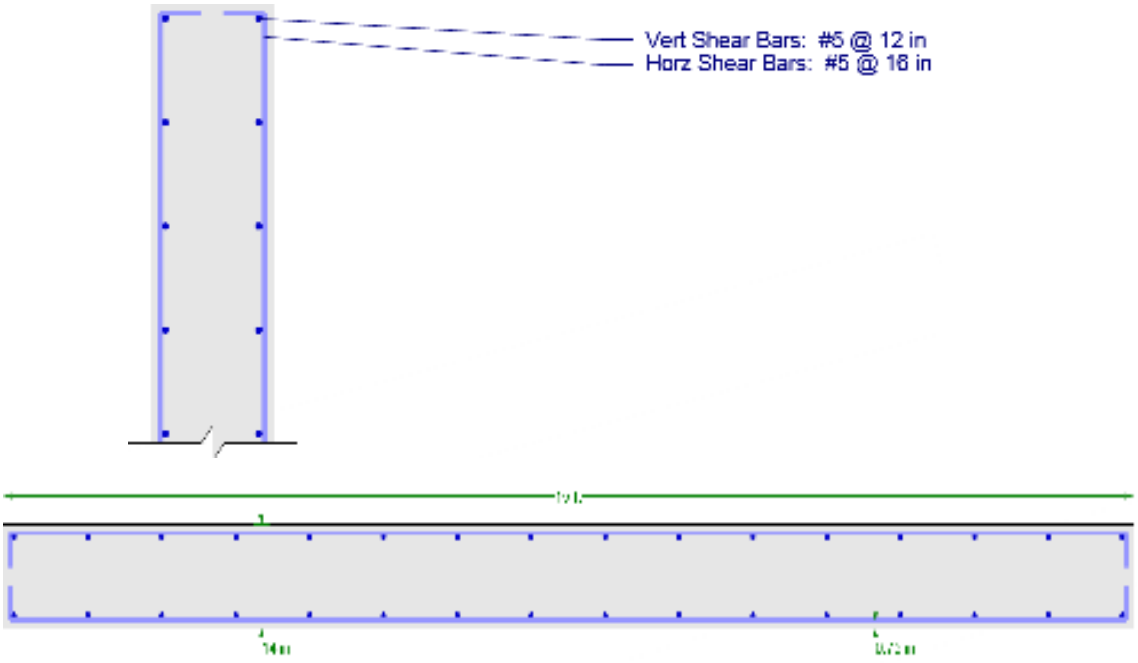

Figure 106: Building (B12-12S-L-O) Ordinary RC Shear Reinforcement Details; Wall Section for Floors 4-6

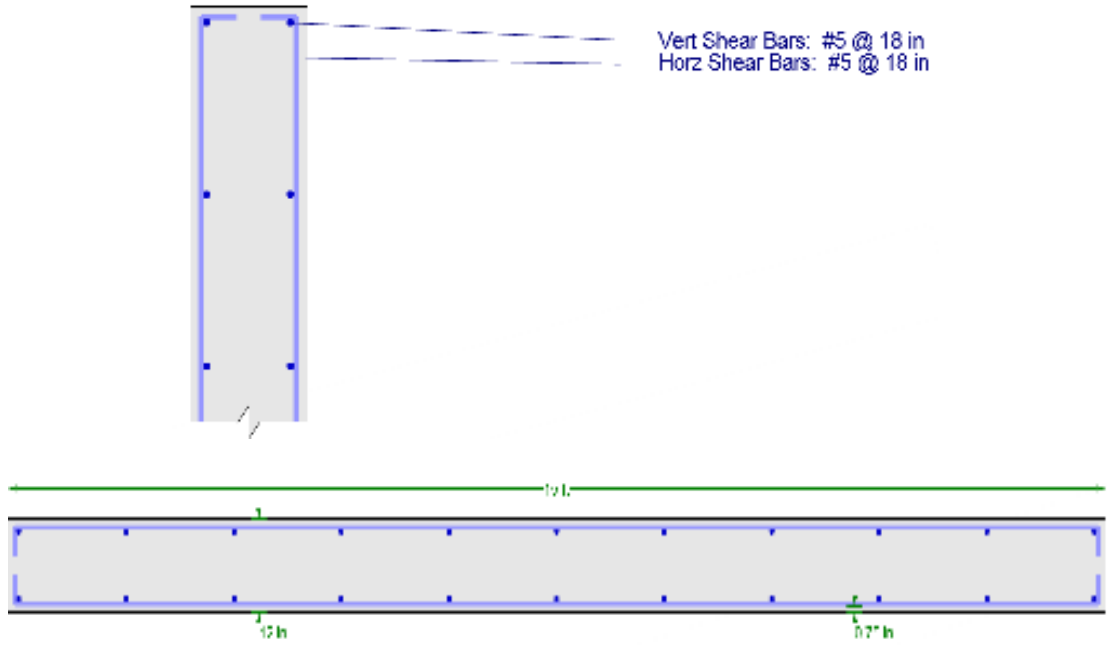

Figure 107: Building (B12-12S-L-O) Ordinary RC Shear Reinforcement Details; Wall Section for Floors 7-9

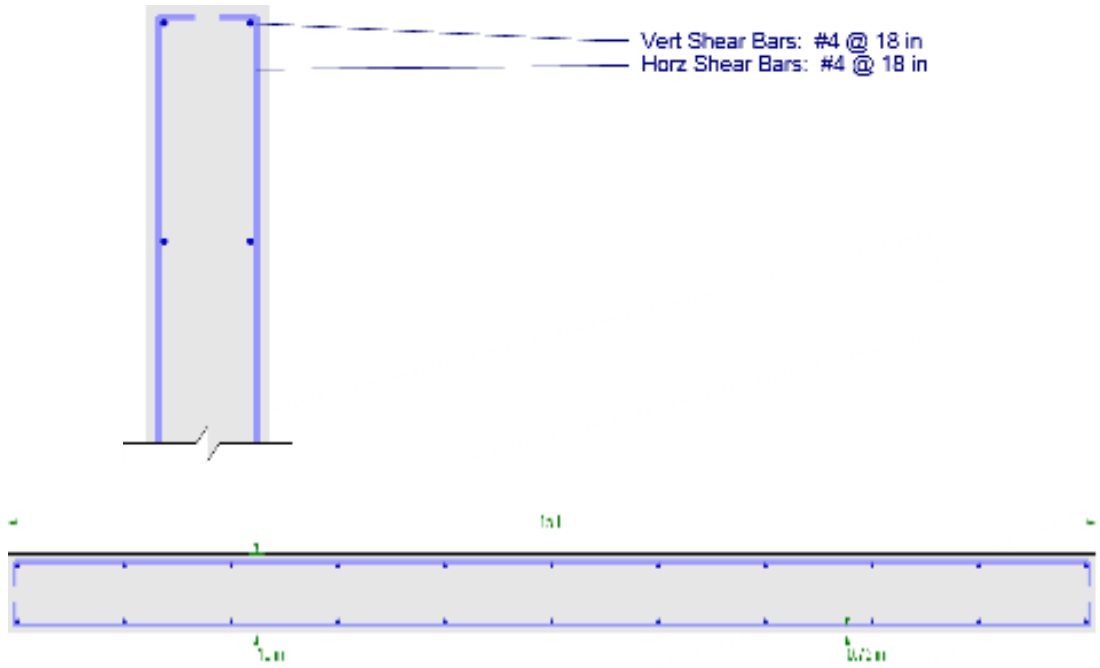

Figure 108: Building (B12-12S-L-O) Ordinary RC Shear Reinforcement Details; Wall Section for Floors 10-12

Appendix B

الكنـــديـــه الأمـــريكيـــه لمـــقـــاولات البـنـــاء ذ.م.م.
AL CANADIAH AL AMERICIAH BLDG. CONT. L.L.C.

23-11-2015

To : **ENGR. NADER ESSAM ALI**
Subject : **Prices of Steel and Concrete**

Concerning the above mentioned subject which you sent to us. The following are our prices :

- Ton Steel Qatari = 2500 dhs/ton
- m3 for Concrete OPC (40N/mm2) including the pump = 250 dhs/m3

Notices:

1. If the quantity is less than 30 m3 the pump will take 500 dhs for the quantity.
2. The prices are for 2 weeks from this date. Any increasing or decreasing in prices we will add or reduce.

Thanking you.
Best Regards.

General Manager

ENG. IBRAHIM RADWAN

Tel.: 06 - 5684860, Fax : 06 - 5684861, P.O.Box : 67565, Sharjah - U.A.E., e-mail : cabc.llc.uae@gmail.com

Vita

Nader Aly was born on June 23, 1990, in Cairo, Egypt. He was educated in private high schools and graduated from Al Shola Private School as class valedictorian in 2007. He received merit scholarship to the American University of Sharjah, from which he graduated summa cum laude in 2011. His degree was a Bachelor of Science in Civil Engineering

In 2012, Mr. Aly began his Master of Science in Civil Engineering at American University of Sharjah. He joined Parsons International office in Dubai in 2012 as a Structural Engineer. After that, in 2015 he started working as a Structural Bridge Design Engineer at Louis Berger Group office in Dubai.